Development and Performance Characteristics of a Family of Gas-Fired Pulsed Combustors

Hassan IPAKCHI

A thesis submitted to Middlesex University in partial fulfilment of the requirements for the degree of Doctor of Philosophy

June 2000

School of Engineering Systems

The work was carried out at the Energy Technology Centre, School of Engineering Systems, Middlesex University, Bounds Green Road, London N11 2NQ, UK.

ABSTRACT

Two nominally 15, and 30 kW Helmholtz-type pulsed combustors were designed and constructed. These were bench mounted with the heat exchangers (i.e. combustion chamber and tailpipe) immersed in the water bath. Their design was based upon the design of a nominally 7.5 kW pulsed unit previously developed at Middlesex University. The design enabled the lengths of the combustion chambers to be varied so that various combustion chamber volumes could be achieved. This provided a new dimension to the study of pulsed combustors which is lacking in many reported works.

It was found that the required input rates could be achieved by scaling up or down each combustion chamber dimensions linearly by a factor of 1.5, while maintaining the geometry identical. Tests showed that the present design of pulsed combustors can operate successfully at various input rates of mains natural gas (93 % methane) with a maximum turn-down ratio of 1.8:1. Results indicated that the three developed combustors would generally operate in the fuel-lean condition. Interestingly, these tests revealed that the amount of excess air reduced as the combustion chamber volume (CCV) was increased.

Systematic investigation on the three developed combustors showed that the temperature within the combustor was principally controlled by the air-to-fuel ratio (A/F). Analysis of the average measured NO_x concentrations at various operating conditions indicated that NO_x emission in this type of pulsed combustor is principally controlled by combustion temperature with no significant influence of combustion chamber volume, tailpipe length or scale of the combustors except in so far as these influenced the A/F and hence the temperature within the combustor. The dominant role of temperature on NO_x production from these combustors become more evident when nitrogen or argon was injected into the system resulting in reduced NO_x emissions at a given A/F. Systematic analysis of data indicated that as the amount of diluent increased, the temperature within the combustor decreased. Almost all the NO_x values recorded were in the form of NO which is believed to be as a result of the high flame temperature (typically above 1850 K). The minimum recorded NO_x value was 5 ppm at the upper limiting value of excess air ratio, λ ; importantly it was found that at these high A/F values there was no significant reduction in overall efficiency of the pulsed units, showing calculated values above 90 %.

Analysis of data indicated that combustion temperature is also a primary factor controlling CO emissions from the present design of pulsed combustors. CO concentrations exhibited U-shaped characteristics when plotted vs λ, showing maximum values at the lowest and highest λ values. By changing water bath temperature (WBT) and hence modifying heat losses to the combustion chamber wall, it was shown that the quenching of the combustion reactions and incomplete mixing of air and gas prior to combustion are contributing factors to CO formation in this type of pulsed combustor.

The developed pulsed combustors were operated successfully with standard test gases. The composition and flame stability of these test gases were similar to the standard test gases G21 (incomplete combustion gas), G222 (light back gas) and G23 (flame lift gas). Analysis of the exhaust gas composition showed similar trends to those obtained when burning mains natural gas; as the heat input was increased, O_2 levels decreased while CO_2 and NO_x emission levels increased. Similarly, CO concentrations showed U-shaped characteristics when plotted against firing rate.

Measurements of peak pulsing pressure and frequency were used as a guide to operation and stability performance of the pulsed units. It was found that the operating frequency was a function of configuration of the combustors and temperature of the internal gases. Frequency of operation showed a reciprocal correlation with volume of combustion chamber and tailpipe length and increased as the heat input was increased. Pulsing pressure amplitude also was influenced by change of configuration of the combustors, increasing as the CCV and tailpipe length were decreased. Analysis of experimental data obtained at fixed configuration of the combustors showed that the peak pulsing pressure was a strong function of the heat release per cycle in the present design of pulsed combustors.

A major drawback of the use of pulsating combustors is the high noise level which is associated with their operation. It was found that it is possible to reduce overall noise levels of the pulsed burners to acceptable values by configuring the system appropriately. This included the use of expansion chambers at the inlet and the exhaust outlet which reduced the overall noise levels to a minimum value of 65 dBA.

Acknowledgments

My special thanks goes to my supervisors Dr. William Maskell, Mr. Peter Barham and Mr. Keith Hargreaves for their supervision, support and many valuable suggestions during this study.

I would like to thank British Gas plc for their financial support of this project. I also would like to thank the principal scientists and engineers of British Gas Research Centre at Loughborough, particularly Dr. M. Tung, Dr. P. Finch, Dr. R.N. Sauba and Mr. A. Suthenthiran for their support and advice.

The general helpfulness and assistance of the entire staff at Middlesex University particularly technicians and library staff at the Bounds Green Campus, and of the staff at the British Library, Chancery Lane, London is acknowledged.

Finally I wish to thank my colleagues at Middlesex University particularly researchers and distinguished members of the Energy Technology Centre including Prof. Frank Tye, Dr. Peter Holmes, Dr. M. Benammar and Dr. I. Markes for their support and for providing an enjoyable time during this study.

Nomenclature

A	Cross sectional area of tailpipe / m^2, or a constant
A_f	Cross sectional area of the float of the gas flow meter / m^2
c_s	Speed of sound / m s^{-1}
C_d	Coefficient of discharge
C_p	Specific heat at constant pressure / kJ kg^{-1} K^{-1} ; kJ $kmol^{-1}$ K^{-1}
C_v	Specific heat at constant volume / kJ kg^{-1} K^{-1} ; kJ $kmol^{-1}$ K^{-1}
CV_g	Gross calorific value / kJ kg^{-1}
CV_n	Net calorific value / kJ kg^{-1}
d	Internal diameter of the tailpipe / m
D_c	Diameter of the ring of the centres of the mixture ports / m
D_p	Diameter of the inlet mixture ports / m
Df	The frequency of the inlet decoupler / Hz
E_a	Activation energy / kJ mol^{-1}
e	Edge to edge spacing of the inlet ports / m
f	Operating frequency of the pulsed combustor / Hz
f_b	Pulsed combustor frequency without decoupler / Hz
f_o	Operating frequency with no flow in the tube / Hz
g	Acceleration due to gravity / m s^{-2}
g_s	Saturated moisture content / kg kg^{-1}
H_R	Enthalpy of reactants / kJ
H_p	Enthalpy of products / kJ
k_i	Reaction rate constant / m^3 mol^{-1} s^{-1} ; ml mol^{-1} s^{-1}
L	Length of the tailpipe or combustion chamber / m
L_{cr}	The critical or minimum length of the inlet pipe / m
L_H	Length of the valve holder / m
L_i	Acoustic loss from the system (the i-th wave damping process)
L_{RH}	The remaining length inside the valve holder between components / m
M	The Mach number
N	Number of mixture ports

n	Number of moles
p	O_2 concentration / %
P	Pulsing pressure / N m^{-2}
P_h	Pressure rise inside combustion chamber / N m^{-2}
P_{atm}	Atmospheric pressure / N m^{-2}
P_{ref}	Reference pressure / N m^{-2}
Q	Heat addition / kJ
Q_u	Useful heat / kJ
q	The volume flow rate of input fuel gas / ml s^{-1}
R	Specific gas constant / kJ kg^{-1} K^{-1}
R_o	Universal gas constant / kJ $kmol^{-1}$ K^{-1}
Re	Reynold number for steady flow
r	Internal radius of the combustion chamber or the tailpipe / m
r_c	Internal radius of the conical end of the combustion chamber / m
r_H	Internal radius of valve holder / m
r_{LR}	Internal radius of the locking ring / m
s	CO_2 concentration / %
S	CO concentration / %
T	Temperature / °C or K
T_i	Initial temperature / °C or K
T_f	Final temperature or adiabatic flame temperature / °C or K
T_{op}	Average operating temperature / °C or K
t	Time / s
U	Internal energy / kJ
v	The flow velocity / m s^{-1}
V	Volume of the combustion chamber / m^3
V_C	Volume of the main cylinder (i.e. combustion chamber volume without the conical section) / m^3
V_{CC}	Effective volume of the combustion chamber / m^3
V_d	Volume of the inlet decoupler / m^3
V_E	Volume of the conical cylinder end / m^3

V_{G1} Scale reading of gas "G2" flow rate

V_{G2} Actual readings of gas "G2" flow rate

V_H Volume of the valve holder / m^3

V_f Volume of the float / m^3

V_{fr} Volume flow rate / $m^3\ s^{-1}$

V_F The remained volume inside the valve holder / m^3

W_g Gross Wobbe number / MJ m^{-3}

W_n Net Wobbe number / MJ m^{-3}

x Location / m, or excess air

X Distance from the rim of the valve holder to the top surface of the lock ring in the downstream of the flame trap / m

Y Distance from the upstream rim of the combustion chamber to the valve holder / m

Greek Symbols:

γ Ratio of specific heat capacities

η Overall efficiency / %

λ Excess air ratio (i.e. actual A/F divided by stoichiometric A/F)

ρ Density / kg m^{-3}

ρ_f Density of the float / kg m^{-3}

σ Relative density of the gas

τ Characteristic time and oscillation period / s

Contents

Chapter Two

Chapter Six

Chapter Seven

Introduction

General

The combustion of fossil fuels is the primary energy source in our present society. However, the burning of fossil fuel is a major contributor to global annual pollutant emissions which have increased substantially since 1900. These emissions include:

1. Nitrogen oxides (NO_x) which affect fish and plant life by increasing environmental acidity. NO_x are one of the ingredients that combine to create photochemical smog. Building erosion can also be attributed in part to NO_x emissions.
2. Carbon dioxide (CO_2) which causes global warming.
3. Carbon monoxide (CO) which is produced from incomplete combustion. Its effect on human health is of most concern because it interferes with the take-up of oxygen by the blood.
4. Hydrocarbons (HCs) which react with NO_x to produce ground level ozone (smog) that damages the lungs and irritates the eyes.
5. Sulphur dioxide (SO_2) which is an acid gas when deposited by rain or dry deposition, and can increase the acidity of soils and water. It also contributes to the erosion of many conventional building materials.
6. Toxic particulates that can cause cancer, birth defects and neurological problems.

According to the Department of Environment and Transport Region (DETR), in the UK alone in 1997, some 1834 ktonnes NO_x, 147 Mtonnes CO_2, 5089 ktonnes CO and 184 ktonnes of Particulate Matter $(PM)_{10}$ were generated from burning fossil fuels.

In the following sections some of the above environmental problems are discussed in more detail.

Greenhouse Effect

The presence of water vapour, carbon dioxide (CO_2), ozone (O_3), methane (CH_4) and nitrous oxide (N_2O), reduce the rate of loss to space of the thermal energy emitted by

the surface and lower atmosphere, thereby increasing the global average surface temperature above the nominal temperature that would occur in the absence of an atmosphere. In another words, the net effect of greenhouse gases in the atmosphere is to keep the Earth's surface more than some 30°C warmer than it would be otherwise. This phenomenon is known as greenhouse effect [Edmonds *et al.*, 1989]. An excess of these greenhouse gases in the atmosphere retains additional heat and contributes to global warming. It is known that a main contributor to the greenhouse climate problem is emissions of CO_2 from fossil fuel combustion. However, the atmospheric concentrations of several other radiatively important gases such as methane and chlorocarbons are also increasing and are expected to affect climate significantly.

Acid Rain

There is not universal agreement concerning the origin of acid precipitation but scientific evidence does indicate that acid precipitation results from the combustion of fossil fuels releasing oxides of nitrogen and sulphur into atmosphere. These oxides undergo transformation in the atmosphere resulting in the formation of HNO_3 and H_2SO_4 which may be transported great distances. Once deposited through the vehicle of rain, snow, hail, mist, or fog they cause damage to vegetation, soils, lakes, rivers, statues and buildings [Cowgill, 1989].

An alternative explanation for the above phenomena is the drastic changes in land use that have been brought about over the last three decades.

Ozone Depletion

The ozone layer acts as a filter for ultra-violet (UV) radiation from the sun, removing radiation of wavelength below 300 nm. Ozone forms from the dissociation of molecular oxygen by short wavelength UV radiation in the upper stratosphere. However, the ozone itself is rapidly photo-dissociated [Harrison, 1992].

Pollutant gases such as nitrogen oxides are potential catalysts for the destruction

of ozone. Although, during the past two decades concern has been raised on the effect of halogen compounds especially the non-toxic, non-flammable and chemically inert chlorofluorocarbons (CFCs) or Freon on destruction of ozone [Hanby 1993]. The CFCs are used as refrigerants, aerosol propellants and gases for production of foam plastics [Harrison, 1992].

Discussion

Most studies of the greenhouse issue have focused on the role of CO_2. Since CO_2 is one of the main products of combustion of fossil fuel, it can be reduced by burning less fossil fuel by utilization of more efficient devices to produce heat and power. Moreover, the use of natural gas instead of coal and oil can be beneficial since the mass of CO_2 emitted per unit of heat released is less for natural gas (i.e. 0.43 ktonne $MWyr^{-1}$) compared to oil (0.62 ktonne $MWyr^{-1}$) and coal (0.75 ktonne $MWyr^{-1}$) [Harrison, 1992]. Clearly elimination of large scale deforestation by burning and encouragement of reforestation particularly in developing countries to promote CO_2 absorption have an important role to play.

Nitrogen oxides (NO_x) are combustion-generated air pollutants that have received much attention particularly during the last two decades. As was mentioned earlier, NO_x is one of the main contributors to the greenhouse effect, acid rain and ozone depletion. There have been a number of techniques proposed to reduce NO_x emissions which are based upon modification of combustion process and treatment of the products of combustion. While these methods are effective in reducing NO_x emissions they have a significant effect on the combustion system, such as lowering the flame temperature, enhancing carbon monoxide (CO) and particulate generation. Subsequently, these affect the overall fuel/energy efficiency and have implications for human health.

From the above, clearly there is a need for combustion devices with high thermal efficiency, reduced pollutant* emissions and ability to use a variety of gaseous fuels with

* The definition of a pollutant is a substance present in a greater than natural concentration which has a detrimental effect on environment.

similar effectiveness. Pulsed combustion devices can satisfy these needs. Pulsed combustion systems have a number of attractive features for heating applications. These include simplicity of construction, compactness for a given heat rating, enhanced heat transfer, high efficiencies, low NO_x and CO emissions and electric power requirement only at start-up.

Gas-fired pulsed combustors for water heating applications have been on the market for a number of years. Nevertheless there is a need to learn more about the physical and chemical processes which control their operation. For instance, a pulsed combustor's operating functions are interrelated, hence, the various components must be developed in relation to each other rather than separately. Thus, for better understanding of the physical processes, there is a need to separate and investigate the various adjustable parameters.

Despite considerable research efforts during the last 25-30 years there is still a requirement for systematic investigation of factors influencing the fundamental operating processes and the emission of pollutant gases from pulsed combustors.

Objectives

This PhD thesis describes experimental investigations performed to obtain an understanding of the fundamental operating principles and exhaust gases emissions of the present design of Helmholtz-type pulsed combustion heating device. The main goal of this effort was the acquisition of information that will be useful for the engineering design of practical systems which employ the pulsed combustion principle. The objectives of this study were:

- The successful design and development of two nominally 15 and 30 kW pulsed combustors.
- The demonstration and the performance characterisation of the newly developed 15 and 30 kW combustors and an existing 7.5 kW pulsed combustor.
- A systematic investigation of the parameters influencing the gaseous pollutant emissions, the overall efficiency and noise emission in this type of combustor

leading to a fundamental understanding of such influences.

- To provide information on fuel flexibility, optimum configurations and operating conditions for this design of pulsed combustor for commercial use.

In the next two sections, the above listed objectives are described in more detail.

Design and Development of the Required Nominal Input Pulsed Combustors

At present, the design of a pulsed combustor must proceed on an empirical basis and it is not possible simply to scale up or down from a successful configuration. One of the major parts of this study was aimed at tackling this weakness. The objective was to design, build and develop two experimental 15 and 30 kW gas-fired pulsed combustion water heaters in addition to the existing nominally 7.5 kW pulsed combustor previously built at Middlesex University with an identical geometry. An important constraint was that the combustors should operate satisfactorily with varying fuel gas flow rates and fuel gas compositions.

Performance Characterisation of the Developed Pulsed Combustors

Once the combustors were constructed and were fully operational, the further objective was to characterise each pulsed combustor, substantiating its operational limitations and establishing the optimum configuration and fuel gas rate in terms of pollutant gases and stable operation leading to optimisation of the present design. In addition, a concern was to achieve maximum overall efficiency with minimum attainable noise.

The task of characterisation of the developed pulsed combustors included further objectives:

a) Systematic measurements of operating frequency and pulsing pressure of the combustors under various operating conditions,

b) To develop an understanding of the effect of these parameters upon stable and satisfactory performance of the developed combustors.

It is well known that the satisfactory performance of a pulsed combustor relies upon satisfying Rayleigh's criterion which states that the heat release and pressure oscillations should be in phase for satisfactory operation of a pulsed combustor [Putnam, 1971a]. Thus, it is a matter of importance to establish the influence of various parameters such as fuel flow rate, air-to-fuel ratio, combustion chamber volume, tailpipe length and flapper valve thickness upon operating frequency and pulsing pressure which are fundamental factors influencing the operation of a pulsed combustor including the processes that lead to heat release [Keller *et al.*, 1989].

c) To carry out a systematic investigation on NO_x and CO production mapping variations with changeable parameters as above in addition to the input fuel gas composition, temperature of the water bath and dilution of mixture charge of air and gas with nitrogen or argon.

As was mentioned earlier, the emission of nitrogen oxides from combustion systems has important environmental consequences and tends to be a problem localised to the vicinity in which the NO_x is generated. Indeed, NO_x control is one of the primary design parameters for utility and industrial power boilers. Although pulsed combustors generally generate low NO_x levels, the development of competing technologies and increasingly strict regulations for low NO_x emissions implies the need for further reduction of NO_x produced from current pulsed combustors. Therefore, one of the main objectives of this work was in this area, providing information on NO_x production in this type of pulsed combustors and to disentangle the coupled effects between the many and various parameters which may influence NO_x emission. Moreover, an attempt has been made to gain a detailed understanding of the underlying mechanisms for NO_x and CO formation in the present design of pulsed combustors.

Chapter One

Background & Literature Review

1.1 Introduction

The successful laboratory development of gas-fired pulsed combustion heating devices has demonstrated their advantages over conventional combustion heating equipment in providing fuel savings and reduced emissions of pollutants. Hence, it is anticipated that pulsed combustion technology may be applied to the commercial and industrial sectors in the near future. However, to put such devices in wide commercial use, more fundamental research and understanding of the chemistry and physics of the pulsed combustion process is required. During this century a great deal of research has been carried out on pulsed combustion systems. In this chapter some of the important reported works, including those with historical significance, will be reviewed and used as a source of additional information and references.

Combustion with self-sustaining oscillations is called "pulsed combustion"* and chambers that are deliberately designed to produce combustion oscillations are usually called "pulsating combustion chambers" or "pulsed combustors". The intention of such designs is the utilization of the higher combustion and heat transfer rates associated with the oscillations. Pulsed combustors are generally designed so that a periodic heat release is obtained at a point corresponding to a pressure anti-node of a fundamental acoustic mode of oscillation of the system. In most cases the oscillation or pulsation is driven if the periodic heat release is in phase with the pressure variation. These oscillations affect the mixing rates between various species, accelerating the combustion process and reducing the amount of excess air required for combustion. Thus, it follows that there is an increase of thermal efficiency caused by reduction of heat losses from the pulsed unit's exhaust [Zinn, 1992]. High heat transfer resulting from these pulsations reduces

---

* The process has been described by various terms including: "pulsatory", "pulsating", "resonant" and "pulse" combustion. Throughout this thesis the term pulsed combustion is used.

the fraction of time during which combustion occurs at high temperature, resulting in lower thermal NO_x formation [Keller and Hongo, 1990].

Acoustical oscillations are generated in most combustion systems but they are generally regarded as being annoying, with damaging effect to the equipment. These oscillations may be categorised as unwanted combustion-driven oscillations. In fact, in the design and operation of industrial and residential continuous combustion furnaces, care is taken to eliminate or prevent such combustion-driven oscillations or pulsations. Such pulsations can disrupt the combustion air supply then resulting in pollutant formation and/or lower efficiency. These pulsations also, cause early fatigue failure and material deterioration [Putnam, 1971a].

The use of the phenomenon of pulsed combustion is not new; technical designs and patents go back as far as 1906. Research and investigations on pulsed combustion principles and their practical application are being continued in several countries including the United Kingdom, United States of America and Japan. In spite of the efforts of many workers, pulsed combustion systems are still not in widespread use.

1.2 Basic Operating Principles of Pulsed Combustors

There appear to be three main types of pulsed combustor for purposeful applications:

i) Quarter-Wave or Schmidt

ii) Helmholtz

iii) Rijke.

One other reported design which is patented as a pulsed combustor is the Reynst combustor also known as a pulsed-pot combustor. More details on this type of pulsed combustor is given later.

The classification of pulsed combustors is related to their geometry and properties which describe the acoustic behaviour of the indicated pulsed combustor [Zinn, 1986]. However, the mechanism of operation is essentially the same for all three basic forms of pulsed combustor.

The means by which the utilized fuel and air are introduced is also a matter of

considerable importance. In the following sections these are discussed.

1.2.1 Quarter-wave Pulsed Combustor

As the name of the combustor implies, the Quarter-wave pulsed combustor operates with the characteristics of the acoustic Quarter-wave tube. It consists of a pipe closed at one end and open at the other. A schematic diagram of a Quarter-wave type pulsed combustor is given in Fig. 1.1. The standing acoustic pressure wave inside the Quarter-wave pipe has its maximum (i.e. antinode) at the closed end where the air and fuel are introduced and minimum (i.e. node) at the open end. The length of the tube is equal to a quarter wavelength of the oscillation which means that a standing wave is produced in the combustor with a wavelength equal to four times the length of the pipe.

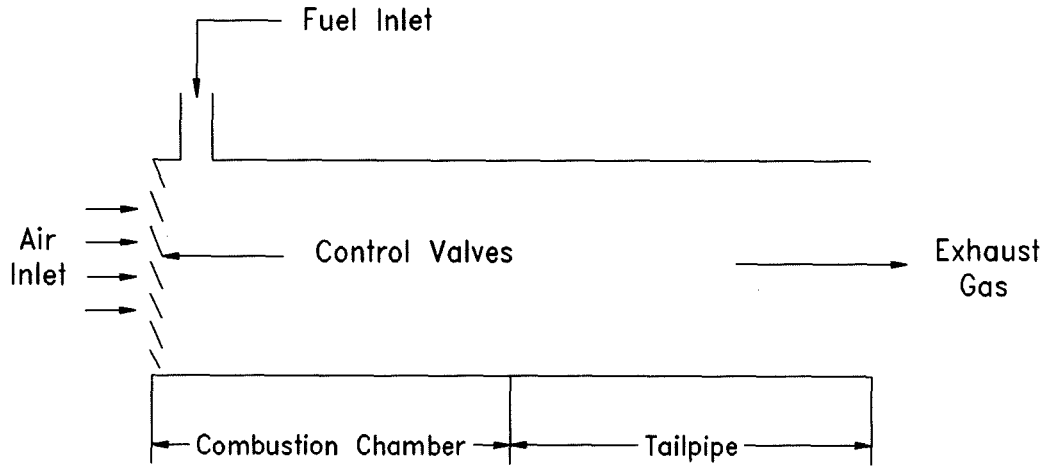

Fig. 1.1 A basic schematic of Quarter-wave type pulsed combustor.

The operating frequency of the system operating in the fundamental mode can be determined by following equation [Hanby, 1971]:

$$f = \frac{c_s}{4L} \tag{1.1}$$

where f is the operating frequency, c_s is the velocity of sound and L is the length of the tube. However, for a more complete picture, the steady component of flow in the tube should be taken into account. Hanby [1971] has reported an analysis of such a flow in a duct. He has described the resonant frequency in the duct is lowered according to:

$$f = f_o(1 - M^2) \tag{1.2}$$

where f_o is the frequency with no flow in tube and M is the Mach number of flow in the tube. When the Mach number is low the above equation has little practical significance. In pulsed combustors the Mach numbers obtained are generally very low [Hanby, 1971].

A Quarter-wave pulsed combustor is fitted with a mechanical or aerodynamic valve(s) and the combustion process occurs near to this, where as mentioned earlier, the magnitude of the pressure oscillations is close to its maximum. The fuel and the air enter into the combustor when the pressure is at a minimum. Inside the combustor a combustible mixture is formed and ignited by means of a spark plug. The resulting combustion process increases the internal pressure. This, in turn, causes the mechanical valves to close and the hot combustion products to move towards the outlet. The inertia of the gases leaving the combustor decreases the pressure there. Consequently, the mechanical valve(s) open and admit new charge(s) of fuel and oxidizer into the combustor. The new charge of fuel and air mix with the remaining previous combustion gases, react and release energy, causing a new pressure increase in the combustor. This periodic combustion process can now continue without the use of a spark plug.

To ensure that the system operates satisfactorily, the duration of the mixing and reaction processes must be such that most of the combustion heat is released when the combustor pressure is near its maximum [Zinn, 1986].

1.2.2 Helmholtz Pulsed Combustor

The Helmholtz-type pulsed combustors consists of a combustion chamber connected to

a smaller diameter tailpipe which may used for conducting the combustion products out of the pulsed combustion system. They are called Helmholtz pulsed combustors, because of their similarity to a Helmhotz resonator.

Helmholtz resonators are often used as alternative devices to Quarter-wave tubes. As in the Quarter-wave pulsed combustor, a mechanical or aerodynamic valve(s) is utilized to periodically admit fuel and combustion air into the combustor [Zinn, 1986]. Figure 1.2 shows schematically the operation of a Helmholtz-type pulsed combustor with a single flapper valve. This is similar to the type of pulsed combustor which was designed and employed for the present study. The principle of operation of the unit may be described as follows:

1. An initial mixture charge of fuel and air is admitted to the combustion chamber through the flapper valve. A fan is used to provide air for the initial air-gas mixture.

2. The mixture charge is ignited by an electric spark plug. As the fuel burns, the combustion chamber pressure rises above atmospheric pressure.

3. The rise of pressure inside the combustion chamber closes the flapper valve and the exhaust gases are forced down the tailpipe.

4. The momentum of the combustion gases flowing down the tailpipe creates a partial vacuum in the combustion chamber. When the pressure within the combustion chamber has decreased sufficiently, the flapper valve opens and allows a fresh charge of air and gas mixture to enter the combustion chamber.

5. As soon as pulsed combustion is initiated, the air blower and spark plug are turned off. The new fuel and air mixture is then ignited without the need for a spark plug. The pulsed unit acts so as to induce its own combustion air and to provide continuous re-ignition of each new air-gas mixture charge.

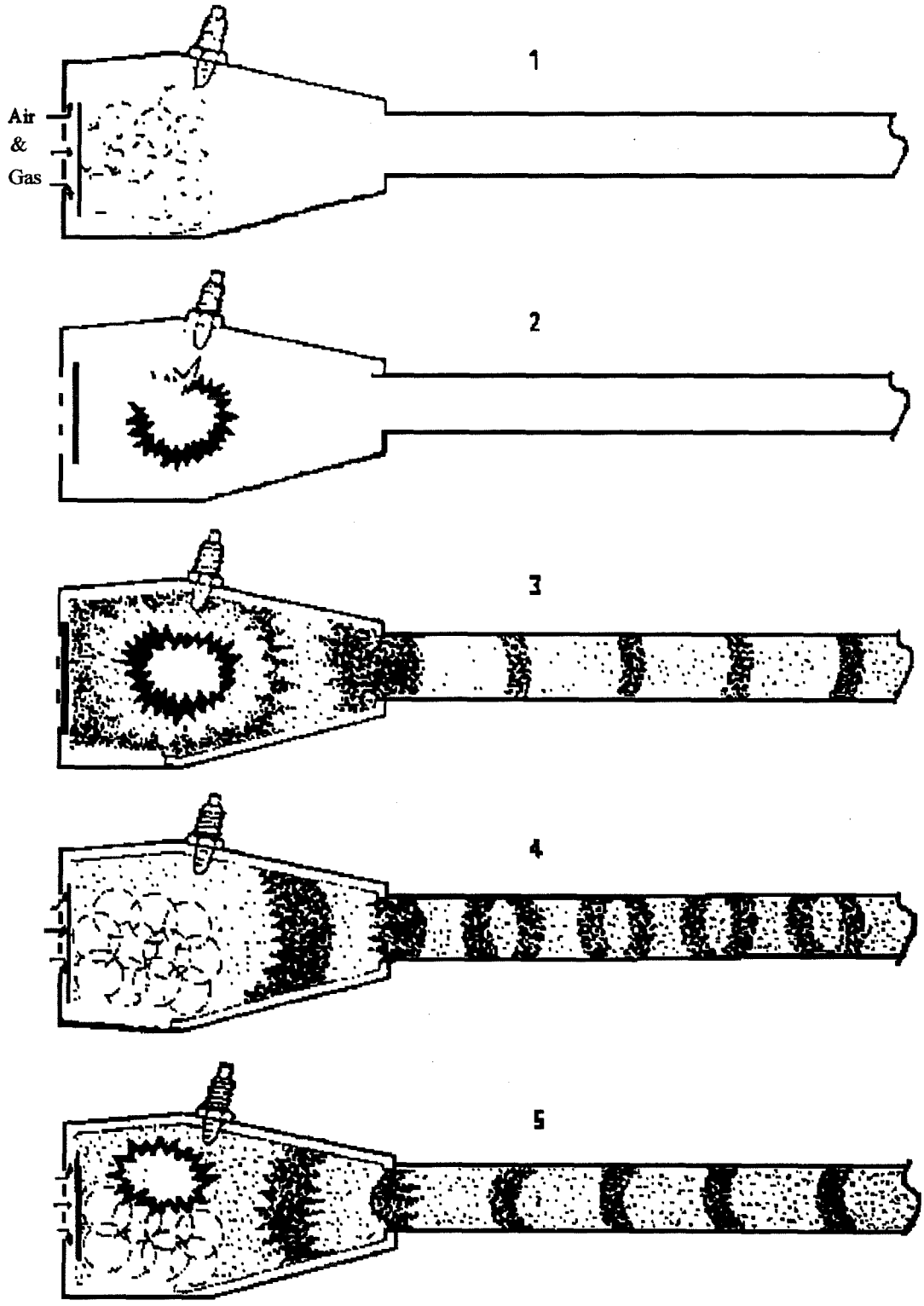

Fig. 1.2 Schematic of operation of a Helmholtz-type pulsed combustor.

For a classical Helmholtz resonator, the fundamental acoustic frequency is given by the following equation attributed to Randall [1951],

$$f = (\frac{c_s}{2\pi})(\frac{A}{VL})^{1/2} \tag{1.3}$$

f is the frequency, c_s is the velocity of sound, A is the internal cross-sectional area of tailpipe, L is the length of the tailpipe and V is the combustion chamber volume. Furthermore, the velocity of sound is given by [Porges, 1977]:

$$c_s = \sqrt{\gamma RT} \tag{1.4}$$

where γ is the ratio of the specific heats of the gas within the combustor, T is its temperature and R is the specific gas constant.

1.2.3 Rijke Pulsed Combustor

Figure 1.3 shows a schematic diagram of a Rijke-type pulsed combustor. Similar to a Rijke tube, it consists of a vertical tube open at both ends. Fuel and air are admitted from one of the open ends and the combustion products leave the combustor through the other end. This type of combustor is more popular when solid fuels (e.g. coal) are used. To attain pulsed combustion operation, the combustion process must be completed within the first half of the combustor, preferably at a distance of $L/4$ from the combustor entrance plane [Zinn, 1986] where L is the length of the tube. It is reported [Wood, 1949] that Rijke produced a sound of considerable intensity by a heated metal gauze stretched across the lower part of a vertical tube open at both ends. He observed that this resulted in the excitation of the fundamental, longitudinal acoustic mode of the tube which may have resulted from velocity variations. This oscillation was

superimposed upon a steady upward flow which was driven by the hot metal gauze [Wood, 1949].

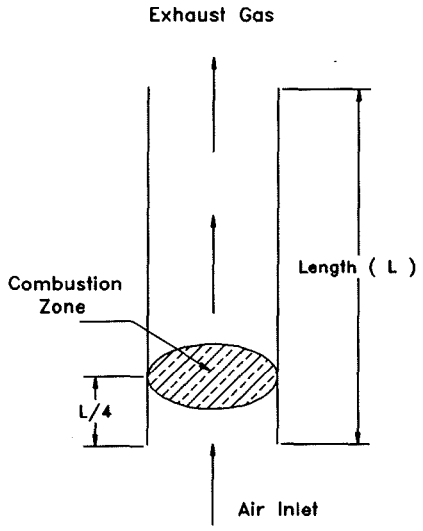

Fig. 1.3 A schematic diagram of a Rijke-type pulsed combustor.

1.3 The Means of Introducing Air and Fuel into a Pulsed Combustion System

The way that air and /or fuel are admitted to a pulsed combustion system is important. Indeed, in some reviews the pulsed combustors are categorized according to their controlling valves. Zinn [1986] produced a good review of these methods which is discussed as follows.

There are two principal ways that air and fuel can be introduced into a pulsed system:

i) A mechanical-valve unit, where an array of flapper valves is used in the entrance region of the air and/or fuel lines to prevent back-flow through the inlet.

ii) An aerodynamic-valve unit, where the inlet is so shaped that the pressure drops in the two flow directions through the inlet are very different at the same flow rate.

1.3.1 Mechanical Valves

Mechanical valves provide a physical barrier to the flow of combustion products out of the combustor, through the combustor's inlet section, during the phase of positive combustor pressure. During the negative pressure phase they open to admit a fresh charge of air or/and fuel to the system. Flapper valves [Griffiths and Weber, 1969], reed valves [Francis *et al.*, 1963] and rotating disc valves [Muller, 1971] are examples of mechanical valves which have been used to date. In recent years, flapper valves have gained wider acceptance and they are used especially in commercial applications which utilize mechanical valves. A potentially serious disadvantage of a highly rated pulsed combustor, such as that which would be required for a typical gas turbine application, is that if it is equipped with a flapper valve(s), the risk of valve failure is likely to jeopardize the reliability of the gas turbine or seriously reduce the life hours expectancy between overhauls. Muller [1971] proposed the use of a rotary valve to counter this difficulty and was able to obtain a substantial pressure rise with an experimental rotary valved pulsating combustor. A disadvantage of such an arrangement is the need to provide a constant speed drive for the rotary valve and also the increased complexity of a gas turbine engine due to the presence of the rotary valve and drive mechanism [Kentfield, 1971].

1.3.2 Aerodynamic Valves

Aerodynamic valves use the fluid mechanical properties of specially designed inlet ducts to prevent combustion products leaving the combustor at the inlet section. In practice the aerodynamic valves cannot completely prevent the outflow of combustion products through the valves during the phase of positive pressure inside the combustor. Just after the high pressure period, high temperature gas in the combusting region is present in both the tailpipe and inlet pipe. Because in most cases the chemical reactions of pulsed combustion are completed in the combustion chamber, forcing the gas through the tailpipe is not important, but gas flowing backward into the inlet would affect the next

phase of combustion cycle. Since such outflow is unacceptable in most practical applications and as a result aerodynamic valves have been very little used.

The principle and techniques of valveless pulsed combustors have been discussed by a number of authors including Lockwood [1982], Kentfield [1986], Putnam *et al.* [1986], Ohiwa and Yamaguchi [1989] and Kishimoto [1991] and some experimental work have been carried to investigate the behaviour of such combustors. However, because of the back-flow of combustion gases into supply lines during the combustion period, the required pressure boost for continuing the pulsation could not be obtained. Therefore, in the valveless combustors, utilization of a blower throughout the operation was necessary. However, this is in contrast to one of the possible advantages of a pulsed combustion system, that it be self-aspirating.

1.3.3 Fans and Compressors

On occasions, especially in applications involving high fuel loadings [Sommers, 1952 ; Babkin, 1965] fans and/or compressors have been utilized to supply the combustion air into the pulsed combustor. While the use of fans increases the capital investment and operating costs of the system, they eliminate difficulties encountered with above mentioned valves such as reverse flow. The use of a fan also considerably increases the maximum limit of gas input rate which can been attained in a pulsed combustor.

1.4 Main Advantages of Pulsed Combustors

Compared to conventional burners, the main advantages of a pulsed combustor system are considered to be as follows:

i) high volumetric heat release rate

ii) high heat transfer rate from the pulsating exhaust gases

iii) high overall thermal efficiency

iv) low NO_x emission levels

v) self-sustaining with no electrical power requirement after start-up.

In addition one can consider the simple construction of these devices and the low-cost of the heat exchanger to be other advantages of such units.

These advantages generally are dependent upon the pulsed combustor design and its application. Furthermore, they are linked to the magnitude of the oscillating velocity of gas stream and thus to the pressure amplitude produced in the acoustic wave by the pulsed combustion process. Flow oscillations increase the rate of mass, momentum and heat transfer generated as a result of pulsation in a flow [Dec and Keller, 1989]. The reported improvements in heat transfer vary from several percent to several orders of magnitude. However, in any anticipated application of pulsed combustion there would be some compromise between the use of a high amplitude of oscillation and the underlying problem of high noise levels. In the following sections some of these advantages are described in more detail.

1.4.1 High Volumetric Heat Release Rate

A wide variety of heat release rates have been reported using pulsed combustion systems by a number of workers. The rates of the various transport processes inside pulsed combustors are high which in turn lead to an increase in the rate of the combustion process. Moreover, the flame propagation rates in pulsating combustors are so high that constant volume combustion may be approached in an open-ended tube [Alebon *et al.*, 1963]. This assumes completed combustion within the combustion chamber. If burning should extend into the tailpipe, the heat release would be reduced accordingly. The approximation of the process to constant volume combustion means that for a given heat output the required size of combustor would be relatively small which results in an increase of combustion intensity.

It has been reported that combustion intensity of a self-aspirating pulsed combustor can be enhanced by reducing the inlet side flow resistance, reducing tailpipe pressure drop and reducing the excess air ratio [Saito *et al.*, 1986].

1.4.2 High Heat Transfer Rate

In a pulsed combustor, the flow in the combustion chamber and tailpipe is pulsatory in nature. This can be expected to give high convective heat transfer coefficients due to high gas velocities and their high fluctuations during a portion of the operation. Thus, heat exchanger areas may be correspondingly smaller for a specific heat output so reducing the cost of the heating system.

Heat transfer studies of pulsed combustion have indicated that heat transfer coefficients are two or three times greater than the steady flow values [Hanby, 1979]. The heat transfer coefficient is related to Reynold number (*Re*) increasing as *Re* increases. It is reported that in the laminar flow region, oscillations in gas velocity intensify heat transfer by 100 to 300 % and in the turbulent region by 20-30 % compared to heat transfer with steady flow conditions [Severyanin, 1982]. Studies have also shown that the rate of convective heat transfer decreased or remained constant when the oscillating amplitude was less than or about the same as the mean velocity, while heat transfer rates were increased when the oscillations were larger than the mean velocity [Hanby, 1969].

Hanby [1979] has reported that the heat transfer coefficient increases along the tube towards the open end, which is the velocity antinode in the standing wave produced. The effect of this is to give a roughly constant rate of heat transfer along the pulsed unit as the increasing heat transfer coefficient is balanced by reducing temperature difference between the gases and the tailpipe walls.

Further improvement of heat transfer in pulsed combustors has been achieved by the use of an insert in the final section of the exhaust tube, reducing its flow area by creating an annulus [Blomquist *et al.*, 1982].

Severyanin reported that the high level of the convective heat transfer due to high gas velocity is reached in the pulsed combustion system at lower power costs than in conventional units [Severyanin, 1982].

1.4.3 High Efficiency

Pulsed combustors are regarded as being high efficiency devices. As mentioned above, there are high heat transfer rates in the combustion chamber and tailpipe, causing a low exhaust gas temperature. This means that the majority of the energy in the combustion products is used leading to heating efficiencies of up to 95% [Dec and Keller, 1989]. Furthermore, less heat exchanger surface area is required than in a conventional steady flow heater because of the intensified convective heat transfer coefficient obtained through the pulsating flow of the combustion products. The increased heat transfer coefficient means that higher thermal efficiencies are possible without the large heat transfer surfaces that would be necessary with constant pressure combustion.

In the pulsed combustion process, because of the turbulence created and the re-ignition of the exhaust gases, combustion is possible with very low excess air levels which in turn result in more efficient and at the same time cleaner combustion.

1.4.4 Low NO_x Emission Levels

Pulsed combustors are known to have relatively low NO_x emission; the average reported values for NO_x are between 30-50 ppm as compared with 58-130 ppm for conventional boilers at similar operating conditions [Corliss *et al.*, 1984]. As was mentioned earlier the rates of heat transfer in the pulsating flow are higher than in the non-pulsating flow. This in turn results in reduced time during which gases are at maximum temperature. Mechanisms responsible for a shorter residence time for combustion gases at high combustion temperature and hence low NO_x values can be the rapid effective mixing of the somewhat cooler fresh reactant with the hot combustion products or readily mix of the low temperature residual products with freshly produced hot combustion products [Saito *et al.*, 1989 ; Keller and Hongo 1990 ; Keller *et al.*, 1994a]. The mechanisms governing the formation of NO_x will be discussed later.

1.4.5 Self-sustained Process

The unit is able to suck in the air required without resorting to external energy sources. The air-blower included in the unit provides the starting air flow and air for purging of the unit. The ignition of the mixture of air and gas takes place automatically after the initial lighting up caused by the spark plug. The appliance vents its combustion products through the tailpipe. In addition, Vishwanath and Thrasher [1986] reported a design of a stand-alone pulsed combustion system, where power generated from the exhaust gases was used to charge a rechargeable battery via a generator and so provide its own electrical power required for start-up.

1.5 Main Disadvantages of Pulsed Combustors

Although the presence of oscillations in pulsed combustors can be advantageous, they can result in a variety of undesirable effects. They can cause the chamber to be mechanically damaged or fail prematurely due to the high rates of wall erosion caused by the violent intense combustion which accompanies the oscillations [Ross, 1954].

Compared to a conventional burner, there are few disadvantages for pulsed combustor. The main disadvantages are:

i) high emitted noise level

ii) limited turn-down ratio

iii) vibration problems.

1.5.1 High Emitted Noise Level

High noise levels are probably the greatest disadvantage in a pulsed combustion system although this no longer provides problems of the same magnitude as those experienced by Reynst [Putnam,1971b]. Noise is still considered to be a major problem when large-scale industrial pulsed combustors are used. It has been shown that the sound pressure level of a pulsed burner is approximately 15 to 30 dB greater than that of a conventional

burner of the same firing rate [Chiu *et al.*, 1981]. Kentfield [1986] has shown that the emitted noise levels in a pulsed combustor are associated with pressure pulses, which are difficult to control. The larger the burner's operating pressure the noisier the unit was. At the same time, increase in thermal efficiency is associated with larger operating pressure.

It has been reported that pulsed combustion noise levels have a linear relation with increasing combustion intensity and that the noise spectrum has several peaks at harmonic frequencies of the operating frequency [Saito *et al.*, 1986]. Saito *et al.* [1986] used an impact testing method and a sound intensity method to determine the local sound intensity and the natural frequency of the system. Using this information they applied appropriate noise reduction methods and reduced the noise emitted from their 6 and 17 kW pulsed combustors to below 45 and 49 dBA respectively. However, the reported noise levels are generally high at around 90-120 dB without silencer and 80-90 dB with the aid of silencers [Reay, 1963 ; Lawton *et al.*, 1982 ; Severyanin, 1982].

One other approach recommended for noise reduction in pulsed combustors is to operate two coupled combustors out of phase with each other [Sran and Kentfield, 1982]. Sran and Kentfield employed a design based on two pulsed combustors with the same frequency joined at the inlet and outlet and with the inlet and outlet spaces surrounded by silencing chambers. The combustors worked naturally 180° out of phase with an assumed fundamental frequency of 60-100 Hz. Hence, the silencing chamber excited at double this frequency. It is known that the control of noise emission with higher frequency is more practical [Hargrave *et al.*, 1986].

Ohiwa and Yamaguchi [1989] experimentally examined a valveless pulsed combustor with wide operation range and found that they were able to operate such a system with 3-8 dB lower noise level than a system with a flapper valve.

1.5.2 Limited Turn-down Ratio

Compared to conventional burners it has been shown by a number of researchers that pulsed burners are more limited in terms of turn-down ratio. In general, a turn-down

ratio of about 50% of the full rate can be achieved with pulsed burners. There may be a number of factors contributing to the problem of limited turn-down ratio in pulsed combustors. However, the main cause is thought to be the limited control of the air flow rate. As will be shown in later chapters, an increase of fuel flow rate automatically increases the air flow rate. However, most pulsed combustors are not fully proportioned in terms of gas and air input rates. This means that the rate of increase of air fails to match the increase in gas rate. Thus, with increasing load the air-to-fuel ratio decreases which in turn limits the turn-down ratio. Conversely, when the gas rate decreases, the excess air level rises. Hence, the air-to-fuel ratio increases to a level that the operation of the pulsed unit can not be sustained. Some researchers [Briffa and Staddon, 1982] suggested that due to the lack of control of excess air, in practice pulsed combustors may only be able to operate at a fixed firing rate. However, work has been reported showing an improvement of the turn-down ratio in pulsed combustors. Corliss *et al.* [1984] have reported a turn-down ratio of 5:1 with their laboratory combustor burning methane. Running mainly with a rich mixture of equivalence ratio of 3.0, Ohiwa and Yamaguchi [1989] reported a turn-down ratio of 11:1 using a valveless pulsed combustor.

1.5.3 Vibration

Structural vibrations are caused by gas pulsations in the intake muffler, air decoupling chamber, combustion chamber and tailpipe. The excitation frequencies are harmonic and sub-harmonic of the fundamental pulsing frequency. If any of these harmonics happens to coincide with one of the many resonant frequencies of the structure, a vibration results. The vibration also contribute to the noise production of the unit.

One of the reported drawbacks to the use of pulsed combustion devices is the adverse effect that pressure fluctuations in the gas supply pipe had on gas meters [Hanby, 1979]. Any pulsations transmitted down the pipe tend to allow more gas through the meter than the device registers.

1.6 History of Development of Pulsed Combustors

The technology of pulsed combustion dates back to the 18th century. It is reported that the first observation of combustion-driven oscillations was in 1777 by Higgins [Wood, 1949]. Later, in 1857, Rijke also reported a similar observation. The observed phenomenon derived from thermo-acoustic noise (i.e. a noise of definite pitch). When Higgins enclosed a hydrogen diffusion flame in a tube with both ends open, he found oscillations occurred for certain lengths of fuel supply line. Due to the audible nature of the pressure waves involved in the oscillatory process the term "singing flame" was often applied to the phenomenon [Wood, 1949]. These oscillations generally had very violent almost explosive characteristics.

These early observations were of great importance in helping towards understanding the process. Later, in 1878, such observations were explained by Lord Rayleigh [Rayleigh, 1945] by outlining the effect of adding heat in a periodic manner on the acoustical frequency and amplitude to a gaseous system in which an acoustic oscillation was occurring. Based on these early investigations Rayleigh produced an important hypothesis which explains why a combustion-driven oscillation can be maintained. According to the Rayleigh criterion, for a combustion oscillation to be maintained, the point of maximum pressure oscillation should be close to the point of maximum heat release i.e. the majority of the heat being added at the point of maximum pressure. In later sections Rayleigh's criterion will be explained in more detail.

At the beginning of this century, investigations on the feasibility of pulsed combustors for gas turbine and aircraft propulsion were carried out and several devices were patented including those of French researchers Esnault-Pelterie, French Patent 1906, and Marconnet, French patent 1908, [Reader, 1978]. Figure 1.4 shows the chamber which Esnault-Pelterie patented in 1906. It consists of a cylindrical resonator tube (3) with flapper valves (2) at both ends controlling the flow of air and fuel from the carburettor (1) which was later ignited with the aid of spark plug (5) and a common discharge nozzle (4) at the centre which drove a turbine wheel (6). This device was intended to drive an aircraft propeller. However, due to the fluctuating nature of the discharge the wheel did not turn at a constant velocity and was of no practical use.

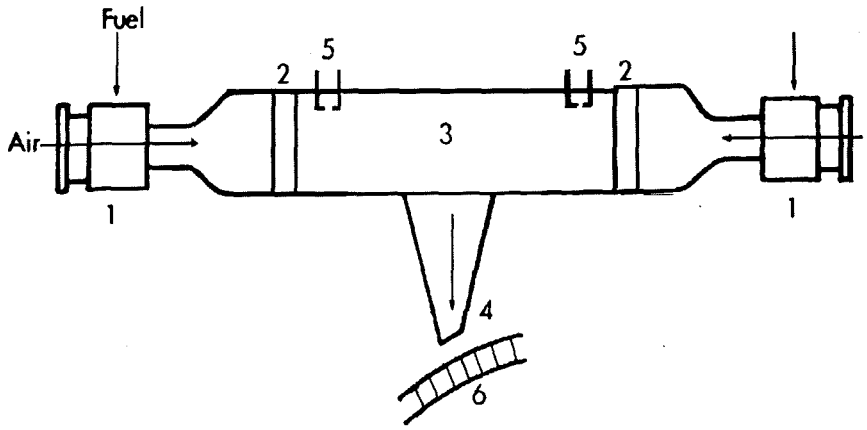

Fig. 1.4 Ensault-Pelterie's push-pull combustion chamber [After Putnam, 1971b].

Esnault-Pelterie's co-worker Marconnet favoured direct use of the jet thrust produced by a single open-ended tube. The Marconnet tube was valveless and had a bulged combustion section. This design was used later as the propulsion unit of the V-I flying bomb. In 1910 a new design was patented by Esnault-Pelterie which enabled significant noise reduction to be achieved. The design as shown in Fig 1.5 consists of two tubes joined at their open ends where there exists a velocity antinode and a pressure node, the tubes operating 180° out of phase with each other. Thus while in one tube combustion was taking place the other was drawing in a fresh charge. This mode of operation not only produced large pressure amplitudes but also operation was relatively quiet.

Almost twenty years later in 1931, Schmidt produced the first operational pulsed-jet [Reader, 1978]. Schmidt's tube was aimed for use as aircraft propulsion units and despite the similarity to Marconnet's research, Schmidt succeeded in obtaining a patent in 1938 [Pugh, 1985]. Schmidt's tube was later modified for use as the engine for the V-1 flying bomb. However, it was not only Schmidt who initiated this new interest but also the Dutch engineer, Reynst.

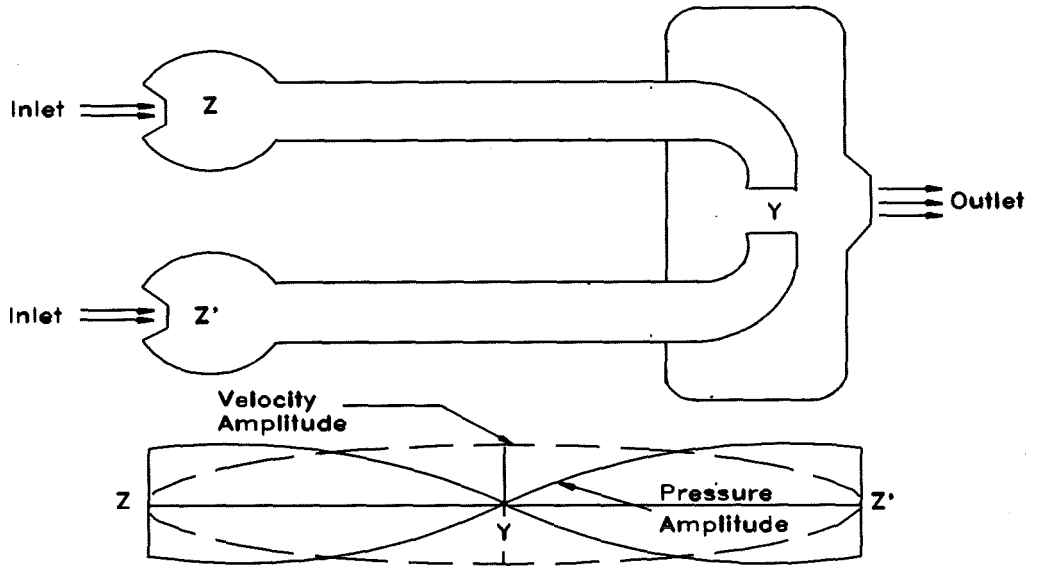

Fig. 1.5 Esnault Pelterie's double tube combustion chamber.

Reynst discovered that a pulsed combustor could work with only one duct which, because of the nature of the process, alternatively acted as an intake and exhaust. The Reynst design is known as a pulsed-pot and was patented in 1938 [Putnam,1971b]. Figure 1.6 shows the basic form of the Reynst pulsed combustor, a valveless resonating combustor which generally looks like a jar. Later, a diffuser placed near the neck of the device separated the incoming mixture which was introduced around the diffuser and the exhaust gases which were passed through the diffuser. The diffuser served to use the outward flow of exhaust gases to create a negative pressure to draw in a fresh charge. Reynst hot pot provided a high heat transfer rate but at the same time it was extremely noisy and could be heard from a very long distance [Blomquist *et al.*, 1982]. Reynst suggested that pulsed combustion devices represent a first step in the evolution of an ideal device which would produce mechanical energy from fuel without the intermediate formation of heat. Reynst suggested a number of designs for water heaters with interesting features such as an interior annular duct to produce a desired type of circulation [Putnam, 1971b].

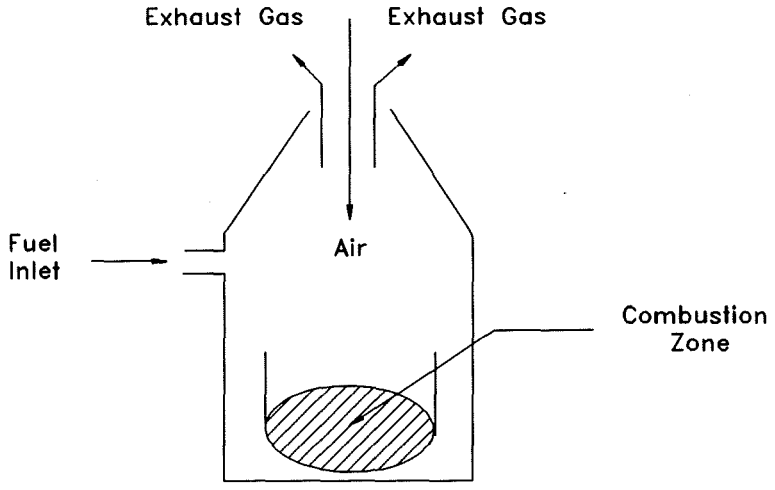

Fig. 1.6 A schematic of the operation of a Reynst-type pulsed combustor.

In 1941, the design of the Schmidt resonator tube was perfected and used to power the famous V-1 flying bomb used during the Second World War. The Argus-Schmidt device had a slightly tapered cylindrical tube open at one end, with flapper valves and fuel injectors at the closed end. During this time French and Americans workers had been following the German experiments and began a new investigation on the pulsed combustion process. The US Navy built and developed a "valveless resojet " in the spring of 1944. This device was similar in construction to the basic Schmidt tube with an aerodynamic valve rather than a mechanical valve. The American investigations on this method of propulsion lasted until 1953 [Reader, 1978]. By that time a German, Huber, had developed and manufactured a 60 kW commercial pulsed combustion air heater which was used as a heating device in buses. A complete description of the operation of Huber's air-heater was reported by Putnam [1971b].

During the 1960s, after a lack of attention for almost a decade, interest in pulsed combustion process was renewed. It was during this period that for the first time systematic investigations on the characteristics of pulsed combustors were carried out.

Workers such as Sommers [1952], Kitchen [1962], Francis *et al.* [1963], Reay [1963], Lockwood [1964], Griffiths & Weber [1969], and Severyanin [1969] carried out important experimental studies on the operating characteristics and development of pulsed combustors. The work of these researchers is examined throughout this study.

In 1969 Hanby showed that experimental data from a Quarter-wave combustor could be matched by using acoustic theory to predict the velocity pulsations and a quasi-steady state assumption to predict the corresponding heat-transfer coefficients [Hanby, 1969]. Quasi-steady state, as applied to oscillating flows, means that at any point in the cycle the flow is assumed to behave as if it were steady at the actual instantaneous velocity. This assumption is valid only for flows with low frequencies or small oscillation amplitudes; mainly it requires that the flow comes to a fully developed equilibrium condition within a time much less than the cycle time. Based on the same work, Hanby reported comparison of the measured operating frequency and pressure amplitude with the predicted theoretical values using a gas-fired organ-pipe type pulsating combustor. He used an aerodynamically-valved combustor and measured pressure fluctuations along the tube at ten sampling ports using a high-temperature transducer. He showed the variation of resonant frequency with root mean square temperature as being a linear relationship. Hanby found a good agreement between theoretical and experimental distribution of pressure amplitude in the combustor [Hanby, 1971]. He did not, however, report any calculation of the magnitude of the amplitudes. His results indicated that high heat transfer and combustion rates can be obtained from such a pulsed combustor, together with radiation of sound at the open end of the combustor.

The renewed interest in pulsed combustion was confirmed by the holding of the first international symposium on the phenomenon of pulsed combustion in UK in 1971. At this gathering it was acknowledged that the potential of pulsed combustion technology had not been fully discerned, and a more systematic analysis and modelling of such devices was required [Reader, 1978]. It was also realised that because of the complexity of the combustion process, with its uncertainties of mixing, kinetics of reaction and non-equilibrium effects, a detailed theoretical analysis was a formidable understanding.

In the late 1970s and during the 1980s the need for high efficiency heating devices as a result of rising prices of fossil fuels, insecurity of supplies and pressure of environmental regulation ensured an increased interest in pulsed combustion systems. In the US two symposia on pulsed combustion technology were held during this period. The first symposium on pulsed combustion technology for heating applications which was held in US, Illinois, Argonne National Laboratory in November 1979 and the second symposium of pulsed combustion applications sponsored by the American Gas Research Institute was held in Atlanta, Georgia in 1982. In both symposia a number of investigations on pulsed combustion heating devices and their performance were reported acknowledging once again the importance and necessity of an analytical approach for better understanding and cheaper development of pulsed combustion devices. The reported studies in these conferences included some analytical predictions on heat transfer in pulsed combustion units.

Ahrens [1979] reported development of a procedure for predicting the influence of design parameters (such as: input rate, combustion chamber volume and tailpipe length) on the thermal performance of a pulsed combustor. He used a simplified analytical model, considering the tailpipe and combustion chamber as being the important components influencing the heat transfer. He applied his model, in an approximation, to the conditions of Hanby's Quarter-wave tube experiments with some modifications such as fuel heating value and input rate. Ahrens's results need to be compared with more experimental data to assess the accuracy and limitation of his model.

Prior to Ahrens's work, a number of workers including Clark and Craigen [1976] had developed the method of characteristics and applied to one-dimensional non-steady flow problems. The method of characteristics utilizes the theory of non-uniform wave propagation according to which the gas flow is determined by the propagation of the pressure wave [Putnam, 1979]. But similar to Ahrens's work none of these workers compared their results with sufficient experimental data to produce an accurate prediction of the performance of pulsed units. The experimental measurements are essential to the development of analytical modelling, since it is only by comparison of predicted and measured results that the quality of an analytical modelling or a simulation

program can be assessed. To apply such methods as described above, the combustion data need to be simplified greatly, such as taking the rate of heat release constant or the flame speed being constant and so on. Moreover, it is claimed that mathematical modelling techniques such as method of characteristics are tedious when done with numerical-graphical techniques and they do not yield closed-form solutions [Putnam, 1979].

Since mid 1980 until recently, the older ideas have been investigated and analytical modelling of pulsating combustion development has been facilitated by advanced instrumentation techniques and computers. A number of theoretical models have been developed. Amongst leading researchers in the field one could name Dhar *et al.* [1982], Ponizy and Wojcickis [1984], Keller [1985], Barr *et al.* [1987], Kishimoto [1991], Zimmer [1991], Dandy and Barr [1991], Fureby and Lundgren [1993] Morel [1993] and AU-Yeung *et al.* [1999] who have developed or used available theoretical models for the simulation of pulsed combustors which are either zero or one-dimensional. During the 1991 International Symposium of Pulsed Combustion an extensive amount of pulsed combustion systems modelling was reported by various leading researchers. Most of these approaches were based upon an assumption of Newtonian mechanics and application of the conservation principle independently to mass, momentum and energy. Barr *et al.* [1987] developed a numerical model which utilized experimental data for heat release and reactant injection to drive the wave motion in a pulsed combustion system. Their methods involved solving the unsteady, one-dimensional equations of continuity, momentum and energy with geometry taken as the variable, along with the ideal (perfect) gas equation. However, some of these models do not clearly take into account the mixing and chemical reaction which in most cases are simultaneous. In most cases they take the assumption that the turbulence level is so high that mixing is essentially instantaneous and so fast that it can be neglected. Kishimoto [1991], characterized a one-dimensional model on a aerodynamic pulsed combustor and provided a comprehensive simulation on influence of the back-flow from the previous cycle on the following injection, mixing of the fresh mixture.

This mathematical modelling without a doubt provided intuition into the pulsed

combustion operation system and a quantitative understanding of primary combustion phenomena such as gas phase chemical reaction, heat transfer from combustion products and above all mixing of reactants and combustion products. But, because of the complexity of processes that occur within a pulsed combustor, with its uncertainties of mixing, kinetics of reaction, and non-equilibrium effects, pure theoretical analysis is difficult if not impossible. Thus, these models have resorted to a certain amount of empirically-determined information, which is system-dependent. Therefore, a truly predictive capability does not yet exist. As a result the design and development of pulsed combustors has proceeded largely by trial and error.

Griffiths and Weber [1969], Windmill [1984], Vishwanath [1985] and Hollowell [1987] have produced good discussions on design and development of experimental and conical pulsed combustion systems (e.g. water heater). Their methodology was based upon experience gained from testing many different pulsed combustor configurations over several years. Vishwanath produced design recommendations for pulsed combustor burners within the input range of 3 to 44 kW. He produced guidelines for sizing different components of a pulsed burner and the expected frequency and pressure using these guidelines. However, as is revealed in later chapters, during the course of present study it was concluded that for the above range of input heat more compact and smaller combustion chamber than those recommended by Vishwanath can be used.

During the last 10 years, fundamental studies have been focused on a more comprehensive understanding of the pulsed combustion process employing advanced combustion diagnostics, including internal flow measurements by Laser Doppler Velocimetry [e.g. Keller *et al.*, 1994b ; Lindholm, 1996], flow visualization in the combustion chamber by Schlieren photography and shadowgraphy [e.g. Keller and Hongo 1990; Keller *et al.*, 1994b; Tang *et al.*, 1995], and heat release rate measurements by an OH chemiluminescence detection method [e.g. Keller and Westbrook, 1986 ; Keller *et al.*, 1990 ; Keller and Hongo, 1990 ; Jones and Leng, 1994]. These techniques provided valuable information on the operation of a pulsed combustor, showing detailed mixing, combustion and ignition processes occurring in a pulsed combustor.

1.7 Applications of Pulsed Combustion

A wide variety of application for pulsed combustion have been suggested. Some of these applications have been investigated experimentally for commercialisation with varying degrees of success. Table 1.1 shows several applications of pulsed combustors that have been proposed during this century.

In most of the research carried out on pulsed combustion systems, gaseous fuels have been found to be the most favourable from testing appliances. However, there are number of reported studies which have been carried out on pulsed combustion using liquid and solid fuels including the use of an oil-fired pulsating combustor in a power station in the former USSR [Babkin, 1965], pulverised coal [Hanby and Brown, 1968] and wood [Moseley and Porter, 1969].

Lockwood [1964] used two augmenters on the Escopette pulsed jet in developing a vertical lift device; this would be particularly valuable where helicopters and related equipment could throw up dirt which might then move into the engine interior. This direction of research eventually led to large drying units composed of multiples of the Escopette-augmenter sets.

Carvalho *et al.* [1984] developed a Rijki-type pulsed combustor burning unpulverised coal consisting of a vertical tube open at both ends with a coal-burning bed at the centre of its lower half. This was a successful design after a number of fruitless studies on burning pulverised coal using a Quarter-wave combustor. This was mainly because the combustion time was often longer than residence time of the coal particles in the combustor. Some of these problems were resolved by preheating the coal and the combustion air.

The majority of pulsed combustion units have been used as heating devices. Development of pulsed combustion systems for heating has been mainly directed to residential sizes of boilers and furnaces. Most of the reported developed pulsating combustors were based upon the principle of a Quarter-wave or Helmholtz resonator which were mainly successful in operation using gaseous or liquid fuel.

Kitchen [1982] reported development of space heating equipment namely the Canadian Pulsomatic boiler which then was used in America as the first commercial

PURPOSE	APPLICATIONS
INDIRECT HEATING OF AIR	Space heating in vehicles Space heating in homes Space heating in industry
DIRECT HEATING OF AIR	Drying in food processing Drying of blood Drying of waste material Wood drying Sand drying Cement block curing Soil sterilization Orchard heating Military smoke and fog generators Insecticide aerosol generators Portable construction heaters Engine and machinery heating glass furnaces and ovens Fume incinerators and pollutant afterburners
HEATING OF LIQUIDS	Hydraulic space heating Steam raising(for heating) with gas, liquid Portable water heating Viscosity control of liquids Chemical processing Petroleum processing Deep-fat fryers
PRESSURE GAIN AND FLUID PUMPING	Pumping fog oil and insecticide Gas-turbine combustors Fan/blower replacement Flue-gas recirculation
THRUST GENERATION	Propulsion Vertical lift devices Torque production Surface cleaning and descaling
OTHER USES	Griddles Snow and ice melting Refuse incineration Gasification MHD power generation Heat pumps Fluidization Coagulation of materials Pilot burner and ignitors for low grade fuels Sawdust incinerator-boiler

Table 1.1 Applications of pulsed combustion.

space heating equipment for the residential applications. Later, the Hydro-pulse boiler [Whitlock *et al.*, 1982] and Lennox furnace were also designed and used for residential applications [Adams, 1982]. The Hydro-pulse boiler manufactured by Hydrotherm Inc. was constructed as a vertical down-fire tube boiler with a more or less similar principle of operation to other pulsed combustion systems. An interesting feature in this design was that an exhaust chamber was used to decouple the pulsation of the combustion cycle from the exhaust and collect the condensed water from the flue gases. Lennox Industries Inc. furnaces were shown to operate properly despite the high sound level and lived up to the predicted efficiency of 90 % plus. Later, the Lennox furnace design was revised to reduce the sound levels and was produced for general distribution in the US [Adams, 1982].

Lucas-Rotax Ltd has developed a pulsed combustor as a domestic hot water boiler for central heating using natural gas or propane as fuel. The boiler was equipped with the small gas valve on the axis of the air valve. In order to protect these valves from hot gas, a flame trap was placed between them and the combustion chamber. The device was designed as a immersion heater with the hot walls of combustion chamber, tailpipe and silencer projecting into the water flowing around them. It was reported that the unit was very quiet in operation and a thermal efficiency of 90 % was claimed [Kitchen, 1982].

In a Russian survey of pulsed investigators world-wide [Severyanin and Dereschuk, 1977] it was agreed that there was a promising opportunity for use of pulsed combustion technology in industrial applications particularly boilers for steam raising and water heating. Severyanin and Dereschuk [1977] described 18 separate devices which used pulsed combustion of gaseous, liquid or solid fuels for applications including drying, steam generation, and air heating.

Putnam, [1971b and 1979] has produced a good review on some of the pulsed combustion applications including propulsion, steam raising, water heating and air heaters.

Adams [1982] gave details of a 10 unit field trial on a condensing air heater. Each heater was rated at 19 kW with around 94 % thermal efficiency.

A review of the literature including the latest reported works shows that the heating applications of pulsed combustors have been successfully commercialized. In most of these applications the energy released from combustion was transferred to a medium such as air, water or industrial liquid through the combustion chamber and tailpipe walls [Zinn, 1992].

Thrasher and Strassemeyer [1987] reported development of a space heater with heat input rate of 5.8 kW and efficiency of over 90 %. The unit could operate with natural gas and propane.

Zinn [1992] has reviewed a new design using pulsed combustion technology to improve the performance of energy intensive and incineration processes. This design utilizes a frequency tunable pulsed combustor to excite large amplitude pulsations in a vessel downstream of the pulsed combustor where the process takes place. This approach would increase the residence time of the process material in the pulsating environment. The combustor operated at the natural acoustic mode of the process volume. This produced resonant driving that maximized the amplitude excited for a given power input.

In recent years Fulton Boiler Works UK Ltd, has successfully developed two 80 and 260 kW pulsed combustors as commercial water heating devices. The design included separate flapper valves for air and gas inlet which then they mixed and ignited inside the combustion chamber. The efficiency of these boilers was up to 96 % with NO_x levels of 35 ppm.

1.8 Fundamental Principles and Background

For the experimental purposes and better understanding of the fundamental outcomes of the present study this section deals with some of the important relevant fundamental background including factors which govern a pulsed combustor's operation, the principles of formation of concerned pollutant gases, their control and methods of minimisation. For instance, despite the fact that general underlying principle of

operation of pulsed combustors have been determined as described in section 1.2 of this chapter, there are other details which require additional study including the mechanism of ignition, combustion and the phase relationship between energy release and pressure oscillations.

1.8.1 Rayleigh Criterion

Lord Rayleigh described his criterion as follow: "If heat is periodically communicated to, and withdrawn from, a mass of air vibrating for instance in a cylinder bounded by a piston, the effect produced will depend upon the phase of the vibration at which the transfer of heat takes place. If heat is given to the air at the moment of high pressure or taken from it at the moment of greatest rarefaction, the pitch is not affected. If the air be at its normal density at the moment when the transfer of heat takes place, the vibration is neither encouraged nor discouraged, but the pitch is altered. Thus, the pitch is raised if heat be communicated to the air a quarter period before the phase of high pressure; and the pitch is lowered if the heat be communicated a quarter period after the phase of high pressure. In general both kinds of effects are produced by a periodic transfer of heat. The pitch is altered, and the vibrations are either encouraged or discouraged" [Putnam, 1971a]. Based on Rayleigh's criterion, to attain pulsed combustion, the driving by the combustion process after ignition must be larger than the acoustic losses within the combustor and the driving by the combustion process is equal to the acoustic losses after the amplitude of pulsation has stabilized at a constant value. These conditions are qualitatively described by the following equation [Zinn 1992]:

$$\int_V \int_\tau P(x,t)\ Q(x,t)\,dt\,dV \geq \int_V \int_\tau \sum_i L_i(x,t)\,dt\,dV \qquad (1.5)$$

where P is the oscillating pressure, Q is the heat addition being functions of x (the location) and t (the time), τ is the oscillation period, V is the combustor volume and L_i is the acoustic loss from the system (the i-th damping process). The left hand side of

equation (1.5) represents the addition of energy to the oscillation by added heat (i.e. driving process) in a cycle and the right hand side characterises the damping (i.e. the energy dissipated) during a cycle within the pulsed combustor which may include more than one loss mechanism.

For the combustion process to drive the acoustic oscillations within the combustor the magnitude of phase difference between Q and P must be less than 90° thus, the left hand integral is positive (i.e. > 0). If the magnitude of phase difference between Q and P exceeds 90°, the left hand integral is negative and the oscillatory combustion process heat addition damps the oscillations, and combustion ceases to operate [Zinn 1992].

A graphical presentation of Rayleigh criterion is shown in Fig. 1.7 [Keller *et al.*, 1989]. The operating frequency of the pulsed combustor is not affected when the instantaneous energy release Q (causing an instantaneous pressure rise) is at the maximum (i.e. case 1, phase angle $3\pi/2$) or minimum pressure points (case 2, phase angle = $\pi/2$) where the pressure amplitude is increased and decreased respectively. The operating frequency has increased when the energy release occurs at π with no effect on pressure amplitude (i.e. case 3). Finally, when the energy release occurs at 2π the operating frequency decreases also with no effect on the pressure wave amplitude (case 4) [Keller *et al.*, 1989]. If the energy release is at some other location than the mentioned above points (representing extreme conditions) then both the operating frequency and the amplitude of pressure wave would be affected.

From the above it is clear that the operating frequency of the pulsed combustor is affected by the phase difference between the energy release and pressure oscillations. The operating frequency is greater than its natural resonant frequency when 0 < phase angle < 180°. The operating frequency of a pulsed combustor is lower than its natural resonant frequency when 180° < phase angle < 360°. When phase angle is equal to zero then there is no effect on the operating frequency, corresponding to the natural resonant frequency of the combustor which is determined by the geometry of the pulsed combustor, temperature distribution and flow characteristics. However, there will be a maximum effect on the pressure amplitude when the phase angle is zero [Zinn, 1992].

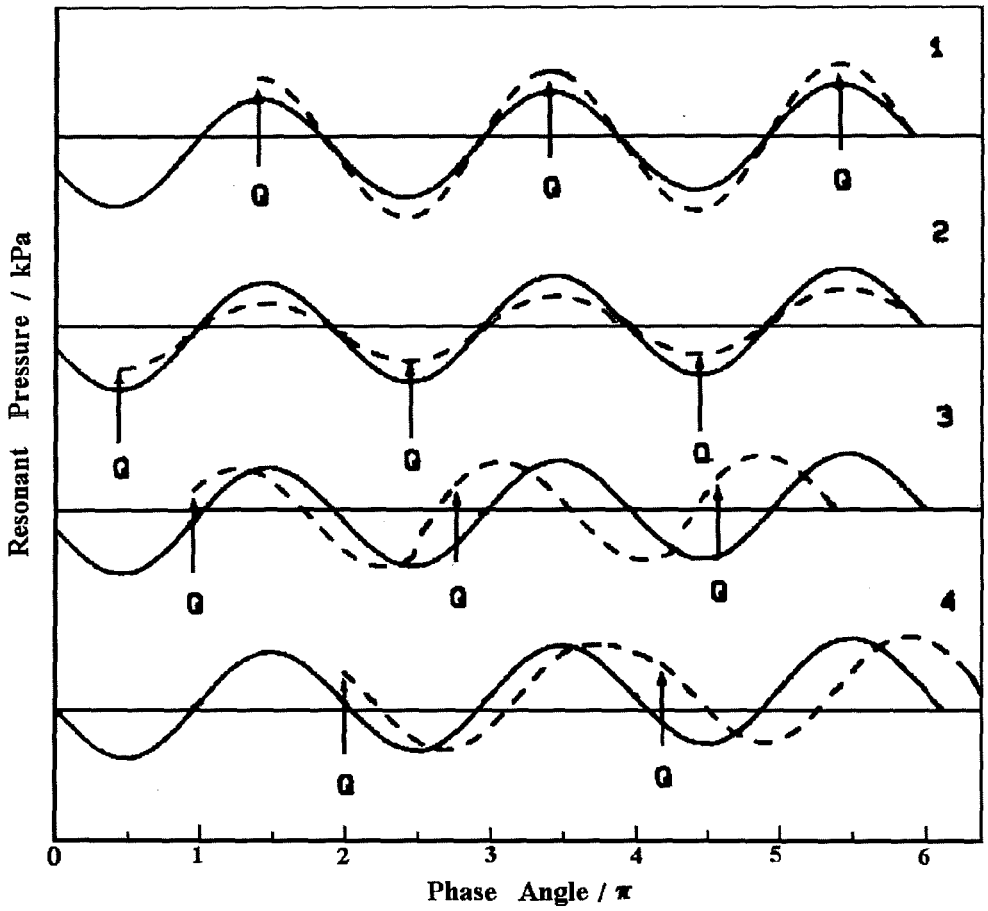

Fig. 1.7 Schematic representation of Rayleigh's Criterion. Symbol Q represents an instantaneous energy release which in turn causes an instantaneous pressure rise. The continuous curve is the undisturbed combustion chamber pressure and the broken line is the pressure after modification by the point source of energy release [After Keller et al., 1989].

1.8.2 Ignition Delay Time

From what was said in the above, it seems that the attainment of pulsed combustion is dependent upon the phase relation between the energy release and acoustic pressure. It is important that the pressure and heat release fluctuations are in phase. To satisfy such a requirement in a Helmholtz-type pulsed combustor there should be a time delay

between ignition of the fresh charge entering the combustor (when the pressure is low) and the process of heat release [Willis *et al.*, 1991]. This means that the ignition of the majority of the fresh charge must be delayed in order to assure the Rayleigh criterion is satisfied. It is also suggested that during injection, the reactants should not ignite. The reactants and hot products mix and at the end of injection the reactants undergo thermal and/or radical ignition [Barr and Keller, 1991].

To simplify such analysis Keller *et al.* [1989] assumed three processes each with its own characteristic time which the total ignition delay time in a Helmholtz-type pulsed combustor depends upon. These characteristic times are as follow:

1) a species mixing time, that is the characteristic time required to mix the fuel with the oxidizer ($\tau_{species}$);

2) the characteristic time required to mix the reactant with hot products, raising the temperature of reactants to the ignition temperature (τ_{mixing});

3) the characteristic time for the chemical reactions to occur ($\tau_{kinetic}$).

They suggested that the total ignition delay time, τ_{total}, for the heat release in a cycle is a monotonically increasing function of these characteristic times [Keller *et al.*, 1989]:

$$\tau_{total} = f(\tau_{species}, \tau_{mixing}, \tau_{kinetic}) \tag{1.6}$$

There is also the fourth characteristic time known as $\tau_{resonant}$ which generally depends upon the configuration or geometry of the unit. In the case of the use of a premixed fuel gas and air charge, similar to the present design of the pulsed combustors in this study, the species mixing time, $\tau_{species}$ is not relevant, hence total ignition delay time is a function of the other two characteristic times, that is:

$$\tau_{total} = f(\tau_{mixing}, \tau_{kinetic}) \tag{1.7}$$

The total ignition delay time prior to energy release is an increasing function of each one of these characteristic times. However, to satisfy the Rayleigh criterion, this total time must be some fraction of the resonant time of the system. The total ignition delay time influences the phase difference between release of energy and the resonant pressure wave and at the same time as described in previous section, the phase difference influences both the amplitude of the pulsations and the operating frequency [Jones and Leng, 1994].

Using a Helmholtz-type pulsed unit Keller *et al.* [1989] tested the above assumption by measuring the response of the system to changes of these characteristic times. Later they measured and theoretically estimated the total ignition delay time in the same pulsed combustor [Keller *et al.*, 1990]. They measured the fluid dynamic mixing time by keeping the kinetic ignition delay time constant. Then they measured the influence of the homogeneous chemical kinetic ignition delay time by maintaining the fluid dynamic mixing time constant. Their predicted results resembled the measured results, an estimated 5 to 12 % and 35 to 45 % of total cycle time being accounted for by homogeneous chemical kinetic delay time and the mixing time respectively. They reported that the measured total delay time was almost constant at around 50 % of total cycle time. This means that more than 90 % of the total ignition delay time is contributed by fluid dynamic mixing time and the rest is balanced by the characteristic chemical kinetic delay time. Therefore, it is always assumed that $\tau_{kinetic} < \tau_{mixing} < \tau_{resonant}$. Although their predicted values for the kinetic delay time were negligible compared with the fluid dynamic mixing time, from their experimental work it is clear that the $\tau_{kinetic}$ has the major influence on the phase difference between energy release and pressure pulsations and hence, combustor operation [Keller *et al.*, 1989].

Without a doubt the described concept would provide a valuable intuition regarding analysis of pulsed combustion system. But as these researchers also have confirmed, the chemical and physical processes leading to ignition are highly coupled, temporally and spatially-varying processes that involve turbulent mixing, injection rates, chemical kinetics and so on, which calls for more understanding of the processes involved.

Jones and Leng [1994] have shown that this type of analysis can be applicable when

using a non-premixed combustor burning natural gas with added hydrogen or propane. In the present study the above theory has been used as a guide to a parametric study of the operating behaviour of the present design of pulsed combustor.

1.8.3 Combustible Gases

The word gas is derived from Greek word meaning 'chaos' or disorder. This is an appropriate name, since the particles are indeed in a state of chaos, colliding and rebounding with a great amount of energy [Hanby, 1993].

Combustible gases (i.e. fuel gases) burn when they are ignited and allowed to combine with oxygen, usually supplied as air. This burning or combustion is in fact a chemical reaction taking place, a reaction which produces heat and changes the gas and air into other gases. During combustion a flame is produced which is a burning mixture of a combustible gas and air. Heat release from the reacting mass and heat transfer to the surroundings are both important in determining the course of a combustion process. In next section the combustible families of gases according to BS EN 437, [1993] are discussed.

1.8.3.1 Families of Gases

To ensure that appliances operate correctly the gas quality must be maintained within close limits. In practice it is kept to a quality range indicated by Wobbe numbers. The Wobbe number gives an indication of the heat input from a burner when using a particular gas. The amount of heat which a burner will provide depends upon the gas composition and the appliance. The latter is fixed by the design adjustment of the appliance and the only alterations in heat input would be brought about by changes in the gas composition, i.e. changes in the characteristics of the gas (i.e. calorific value and the relative density). The Wobbe number links these two characteristics and is obtained by dividing the calorific value by the square root of the relative density, thus:

$$Wobbe\,Number = \frac{Calorific\,Value}{\sqrt{Relative\,Density}} \tag{1.8}$$

it has unit of MJ m^{-3}. Indeed, if there is a significant difference between the Wobbe numbers such as in the case of natural gas (i.e. 50 MJ m^{-3}) compared with town gas (i.e. 27 MJ m^{-3}) then the conversion of appliances becomes necessary to change from one to the other. This was the case in 1966 when the mains distributed fuel in the UK changed from town gas to natural gas.

Kunsagi [1971] reported in the United State that his pulsed unit could not operate satisfactorily although a similar design was run successfully in Sheffield, England. Later, they found out that the unit was operated in the UK using town gas with main combustible components CO and of H_2 with relatively low heating value and air-to-fuel ratio for combustion, while they were operating their pulsed unit in the USA with natural gas containing 96 % methane, with volumetric air-to-fuel ratio of approximately 10:1. This indicates that the air requirement for the same heat release from the combustion of town gas is substantially less than that from the combustion of natural gas and as a result same burner cannot operate with both fuels.

There are three 'families' of gases which have been agreed internationally; each family may be divided into groups, themselves being divided into ranges, as a function of the Wobbe number. The first family covers manufacturing gases having Wobbe number between 22.4 to 29.8 MJ m^{-3}, family two covers natural gases with Wobbe number ranging from 39.1 to 54.7 MJ m^{-3} and finally the third family covers liquid petroleum gases with minimum Wobbe number of 72.9 and maximum Wobbe number of 87.3 MJ m^{-3} [BS EN 437, 1993].

Manufactured gases are generally made from coal, oil feed-stockers or naphtha and also include liquid petroleum gases and air mixtures. United Kingdom natural gas comes from a well-head in the North sea and from Morecambe Bay and also imported from other countries [Jasper *et al.*, 1990]. Finally, liquid petroleum gases include compressed propane (C_3H_8) or the less volatile butane (C_4H_{10}) and mixtures like calor gas.

In this study the term 'test gas' is used, referring to gases intended for the verification of the operational characteristics of appliances using combustible gases. These gases by definition consist of reference gases and limit gases [BS EN 437, 1993].

Reference gases are test gases on which appliances operate under nominal conditions when they are supplied at the corresponding normal pressure. Limit gases are the test gases representative of the extreme variations in the characteristics of the gases which could be supplied via the main [BS EN 437, 1993].

Table 1.2, shows the composition and principle characteristics of the different test gases corresponding to the gases of second families. These values which are measured and expressed at 15°C, are derived from ISO/DIS 6976 1992. Also, the net and gross calorific values of these gases together with the net and gross Wobbe numbers of the gases of the second family at 15 °C and 1.013 bar are given in table 1.2. The static pressure for the group "H" of the second family, which should be applied at the gas inlet connection to the appliances whilst in operation are between the limits of 17 mbar and 25 mbar. For the present work the test gases NGB, NGD and NGC were used. The composition of these test gases were close to test gases of the second family group H [see Appendix II]. The NGB, NGC and NGD test gases simulate conditions for incomplete combustion, light back and flame lift respectively. In the following sections these conditions better known as flame stability, are briefly examined.

Flame Lift

Flame lift of a flame from a burner is a process in which the base of the flame lifts from the burner exit port. Flame lift or blow-off generally occurs when the burning velocity is low and/or flow rate is high, affecting both laminar and turbulent flames. The process may reach a metastable state in which the base of the flame sits up to several centimetres above the burner. Such a state often seems quite stable and a small increase in flow does not affect it. However, a moderate flow increase or merely fluctuations in flow are usually sufficient to drive the flame away from the burner completely and hence to extinguish it which is known as blow-off. This is because the gas diffuse into surrounding air and mixture becomes too weak to burn. Flame blow-off is a particularly

vexing problem for the combustion designers since it places a limit on burner output and for large flames, it requires relatively complex flame detection and automatic fuel shut-off systems for safety reasons.

Gas Group	Test Gas	Designate.	Composition / volume %	W_n	CV_n	W_g	CV_g	σ
				/ MJ m^{-3}				
H	Ref. Gas	G 20	CH_4 = 100	45.67	34.02	50.72	37.78	0.555
	Incomplete comb. Limit gas	G21	CH_4 = 87 C_3H_8 = 13	49.60	41.01	54.76	45.28	0.684
	Light back limit gas	G222	CH_4 = 77 H_2 = 23	42.87	28.53	47.87	31.86	0.443
	Flame lift limit gas	G23	CH_4 = 92.5 N_2 = 7.5	41.11	31.46	45.66	34.95	0.586
L	Ref. & light back limit gas	G25	CH_4 = 86 N_2 = 14	37.38	29.25	41.52	32.49	0.612
	Incomplete Comb. & sooting limit gas	G26	CH_4 = 80 C_3H_8 = 7 N_2 = 13	40.52	33.36	44.83	36.91	0.678
	Flame lift limit gas	G27	CH_4 = 82 N_2 = 18	35.17	27.89	39.06	30.98	0.629
E	Ref. Gas	G20	CH_4 = 100	45.67	34.02	50.72	37.78	0.555
	Incomplete Comb. & sooting limit gas	G21	CH_4 = 87 C_3H_8 = 13	49.60	41.01	54.76	45.28	0.684
	Light back limit gas	G222	CH_4 = 77 H_2 = 23	42.87	28.53	47.87	31.86	0.443
	Flame lift limit gas	G231	CH_4 = 85 N_2 = 15	36.82	28.91	40.90	32.11	0.617

W_n = net Wobbe number, W_g = gross Wobbe number; CV_n = net calorific value, CV_g = gross calorific value; σ = Relative density of the gas

Table 1.2 ***Characteristics of the test gases, gas dry at 15°C and 1013.25 mbar [After BS EN 437, 1993].***

Light Back

Light back in which the flame propagates back through the burner port or upstream into the burner tube, usually causes explosion in the unburnt fuel-air mixture. This is a problem by definition confined to premixed flames. Light back generally occurs when the flow rate is low and the burning velocity is high (e.g. hydrogen). Neglect of the fundamentals of the phenomenon has led to unsatisfactory empirical correlations being the only guides available to the applied scientist solving practical problems [Jones, 1989].

According to the British Standards requirement for heating appliances, neither flame lift (when burning G23) or light back (when burning G222) is permitted and the burner should operate in a stable condition with reference gas (G20) as well as these limit gases [BS 5258, 1986].

Incomplete Combustion

In the reaction zone of the flame, the constituent gases form intermediates before reacting to form the final products of combustion, carbon dioxide (CO_2) and water vapour (H_2O). These intermediates include carbon, carbon monoxide, alcohols and aldehydes.

If combustion is interrupted before completion then incomplete combustion products can be released from the flame. Of the products of incomplete combustion, carbon monoxide is the most dangerous. It is a toxic gas and a concentration of only 0.4 % in the air can be fatal within a few minutes.

Due to the perils of poor combustion , minimum standards of combustion have been laid down by the British Standards Institution (BSI) so that all approved appliances must conform to the specification of BS 5258. Standards in United Kingdom, are based on the ratio carbon monoxide to carbon dioxide (CO/CO_2) produced; this must not exceed 0.02 under specified conditions. However, new European Union standards are based upon CO emissions only. According to these new regulations, the CO emissions must not exceed 1000 ppm.

1.8.3.2 Fuel Flexibility of Pulsed Combustors

There are few documented data on the influence of fuel gas composition on the performance of pulsed combustion systems. Griffiths *et al.* [1982] established the effect of fuel gas composition on furnace and boiler performance in terms of NO_x production for a large number of residential units for various fuel compositions in each case. They reported that for three compositions, that is adjustment (CH_4 = 83.4 %, C_3H_8 = 8.6 %, N_2 = 8.0 %), yellow-tip limit (CH_4 = 91.2 %, C_3H_8 = 8.8 %) and lifting limit (CH_4 = 81.8 %, C_3H_8 = 5.5 %, N_2 = 12.7) gases NO_x data were similar. Two of the systems tested were pulsed combustors. The combustors operated satisfactory burning these gases and showed significantly lower NO_x than continuous combustion units.

Corliss *et al.* [1984] also studied the characteristics of a propane-fired aerovalved pulsed combustor and found that there was not a significant difference in the overall pattern of NO_x emission as a function of air-to-fuel ratio compared with other studies. The NO_x concentrations showed a continuous decrease with increasing excess air. Moreover, they found that there was no effect of operating frequency on NO_x emission by dividing the data into two groups above and below 110 Hz.

Windmill [1984] investigated the fuel flexibility of a pulsed unit using the test gases NGB, NGC and NGD. He found that it was possible to operate a pulsed unit with these test gases and he produced some data on CO/CO_2 ratio. But these studies were relatively uninformative concerning the behaviour of pulsed units burning these test gases.

Keller and Westbrook [1986] reported an investigation into the response of a valved pulsed combustor to changes in fuel chemistry. They operated on a Helmholtz-type combustor using methane and methane with added ethane. They showed that changes in fuel composition changed the chemical kinetic mechanism which in turn affected the chemical ignition delay timing, resulting in modification of the phase relationship between heat release rate and the resonant pressure wave arising from the combustion process. Thus, when burning pure methane the lean stability limit was lower than for the mixed methane-ethane fuel.

Jones and Leng [1994] reported effect of burning various proportion of hydrogen

or propane in methane on performance of a non-premixed pulsed combustor. By measuring pressure and heat release rate they determined the phase difference between two oscillations. They showed that addition of hydrogen decreases the magnitude of pulsing pressure and rises the operating frequency and phase angle between heat addition and pressure oscillations. The also reported deterioration of performance of their combustor when burning propane plus methane, showing a rise in operating frequency and phase difference. They attributed these changes to variation in total ignition delay time.

1.8.4 Gaseous Emissions From Combustion

Emissions have come to be seen in a wide context, with scientific credibility being given to concerns about long-tem irreversible changes to the climate of the planet and in particular the global warming issue. The harmful aspects of emissions can be categorised by their perceived consequences such as changes in air quality producing deterioration in human, plant and animal health.

Gaseous pollutants emitted from combustion processes may be categorised as follows [Hanby, 1993]:

i) Products of incomplete fuel combustion such as carbon monoxide (CO) and gaseous hydrocarbons (HC).
ii) Oxides of nitrogen (NO_x).
iii) Carbon dioxide (CO_2).
iv) Emissions resulting from fuel contaminants such as sulphur, which could results in sulphur dioxide (SO_2) and sulphur trioxide (SO_3). These emissions can be influenced by fuel selection.
v) Emissions resulting from additives. Additives are generally used to achieve specific objectives but may cause some other emission problems.

In the next sections the formation of some of the principal pollutant gases from

combustion process are discussed and some of the methods which may control their emissions are reviewed.

1.8.4.1 Origin of NO_x Emission

Oxides of nitrogen have been identified as significant atmospheric pollutants. The oxides of nitrogen are: nitric oxide (NO), nitrogen dioxide (NO_2) and nitrous oxide (N_2O). Of these, the two compounds that are of interests in combustion systems are NO and NO_2. There is a growing interest in the emission of nitrous oxide (N_2O) from flames but measurements have generally shown concentrations to be low except possibly in fluidised bed combustion [Leckner and Gustavsson, 1991].

A considerable amount of experimental and theoretical work has been directed at understanding and predicting concentrations of NO in combustion gases and the mechanism of the formation of NO in flames utilizing various types of hydrocarbon fuels including propane-air and methane-air flames [Allen, 1990 ; Bowman, 1992].

The formation of NO_x is a complex process involving the high temperature fixation of atmospheric and fuel bound nitrogen. It involves many chemical reactions in both equilibrium and non-equilibrium processes that takes place in the pre-combustion, combustion and post-flame region. As a consequence, NO_x is referred to as being thermal, prompt and fuel NO_x depending upon the process responsible for its formation.

Thermal NO_x

This refers to NO_x formed through a mechanism in which, at flame temperatures, reactions occur which result in the decomposition of some oxygen and nitrogen molecules into oxygen and nitrogen atoms. These *O* and *N* atoms can then react with nitrogen and oxygen respectively to form NO. The simple chain reaction for the formation of NO was proposed by Zeldovich and this mechanism is thought to be the main route of the formation of thermal NO_x in combustion systems. The chemical

reaction processes are as follows [Bowman, 1992]:

$$O + N_2 \rightleftharpoons NO + N \tag{1.9}$$

$$N + O_2 \rightleftharpoons NO + O \tag{1.10}$$

The nature of the above reactions is such that there is a strong dependence on temperature, and a lesser sensitivity to oxygen concentration. This suggests reducing excess air and flame temperature as practical means of controlling the formation of thermal NO although these two are to some extent mutually incompatible. In addition to the above two reactions the dissociation of O_2 should be considered [Miller and Bowman, 1989]:

$$O_2 + M \rightleftharpoons O + O + M \tag{1.11}$$

where M represents a catalyst. This is the major source of oxygen, the reactant in reaction (1.9).

There is a third reaction which has been shown to contribute at and near fuel- rich conditions as follows [Iverach *et al.*, 1973]:

$$N + OH \rightleftharpoons NO + H \tag{1.12}$$

However, since most practical gas flames are fuel-lean, the above reaction can usually be neglected.

The rate constant k_i is generally expressed in the Arrhenius forms:

$$k_i = A \exp\left(\frac{-E_{ai}}{RT}\right) \tag{1.13}$$

in $m^3\ mol^{-1}\ s^{-1}$ where A is a pre-exponential factor, E_a is the activation energy and i is the index of reaction considered.

It is known that the rate-determining step governing the formation of virtually all NO in the post-flame gases is reaction (1.9) [Bowman, 1992] and based on the evaluation of Hanson and Salimian [1984] the rate expression used for this reaction is as follows:

$$k_{1.9} = 1.84 \times 10^8 \exp(\frac{-38370}{T}) \quad m^3 mol^{-1} s^{-1} \tag{1.14}$$

The rate of formation of NO is significant only at high temperature (greater than 1500 K) as fixation of nitrogen requires the breaking of the strong N_2 triple bound [Baulch *et al.*, 1973]. This effect is represented by the high activation energy of reaction (1.9) i.e. 319 kJ mol^{-1} which makes it the rate-limiting step of the extended Zeldovich mechanism [Bowman, 1992]. Providing there is sufficient oxygen, the rate of consumption of free nitrogen atoms becomes equal to the rate of its formation and therefore a quasi-steady state can be established. This assumption is valid for most combustion cases except in extremely fuel-rich combustion conditions [Bowman, 1992].

Prompt (Fenimore) NO_x

It is known that during combustion of hydrocarbon fuels, the NO_x formation rate can exceed that due to direct oxidation of nitrogen molecules. The prompt NO_x refers to NO formed by reactions of N_2 with hydrocarbon radicals in the flame. The mechanism of formation of prompt NO_x was identified first by Fenimore [Fenimore, 1971] who concluded that NO formation rates in the vicinity of the flame front were quite rapid and inconsistent with the post combustion zone mechanism for NO formation. It is reported that prompt NO_x can form significantly in some combustion environments, such as in low temperature, fuel-rich conditions and where residence times are short. Surface burners, staged combustion systems and gas turbines can create such conditions [Iverach *et al.*, 1973].

The actual formation of prompt NO_x involves a complex series of reactions and many possible intermediate species. A number of species resulting from fuel fragmentation have been suggested such as CH, CH_2, C_2H as the source of prompt NO_x in hydrocarbon flames [Hayhurst and Vince, 1983]. However, the major contribution is from CH for which the suggested primary step and the rout accepted is as follows [Harris *et al.*, 1976 ; Williams *et al.*, 1997]:

$$CH + N_2 \rightleftharpoons HCN + N \tag{1.15}$$

$$N + O_2 \rightleftharpoons NO + O \tag{1.16}$$

$$HCN + OH \rightleftharpoons CN + H_2O \tag{1.17}$$

$$CN + O_2 \rightleftharpoons NO + CO \tag{1.18}$$

Fuel NO_x

Emissions of NO_x from systems burning fuels containing nitrogenous compounds are much higher than those obtained from pure hydrocarbon fuels. The nitrogen in the fuel is a particularly important source of nitrogen oxide emissions for residual fuels oil and coal, which typically contain 0.3-2 % nitrogen by weight. As the nitrogen content of the fuel (i.e. % N_2 in fuel) increases, the fuel NO_x becomes a more significant contributor to the total emissions with a corresponding decline in the significance of thermal NO_x [Hanby, 1993]. Studies of fuel NO formation have shown that the process is relatively insensitive to temperature and mostly depends upon the amount of oxygen in the burner zone (i.e. decreases as the oxygen decreases), nitrogen in the fuel (i.e. increases as the nitrogen in the fuel increases) and type of flame (i.e. less for diffusion flame than premixed flame) [Fenimore, 1972 ; Bowman, 1992 ; Hanby, 1993]. It is noted that the

presence of molecular nitrogen in the natural gas does not constitute fuel nitrogen, therefore, fuel NO_x is not a significant component of NO_x emission in this study.

Formation of Nitrogen Dioxide (NO_2)

It is apparent that NO_2 can be formed in combustion processes of turbulent diffusion flames, gas turbines, diesel and spark-ignition engines [Johnson *et al.*, 1979]. The precise mechanism for the formation of NO_2 is not fully understood. The most generally accepted theory is that the nitrogen dioxide results from the reactions of NO with O_2, O, OH and HO_2 in the flame. Some of the reactions are as follows [Johnson *et al.*, 1979]:

$$2NO + O_2 \rightarrow 2NO_2 \tag{1.19}$$

$$NO + O + M \rightarrow NO_2 + M \tag{1.20}$$

where M is a third-body molecule.

The conversion of NO to NO_2 by the HO_2 mechanism is [Johnson *et al.*, 1979 ; Hargreaves *et al.*, 1981 ; Bowman, 1992]:

$$NO+HO_2 \rightarrow NO_2+OH \tag{1.21}$$

and the destruction steps are as follows [Johnson *et al.*, 1979]:

$$NO_2+O \rightarrow NO+O_2 \tag{1.22}$$

$$NO_2+H \rightarrow NO+OH \quad (1.23)$$

The HO_2 is believed to result from the reaction of *H* radicals with molecular oxygen and a third-body according to the reaction [Johnson *et al.*, 1979]:

$$H+O_2+M \rightarrow HO_2+M \quad (1.24)$$

This HO_2 formation reaction is favoured at relatively low temperatures. Once formed, the HO_2 radical is not very reactive and remains to react with NO already formed by other flame reactions in the high-temperature region of the flame which are transported by diffusion to the low-temperature regions. At higher temperatures (e.g. temperatures > 1500 K) alternative reaction paths are more important and NO_2 formation is not favoured [Hargreaves *et al.*, 1981].

Emissions of Nitrous Oxide (N_2O)

Emission of nitrous oxide from combustion processes has attracted interest because of the possible impact on the depletion of stratospheric ozone and on the greenhouse effect. N_2O is relatively inert gas and does not act as an acidifying agent nor a contributor to the deposition of nitrates which are the reported hazards of the other nitrogen oxides, NO and NO_2. The natural source of nitrous oxide is mainly biological activity; emission from soil and from the ocean is a result of side reactions in the nitrification/de-nitrification cycle [Bollin *et al.*, 1986].

A very low emission of N_2O have been observed from gas-fired devices including gas turbines, large gas-fired boilers and laboratory-scale combustors [Arai, 1994]. But relatively substantial emission of N_2O has been observed from fluidised-bed combustion with possible dependence upon variables including temperature, bed material together with design, pressure and load [Lyngfelt *et al.*, 1995].

1.8.4.2 Factors Influencing NO_x Emission

In order to control NO_x emission first it should be established and understood that what factors may influence NO_x emission. The important parameters are [Coe, 1980]:

i) excess oxygen available
ii) flame temperature
iii) combustion speed
iv) furnace size and configuration
v) burner design
vi) fuel bound nitrogen.

Excess Air Available

It was shown in equation. (1.9), that the formation of NO can be initiated by oxygen atoms, possibly formed by the dissociation of molecular oxygen. A number of studies have shown the clear dependence upon NO_x formation with oxygen concentration. Coe, [1980] using a forced draft diffusion flame burner showed that the net result of rate dependency on oxygen atom concentration is that a higher formation of nitric oxide occurs when there is a high level of excess oxygen available. He found that NO_x formation had a greater degree of dependency upon excess oxygen when the burner was fired with oil or oil and gas simultaneously (i.e. duel fuel 50/50 gas and oil) while firing gas only showed very little change in NO_x formation as excess oxygen was varied.

Flame temperature

Studies have shown that without a doubt flame temperature is a major factor in the formation of nitric oxide. In fact, the formation of nitric oxide by oxidation of atmospheric nitrogen is strongly dependent upon temperature with a lesser sensitivity to oxygen concentration. It should be noted that depending on burner design, although temperature has a great role on NO_x formation, availability of excess oxygen atoms may

well be an overriding consideration.

Combustion Speed

One of the main factors which influences the formation of NO_x in a combustion process is the residence time. This is the period during which the chemical reactions occur at the high temperature in the combustion zone. Because the formation of oxides of nitrogen is a slow process and continues even after combustion, the residence time of combustion products at high temperature should be kept short to minimise NO_x emissions.

Furnace Size and Configuration

The size of furnace in NO_x formation is important, simply because of its correlation with temperature. In fact, the main objective in the design of a low NO_x furnace is to increase the furnace cooling surface in the flame zone. The higher the heat release per unit volume of the furnace the greater the potential for NO_x formation [Coe, 1980]. Maldistribution of heat through the furnace can cause "hot spots" and enhanced NO_x generation [Coe, 1980].

Changing the configuration of a burner is a matter of importance in relation to NO_x formation. A furnace should be designed to utilize maximum cooling surface. This may be done by directing the flame along a wall or maximising the heat removal rate [Johnson and Rawdon, 1977].

Burner Design

The type of burner determines the baseline NO_x formation characteristics. The principles of designing burners for reduced emissions of NO_x follow from the above-mentioned considerations including oxygen control and limitation of peak temperature which have a fundamental role in NO_x formation. In some burners the mixing of fuel and air is

delayed to produce a low-temperature, diffusion-controlled flame [Johnson and Rawdon 1977]. Finally, the direction of injection of fuel may influence NO_x formation particularly in turbulent flame burners. It has been reported that in a turbulent flame burner if the fuel was injected perpendicular to the secondary air stream rather than parallel to the air stream then the emission of NO_x was slightly reduce [Bagwell *et al.*, 1970].

Fuel Bound Nitrogen

Experimental investigations have shown that the formation of oxides of nitrogen increases as fuel-bound nitrogen increases. The nitrogen in the fuel can form either N_2 or NO_x in the combustion products. The relative proportion of these depends upon the amount of nitrogen present in the fuel. It has been reported that as fuel-bound nitrogen increases the percent conversion to nitric oxide decreases. If this is about 0.1 % by weight, then the conversion of nitrogen in the fuel to NO_x is high. Whereas for fuels containing significant amounts of nitrogen (i.e. more than 0.5 % by weight) possibly 50 % of the nitrogen forms NO_x [Hanby, 1993].

1.8.4.3 Methods of Controlling and Reducing NO_x

In view of the above-mentioned contributing factors to NO_x emission, a number of methods have been suggested and investigated for the reducing NO_x emissions. The most popular methods are [Murphy and Putnam, 1985]:

i) Secondary-Air Baffling
ii) Catalytic and Radiant Burners
iii) Flame Inserts
iv) Burner Adjustments
v) Staged Combustion
vi) Exhaust Gas Recirculation.

Some of these methods have been described previously. The last two of the above

measures are the most common currently in use.

Staged Fuel and Combustion Air

From what has been said so far it can be concluded that the most important factors limiting NO_x concentration are: temperature, oxygen concentration and residence time. Staged combustion generally takes advantage of the effect that temperature plays on NO_x to retard its development. In the burners known as low-NO_x burners, the design is such that the fuel, the air or both are added in stages. A staged fuel/air supply gives a more gradual mixing of the fuel and combustion air which in turn lowers the peak flame temperature.

The staged combustion is especially used in fuel-rich burners. Combustion of fuel-rich mixture results in reductions in NO_x but at the same time, large quantities of carbon monoxide and hydrogen are produced. Consequently, secondary treatment of the gases is usually carried out by addition of air after the primary combustion zone to facilitate the complete oxidation of products formed in the primary zone. A practical amount of excess air is usually added to ensure complete combustion [Coe, 1980]. A good review of staged combustion is given by Allen [1990]. NO_x reduction of up to 70 % was reported using staged combustion when firing with natural gas and 40 to 50 % when firing with coal or oil [Turner and Siegmand, 1972].

Exhaust Gas Recirculation (EGR)

Exhaust gas recirculation reduces the temperature and oxygen concentration in the combustion zone and as a result lowers the thermal NO_x emission. Exhaust gas recirculation can be either external where combustion products are returned from the point of entry to the flue, or internal where the post-flame front gases are recirculated to the burner head. The amount of exhaust gas recirculation may be limited by flame stability and diminishing returns of recirculation. In car engines the NO_x production can be reduced up to 60 % using EGR although this involves an increase in the release of

unburned hydrocarbons (HC). The maximum limit of EGR is set by the increase in the HC emission, increase in consumption of fuel and the worsening smoothness of running of the engine.

1.8.4.4 NO_x Emission From Pulsed Combustors

It has already been mentioned that the pulsations in pulsed combustors increase the heat transfer through the heat exchangers reducing the time during which the combustion products remain at high temperature which can result in a reduction in thermal formation of NO_x. It has also been suggested that in pulsed combustion burners, because of incomplete clearing of the combustion chamber of combustion gases at the end of each cycle the burner possesses intrinsic exhaust gas recirculation (EGR) which may contribute to the low NO_x emission levels in the pulsed combustors [Murphy and Putnam, 1985]. Keller and Hongo [1990] carried out experimental measurements of velocity and temperature at various points along a Helmholtz-type pulsed combustor and concluded that the rapid effective mixing of the cooler combustion gases inside combustion chamber and the hot combustion products are responsible for the low NO_x emissions from pulsed combustors, creating a short residence time at high temperatures and hence quenching the production of NO.

During last two decades there have been number of reported studies on NO_x emissions using various types of pulsed combustors [e.g. Corliss, 1984 ; Keller *et al.*, 1994a; Lindholm *et al.*, 1995, Jones and Leng, 1996 ; AU-Yeung *et al.*, 1998] and different types of fuels [e.g. Keller and Westbrook, 1986 ; Jones and Leng, 1996]. In general these studies have shown that pulsed combustors can be categorised as low-NO_x devices since the NO_x concentrations in these devices are almost half of the amount produced by steady flow conventional burners operating in similar conditions. However, the trend of environmental regulations particularly during the last decade has been demonstrated towards the category of ultra-low NO_x emissions (i.e. < 5 ppm). Thus, further reductions of NO_x emissions are needed in pulsed combustors. In recent years the conventional techniques for control of NO_x formation have been adopted in pulsed

combustion devices. These methods are mainly exhaust gas recirculation, fuel staging and air staging.

Saito *et al.* [1989] proposed a NO_x reduction model of a valved pulsed combustor with the assumption of rapid combustion and quenching, rich-lean two stage combustion and exhaust gas recirculation (EGR). Michel and Belles [1991] investigated the influence of exhaust gas recirculation on NO_x emissions from a pulsed combustor. They found that NO_x concentrations were reduced approximately 20 % with an EGR rate of 4 %. At recirculation rates of greater than 6 % they found that CO emission rose to unacceptable levels although, they did not indicate any detailed reasons for the cause of such an effect. Similarly, Lindholm [1995] has reported reduction of NO_x emissions to around 50 % by the EGR method (i.e. EGR rate of 7.0 %). Lindholm [1995] reported for a given air-to fuel ratio EGR lowered the operating frequency and increased pressure amplitude in the combustion chamber which were favourable for low emissions of NO_x. She indicated that the effect of EGR is influenced by these parameters and due to the fact that higher pressure amplitude leads to an enhanced heat transfer and hence lower temperature inside combustion chamber, the possibility of reduction of NO_x increases [Lindholm, 1995].

Using air staging and fuel staging Kelly *et al.* [1991] managed to reduce NO_x levels from an aerovalved pulsed combustor by up to 28 % and 17 % less than the baseline NO_x emissions (57 ppm) respectively. They reported a minimum achievable NO_x of 26 ppm from their propane-fired pulsed combustor by combining fuel staging and air staging methods.

Keller *et al.* [1994a] reported reduction of NO_x and CO to less than 5 ppm by controlling the combustion temperature and the residence time. The latter was achieved by changing the injection geometry (i.e. rate and direction of vorticity deposition into combustion chamber), thereby controlling the rate of fine-scale fluid dynamic mixing. Increase in fine-scale mixing provided 10 % reduction in NO_x concentration (i.e. 3.0 ppm) which was within the scatter of data. Their CO data was remarkably low for this type of combustors, showing a minimum concentration of 2.5 ppm.

Jones and Leng [1996] measured NO_x and CO emissions from a non-premixed

pulsed combustor burning methane and methane with added hydrogen and propane. They found the NO_x concentrations and the relative proportions of NO and NO_2 from their combustor is correlated with flame temperature. NO_x data when burning methane with added hydrogen or propane showed higher values compared with burning methane only. This was attributed to a decrease in excess air and resulting higher flame temperature. They found that CO concentration decreased with addition of hydrogen which also attributed to the variation in flame temperature.

Recently, AU-Yeung *et al.* [1998] have reported an inverse relation between frequency and the NO emissions from a Schmidt pulsed combustor. They proposed that there is a scope for reducing NO emissions further if operational frequency can be raised.

From the literature it is concluded that low emission of NO_x from pulsed combustors is resulted from short residence time of combustion gases within the combustor at high temperature. However, a possible problem is the effect of the NO_x reduction methods upon operating efficiency and emission of other pollutant gases.

1.8.5 Formation of Carbon Monoxide (CO)

Carbon monoxide is a component of the flue gas resulting from incomplete combustion of the hydrocarbon fuel. The simplest reacting system is the dissociation equilibrium [Hanby, 1993]:

$$CO + \frac{1}{2}O_2 \rightleftharpoons CO_2 \tag{1.25}$$

though the equilibrium constant is such that the equation predicts low CO concentrations for percentage concentrations of oxygen. Generally, higher than the equilibrium concentrations of CO are measured in boilers and furnaces since the rate of formation of CO is considerably faster than that of its further oxidation to CO_2 [Hanby 1993].

Although formation of carbon monoxide as a combustion product is particularly associated with sub-stoichiometric (i.e. fuel-rich) combustion, CO may also be detected in the presence of excess air. In this case, the CO concentration primarily depends upon

an inhomogeneous mixture of fuel and air. In addition, CO can be detected at the extreme fuel-lean mixture condition (i.e. high excess air) where the temperature inside the combustion chamber is low and hence the concentrations of radicals such as OH which influence oxidation of CO are less [Hanby, 1993];

$$CO + OH \rightleftharpoons CO_2 + H \tag{1.26}$$

In the above equation the reaction is forward from left to right at high temperature and vice-versa at low temperature.

1.8.6 Carbon Dioxide Emissions (CO_2)

One of the principle products of combustion of hydrocarbon fuels is carbon dioxide. The equation below shows the stoichiometric or theoretical combustion reaction of methane:

$$CH_4 + 2O_2 \rightarrow CO_2 + 2H_2O \tag{1.27}$$

CO_2 emission is mainly important because of its contribution to the greenhouse effect. Furthermore, the carbon dioxide content of a combustion gas is an important criterion of efficient and economic combustion.

The control of CO_2 emission via the design and operation of combustion equipments is limited. The most important action for any given level of energy demand is to design and operate combustion devices so as to burn fuel as efficiently as possible. More efficient means less use of fuel for a required heat output which in turn means less CO_2 emission. The employment of combined heat and power schemes and pulsed combustion technology which have high efficiency may be one solution to the problem of CO_2 emission. Of course burning natural gas produces less CO_2 (for a given heat release rate) than other common fossil fuels.

Chapter Two

Design and Development

2.1 Introduction

In order to design a pulsed combustor with a given output the designer needs an estimate of the likely efficiency and the constraints on overall size and sound level. However, the initial design will be only an approximation since the knowledge of pulsed combustion technology is still limited. The first step is to establish a set of combustion system components that will provide satisfactory performance in all respects including: ignition, resonant burning, and clean (i.e. low CO) combustion, with the constraints imposed by the particular application. This is an empirical process, with no precise design rules, carried out by assembling and trying various combinations of components on the laboratory test-bench. Because there is, as yet, no comprehensive mathematical model of the pulsed combustion process, the design process draws on the accumulated know-how and observations derived from previous experience gained in the course of devising and operating pulsed systems and adapting them to practical applications. It should be noted that the processes occurring in a pulsed combustion device are strongly coupled and small geometrical changes can result in a substantial effects on performance.

2.2 Design and development of the nominal Input Pulsed Combustors

The pulsed combustors used in this study were of the Helmholtz-type (as described in Chapter 1) which implies that their operation depends upon the resonant coupling between the combustion process and the acoustic wave developed in the tailpipe [Putnam, 1971a]. The Helmholtz-type combustor is suitable for immersion tube heating, and as a result, was chosen for this study.

The nominally 7.5 kW pulsed combustor employed in this study, was previously

constructed in the laboratories of the Energy Technology Centre (ETC) at Middlesex University [Suthenthiran, 1990]. Its design was based upon an earlier prototype [Hargreaves and Patterson, 1986]. For the present study two additional combustors of nominally 15 and 30 kW were designed and developed. Their designs were similar to that of the 7.5 kW pulsed unit. Later, some modifications were made to the 7.5 kW pulsed burner to improve operation. These alterations were mainly to the air decoupler, tailpipe and the flapper valve. It should be noted that the ratings used to identify the combustors (7.5, 15 and 30 kW) represent the maximum heat input rates.

The geometry of the basic components of the three combustors was identical. Reference was made to Griffiths & Weber [1969] and Vishwanath [1984 and 1985] for guidelines to the design of pulsed combustors particularly in sizing the air and gas delivery systems. The design approach was similar to that of the Vishwanath [1985] following his recommended flow chart shown in Fig. 2.1. Sizing of most of the add-on components was done mainly by a trial and error process, guided by the achievement of satisfactory operation of the assembled units.

2.2.1 Design for Purpose

The specific chosen application normally determines the requirements and size restrictions of the design to be generated. In the case of the 7.5 kW combustor the application was for a compact water heater for use in a household. For development purposes the pulsed unit was set up on the test-bench in a water bath. The nominally 15 and 30 kW pulsed combustors were also designed for use as a water heating appliances.

2.2.2 Determination of Input Rate

The gas input rate is determined by the required nominal output. It should be borne in mind that pulsed combustion systems have a somewhat limited turn-down ratio

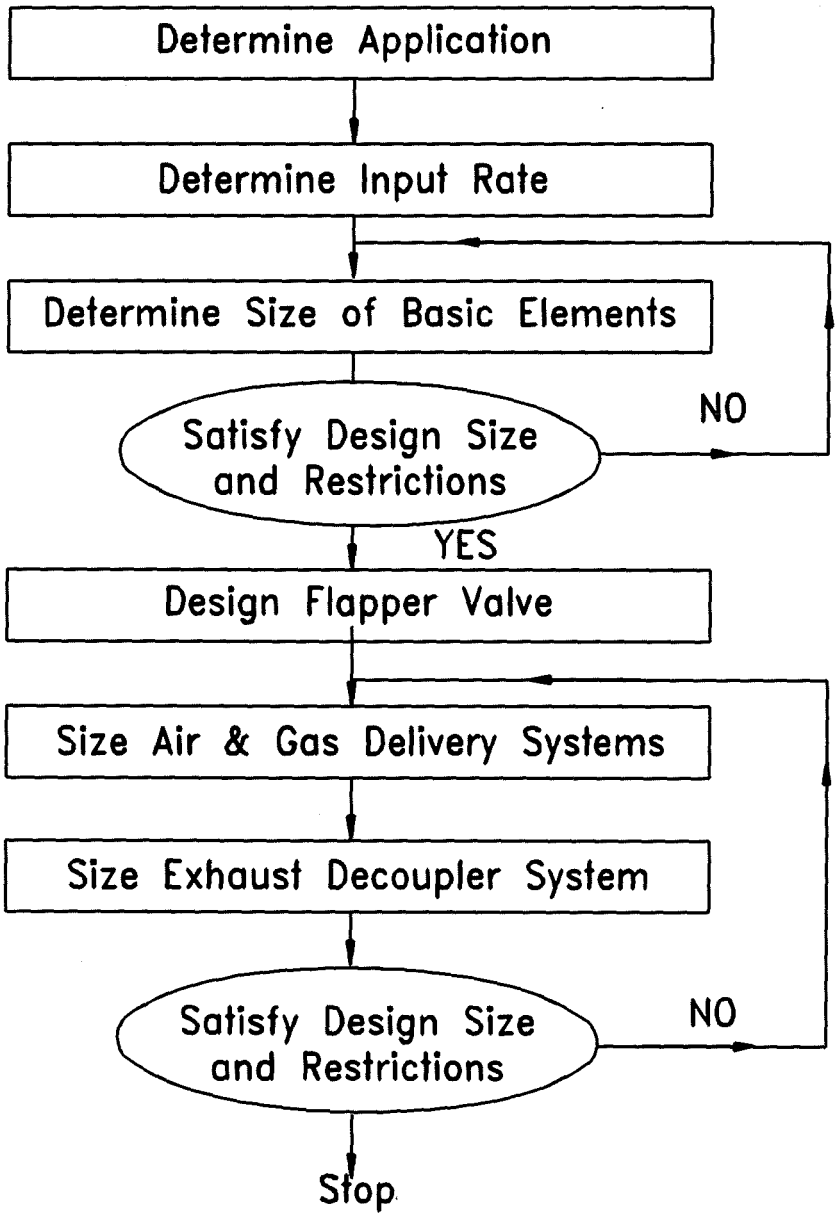

Fig. 2.1 Flow chart used for the design of the nominally 15 and 30 kW combustors [After Vishwanath, 1985]. Fuel gas input rate was determined with respect to the fuel gas composition.

compared with conventional burners. Maximum fuel gas input rates of 200, 380 and 840 ml s^{-1} were anticipated for the 7.5, 15 and 30 kW pulsed combustors respectively. Initial tests on the developed combustors showed that to start the 7.5, 15 and 30 kW pulsed combustors gas input rates of 150, 250 and 550 ml s^{-1} were required respectively when the toroidal air fan was switched on. The starting input gas rate was not influenced greatly by changes of configuration (i.e. tailpipe length, combustion chamber volume and flapper valve thickness) of the pulsed units.

2.2.3 Sizing the Basic Elements

For the present design of pulsed combustors the basic elements were:

a) Mixer head,

b) Combustion chamber,

c) Tailpipe.

These components were designed such that they could be modified or replaced as needed in order to develop a smooth running system, with satisfactory combustion at the desired input rate.

2.2.3.1 Mixer Heads

Air and fuel gas were mixed in the cylindrical brass mixer head before entering the combustion chamber via the flapper valve. The mixer heads were designed to give a (limited) variable mixing volume for fuel gas and air which could be achieved by adjustment of the mixer head position within the combustion chamber. However, a series of tests showed that the mixer head volume did not have a significant effect on the combustor's operation. This may well be because of the position of the flapper valve which was located downstream of the mixer head in the present design. The mixer heads had volumes of around 50, 240 and 900 ml for the nominally 7.5, 15 and 30 kW pulsed combustors respectively.

The dimensions of the mixer heads are shown in Fig. 2.2 to 2.4. Figure 2.5 shows

MATERIAL: BRASS

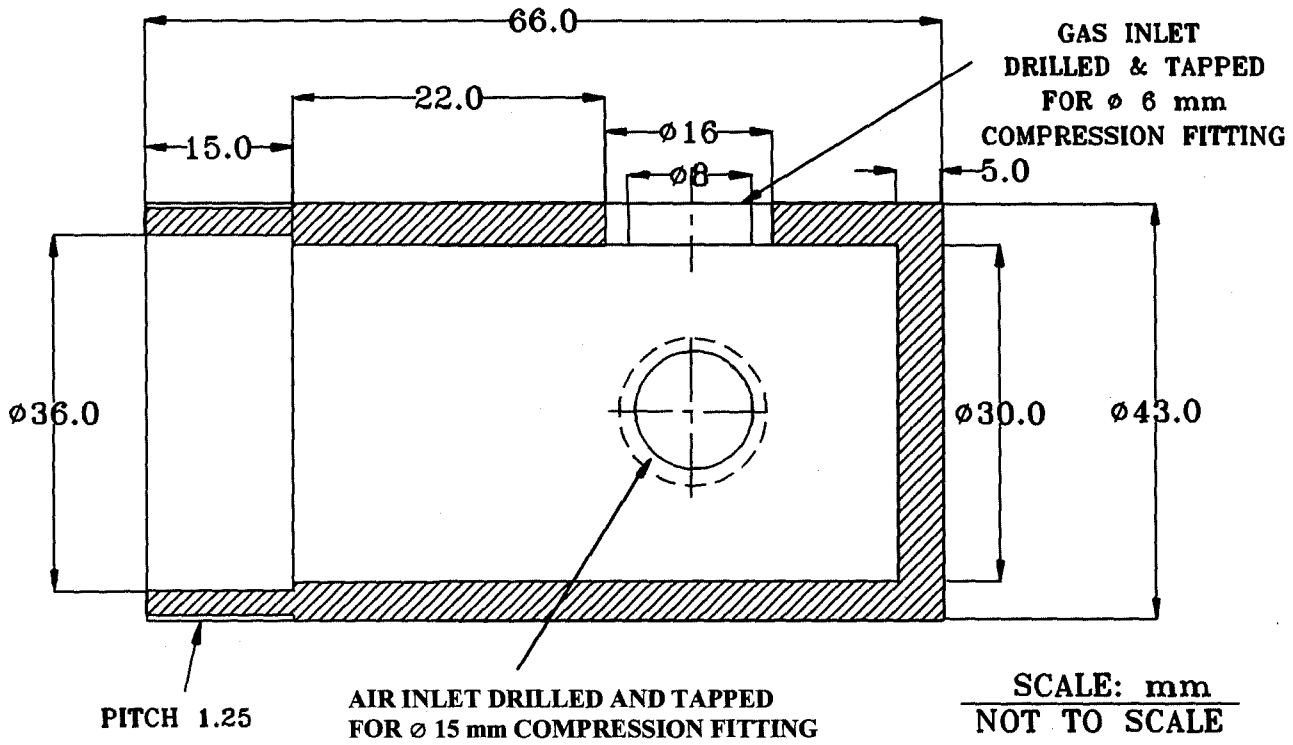

Fig. 2.2 Sectional view of the mixer head for the 7.5 kW pulsed combustor.

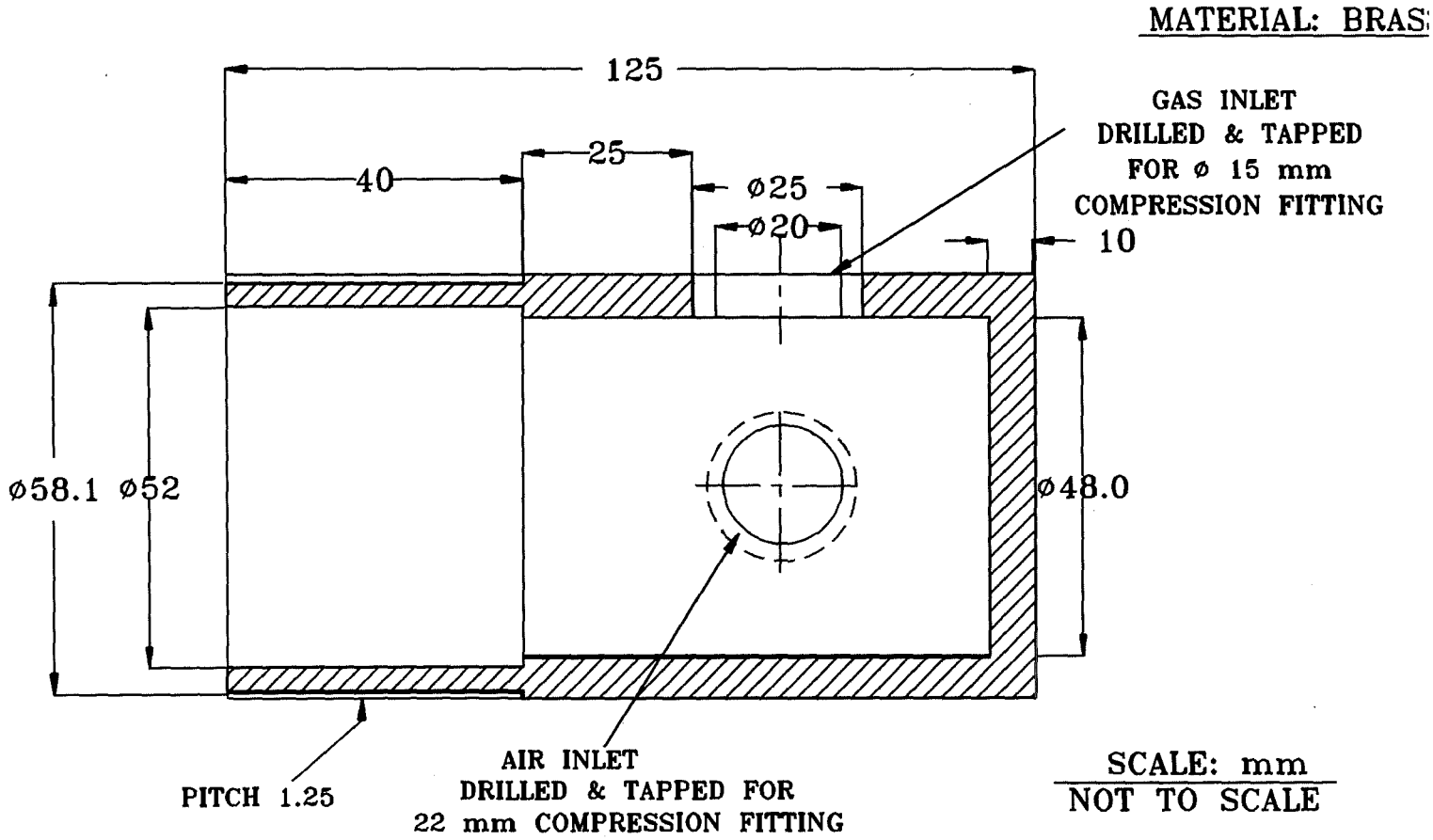

Fig. 2.3 Sectional view of the mixer head for the 15 kW pulsed combustor.

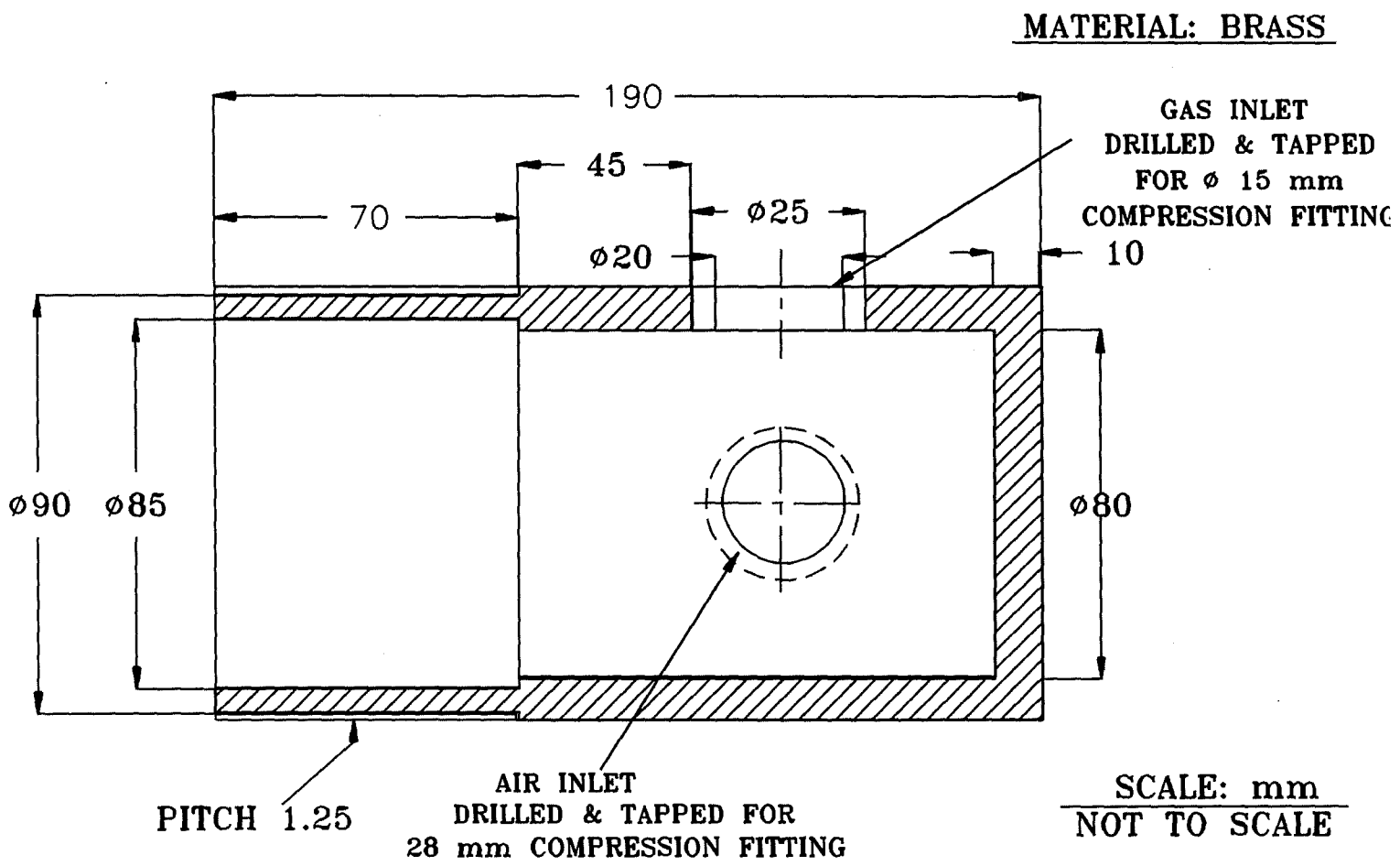

Fig. 2.4 Sectional view of the mixer head for the 30 kW pulsed combustor.

a photograph of the machined mixer head. As shown in the figures the mixer heads were fitted with two inlet ports (one for gas and one for air) 90° apart and at a distance of at least 2.5 cm from the back end of the mixer head, so that the air and gas streams were introduced at right angles to each other for good mixing. The air and gas inlet ports on the mixer head were designed such that their size could be altered to use various diameters of air and gas inlet pipes as desired and in this way to achieve optimum operation of the pulsed units. Tests showed that the 7.5, 15 and 30 kW combustors could operate successfully with air inlet port diameters suitable for compression fittings of ⌀15, ⌀22 and ⌀28 mm respectively. The gas inlet ports for the 15 and 30 kW combustors were sized such that a ⌀15 mm compression fitting could be fitted. The mixer head of the 7.5 kW combustor had incorporated with a gas inlet port suitable for a ⌀ 6 mm compression fitting.

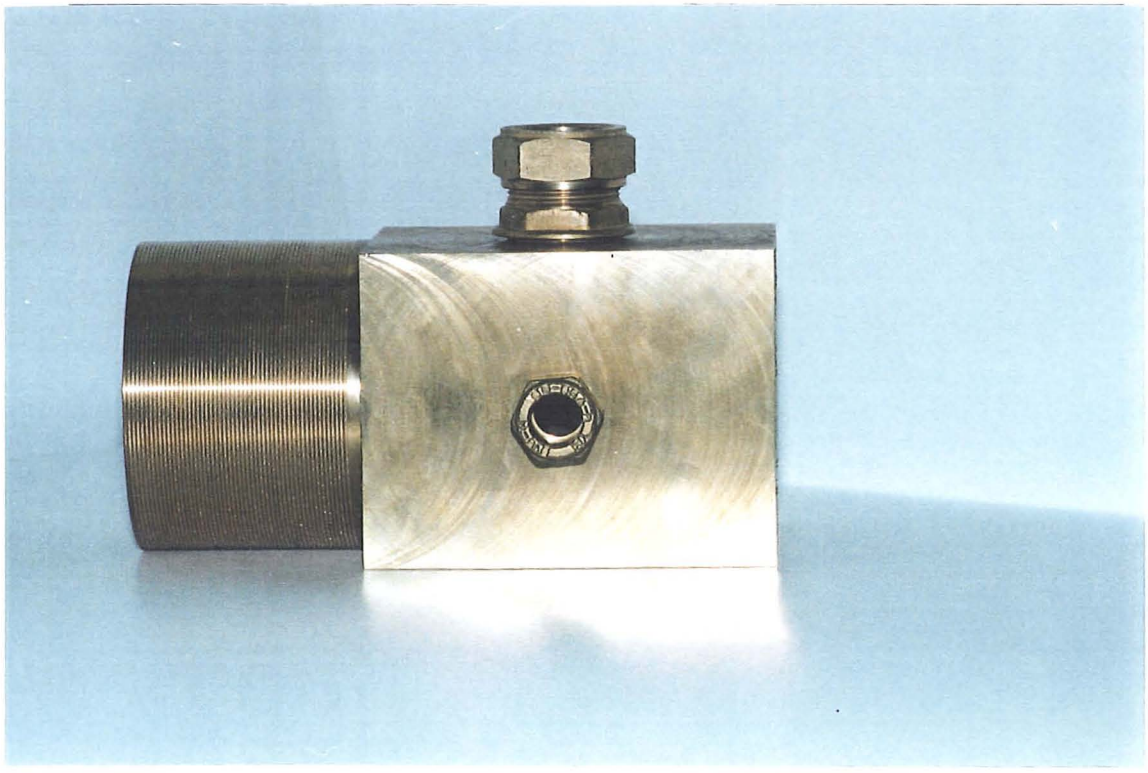

Fig. 2.5 A photograph of the developed mixer head for the present design of pulsed combustor.

2.2.3.2 Combustion Chambers

As the name implies this is where the combustion occurred and since the pulsed combustors were designed to be of the Helmholtz-type the combustion chamber corresponded acoustically to a resonator cavity.

The combustion chambers of the nominally 15 and 30 kW pulsed combustors were sized by taking into consideration the combustion chamber volume and nominal heat input of the previously designed 7.5 kW pulsed burner. The geometry of the three combustion chambers was identical but their dimensions were increased linearly by a factor of 1.5 from one combustor to the next larger. Thus, the combustion chambers were designed and sized to give the effective volume ranges of 80 to 120 ml, 270 to 400 ml and 1000 to 1400 ml for the 7.5, 15 and 30 kW pulsed combustors respectively. These volumes could be achieved by adjusting the position of the flapper valve carrier inside along the combustion chamber. A calculation method for the effective combustion chamber volume is given in Appendix I.

Figures 2.6 to 2.8 show the actual dimensions of the developed combustion chambers. The chambers were cylindrical in shape and constructed from brass and the outer surface acted as part of the heat exchanger surface. Each combustion chamber was fitted with a slot situated downstream of the flapper valve assembly for mounting a spark plug. Figure 2.9 shows a photograph of the combustion chambers.

Since the developed pulsed combustors were test-bench prototypes, there was no restriction on the available space. For commercial use, however, it is important to take a number of factors into consideration when sizing the combustion chamber, including: space available within a proposed pulsed combustion appliance and sufficient heat transfer area to provide a high thermal efficiency at the proposed gas input rate.

In the design of a pulsed combustion unit, despite the fact that pulsating combustion occurs mainly and possibly entirely inside the combustion chamber (see Chapter 6), the combustion chamber and adjacent tailpipe should be treated as a single integral unit. They should be sized so that the natural frequency of the gas-column inside the entire unit is in resonance with the rate of pulsation produced in the combustion chamber [Griffiths and Weber, 1969]. This was explained in Chapter 1 and should be

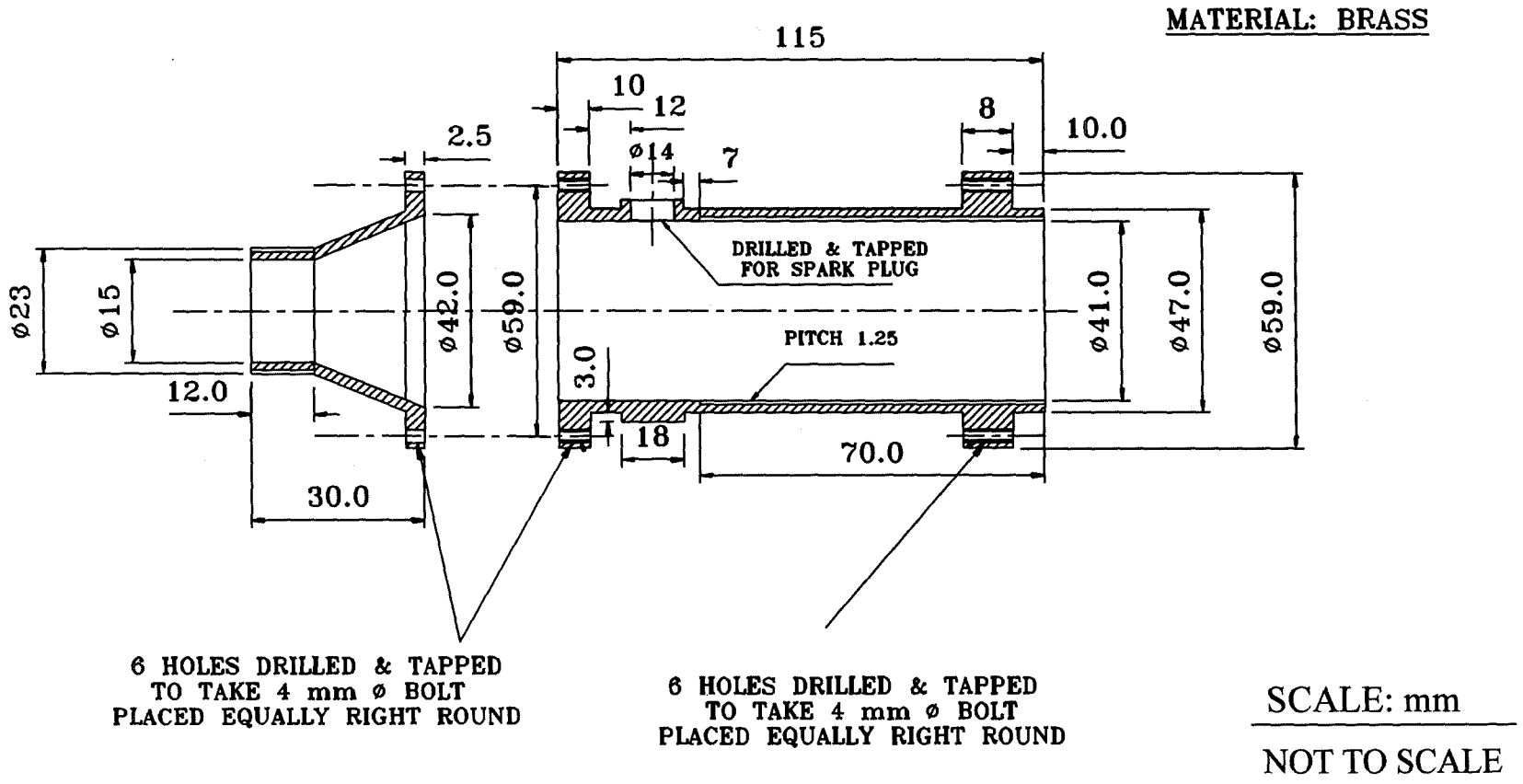

Fig.2.6 Sectional view of the combustion chamber for the 7.5 kW combustor.
Flow direction was from right to left. Flapper valve location is shown in Fig. 3.1

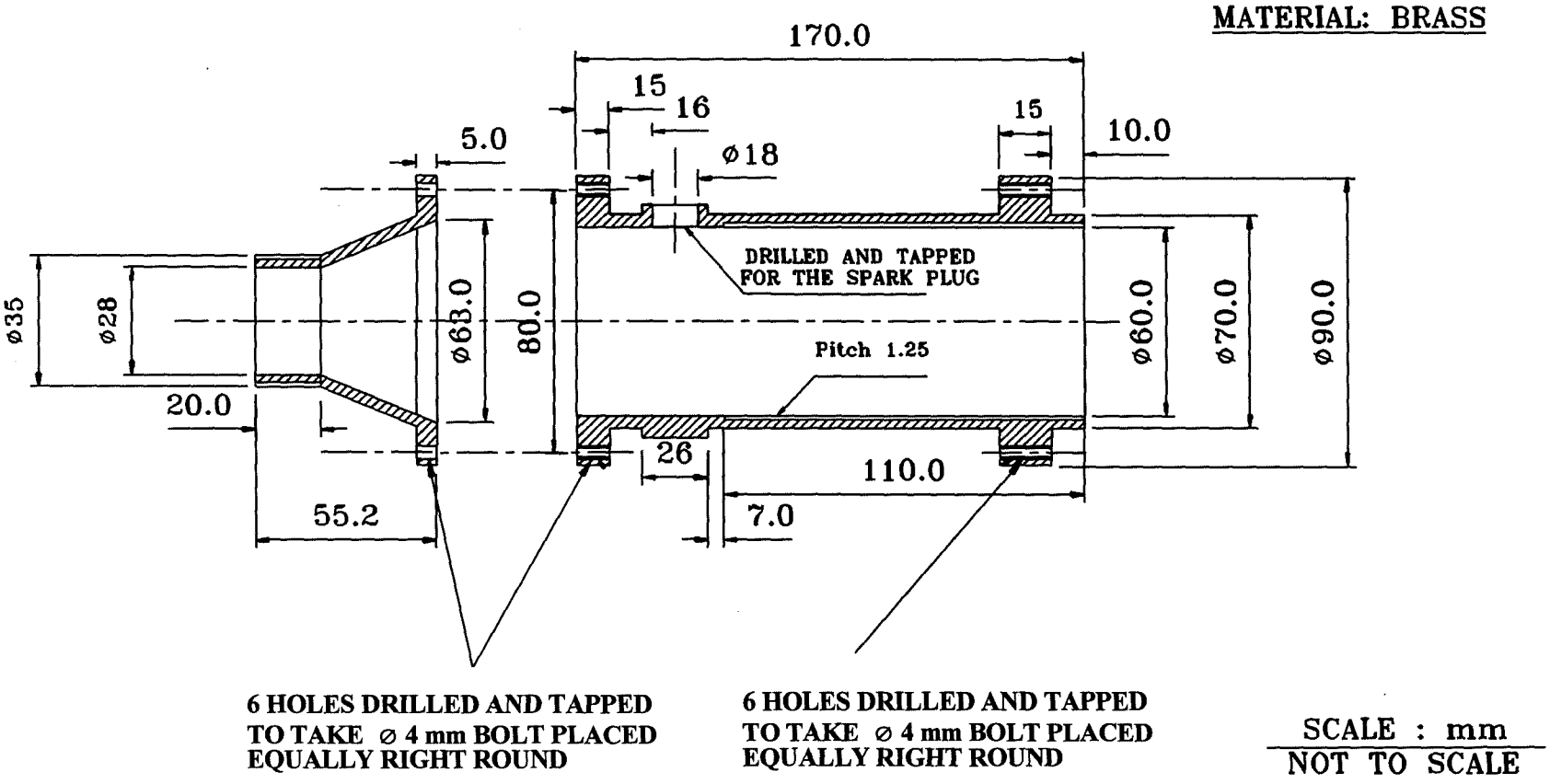

Fig. 2.7 Sectional view of the combustion chamber for the 15 kW combustor.
Flow direction was from right to left. Flapper valve location is shown in Fig. 3.1

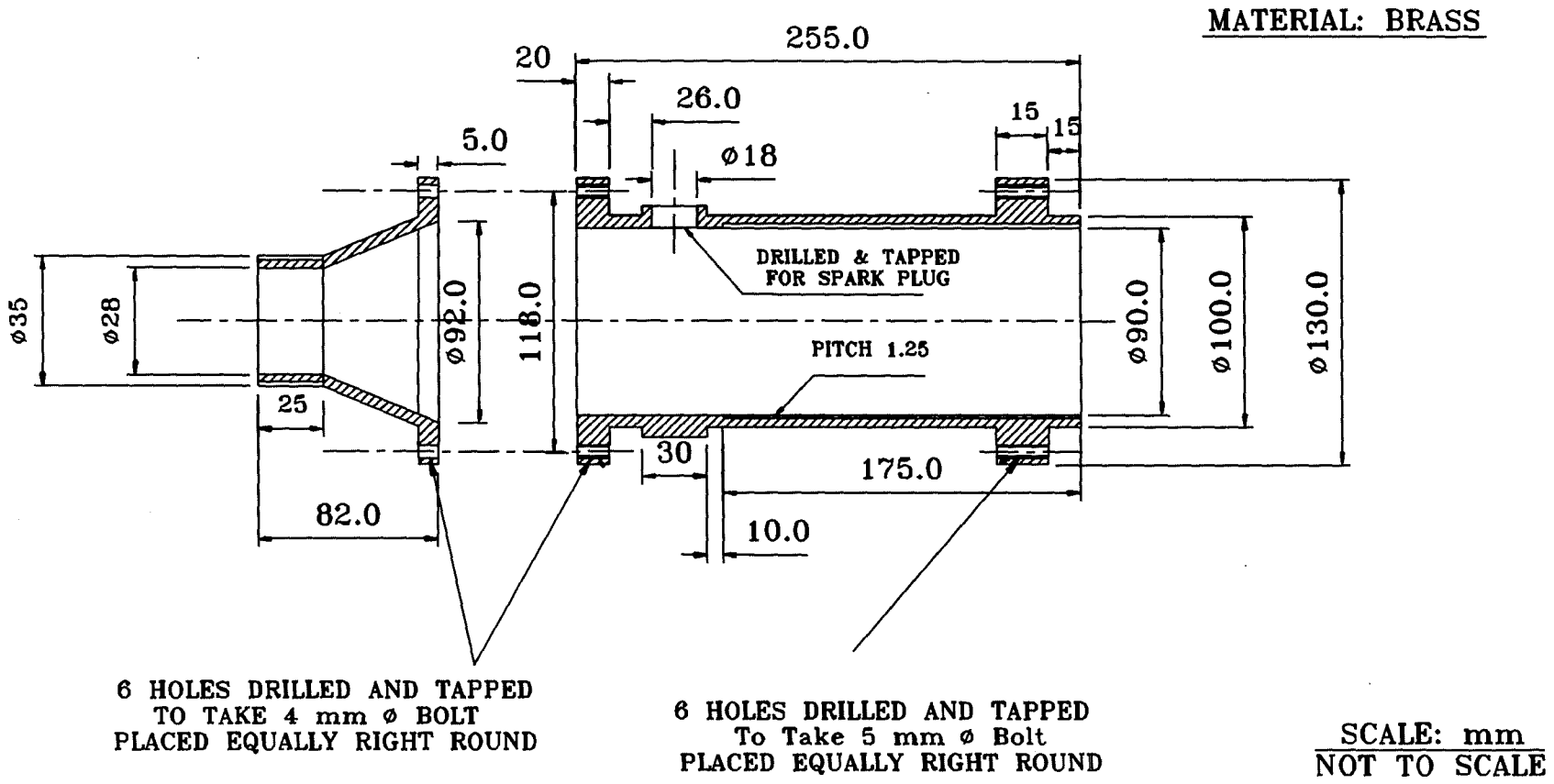

Fig. 2.8 Sectional view of the combustion chamber for the 30 kW combustor.
Flow direction was from right to left. Flapper valve location is shown in Fig. 3.1

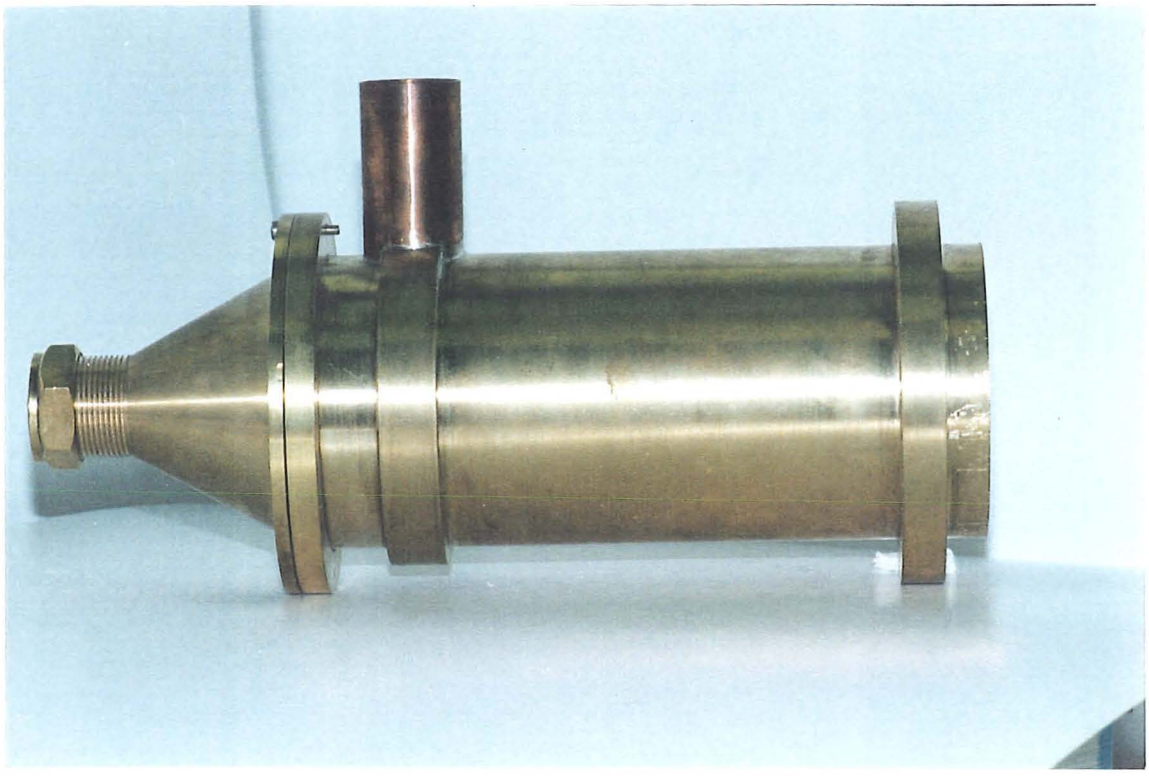

Fig. 2.9 A photograph of the developed combustion Chamber.

accomplished for the successful operation of a pulsed unit. Hence, for this study the combustion chamber volume and tailpipe length for each pulsed unit were chosen so as to satisfy such requirements. Development proceeded on a trial and error basis. It was found that there were minimum combustion chamber volumes of 80, 280 and 1060 ml respectively using which the 7.5, 15 and 30 kW pulsed combustors would operate. Tests showed that the fuel gas input rate for each pulsed combustor was influenced by the combustion chamber volume; higher gas input rates could be used with larger combustion chamber volumes. For instance, in the case of the 15 kW pulsed combustor, with a combustion chamber volume of 300 ml the pulsed unit operated at a maximum gas input rate of 360 ml s^{-1} whereas with a combustion chamber volume of 380 ml the pulsed combustor could be operated with complete combustion at a maximum gas input rate of

385 ml s^{-1}. These effects are discussed in greater detail in later chapters where the operating frequency and pulsing pressure of pulsed combustors are analysed.

2.2.3.3 Tailpipes

Studies have shown [Francis, 1963 ; Gill and Bhaduri, 1978; Keller *et al.,* 1989] that the tailpipe dimensions for a particular combustion chamber size are the geometrical factors which have the greatest effect on operating frequency and pressure in a pulsed system. This is analysed in more detail in Chapters 4 and 5.

In the same way as for the combustion chamber, the size and shape of tailpipe is dependent upon the availability of space and the required area of heat transfer for a given pulsed combustor. The tailpipe can be used in the form of a coil [Adams, 1982] or in the form of a single tube or multiple tubes [Whitlock *et al.,* 1982]. It should be noted that tailpipes should not have sharp bends in them as these impede gas flow and influence the smooth running of the combustor. Tailpipes generally are used as the main source of heat transfer especially in water heating devices.

For the present design of the 7.5, 15 and 30 kW pulsed burners, copper tubes of 12, 15, and 22 mm outside diameter* respectively were used where the tailpipes imitated the neck of a Helmholtz resonator. Various lengths of tailpipe were tested. These included tailpipe lengths of 1500, 2000 and 2300 mm for the 7.5 kW pulsed combustor, 1500, 2000 and 2500 mm for the 15 kW pulsed unit and finally, 2000 mm for the 30 kW pulsed burner. The experimental investigations for this study were carried out using the above given tailpipe dimensions. A photograph of the typical tailpipe used in this study is shown in Fig. 2.10.

In the same way as with the combustion chamber volume, the results from initial tests investigating the operating limits of the pulsed combustors showed that there was a minimum tailpipe length below which the pulsed unit could not be operated successfully, i.e. on the basis of ease of starting and continuous running. These tests

---

* Throughout this chapter the given values represent the outside diameter of the tailpipes. However, for the relevant calculations the average inside diameter values are used.

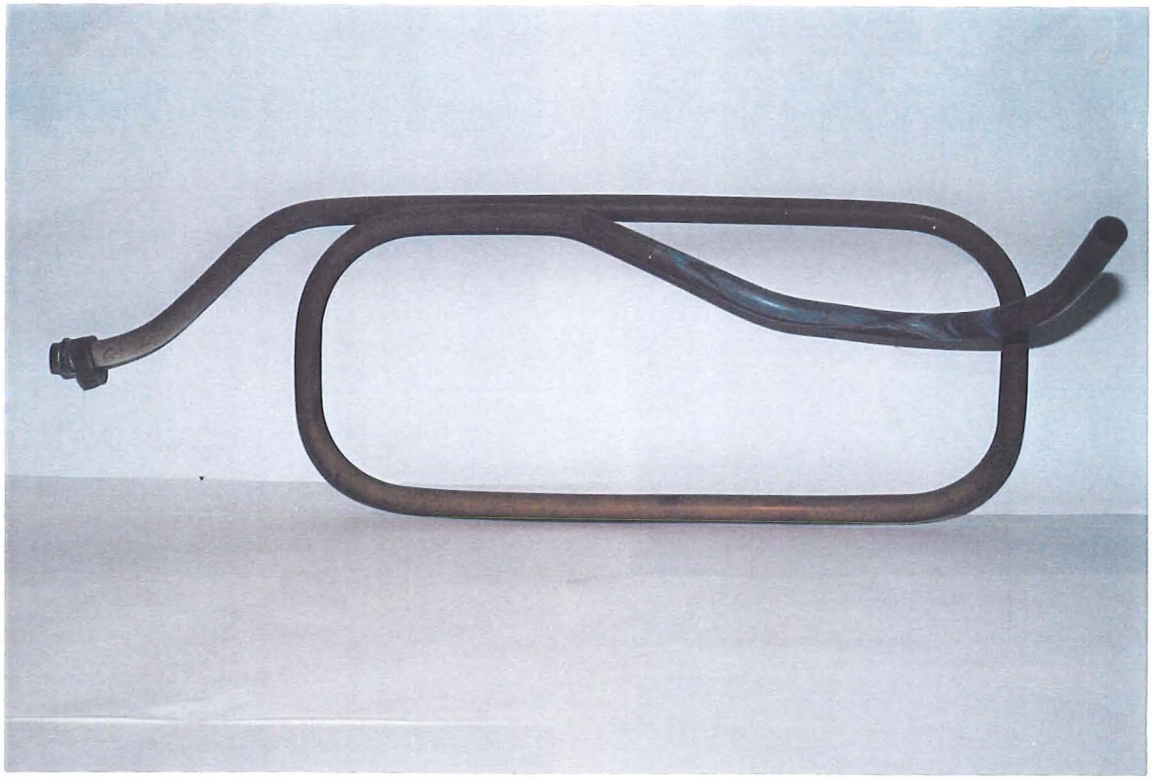

Fig. 2.10 A photograph of the tailpipe.

showed that the 7.5, and 15 kW pulsed combustors would not run continuously with a tailpipe length and diameter below 1500 mm & 10 mm or 1300 & 12 mm respectively. It was also found that the pulsed units could operate with higher fuel gas input rates when a longer tailpipe was used compared to shorter tailpipes. However, the minimum fuel gas input flow rate was increased with a longer tailpipe. This may be because of the effect of this parameter upon the operating frequency of the pulsed units. As will be shown later in Chapter 4, the fundamental frequency of a pulsed burner is primarily determined by the physical size of the system, and most burners operate at this fundamental frequency.

In this study, tailpipes longer than 2500 mm were not used. This was mainly because of the design restrictions and the fact that the requirements for the chosen

applications (e.g. overall efficiency) were satisfied with the elected tailpipe lengths.

2.2.4 Valve Assembly

Figure 2.11 shows a diagram of the valve assembly used for the three pulsed combustors. As can be seen the valve manifold** incorporates a flapper valve, a spacer, clearance plate, bolt, flame trap and lock rings. By adjustment of the position of the valve manifold various combustion chamber volume can be achieved. The flapper valve is used to control the flow of the air and gas mixture into the combustion chamber. The design of the flapper valve was similar to that in the previous pulsed combustor built at Middlesex University [Suthenthiran, 1990] which was based on the principles obtained from Skinner [1989]. The valve was in the shape of a ring allowing the flapper valve to float over a spacer. A photograph of the flapper valve body with incorporated components is shown in Fig. 2.12.

In operation the flapper valve moves freely over the spacer and opens against the clearance plate as a result of the differential pressure of the mixture of air and gas and that inside the combustion chamber once during each cycle. Back pressure from each combustion pulse forces the flapper against the valve body closing off the ports through the mixture is supplied. The sectional and face views of the flapper valve carrier are given in figures 2.13 to 2.15, for the nominally 7.5, 15 and 30 kW combustors respectively. Shown also in Fig. 2.16 are the actual dimensions of the lock rings used for keeping the flame trap in position for each combustor.

Valve life in pulsed combustion devices has posed some design problems. It is reported that the flapper valves used in the German V-1 flying bombs had an operating life of about half an hour [Manganiello, 1948]. Later, these vane-type spring steel flapper valves were coated with materials such as neoprene which gave them more durability (i.e. around 200 hour of operation). The major problems associated with these

**

The names valve manifold, flapper valve carrier and flapper valve body have similar meanings throughout this thesis.

NO.	DESCRIPTIONS	NO. OFF
1	COMBUSTION CHAMBER	1
2	LOCK RING	2
3	FLAME TRAP	1
4	BOLT	1
5	CLEARANCE PLATE	1
6	SPACER	1
7	FLAPPER	1
8	VALVE MANIFOLD	1
9	WASHER	1
10	NUT	1

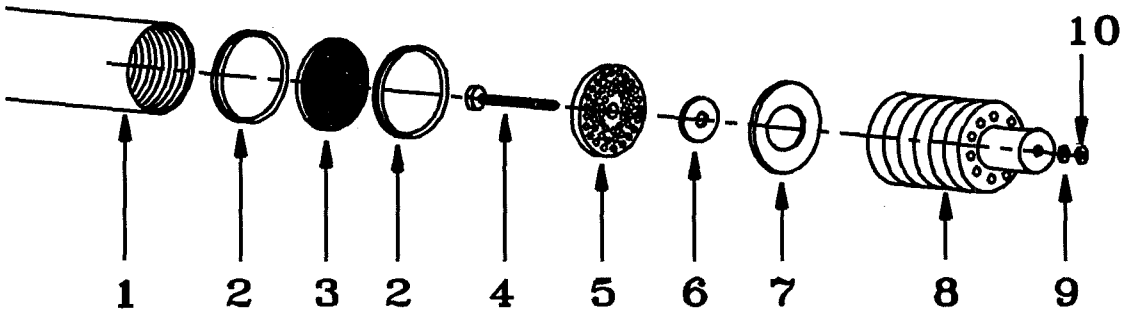

Fig. 2.11 Schematic arrengement of the flapper valve assembly for the three developed combustors.

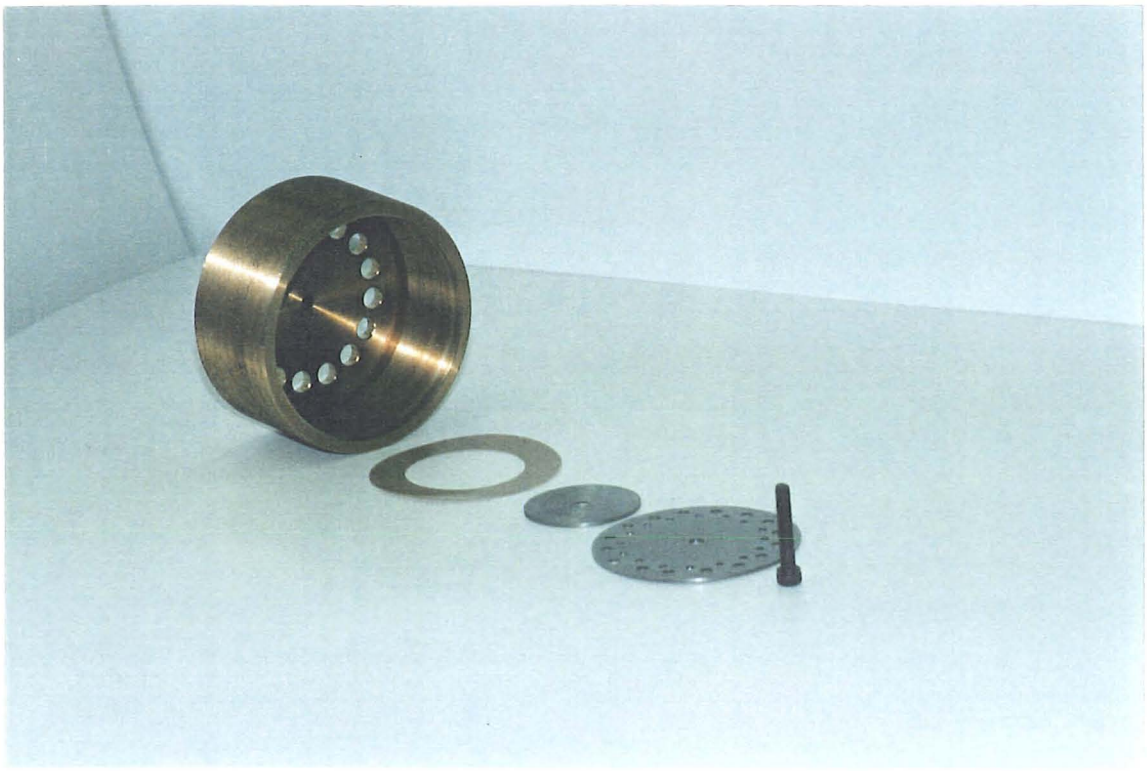

Fig. 2.12 A photograph of the flapper valve assembly.

valve are those of fatigue and flame leakage. The use of sandwich type valves, in which the inner plate took up most of the impact and the outer plate most of the heat, as well as valve designs which provided protective cold cushions of air and reduced amplitude of valve motion have been reported [Belles, 1986].

In the present pulsed combustor design, the constraints on the choice of material were that it should seal against back-flow when seated while being of low mass so that it could respond quickly to pressure changes inside the combustion chamber. It should also be hard wearing to provide satisfactory service over extended periods of operation. Furthermore, it should be able to withstand the high temperatures to which it is subjected. Various materials including PTFE- coated fibre glass, Viton*** rubber and

***

Viton is a trademark that falls within the generic family of synthetic rubbers called fluoro elastomers.

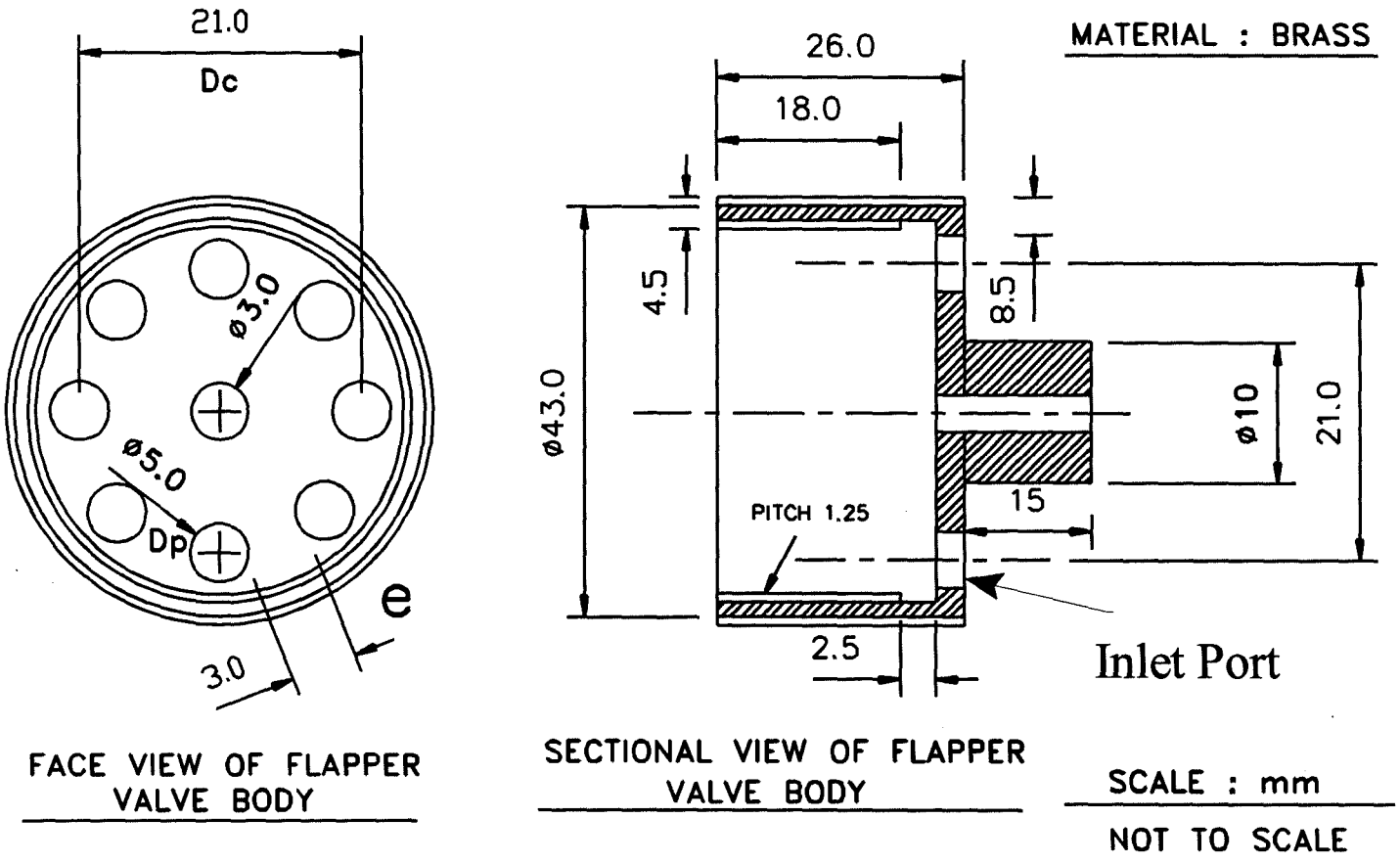

Fig. 2.13 Sectional and face view of the flapper valve carrier used for the 7.5 kW combustor.

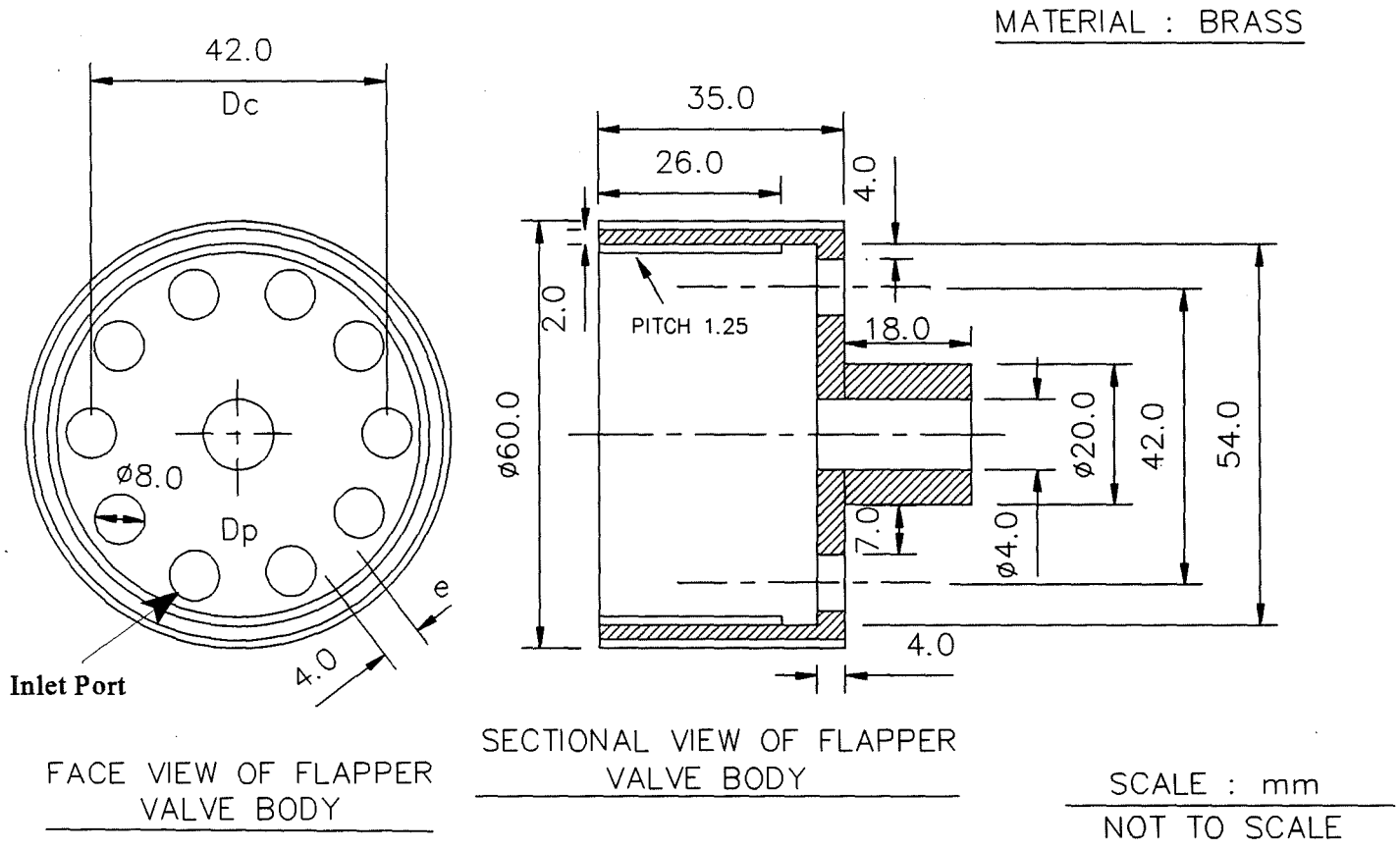

Fig.2 .14 Sectional and face view of the flapper valve carrier used for the 15 kW combustor.

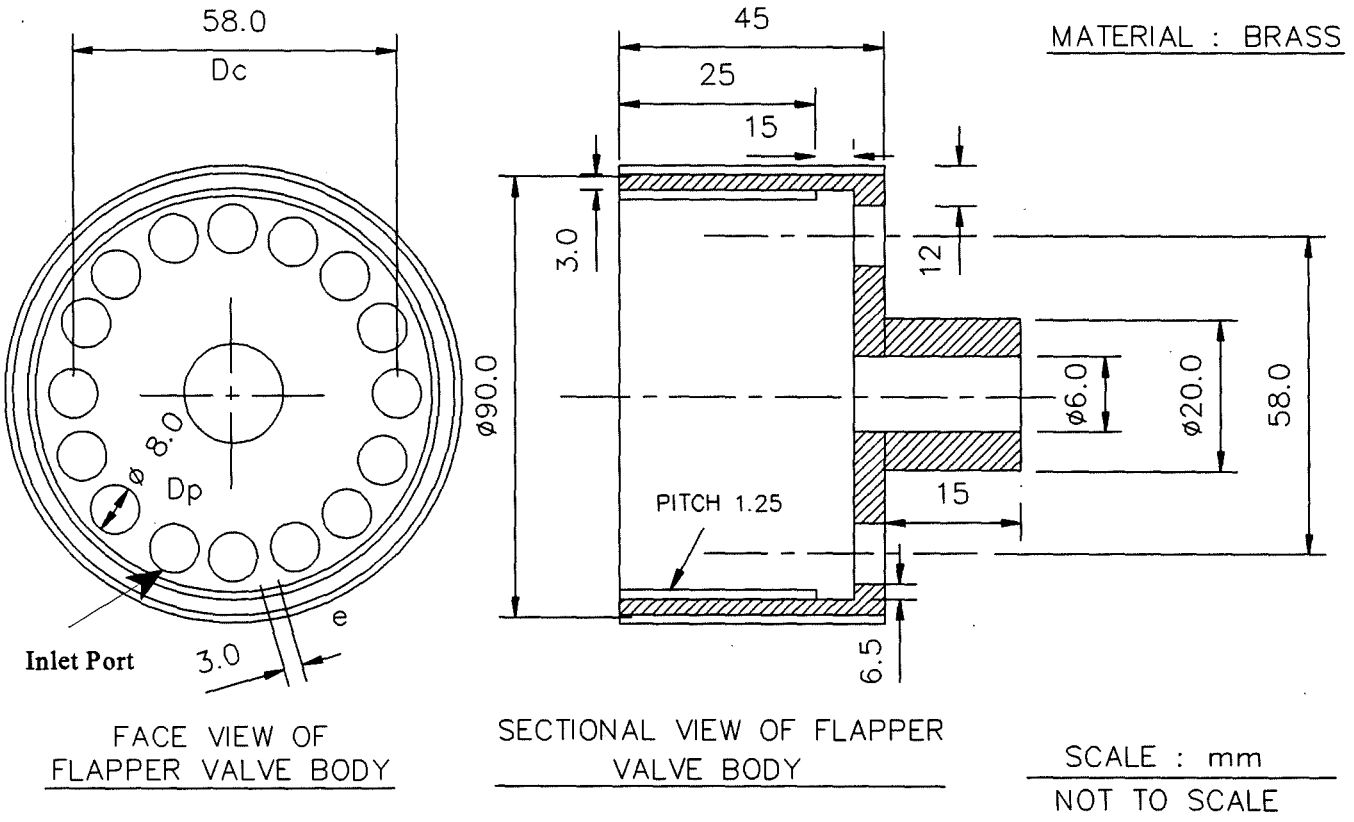

Fig. 2.15 Sectional and face view of the flapper valve carrier employed for the 30 kW combustor.

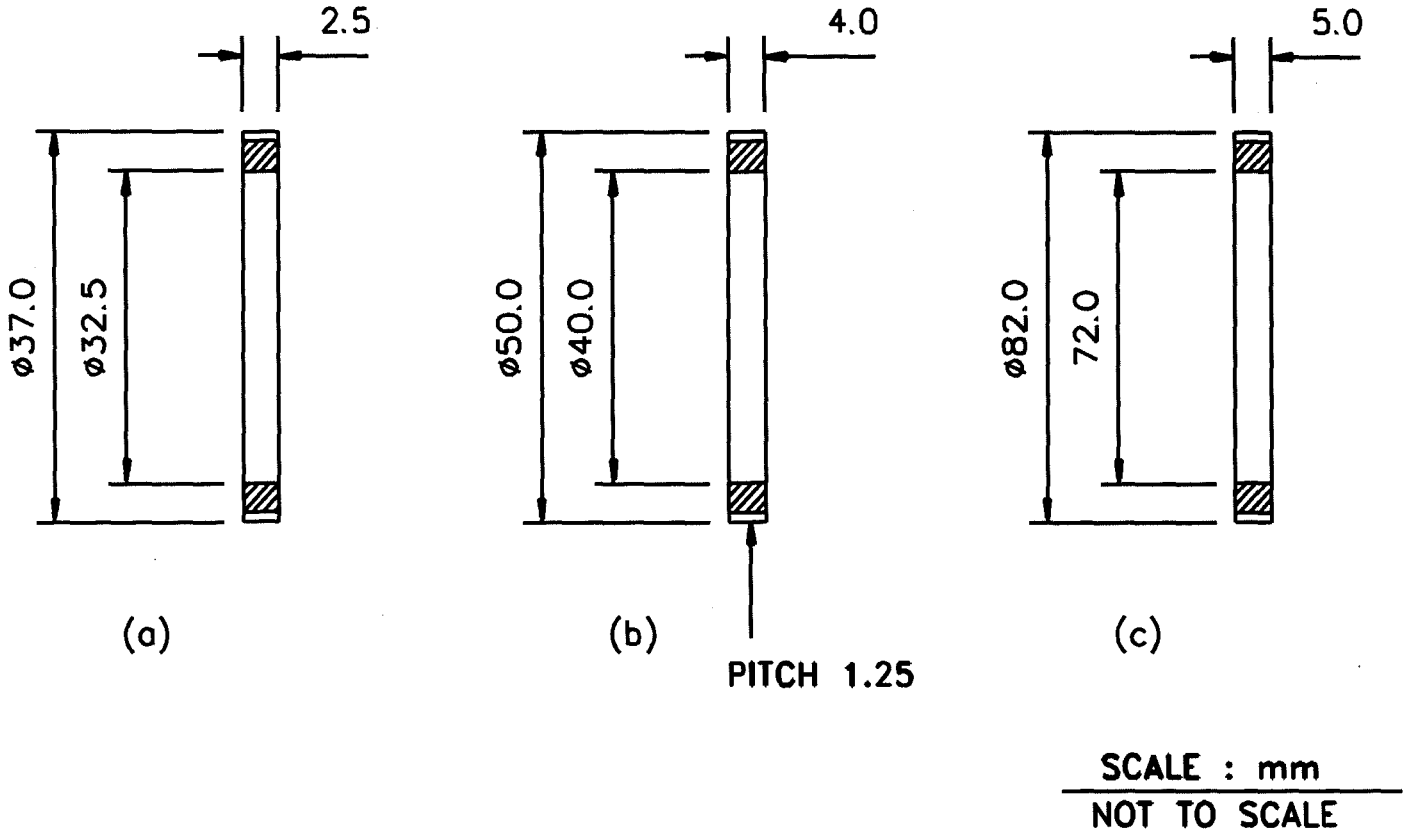

Fig. 2.16 Sectional views of the lock rings used for the a) 7.5 kW, b) 15 kW and c) 30 kW combustors.

silicone rubber coated fibre glass were tested. Fig. 2.17 shows a photograph of flapper valves made of these materials with thicknesses ranged from 0.13 to 0.7 mm. It was found that PTFE- coated fibre glass with an operating temperature range of -50°C to 250°C was a suitable material to satisfy the above requirements. The material served without deterioration for up to 250 hours of operation. A flapper valve thickness of 0.15 mm was found to be the most appropriate with respect to operation of the pulsed units. Thus, most of the tests in this study were carried out with flapper valves using the above material and thickness. Tests showed that combustors would not operate with a flapper valve thickness of over 0.7 mm.

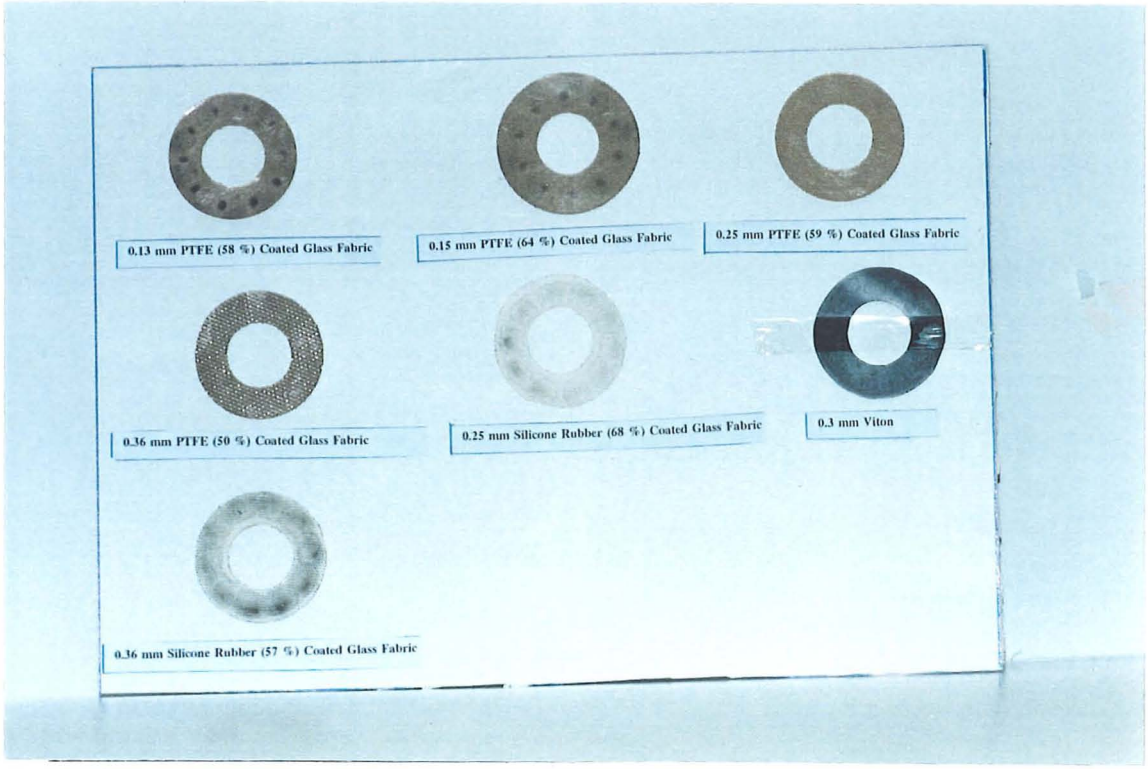

Fig. 2.17 photograph of the flapper valves made of the specified materials.

A flame trap (positioned between two locking rings downstream of the backing plate) was used to prevent the destruction of the flapper valve and potential explosion resulting from a flame travelling back into the mixer head. In most tests carried out for

this study, a brass disc with 1 mm diameter equally spaced holes was used as a flame trap. Tests showed that the pulsed units could operate successfully with other materials such as mild steel and ceramic. These tests showed that the successful operation of the pulsed units was not so much dependent upon the material used for the flame trap but more upon the size of the holes in the flame trap. This is because of the position of flame trap in the present design, where there is a requirement that the holes are of sufficient size to provide enough flow area for the mixture charge passing into the combustion zone. For a similar reason, it was found that an adequate clearance between the outer edge of backing plate and the valve chamber wall was necessary to attain successful operation of the pulsed unit. Indeed this was one of the main parameters identified in this study for successful operation of the present design of pulsed combustors. This is because it is the only route by which the mixture charge could travel from the inlet mixture ports to the combustion zone. Hence, there should be enough clearance and hence flow area to allow sufficient mixture charge of air and gas to enter the combustion zone. Obviously, the size of the clearance is dependent upon the dimensions of the valve carrier and inlet ports. Inlet ports should be as large as possible allowing ample flow of the mixture charge into the system. As a result of a series of tests on the three combustors, a minimum clearance of 4 mm was used.

Performance of the pulsed combustors was investigated with various test gases including NGC. To achieve successful operation of the pulsed unit using the test gas NGC, which had high contents of H_2 (i.e. 36 %), the flame trap required an additional coarse wire mesh. Tests showed that a ceramic flame trap plus coarse wire mesh resulted in better operation of the pulsed combustor. Using NGC the unit back-fired and the combustor could not be run without the coarse wire mesh. This was thought to be because the higher H_2 percentage contents in the NGC gas increased the burning velocity of the gas which in turn may have caused the flame to propagate back into the mixer head. Kitchen [1982] also reported that his pulsed combustor with a single tailpipe centred on a cylindrical combustion chamber would not operate on manufactured gas which had a rate of flame propagation of 670 mm s^{-1}. However, when natural gas (with a flame speed of about 300 mm s^{-1}, almost half of the manufactured gas) was used for

the same combustor configuration the unit operated successfully. Previous work at Middlesex University by Suthenthiran [1989] and the work of Windmill [1984] have shown similar observations as in this study when burning NGC.

The number of mixture inlet ports on the flapper valve body for each combustor was determined using the equation below [Griffiths and Weber, 1969]:

$$N = \frac{\pi D_c}{D_p + e} \tag{2.1}$$

where: N is number of inlet mixture ports,

D_c is the diameter of the ring of the centres of the ports,

D_p is the inlet mixture ports diameter,

e is the edge to edge spacing of the inlet ports, which should be as small as possible to provide more ports and hence greater total inlet area.

The actual dimensions and number of inlet mixture ports are given in Fig. 2.13-2.15. Other parameters such as the spacer thickness which determines the flapper movement spacing or clearance between the wall of combustion chamber and the backing plate were chosen by a trial and error procedure. Griffiths and Weber [1969] have reported detailed calculation of such parameters but these calculations do not necessarily apply for all applications. They may, however, provide a useful guide.

2.2.5 Air and Gas Delivery Systems

The air and gas delivery systems for the present design of pulsed units were comprised of air and gas lines, air and gas decouplers, gas orifice (placed as a restriction in the outlet of the gas decoupler) and an air blower. A radial orientation of the air and gas lines at the mixer head with 90° separation was employed to give good mixing. The following sections describe the design and sizing procedures of the air and gas delivery systems.

2.2.5.1 Gas Orifice Size

Figure 2.18, shows the relationship of the gas orifice size with the gas heat input rate recommended by Vishwanath [1984]. From this graph, for a given heat input rate the approximate gas orifice diameter for the present combustors was determined. Once the approximate orifice size was established, the actual size of gas orifice was determined using previous pulsed combustion studies carried out in the laboratories of the ETC and by a trial and error approach in order to maintain practical operation of each pulsed unit.

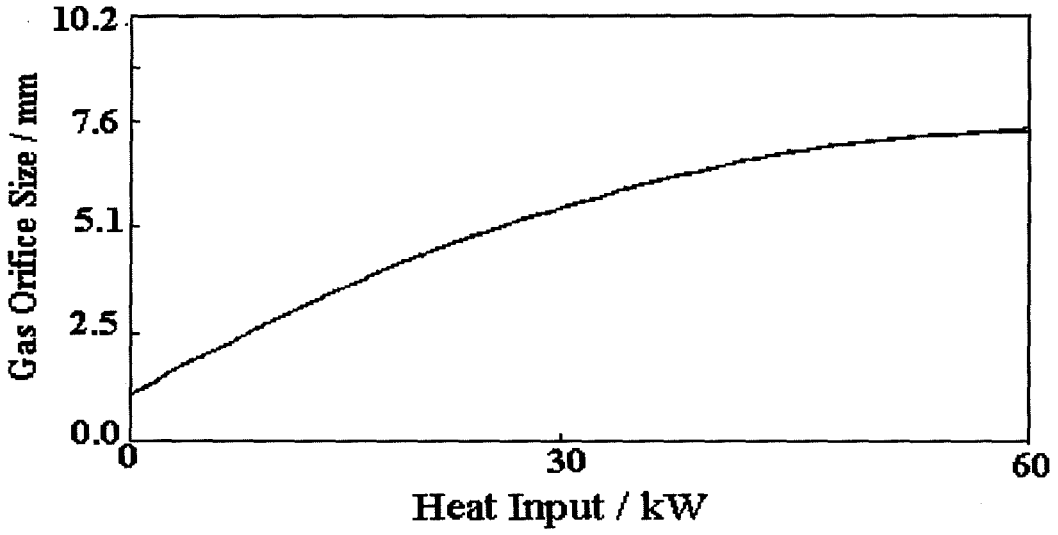

Fig. 2.18 Heat input rate versus gas orifice size (After Vishwanath, 1984).

The above procedure led to the satisfactory operation of the 7.5 and 15 kW combustors when using a gas orifice of 3 mm diameter and of the 30 kW combustor with a gas orifice diameter of 4 mm. No further study on the effect of the gas orifice diameter on the operating conditions of the pulsed units was carried out. However, it is reported that the orifice size may influence the fuel injection timing and amount of excess air in a non-premixed combustor although operating frequency was found to be almost independent of orifice diameter [Corliss *et al.*, 1987].

2.2.5.2 Air and Gas Decouplers

The air and gas decouplers employed in this study, were simply expansion chambers placed in the path of the air and fuel gas lines into the system, to provide stable operation of the pulsed combustors and to reduce the noise level. It is known that the design of the decoupler has a significant impact not only on sound emissions but also upon the stability of a pulsed combustion burner [Vishwanath, 1984]. To design and size the air decoupler for this study, guidelines given by Griffiths and Weber [1969] and Vishwanath [1984 and 1985] together with trial and error procedures were used. Vishwanath considered that the inlet pipe length, inlet pipe diameter and decoupler volume were the important parameters that influence the design of an inlet decoupler.

Air decoupler volumes of 550, 1300 and 1800 ml with inlet air pipe diameters of 15, 22 and 28 mm to the mixer head were found to be satisfactory for the 7.5, 15 and 30 kW combustors respectively.

A series of tests was conducted with changes to the length, diameter and the position of the inlet and outlet of the air decouplers while keeping the volumes constant. It was found that there was no detectable change in the performance of the combustors, indicating that the volume of the decoupler was the most significant parameter and that the shape and the location of the inlet and outlet on the air decoupler was not critical to the operation of the combustor.

Similarly, for each combustor a gas decoupler was employed to prevent pressure pulsations from being transmitted to the gas flow meter and the supply line, allowing more accurate and precise readings of the gas flow rates. Preliminary tests showed that gas decoupler volumes of 200, 670 and 1100 ml were adequate in the case of the nominally 7.5, 15 and 30 kW pulsed burners respectively.

2.2.5.3 Determining the Length of the Air Inlet Lines

To determine the length of the air inlet line from the fan into the air decoupler, Vishwanath's guidelines were followed by first determining the decoupler frequency (*Df*) which was assumed to be approximately 60 % of the frequency of the unit without

decoupler (f_b) [Vishwanath, 1985]:

$$Df = 0.6 \times f_b \tag{2.2}$$

and then by calculating the critical (i.e. minimum) air inlet pipe length. This was obtained using the following equation [Vishwanath, 1985]:

$$L_{cr} = [\frac{12 c_s}{2\pi Df}]^2 [\frac{\pi d_p^2}{4V_d}] \tag{2.3}$$

where: L_{cr} is the critical or minimum inlet pipe length

c_s is the speed of sound at the ambient air temperature

Df is the inlet decoupler system frequency

d_p is the internal inlet pipe diameter

V_d is the inlet decoupler volume.

Substituting the known values in to equation (2.3) an approximation of the critical inlet pipe lengths for the nominally 7.5, 15 and 30 kW pulsed combustors were calculated to be 470, 790 and 900 mm respectively. Since the inlet pipe length should be of value greater than L_{cr} [Vishwanath, 1984 and 1985], and taking into consideration the available space and arrangement of the units, inlet pipe lengths of 1000, 1250 and 1400 mm were chosen. Tests showed that the above lengths provided satisfactory operation of the pulsed combustors.

For the nominally 7.5 and 15 kW pulsed burners a gas line diameter of 15 mm and lengths of 500 and 700 mm were used from the rotameter to the decoupler. These values were increased to 22 mm diameter and 1100 mm length in the case of the nominally 30 kW pulsed burner. These values were obtained by a trial and error procedure.

2.2.5.4 Sizing the Exhaust Decoupler System

The main reason for the use of an exhaust decoupler in the present design was to reduce

noise emission. However, it may also influence the operating condition of the pulsed unit. It has also been reported that the exhaust decoupler could be also used as an additional heat transfer area [Griffiths and Weber, 1969].

In the case of the exhaust decoupler system, the parameters likely to affect the performance are the decoupler volume, vent pipe diameter and length [Vishwanath, 1984]. The exhaust decoupler should be sized so as to obtain a volume as large as possible within the available space for each pulsed combustor. It has been reported that with larger volumes, greater reduction in exhaust noise emissions can be achieved [Griffiths and Weber, 1969 ; Vishwanath, 1984 and 1985]. For the present design of pulsed units a well-baffled motor car silencer of 6000 ml volume was used. To compare the performance of the three combustors under investigation it was decided to use the same exhaust decoupler configuration for each combustor.

The vent pipe diameter and length may also affect the unit's performance. The vent pipe diameter should be adequately sized so that the emitted noise is reduced while not adversely affecting the stable operation of the burner [Vishwanath, 1984]. Vishwanath recommended similar calculation for the vent pipe length to those used to calculate the critical length of the inlet line. The exhaust silencer used in the present study had a vent pipe length of 150 mm with a 45 mm internal diameter.

2.3 Turn-down Ratio

One of the limitations of a pulsed combustor is an inherent relatively low turn-down ratio compared with conventional systems. In fact, this disadvantage may be one of the main reasons which has prevented the widespread use of pulsed combustors for commercial purposes. During the initial testing of the developed pulsed combustors it was observed that there is a lower limit and upper limit of the input fuel gas rate within which each combustor could operate. The failure to operate with higher gas input rates than the upper limit may be attributed to a) insufficient combustion air inside combustion chamber to sustain combustion and b) decrease in cycle time to complete the combustion process. As mentioned in previous chapter there should be sufficient heat release to provide the

driving force necessary to overcome the damping in the combustor. Tests showed that the nominally 7.5, 15 and 30 kW combustors generally failed to run at gas input rates of higher than 240, 390, and 860 ml s^{-1} respectively. In this study, tests also showed that the pulsed units failed to run at gas input rates below 116, 190 and 410 ml s^{-1} for the 7.5, 15 and 30 kW combustors respectively. Failure of operation at lower gas input rate can be attributed to the associated high levels of excess air (see Chapters 4 and 6) and possible high phase difference (i.e. above 90°) between heat release and pressure oscillations. High excess air results in insufficient energy transfer from the initial mixture control volume to propagate the flame, and the mixture become non-flammable. Phase angle data was not available to confirm the effect.

Results obtained from a series of tests showed that these limits and hence the turn-down ratio of the pulsed systems can be altered by changing the configuration of the unit. Table 2.1 shows the influence of the configuration of the pulsed unit on the turn-down ratio. It can be seen that the turn-down ratio of the pulsed combustors improved with increasing tailpipe length, combustion chamber volume and with increase of the flapper valve thickness. The maximum turn-down ratios achieved for the developed nominally 7.5, 15 and 30 kW pulsed combustors were almost similar at 1.75:1.

It is shown in Chapters 4 and 5 that a change of configuration of the pulsed units affected the operating frequency of the systems and may in turn modified the turn-down ratio. It should be noted that the consequence of an increase in the turn-down ratio may be higher pollutant emissions and noise levels.

Windmill [1984] has reported an improvement of turn-down ratio by reducing the mixture inlet area of the pulsed combustor. The validity of the above was examined using the 15 kW pulsed combustor. The mixture inlet area of the pulsed system was reduced by blocking symmetrically 2 and then 4 of the 10 inlet ports. As more inlet mixture ports were blocked the maximum gas input rate at which system would run for a given configuration was decreased (i.e. from 14 kW to about 12 kW). It appeared that the turn-down ratio of the unit with 4 inlet ports blocked was greater than with other configurations of the pulsed combustor. When 6 of 10 ports were blocked the pulsed system did not operate successfully. The results obtained are presented in table 2.2.

The Nominal Input Pulsed Combustor	Combustion Chamber Volume / ml	Tailpipe length / mm	Flapper Valve Thickness / mm	Lower Limit of Gas Input / ml s^{-1}	Upper Limit of Gas Input / ml s^{-1}	Turn-Down Ratio
7.5 kW	80	1500	0.15	118	200	1.70:1
	95	1500	0.15	126	216	1.71:1
	110	1500	0.15	130	225	1.73:1
	110	2300	0.15	142	249	1.76:1
15 kW	300	1500	0.15	208	356	1.71:1
	350	1500	0.15	217	375	1.73:1
	385	1500	0.15	222	389	1.75:1
	350	2000	0.15	224	395	1.76:1
	350	2500	0.15	219	389	1.78:1
	350	1500	0.13	208	333	1.60:1
	350	1500	0.25	222	383	1.73:1
	350	1500	0.36	226	395	1.75:1
30 kW	1100	2000	0.15	417	695	1.66:1
	1164	2000	0.15	443	745	1.68:1
	1216	2000	0.15	459	778	1.69:1
	1269	2000	0.15	486	834	1.71:1
	1300	2000	0.15	497	861	1.73:1

Table 2.1 ***Variation of turn-down ratio with configuration of the pulsed units***

Number of Mixture Inlet Ports Blocked	Lower Limit Gas Input Rate / ml s^{-1}	Upper Limit Gas Input Rate / ml s^{-1}	Turn-Down Ratio
0	217	375	1.73:1
2	190	335	1.77:1
4	175	315	1.80:1

Table 2.2 ***Variation of turn-down ratio with change of total mixture inlet area.***

Chapter Three

Instrumentation and Experimental Techniques

3.1 Introduction

In previous chapters, details of the design and construction of the pulsed combustors have been discussed and their underlying principle of operation was explained. In this chapter the general experimental arrangement of the pulsed units is shown and detailed description of the instrumentation and methods of measurement employed in this study are reviewed.

The performance of the pulsed combustor units is dependent upon the fuel gas composition and its firing rate (fuel consumption) and upon the geometry and configuration of the components of the unit. As these were changed measurements of the following performance outputs were made:

- Excess air ratio
- Cycle time or operating frequency
- Pressure oscillations*
- NO_x and CO emission levels
- Overall thermal efficiency of the unit as a water heater
- Temperatures within the unit
- Noise levels.

The analysis of data obtained from these measurements enables us to provide detailed information and understanding of the operation and performance of pulsed combustor units which can be used for improving design and further development of such units.

---

* Throughout this thesis the term pressure oscillation, pulsing pressure and operating pressure have similar meanings.

Details are given below of the instrumentation and measuring techniques required for the measurements of gas input rates, temperatures of flue gases, gaseous emission concentrations, operating frequency, pulsing pressure and noise emission levels.

3.2 The Laboratory Arrangement of the Pulsed Units

A schematic diagram of the experimental arrangement of the pulsed combustors designed and constructed for the present study is shown in Fig. 3.1. The combustors were of the Helmholtz-type, with cylindrical components. Each unit was mounted in a 0.062 m^3 volume water tank with the combustion chamber and the exhaust tube immersed in the water.

For each combustor a toroidal fan was employed to supply air during the ignition sequence. A spark plug (Bosch) connected to an ignition system was used to ignite the mixture of air and fuel gas and was positioned in the path of the mixture of air and gas (the reactants) downstream of the flapper valve assembly inside the combustion chamber. Once pulsing combustion was established, the fan together with the spark plug were switched off. During the initial tests it was found that the width of the gap of the spark plug should be set at around 4.0 mm for successful ignition to be achieved.

Natural gas was fed from the mains and was pressurised by a gas booster pump. A pump, Model M5 (The Utile Engineering), having a maximum duty of 5.5 $m^3 h^{-1}$ / 650 mbar at room temperature was employed for the 15 and 30 kW combustors and a gas booster pump Model EM15 (The Utile Engineering), with maximum duty of 2.0 $m^3 h^{-1}$ / 254 mbar at room temperature for the 7.5 kW combustor. Low and high pressure switches were used before and after the gas booster pump respectively, to shut off the flow of gas should there be significant leakage in the line. An adjustable low pressure regulator Model 226 MK (Dunkins Ltd.), to eliminate fluctuations in the line pressure, was fixed in series with the gas compressor allowing the gas to exit at a steady gauge pressure up to 25 mbar. The fuel gas flow rate was controlled by a valve in the line immediately before a calibrated rotameter.

The air flow rate could not be measured directly by a variable area flow meter due

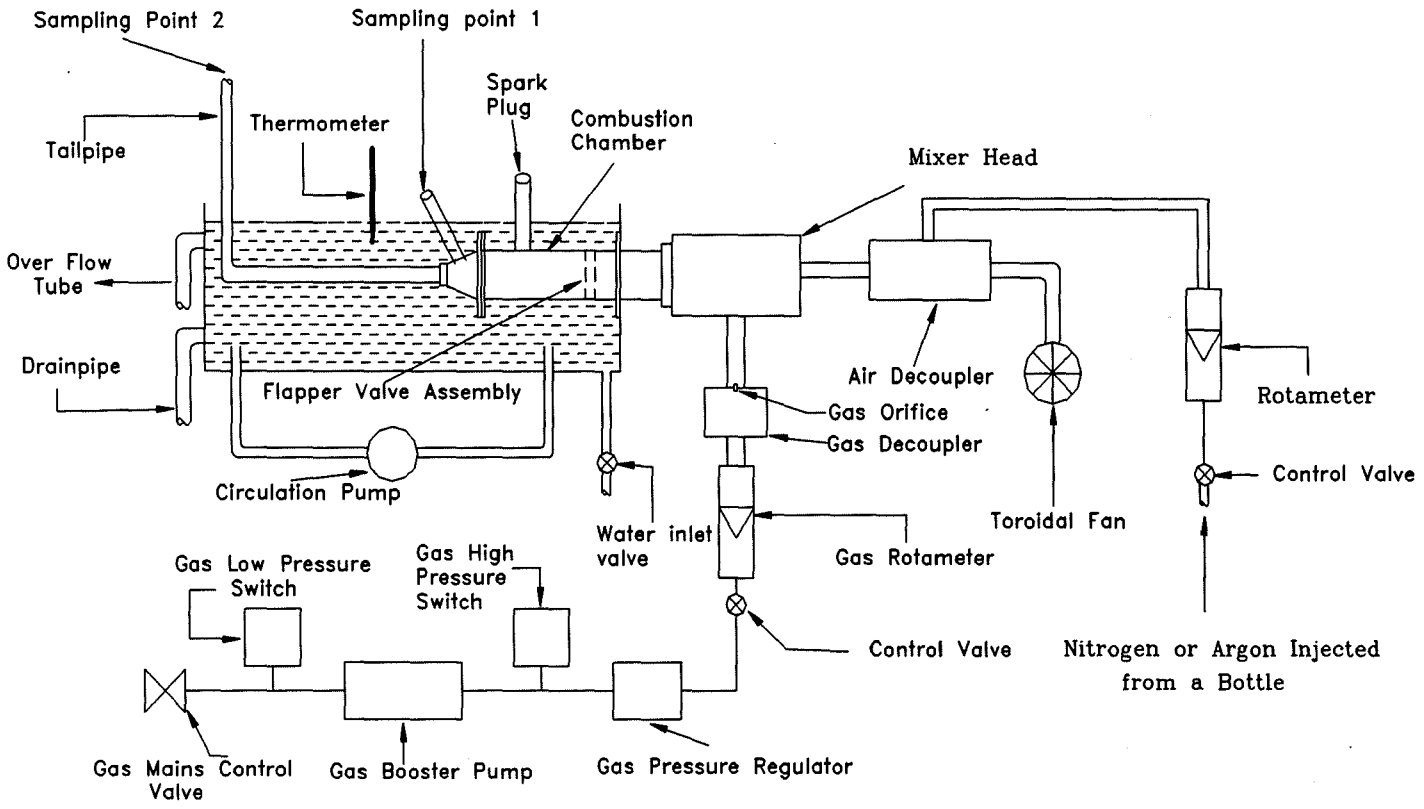

Fig. 3.1 A schematic representation of the experimental arrangement of the developed pulsed combustors.

to pressure fluctuations within the inlet delivery system. An attempt was made to measure the air consumption rate by using an orifice plate, but the orifice plate restricted the air flow to the combustor and halted its operation. Therefore, the air flow rate was calculated from the oxygen concentration in the exhaust gases and the known fuel gas composition and flow rate.

3.3 Measurement of the Input Gas Flow Rate

The fuel gas volume flow rate into the pulsed units was measured using a calibrated (at 15 °C and 1020 mbar absolute) rotameter (type 2000, KDG Ltd) immediately downstream of the control valve.

This study included measurements of the performance of the pulsed combustors burning various test gases and with addition of nitrogen or argon. The test gases were fed directly from a cylinder to the mixer head via the low pressure regulator and calibrated rotameter. The flow rate of these test gases was measured using a rotameter calibrated for mains natural gas. Hence a correction was required to the readings to determine the actual flow rate of these test gases. The following relation was used for correction of the readings:

$$V_{G_2} = V_{G_1}\sqrt{\frac{\sigma_{G_1}}{\sigma_{G_2}}} \qquad (3.1)$$

where: V_{G1} is scale reading of G_2 flow rate,

V_{G2} is actual value of G_2 flow rate,

σ_{G1} is the relative density of gas G_1 and

σ_{G2} is the relative density of gas G_2.

Detailed derivation of the above equation is given in Appendix III.

The added N_2 or Ar volume flow rate was measured using a smaller rotameter (Type 1100 KDG Ltd) calibrated for nitrogen at 15 °C and 1020 mbar. Thus, equation (3.1) was used when argon was passed through it to obtain correct readings of the argon

volume flow rate. The flow of either nitrogen or argon from the bottle was controlled by a pressure regulator and a control valve upstream of the rotameter (see Fig. 3.1). In addition, to ensure that the readings were correct, the nitrogen or argon input pressure was monitored constantly throughout all the tests using a manometer placed immediately upstream of the rotameter. Temperature also was checked and found to be close to calibration temperature, i.e. 15 °C, in all cases.

3.4 Temperature Measurement

An important parameter when analysing the data relating to gaseous emissions from the pulsed combustors is the temperature of the gases inside the combustion chamber and in the tailpipe. Therefore, at two sampling points the time-averaged flow temperature was monitored using type "K" (chromel-alumel) thermocouples. The thermocouples were enclosed in mineral insulated metal sheaths, so that they could be used above 800 °C [BS 1041- part 4, 1992]. The thermocouples were directly connected to a high input impedance digital meter (Comark, Model 2501). The meter incorporated cold junction compensation and built in linearization circuitry. In these temperature measurements no radiation corrections were made.

During the experimental measurements the water bath temperature was maintained constant at a value above the dew point of the exhaust gases. The temperature of water inside the tank was measured using a mercury thermometer immersed in the water. For most tests the water bath temperature was kept at 65±1°C which was some 5 °C above the dew point of the exhaust gases at stoichiometric conditions. The dew point of the exhaust gases was calculated based upon the volumetric percentage of water vapour in the combustion products (see Appendix VI).

3.5 Measurement of Combustion Products

A volumetric analysis of the combustion products enables the performance of the

combustors to be characterised and can also be used to calculate other important parameters. For example, in this study O_2 measurement was used to calculate the excess air in the combustion chamber and hence the air flow rate.

The combustion products were analysed for CO and CO_2 using an infra-red analyser (Analytical Developments, model WA-558A) and O_2 using a paramagnetic analyser (Servomex, OA500 model). For NO and NO_x (i.e. NO + NO_2) concentration a chemiluminescent analyser (Rotork Analysers, model 443) was employed and NO_2 was determined by the difference of the two gases.

Exhaust gas samples were withdrawn from the end of the tailpipe (i.e. sampling point 2), using a stainless steel probe with a polypropylene sample line. These materials provide non-reactive surfaces to contact with the exhaust samples; it is well known that NO and particularly NO_2 are reactive gases. At the beginning of the sample line a water trap was used together with a coarse filter to prevent any condensate and particulates from entering the analyser. The exhaust gas samples were dried completely with the aid of a drying column containing anhydrous $CaCl_2$ before entering the infra-red analyser. Soda lime was used to strip carbon dioxide from clean air zero gas and provide a supply of CO_2-free air for purging the carbon dioxide analyser optical path in addition to the zero gas for setting up the analyser.

For the NO_x measurements the sample gases were passed through a heated line to the analyser and dried by a permeation dryer within the analyser. It is known that NO_x (especially NO_2) is soluble in water. Also, removal of water from the sample can minimize the quenching error which is associated with the chemiluminescent method.

All the employed analysers were calibrated before each set of test measurements by using bottled span gases. The span gases were a mixture of known concentrations of the gases required for analysis (e.g. 80 ppm NO balanced with nitrogen). The analysers also calibirated for zero readings using purified bottled air.

The principles of gas analysis by infra-red absorption, oxygen measurements by magnetic means and chemiluminescent gas methods for NO_x measurements are given in Appendix IX.

3.6 Measurement of Pulsing Pressure and Frequency

The pulsating pressure for each pulsed combustor was measured at the outlet of the tailpipe (sampling point 2) using a low pressure quartz transducer (Kistler, type 7261). The pressure transducer was firmly mounted above the vertical tailpipe outlet with adjustable position and orientation. After a series of preliminary tests it was found that the trace with the least noise levels was obtained by placing the transducer 30 mm from the tailpipe outlet in line with and facing it. This was in agreement with Suthenthiran investigation [1988].

Signals from the transducer were displayed on a storage oscilloscope (Model 221, Tektronix). The measuring range of the transducer was between -1 to 10 bar with sensitivity of 2200 pC bar^{-1} or 20 V bar^{-1}. The transducer had been calibrated by the manufacturer and had a resonance frequency of 2.5 kHz. The electrical charge signals yielded by the piezoelectric sensor were converted into a proportional voltage with the aid of a charge amplifier (Kistler, type 5039A) positioned in series with the oscilloscope. The charge amplifier was set up to operate at two ranges of 2.0 and 0.5 bar at full-scale (i.e. 10 Volts). A block diagram of the arrangement of the apparatus is given in Fig. 3.2.

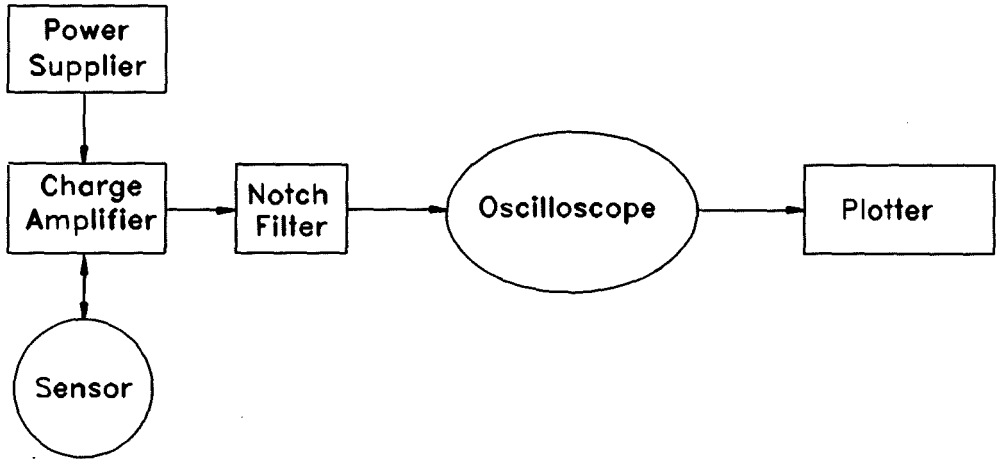

Fig. 3.2 A block diagram of the experimental arrangements used for pulsing pressure measurements.

The initial observed pressure pulsation signals were a complex waveform produced by the compounding of the fundamental frequency and included noise of relatively constant frequency of around 2.0 kHz. A notch filter was incorporated between the transducer and the oscilloscope to condition the trace by blocking the unwanted noise. A typical trace of signals is shown in Fig. 3.3. The frequency of pulsing was determined from the trace by measuring the peak to peak time. The presented pulsing frequency and pressure data in this report were obtained from an average of more than 250 cycles in each case.

3.7 Noise Measurement

In this study the noise characteristics of the pulsed combustors were investigated. Sound measurements were made using a Bruel & Kjaer precision sound level meter Model 2203 and active filter set type 1613 as these allowed a detailed analysis of the sound spectrum to be made. These readings were confirmed using a digital impulse sound level meter model D1422 (DAWE Instruments). All the measurements were carried out with the sound level meters situated 1 metre from the given source of noise and at 45° angle to horizontal, in line with the source.

The Bruel & Kjaer sound level meter was of type 1 requirements for both free field and random incidence measurements. It had an accuracy of ±1dB with a typical frequency range (within + 0.5 to -3 dB) better than 10 Hz to 25 kHz in all ranges. Figure 3.4 shows a schematic diagram of the sound level meter (type 1) which was employed in this study.

The type 1 sound level meter comprised a sensitive microphone which was of the condenser type acting as a capacitor with constant charge, a 10 dB step attenuator, a battery-powered amplifier, weighting networks and slow and fast averaging responses. The microphone employed converted the sound to an equivalent electrical signal. However, the electrical signal produced was weak and so it was amplified by a preamplifier before being processed. The amplifier frequency response was flat within 2 dB from 2 to 15000 Hz, although it should be noted that the overall frequency

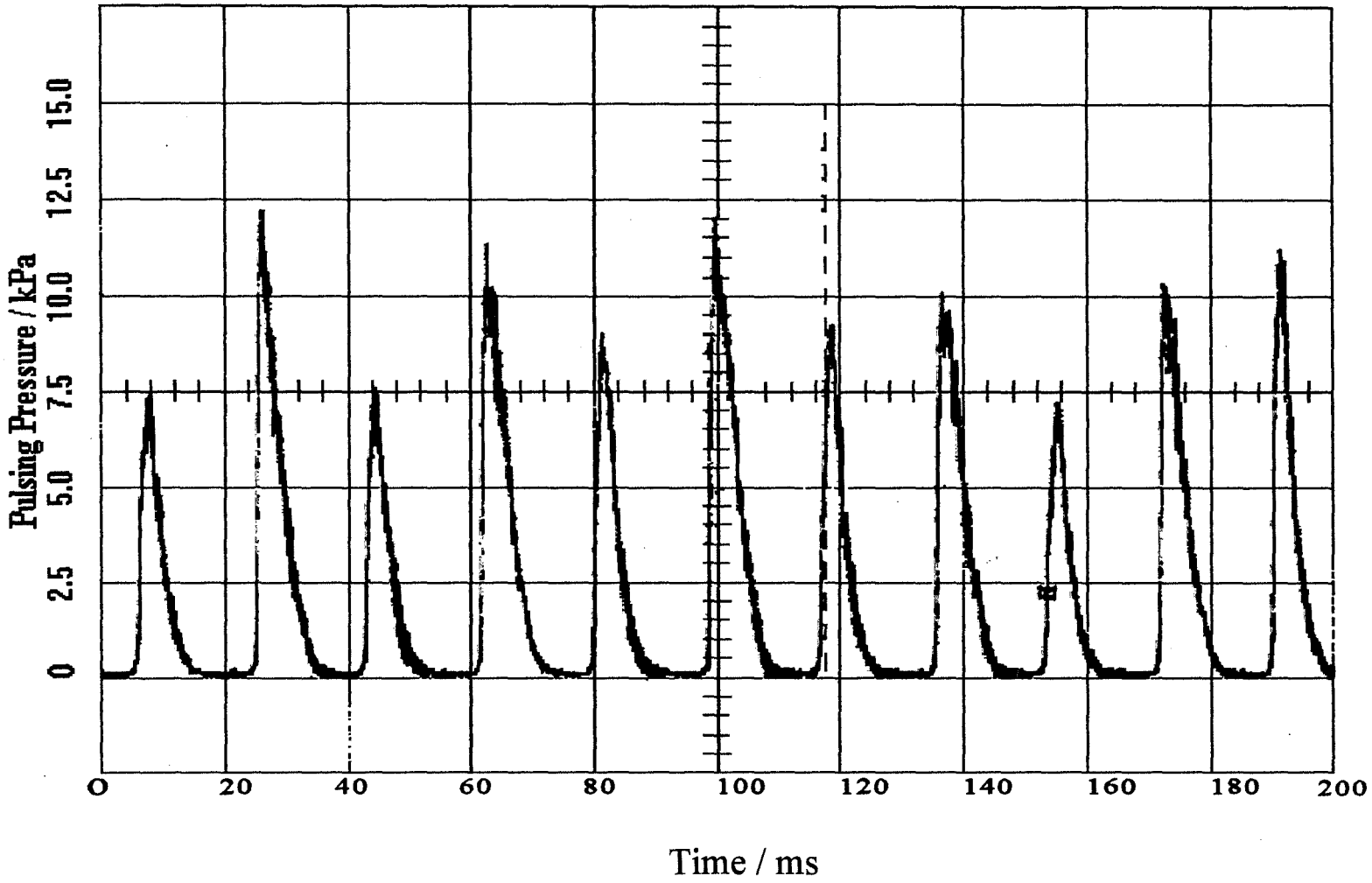

Fig. 3.3 A typical trace of pressure against time from the developed pulsed combustors measured at the tailpipe exit.

response is usually determined by the microphone characteristic. The amplifier was equipped with an input stage which had a high input impedance to match the condenser microphone.

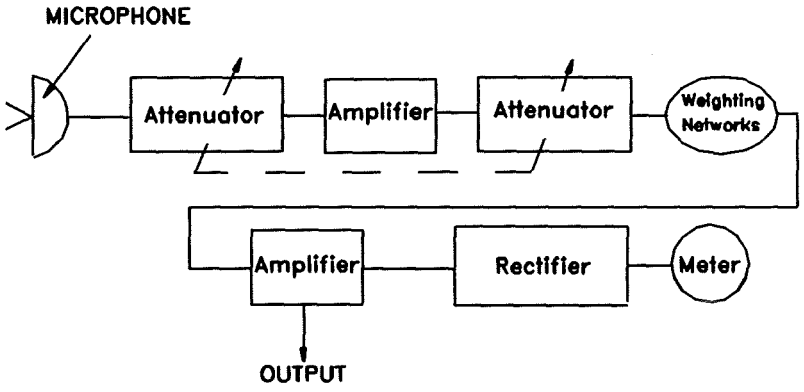

Fig. 3.4 ***A schematic representation of the type 1 sound level meter [After Warring, 1974].***

3.7.1 Frequency Analysis

The principle uses for frequency analysis in noise control are:

a) to identify dominant sources of noise,

b) to optimize the selection of methods, materials and structures for controlling noise.

The analysis can be performed in either "real time" or "extended time". In this study the former was used and refers to a frequency spectra that is calculated and presented with virtually no delay - essentially in real time. For the frequency analysis in this study an octave filter set type 1613 (Bruel & Kjaer) and a dual channel signal analyser type 2032 (Bruel & Kjaer) were employed. Although, the dual channel signal analyser was primarily designed for dual channel measurements it had the features required in a single channel Fast Fourier Transformation (FFT) analyser. The resolution of the analyser in the frequency domain was 801 lines, with a frequency span from 1.56 Hz to 25.6 kHz. The real time frequency of the analyser was greater than 5 kHz in dual channel

operation, rising to greater than 10 kHz for single channel operation. Before using the 2032 analyser it was calibrated with reference to the sensitivity of the microphone used i.e. 47.3 mV/ Pa.

With the aid of FFT processing, the time-domained samples were transformed to frequency domain signals, allowing the frequency domain representation of the primary signals to be obtained. The heart of spectral analysis is the Fourier transform. It exists for all transients of finite energy which include all signals of finite duration and finite amplitude. The Fourier transform identifies or distinguishes the different frequency sinusoids and their respective magnitudes which combine to form an arbitrary waveform. In this way the noise relevant to any specific frequency was identified. The samples taken in the present work were an average of 1000 readings. Hard copy of sound vs frequency traces were obtained using a graphics recorder type 2313 (Bruel & Kjaer).

Chapter Four

Operating Frequency

4.1 Introduction

Pulsed combustion is acoustical in nature and occurs via a cyclic process and therefore, frequency is a fundamental parameter. It is evident that the frequency and hence cycle time sets a limit on the time available for ignition and burning of the premixed charge of gas and air admitted during each cycle and determines the volume of the charge per cycle for a given mean gas flow rate. In addition, the fundamental frequency has an important bearing on the noise quality and the design of measures to attenuate the noise. There have been a number of studies regarding pulsing frequency of mechanically-valved pulsed combustors [e.g. Corliss *et al.*, 1987 ; Keller *et al.*, 1989] but data are generally sparse concerning the factors controlling the pulsing frequency for a premixed pulsed combustion system of design similar to that used in this study.

In the light of the above, a systematic investigation was carried out in which the influence of adjustable parameters upon the operating frequency was studied. Parameters included:

i) input firing rate,
ii) air-to-fuel ratio (A/F); this is normally a dependent variable once the air fan has been switched off after ignition but can be adjusted by running the air fan,
iii) combustion chamber volume,
iv) tailpipe length,
v) thickness of the inlet mixture flapper valve.

Such experimental measurements of the pulsing frequency of the present design of pulsed combustors, provided an extensive body of data which is reported in this chapter. The analysis of this data contributed to a better understanding of the fundamental processes governing the operation of the present type of pulsed combustion system. This, together with other aspects of this study, enabled the optimum operating

conditions for these appliances to be determined and provided information on scaling and characteristics of the pulsed combustors which can be used in the designs of practical systems.

4.2 Effect of Fuel Gas Flow Rate

Experimental measurements of the pulsing frequency of the three nominally 7.5, 15 and 30 kW pulsed combustors at various fuel gas flow rates were carried out. In these tests the geometry of the combustors remained constant and the air fan was switched off once pulsing was achieved. A detailed description of the measurement methods and apparatus employed for these tests is given in Chapter 3. Figure 4.1 shows the variation of operating frequency of the pulsed combustors with the fuel gas input rate. It can be seen that operating frequency increased as the fuel gas rate increased and was typically in the range of 35-60 Hz.

The observed trend in variation of frequency with input gas flow rate (Fig. 4.1) can be ascribed to the resultant variation in the combustion gases temperature. In these self-aspirating combustors, as the fuel gas rate was increased the amount of excess air decreased and consequently the temperature of combustion gases increased as shown in Fig. 4.2. Equations (1.3) and (1.4) indicate that an increase in the frequency with fuel gas rate would be expected in line with the findings here.

According to equation (1.4) an increase in the temperature of combustion gases increases the velocity of sound. As shown in equation (1.3) for a Helmholtz resonator the resonant frequency is proportional to the velocity of sound. Therefore, an increase in the temperature of the combustion gases due to an increase in the fuel gas flow rate increased the resonant frequency and hence the operating frequency of the pulsed combustors.

Another possible contributing factor to the observed increase of frequency with increase of fuel gas input rate is the subsequent variation in the total ignition delay time. In Chapter 1 it was explained that to fortify pulsation in a pulsed combustor,

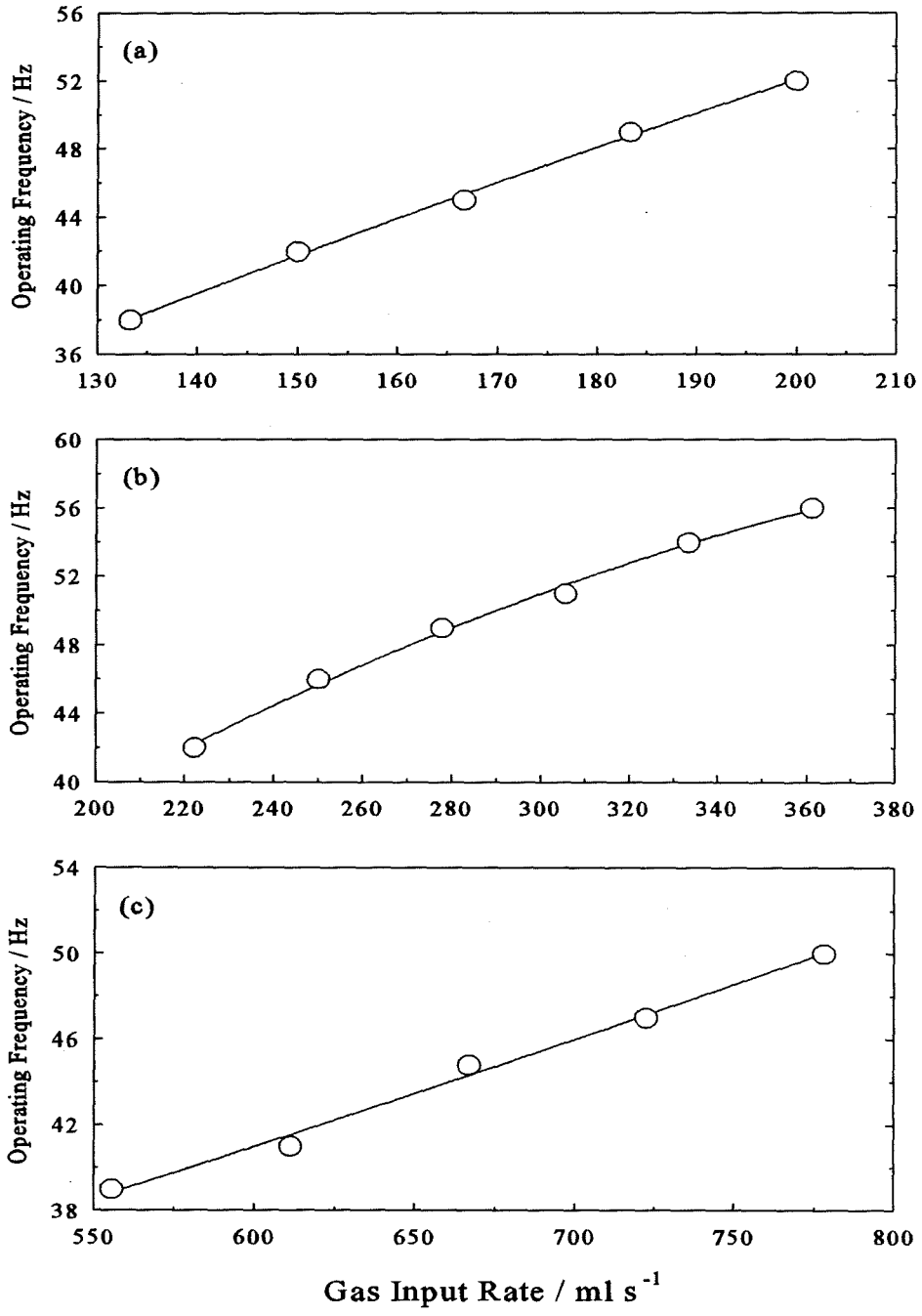

Fig. 4.1 Variation of operating frequency with fuel gas input rate for a) the 7.5 kW combustor with combustion chamber volume of 110 ml, b) the 15 kW combustor with combustion chamber volume of 370 ml and c) the 30 kW combustor with combustion chamber volume of 1270 ml. Tailpipe length and flapper valve thickness were kept constant at 2000 mm and 0.15 mm respectively for the three combustors.

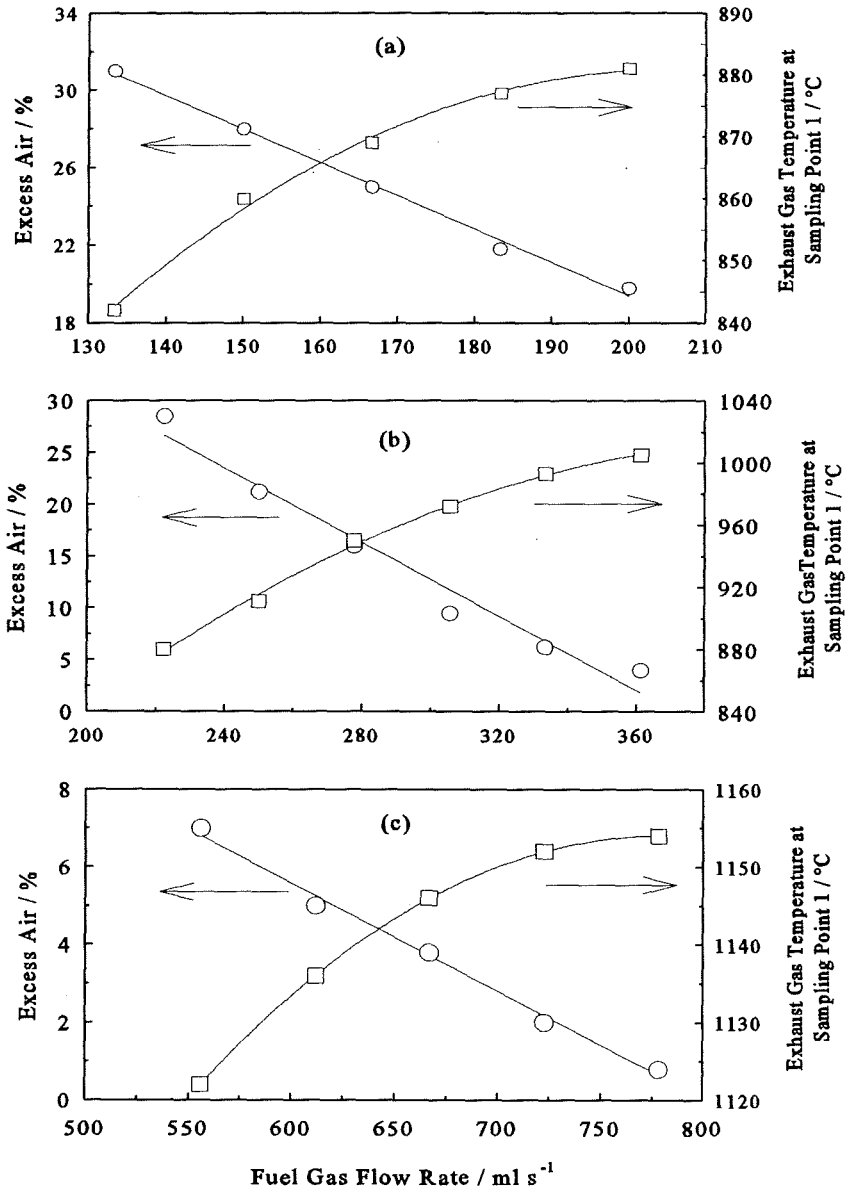

***Fig. 4.2** Variation of percentage excess air and measured temperature in the combustion chamber (i.e. sampling point 1) for a) the 7.5 kW combustor with combustion chamber volume of 110 ml, b) the 15 kW combustor with combustion chamber volume of 370 and c) the 30 kW combustor with combustion chamber volume of 1270 ml. Tailpipe length of 2000 mm and flapper valve thickness of 0.15 mm was used for the three combustors.*

there should be an ignition delay time so that the Rayleigh criterion is satisfied. It was also explained that the total ignition delay time is a function of each of the characteristic times [Keller *et al.*, 1989] for the governing processes including the time for the chemical reactions to occur (i.e. $\tau_{kinetic}$) and the time required for mixing the reactants with remaining combustion gases (i.e. τ_{mixing}). The change in the total ignition time in turn influences the phase relationship between the energy release and the pressure oscillations and hence frequency as described in Chapter 1, section 1.8 [Keller *et al.*, 1989 ; Jones and Leng 1994]. With the reference to the above assumptions, the effect of the fuel gas rate and other changeable parameters, upon operating frequency of the developed combustors is discussed below.

The rise of the flame temperature subsequent to an increase in the fuel flow rate increases the chemical reaction rate. This can be shown by an Arrhenius type equation for the oxidation of fuel [Williams, 1990]:

$$Reaction\ Rate = A[Fuel][Oxygen]\exp(\frac{-E_a}{R_0 T}) \qquad (4.1)$$

where A is a constant, E_a is the activation energy, R_0 is the universal gas constant, T is the flame temperature. The above equation states the correlation of reaction rate with fuel, oxidizer and temperature. According to the equation (4.1) an increase in temperature subsequent to an increase in the fuel gas rate (as shown in Fig. 4.2), would increase the rate of chemical reaction. This in turn would decrease the characteristic time $\tau_{kinetic}$. The decrease of $\tau_{kinetic}$ therefore reduces the total ignition delay time (see equation 1.7). Furthermore, Keller *et al.*[1989] have reported that the characteristic time required to mix the reactants with the hot products, τ_{mixing}, has an inverse dependence upon the velocity of the inlet jet. Thus, as the fuel gas rate was increased, τ_{mixing} was decreased due to an increase in the total volume injection rate of the mixture of air and gas. This in turn also reduced the total ignition delay time. It is reported that shortening the total ignition delay time causes an increase of phase difference between the energy release and the pulsing pressure which then influences (i.e. increases) the operating frequency of the pulsed units as seen in Fig. 4.1 [Keller *et al.*, 1989 ; Jones and

Leng 1994]. In this study no phase angle data was obtained due to unavailability of the required instruments.

4.3 Effect of Boosting Air Supply

The air-to-fuel ratio (A/F) at a given fuel gas flow rate could be boosted by running the air fan during pulsating combustion. A series of tests was conducted using the 15 kW pulsed combustor with a fixed configuration. The results of these tests are shown in Fig. 4.3. At any given fuel flow rate and a fixed configuration, running the combustor with the fan decreased the operating frequency compared with the situation when the air fan was switched off. With the air fan on, values of the excess air (Fig. 4.4a) increased while the exhaust gas temperature at sampling point 1 decreased (Fig. 4.4b).

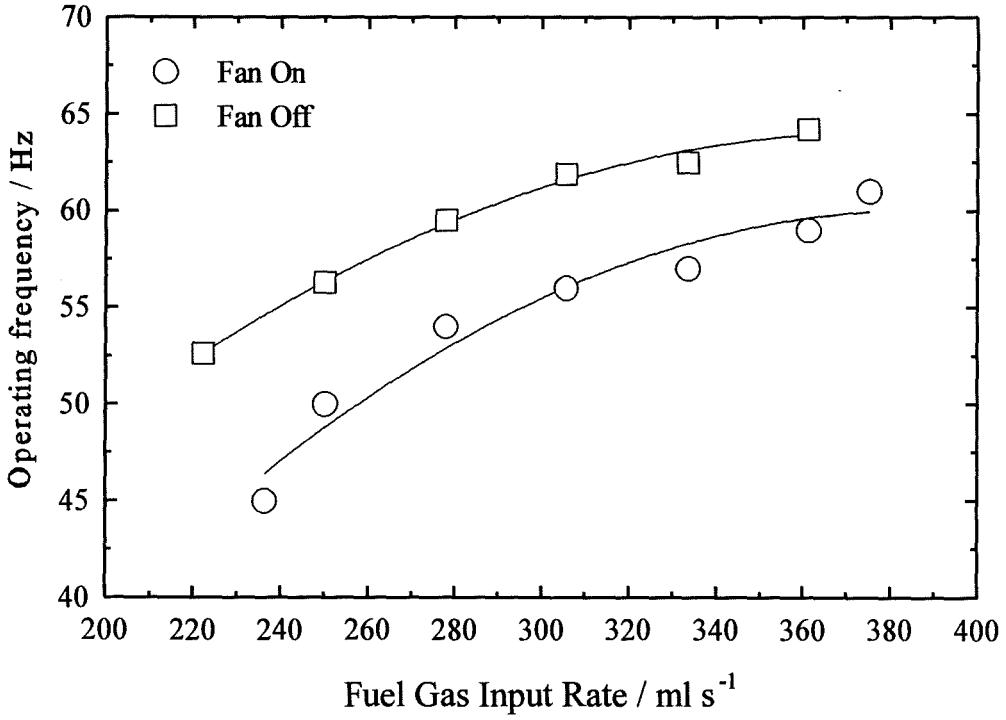

***Fig. 4.3** Effect of increasing the air flow rate by leaving the air fan on after ignition sequence, upon the operating frequency of the nominally 15 kW pulsed combustor at various fuel gas flow rates. The combustion chamber volume and tailpipe length were kept constant at 370 ml and 1500 mm respectively.*

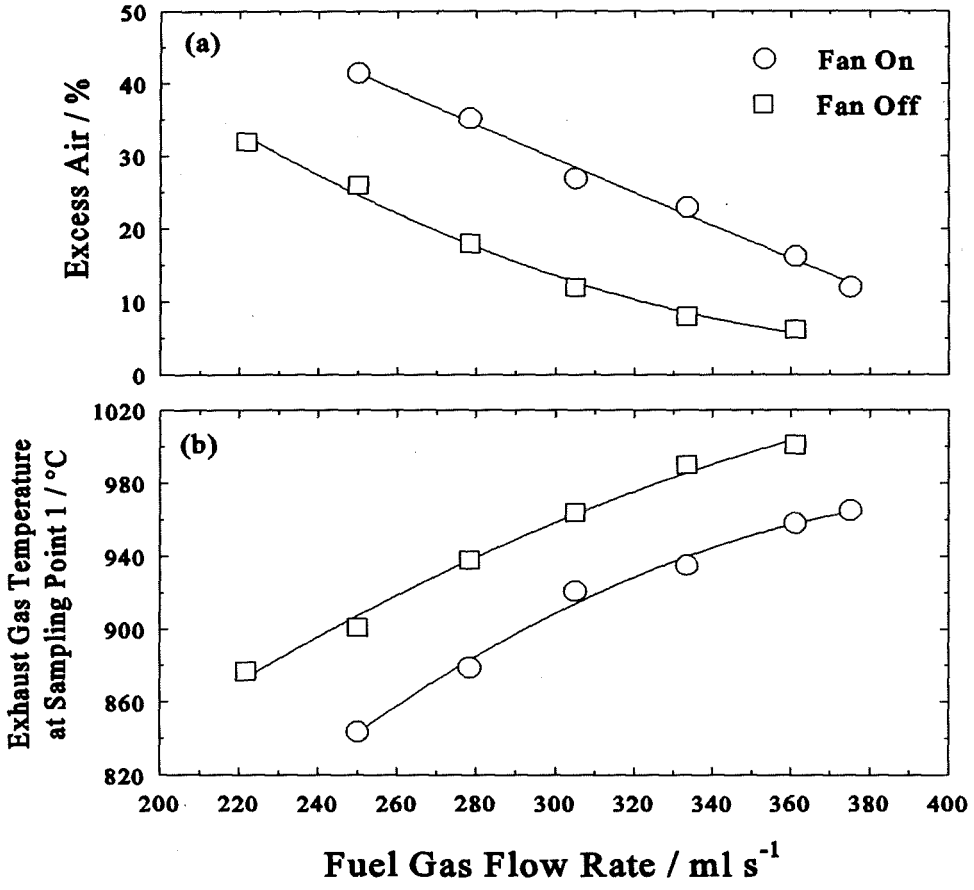

***Fig. 4.4** Effect of operating the 15 kW pulsed combustor with the air fan upon the a) excess air and b) exhaust gas temperature inside the combustion chamber (sampling point 1). The tailpipe length and combustion chamber volume used were 1500 mm and 370 ml respectively.*

The decrease in the frequency of pulsing at a given fuel rate when the air was boosted was an interesting effect and may have resulted from two main causes:

i) decreased flame temperature due to dilution by the increased air,

ii) increased total ignition delay time due to increased chemical reaction time ($\tau_{kinetic}$).

Additional insight may be gained by plotting the measured frequency against the excess air ratio, λ, as shown in Fig. 4.5 and Fig.4.6. Fig. 4.5 shows the data in Fig. 4.3 vs λ for both fan on and off operating conditions; and it is seen that all the data

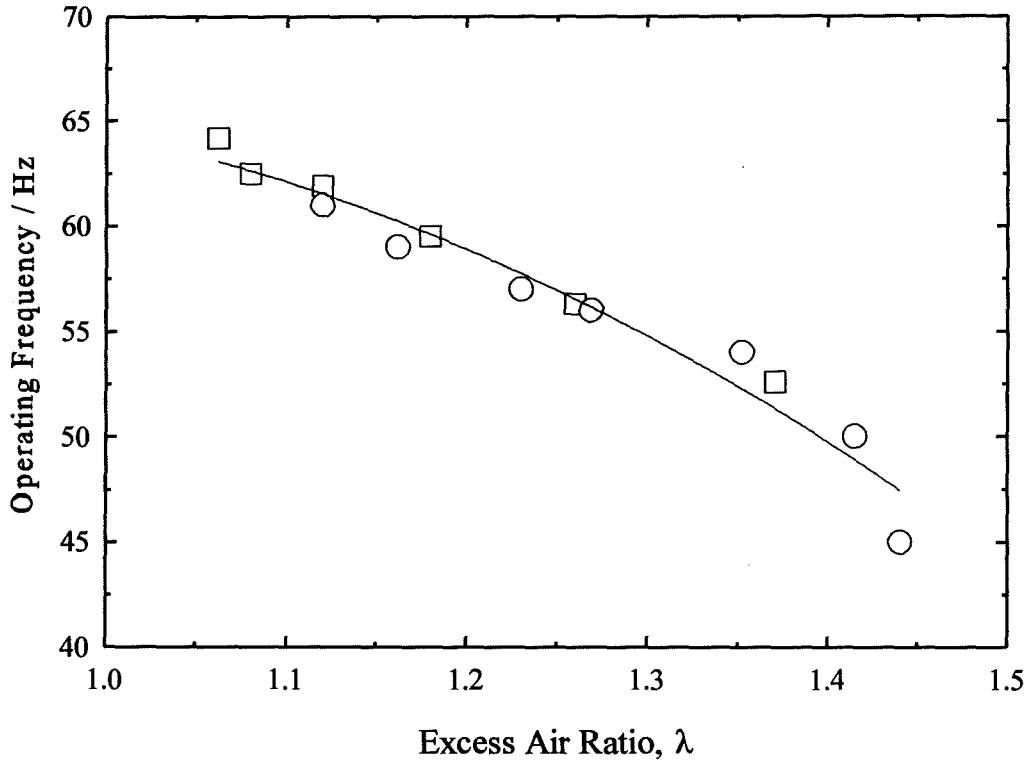

***Fig. 4.5** Variation of frequency with excess air ratio, λ using the nominally 15 kW combustor. Configuration used was: combustion chamber volume of 370 ml, tailpipe length of 1500 mm and flapper valve thickness of 0.15 mm. Symbols as in Fig. 4.3.*

follow a single curve. It will be shown later in Chapter 6 that in the present type of pulsed combustors the combustion temperature is principally fixed by the A/F. This is also shown in Fig. 4.7, where the measured exhaust gas temperature at sampling point 1 is plotted against λ, for the 15 kW combustor operating with the air fan switched on and off. It follows that for a given configuration of each combustor, the operating frequency of the present type of pulsed combustor is principally dependent upon the temperature within the combustor.

In the case of the 30 kW pulsed combustor the pulsed unit could be operated under fuel-rich condition (i.e. $\lambda < 1$). For values of λ less than 1 the frequency decreased as the mixture became richer (Fig. 4.6c). Under fuel-rich condition there

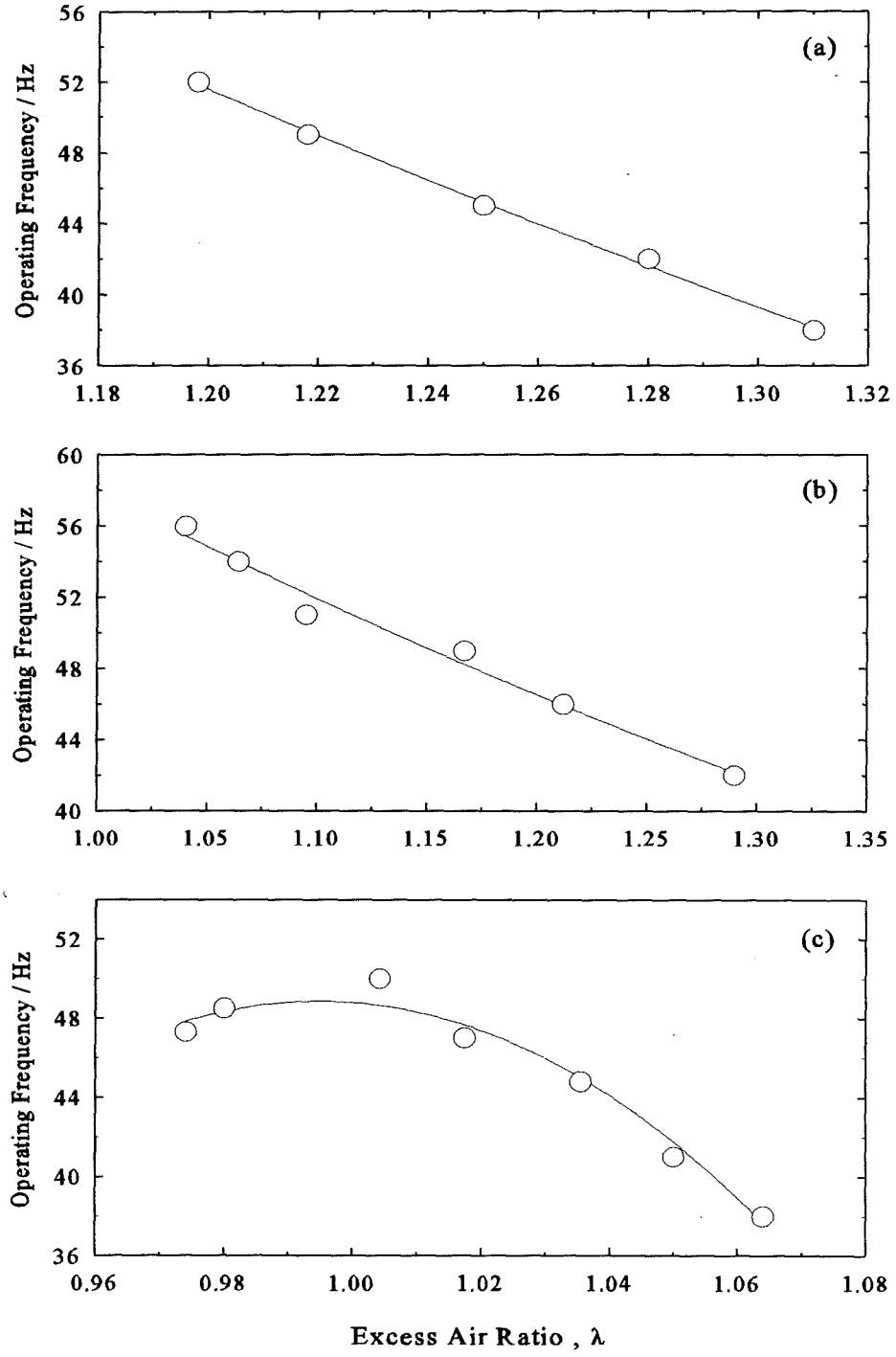

Fig. 4.6 Variation of operating frequency with excess air ratio, λ for a) the 7.5 kW combustor with combustion chamber volume (CCV) of 110 ml, b) the 15 kW combustor with CCV of 370 ml and c) the 30 kW combustor with CCV of 1270 ml. Tailpipe length and flapper valve thickness were 2000 mm and 0.15 mm respectively.

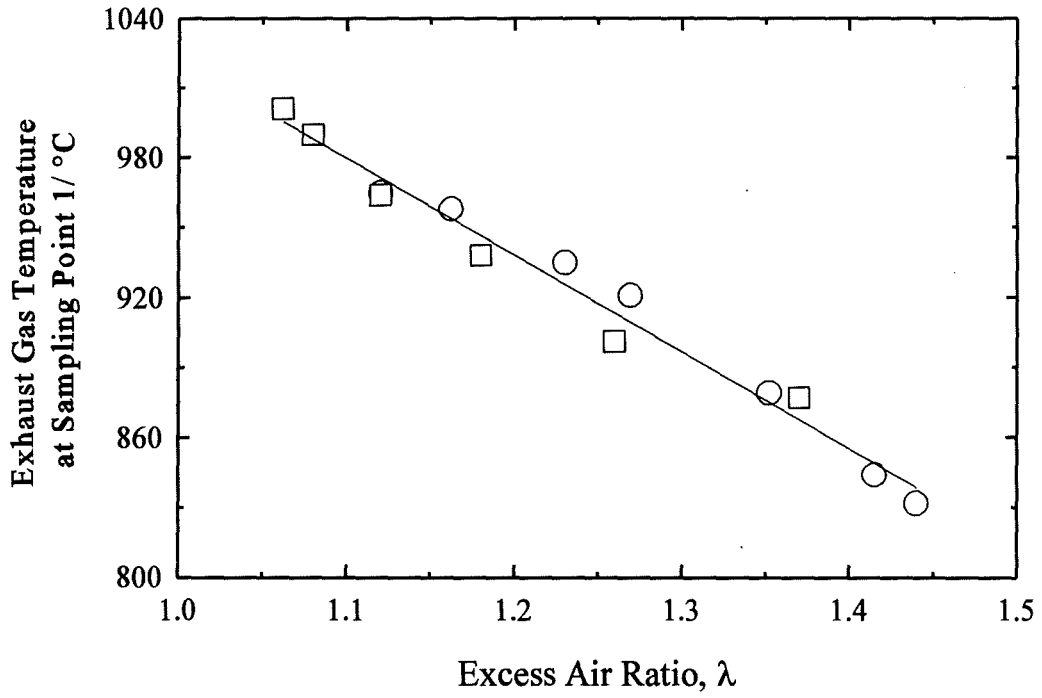

Fig. 4.7 Variation of exhaust gas temperature with excess air ratio. Configuration, Data and symbols as in Fig. 4.4

is insufficient oxygen to burn the gas completely. This results in a reduction of the energy released giving a decrease in the flame temperature and hence frequency (Fig. 4.6c).

According to the equation (4.1) an increase in the excess air brought about by running the pulsed combustor with the air fan on should give a reduced combustion reaction rate because of the reduction in *exp* $(-E_a/RT)$ and the product of mole fractions of fuel and oxidiser. This increases $\tau_{kinetic}$ and hence the total ignition delay time according to equation (1.7). But on the other hand, when running the air fan during the cycle, the inlet velocity is expected to increase. As mentioned earlier, the inlet jet velocity has an inverse relationship with τ_{mixing} [Keller *et al.*, 1989]. Thus, running the combustor with air fan should result in a reduction of τ_{mixing} which consequently should reduce the total delay ignition time (see equation 1.7). Therefore, it may well be that one effect partially offsets the other resulting in little influence on the total ignition delay

time and thereby little effect on the phase difference. However, in this work data on phase angle was not available.

4.4 Effect of Configuration upon Operating Frequency

There has been a number of reported works on the effect of the configuration upon the frequency of pulsed combustors but data generally are lacking for the premixed Helmholtz-type pulsed combustor especially for the effects produced by variation in the combustion chamber volume.

In this study variations in configuration included modifications to the combustion chamber volume (CCV), tailpipe length and flapper valve thickness.

4.4.1 Effect of Combustion Chamber Volume

The design of the combustors allowed the volume of the combustion chamber to be varied by setting the position of the flapper valve carrier within the cylindrical bore. Thus, the length of the combustion chamber was variable but the diameter was fixed for a given combustor.

Tests were carried out burning mains natural gas at a fixed tailpipe length and flapper valve thickness to identify the effect of varying the combustion chamber volume upon the operating frequency of the three developed pulsed combustors. The variation of the operating frequency with fuel gas rate for the combustors at given combustion chamber volumes is shown in Fig. 4.8. In all cases, at a given fuel flow rate, and with fixed tailpipe and flapper valve dimensions, the operating frequency decreased as the CCV was increased. Thus, the combustion chamber volume is shown to have an important influence on the operating frequency.

Interestingly, excess air values increased with decreasing combustion chamber volume at given fuel gas flow rates (see Fig. 4.9). These data were usefully developed to show frequency vs λ as shown in Fig. 4.10. As mentioned earlier in the

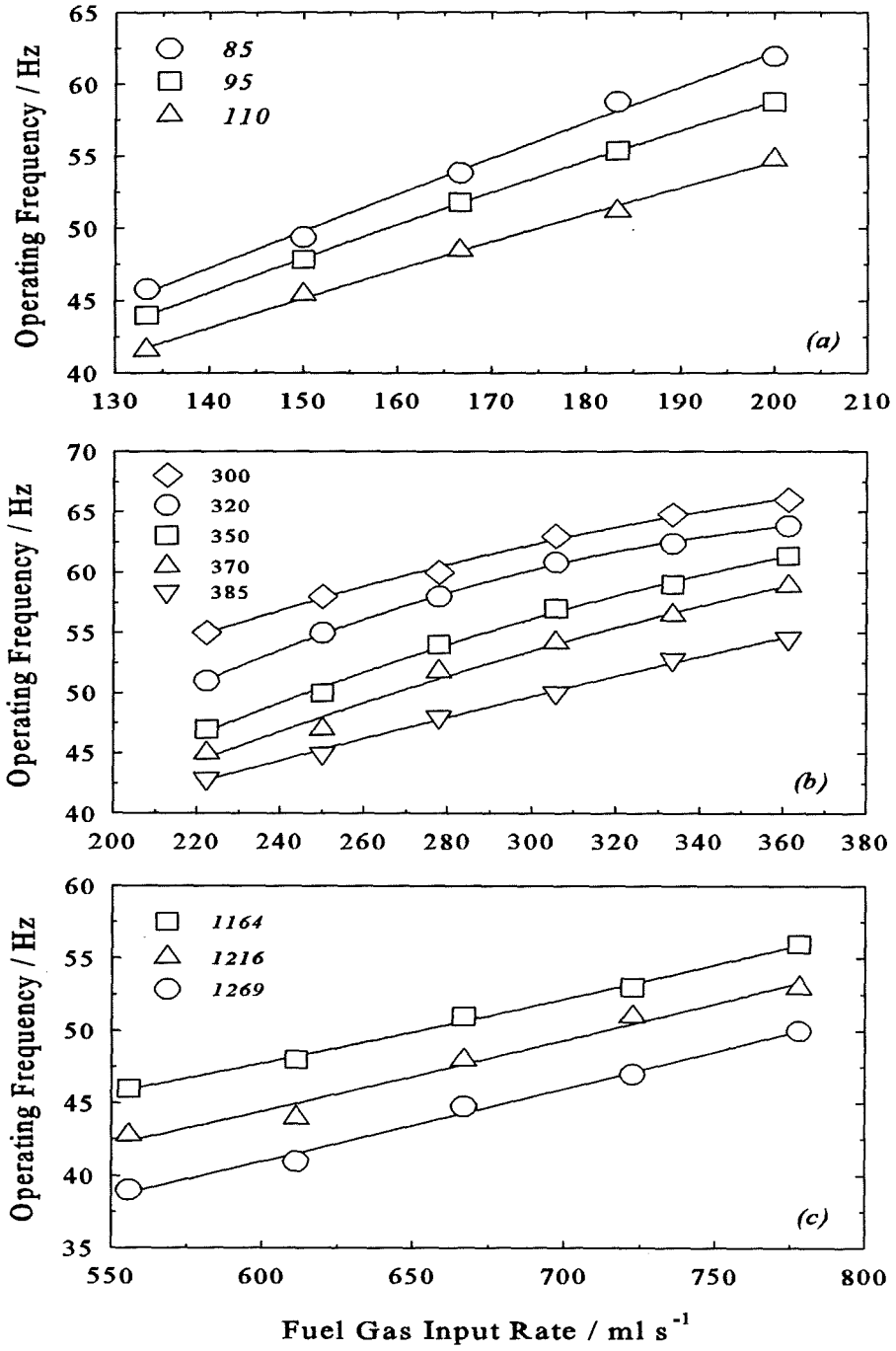

***Fig. 4.8** Effect of change of combustion chamber volume upon operating frequency as a function of input fuel gas flow rate for a) the 7.5 kW combustor with tailpipe length of 1500 mm, b) the 15 kW combustor with tailpipe length of 1500 mm and c) for the nominally 30 kW combustor with tailpipe length of 2000 mm. The specified combustion chamber volumes in the figures are in ml.*

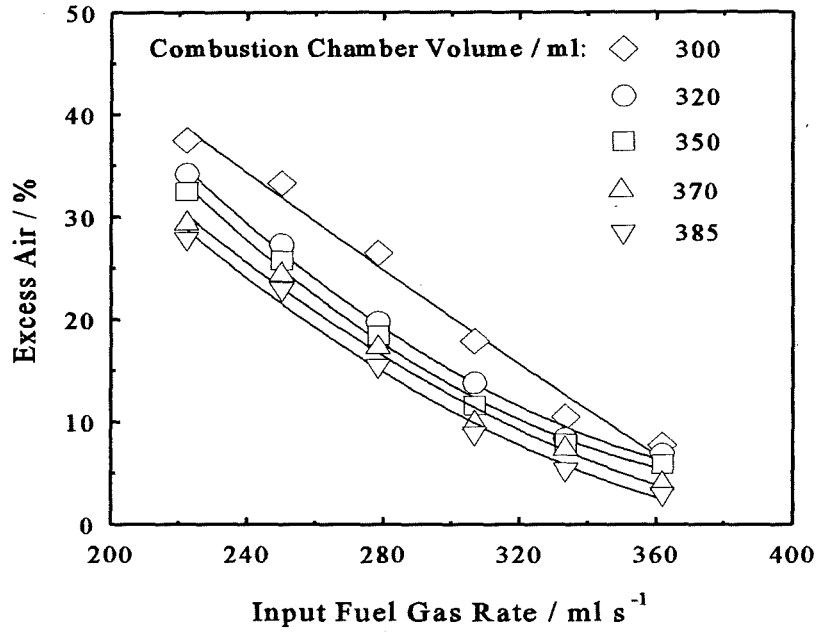

Fig. 4.9 Variation of excess air with fuel gas flow rate for the 15 kW combustor at specified combustion chamber volumes. Tailpipe length was fixed at 1500 mm and the flapper valve thickness was 0.15 mm.

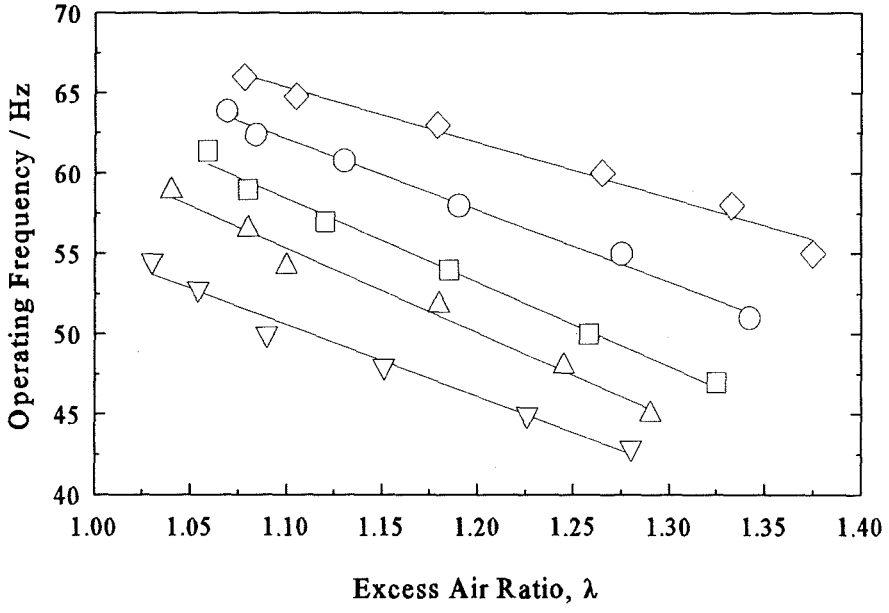

Fig. 4.10 Operating frequency vs λ for the 15 kW combustor at fixed tailpipe length and flapper valve thickness. Symbols as in Fig. 4.9.

present design of pulsed combustors the combustion temperature was fixed principally by A/F. It can be seen from Fig. 4.10 that for a given λ value and hence temperature of combustion gases, the operating frequency of the combustor decreased with the increase of CCV. The trend of results obtained agrees well with the trend of equation (1.3) applied for a Helmholtz resonator, which indicates a reciprocative relation of resonant frequency with CCV. The comparison of theoretical and practical values are shown below in section 4.5.

4.4.2 Effect of Tailpipe Length

Results for the nominally 7.5 and 30 kW combustors are shown in Fig. 4.11. These were obtained at a fixed fuel gas rate, combustion chamber volume and flapper valve thickness while the tailpipe length was varied. It was found that the pulsing frequency decreased with increase of tailpipe length. Equation (1.3) indicated that such an effect would be expected other factors remaining constant. According to equation (1.3), the resonant frequency of a Helmholtz resonator varies inversely with the tailpipe length at any given acoustic mode. Considering the tailpipe acting as a resonator tube, the frequency of oscillation should be proportional to the reciprocal of the time required for a pulse to travel at the velocity of sound along the length of the tube and back. Therefore, lengthening the tailpipe increased the natural resonance time which is the inverse of the natural resonant frequency. The results obtained show a similar trend to those noted for the design of a pulsating combustor by many workers including Francis *et al.* [1963], Gill and Bhaduri [1978] and Hargrave *et al.* [1986].

Some workers, including Francis *et al.* [1963], and Cheng *et al.* [1988], have reported a "frequency jump" to a higher acoustic mode. Francis *et al.* measured the frequency of a Schmidt-type pulsed unit with tailpipe length ranging from 1320 mm to 5280 mm. They observed that between a length of 2970 mm to 3300 mm, the fundamental frequency roughly doubled and between 4620 mm and 4950 mm it increased by one half. From their results including the pressure measurements inside

combustion chamber they deduced that as the tailpipe length was increased the frequency followed the curve for the first mode until the pressure antinode was a considerable distance down the tailpipe [Francis *et al.,* 1963]. This situation is apparently unstable, and the frequency jumps to the second mode, at which there is again a pressure antinode close to the combustion zone. Such frequency jumps did not occur in this study. This could be because of the limitation in the maximum and minimum tailpipe length used in this study.

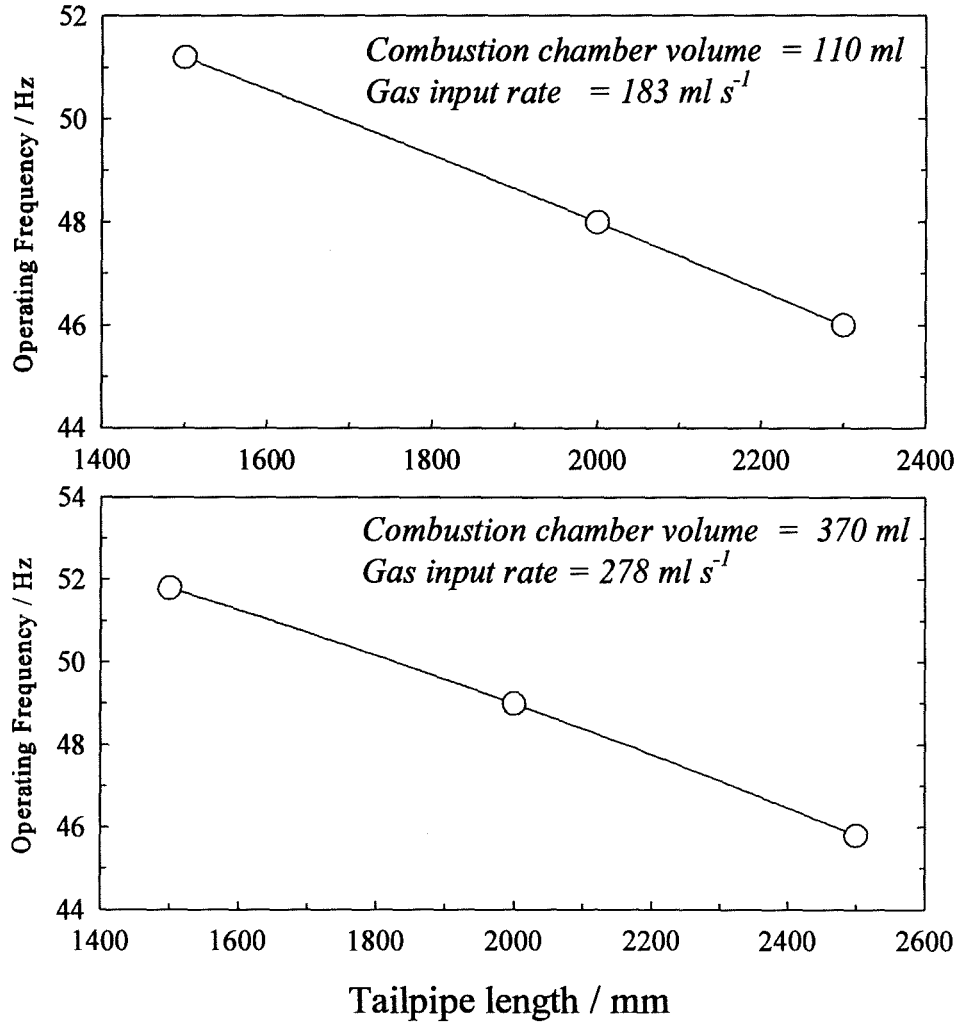

Fig. 4.11 ***Variation of operating frequency with tailpipe length for a) the 7.5 kW combustor and b) the 15 kW combustor at constant gas input rate and combustion chamber volume.***

4.4.3 Effect of Flapper Valve Thickness

In the design of the combustors used in this work, the mixture flapper valve was the only moving part once pulsing was established. A detailed description of the flapper valve used in this study is given in Chapter 2.

Results using flapper valves of PTFE-coated glass fibre material of various thicknesses are shown in Fig. 4.12. Clearly, the frequency was sensitive to flapper valve thickness, showing that for a given fixed flapper valve material, CCV, tailpipe length and fuel gas rate, the operating frequency increased as the flapper valve thickness decreased. Typically, the difference in frequency when using 0.13 and 0.36 mm thickness material was from 55 to 45 Hz, equivalent to cycle times of 18 and 22 ms. The difference of 4 ms was probably largely due to the increased time required

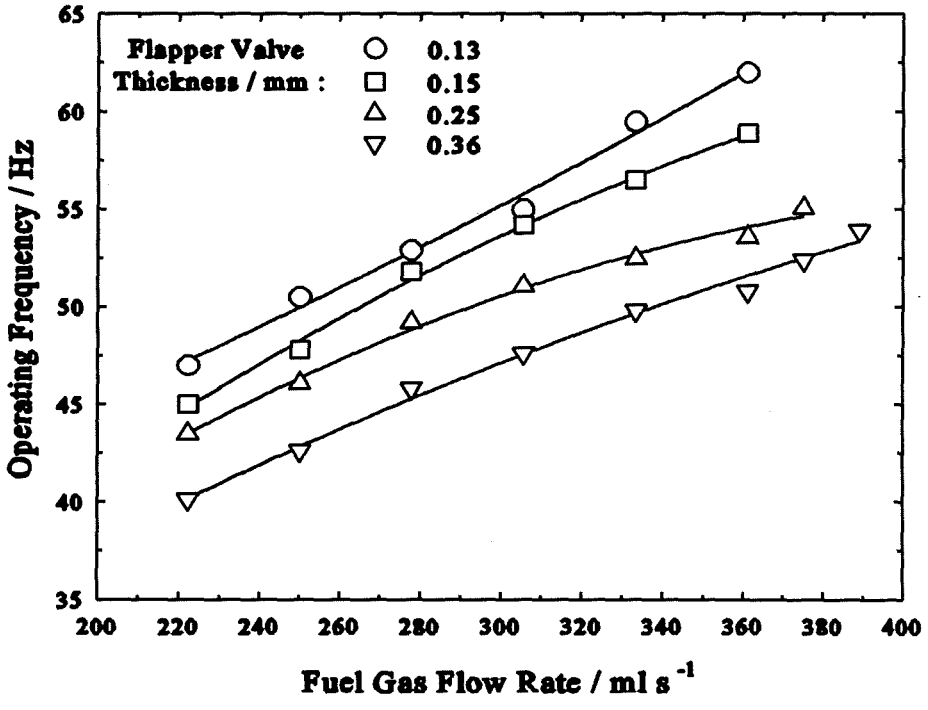

Fig. 4.12 ***Effect of flapper valve thickness upon operating frequency of the nominally 15 kW combustor. The flapper valve material was PTFE-coated glass fibre. The measurements were carried out at combustion chamber volume of 370 ml and tailpipe length of 1500 mm.***

to close the valve when using the thicker flapper materials due to their increased mass (inertia).

4.5 Comparison of Practical and Theoretical Values

In Chapter one it was mentioned that Francis *et al.* [1963] and Bhaduri *et al.* [1968] reported a theoretical analysis which applies a damped spring-mass vibration analogy to Helmholtz resonator oscillations. Thring [1968] also carried out such an analysis which did not include a number of factors such as combustion and induction of fresh charge of reactants. Although later, such calculations were conducted by other researchers, the fact that the governing processes of a pulsed combustor are coupled gives these analysis less credibility. Here, a very simple approach is used to verify the trend of the experimental values.

The experimental results presented in sections 4.4.1 and 4.4.2 show that the developed combustors behaved like a classical Helmholtz resonator whose short neck was replaced by a long tailpipe. Therefore, equation (1.3) may be used to obtain theoretical values of the operating frequency of the pulsed units. A problem encountered was that the temperature of the gases in the tailpipe changes greatly from one end to another. According to equation (1.4) the velocity of sound is dependent upon the temperature of the exhaust gases and this varies along the tailpipe. Therefore, in order to apply equation (1.3) it was necessary to calculate a mean temperature and to use this to estimate the mean velocity of sound.

Fig. 4.13, shows the measured values compared with the frequencies calculated using equation (1.4) and (1.3) respectively. An average temperature T was assumed calculated as the mean between the calculated adiabatic flame temperature and the measured outlet exhaust gas temperature at sampling point 2. The calculated frequencies are of the correct order of magnitude but do not show the variation with fuel gas rate that was measured. One reason may be the variation of temperature of the combustion gases along the tailpipe whereas in the calculation of the theoretical operating frequency, the mean temperature was calculated from two values only.

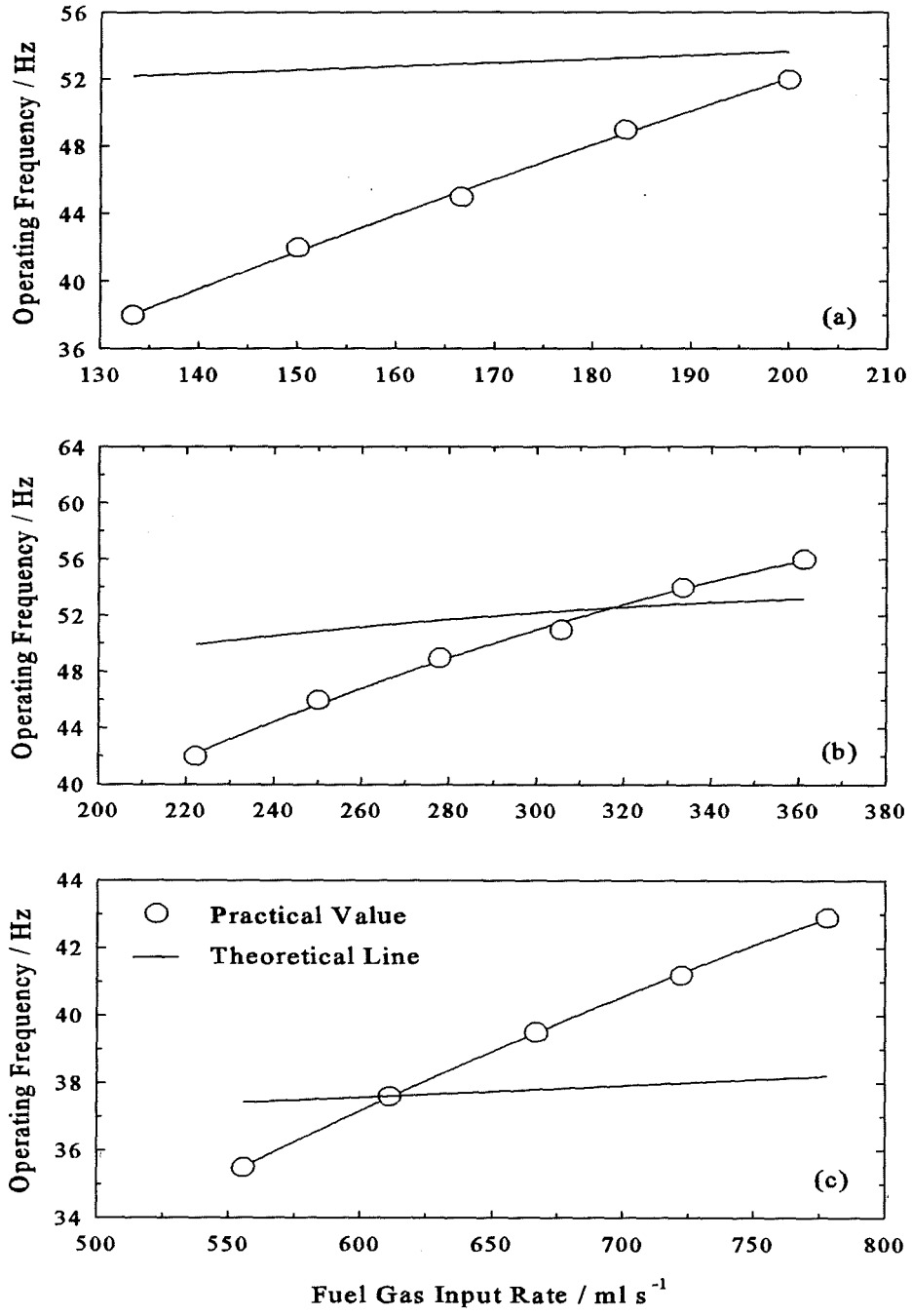

Fig. 4.13 ***Comparison of theoretical and practical values of the operating frequency for a) the 7.5 kW combustor with 110 ml combustion chamber volume, b) the 15 kW combustor with 370 ml combustion chamber volume and c) the 30 kW combustor with 1270 ml combustion chamber volume, using fixed tailpipe length of 2000 mm and flapper valve thickness of 0.15 mm.***

Furthermore, this simple treatment ignores the influence of the flapper valve thickness, effects associated with ignition delay and its influence on the phase relationship between energy release and pressure oscillations in regard to the Rayleigh criterion.

Shown in Fig 4.14 and 4.15 are the comparisons of theoretical values of operating frequency with measured values, at various combustion chamber volumes and tailpipe lengths respectively. The theoretical results display similar trends to the practical values showing a decrease in the operating frequency as the combustion chamber volume (Fig. 4.14) and tailpipe length (Fig. 4.15) were increased. It can be seen that the dependence on combustion chamber volume was substantially greater than that given by equation (1.3) treating the system purely as a Helmholtz resonator. Furthermore, it was found that the experimentally determined decrease in frequency with increase in tailpipe length was less than that predicted by equation (1.3) as shown by the theoretical line in Fig. 4.15. Such correlation of predicted values with practical values are in line with results reported by Gill and Bhaduri, [1978] obtained using a Helmholtz-type combustor. They have also reported that the operating frequency of their pulsed combustor increased as the tailpipe diameter increased [Gill and Bhaduri, 1978].

4.6 Summary and Conclusions

In this chapter the influence on the operating frequency of the input firing rate and configuration parameters, i.e. combustion chamber volume (CCV), tailpipe length and flapper valve thickness has been investigated. Comparisons of the observed behaviour with the theoretical equation for a Helmholtz resonator have also been shown. The following relationships have been observed:

- The frequency increased as the input fuel gas flow rate was increased. This was believed to be as a result of two effects.
  a) The increase in temperature. Temperature inside the combustion chamber increased with increase of the fuel gas flow rate. This in turn increased the

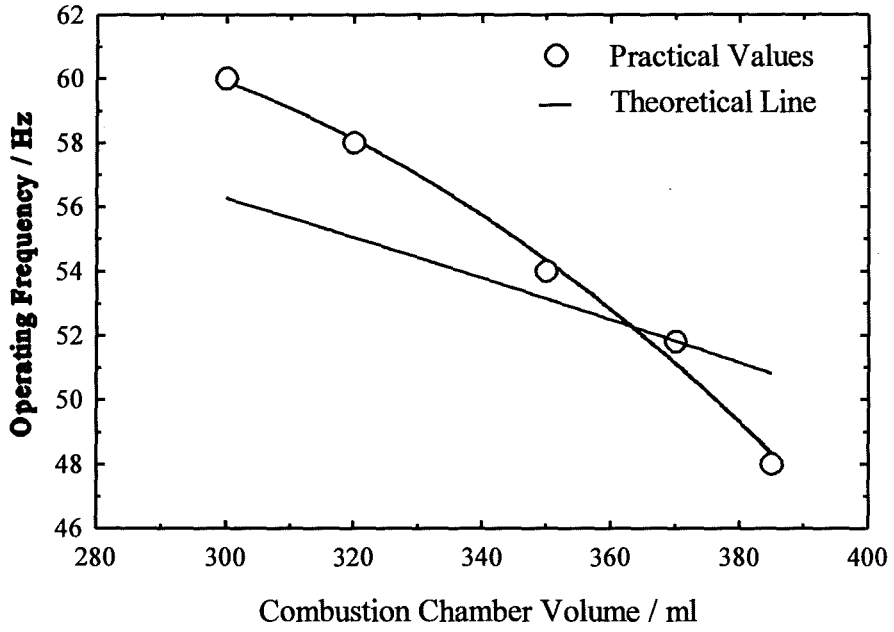

Fig. 4.14 ***Comparison of predicted and measured values of frequency as a function of combustion chamber volume for the 15 kW combustor at fixed fuel gas input rate of 277 ml s^{-1} and tailpipe length of 1500 mm.***

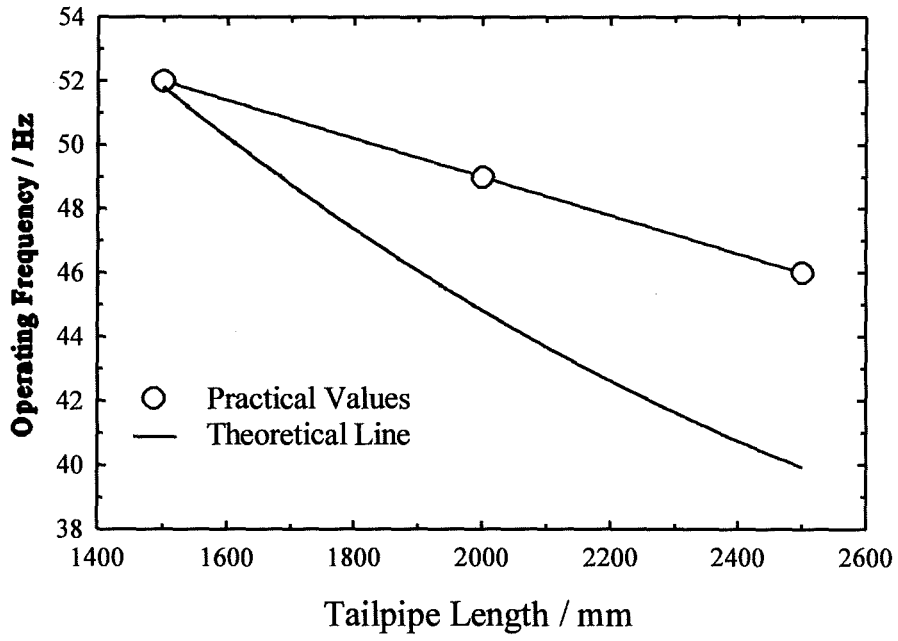

Fig. 4.15 ***Correlation of theoretical and practical values of frequency vs tailpipe length for the nominally 15 kW combustor at constant fuel gas input rate of 277 ml s^{-1} and fixed combustion chamber volume of 370 ml.***

speed of sound and hence natural resonant frequency according to the equations (1.4) and (1.3) respectively.

b) Increase in phase difference between heat addition and pressure oscillations. Increasing the fuel gas flow rate resulted in shortening the time for mixing of the reactants with hot residual product τ_{mixing}. As the fuel gas flow rate increased the total volume flow rate of mixture charge into the combustor increased and hence the total flow velocity increased. Characteristic mixing time is inversely proportional to the inlet flow velocity [Keller *et al.* 1989]. Furthermore, increased flame temperature resulted in faster chemical reactions and hence shorter $\tau_{kinetic}$. Decrease in the above characteristic times resulted in a shorter total ignition delay time. It is known that shorter total ignition delay time results in an increase in the phase difference between energy release and pressure oscillations. This, in turn, results in an increase in operating frequency.

- Boosting the air and hence air-to fuel ratio (A/F) at a given fuel gas rate reduced the frequency of operation. Re-plotting the data as frequency vs λ brought the two sets of data into a single line indicating that for a given fixed configuration of the unit, operating frequency was a function of the gas temperature within the combustion chamber and the tailpipe. This follows from the fact that for the present design of pulsed combustor the temperature within the combustor was principally fixed by A/F. In this study no phase angle data was obtained. Clearly in order to be conclusive on variation of operating frequency with the adjustable parameters, it is necessary to have more information on phase difference between energy release and pressure oscillations.
- For a given gas input rate and fixed tailpipe length and flapper valve thickness, the operating frequency of the pulsed units decreased as combustion chamber volume was increased.
- The operating frequency decreased as the tailpipe length was increased when the CCV, flapper valve thickness and fuel gas flow rate were kept constant.
- The operating frequency of the system was dependent upon the thickness of the flapper valve.

- The experimental results indicated that the developed combustors indeed behave as does a Helmholtz resonator. Thus, frequency can be estimated using the theoretical equation for a Helmholtz resonator. The theoretical values were similar in magnitude to the observed values but there were also clear differences. This may be due to the inadequate estimation of exhaust gas temperature used in equation (1.4). In addition, no term exists in the theoretical equation (1.3) concerning the flapper valve stiffness or mass. Furthermore, it should borne in mind that the governing processes in a pulsed combustor of this type are coupled.

From the above it can be concluded that the operating frequency of the present design of pulsed combustors was a function of their geometry and of the temperature of combustion gases inside the combustion chamber. This is in accordance with equation (1.3), an approximation for a Helmholtz resonator, indicating that the present combustors behaved similarly to a Helmholtz resonator as was intended.

The trend of results also indicated that the operating frequency of the pulsed combustors can also be influenced by total ignition delay time and thus phase difference between energy release and pressure oscillations as described by researchers such as Keller *et al.*[1989] and Jones and Leng [1994]. However, no phase angle data was available in this study to confirm the theory.

Chapter Five

Pulsing Pressure

5.1 Introduction

The Helmholtz pulsed combustor is an oscillating system with an underlying acoustic nature. When combustion occurs in the combustion chamber, there is a rise in pressure in the chamber which causes the combustion gases to be propelled to the atmosphere via the tailpipe. When this pressure wave reaches the outlet, an expansion wave runs back along the tailpipe and the cycle is then restarted. The resulting pressure fluctuations of the exiting gases can be sampled by placing a pressure transducer near to the outlet of the tailpipe, pointing towards the outflowing gases and on the axis of the pipe.

In Chapter 1, it was indicated that the successful operation of a pulsed combustor depends upon the phase relationship between the heat addition and the resonant pressure wave. Some of the difficulties encountered in getting a new design to resonate may be due to a mismatch between the essential chemical and gas-dynamic rate processes and the time available for them to be completed during the period of a single cycle at resonance [Belles, 1986]. Workers such as Keller *et al.* [1989] or Jones and Leng [1994] have made quantitative measurements of the pulse pressure and heat release rate principally to gain a greater insight into these processes and hence the operation of the pulsed combustion system. Their interpretation has centred on the Rayleigh criterion as a means of explaining the observed variation of pulse pressure in response to changes in the adjustable parameters.

In this chapter, results obtained from the investigation of the effect of adjustable parameters on pulsing pressure of the developed combustors are presented. These results, together with frequency data, provide greater insight towards understanding the governing processes, optimisation and scaling of this type of pulsed combustor.

5.2 Results at Fixed Configuration

The experimental methods for pressure measurements were outlined in Chapter 3 and a typical pressure-time wave curve was shown in Fig. 3.3 of that Chapter. Such diagrams allow both the maximum pulse pressure at the outlet of the tailpipe and frequency of operation of the combustors to be readily determined. The values quoted below were calculated by averaging results from some 250 pulses in each case.

5.2.1 Effect of Input Gas Flow Rate on Operating Pressure

Experimental measurements of the peak pulsing pressure from the three nominally 7.5, 15 and 30 kW pulsed combustors at various fuel gas flow rates were carried out. Figure 5.1 shows the variation of the peak pulsing pressure of the developed pulsed combustors with the gas input rate. It can be seen that as the gas input rate was progressively increased, the peak pulsing pressure at the outlet increased. The three nominally 7.5, 15 and 30 kW pulsed combustors were operated over fuel gas input ranges of 135 to 200, 220 to 360, and 560 to 780 ml s^{-1} respectively. The peak pulsing pressure measurements at the outlet of the tailpipes showed an increase of around 9 to 11, 9 to 12.5 and 11.5 to 15 kN m^{-2} (gauge pressure) with an increase of the given ranges of fuel gas flow rate for the nominally 7.5 (Fig. 5.1a), 15 (Fig. 5.1b) and 30 kW (Fig. 5.1c) combustors respectively. These observations and the effect of the change of configuration on the peak operating pressure of the pulsed units are discussed in later sections of this chapter.

5.2.2 Effect of Running with the Air Fan "On"

In Fig. 5.2, results for the peak pulsing pressure are shown for the nominally 15 kW combustor as a function of fuel gas input rate under operating conditions with the air fan turned on or off. These measurements showed that at a fixed firing rate and configuration, the peak pulsing pressure at the outlet of the tailpipe was higher when the air fan was kept on, compared with when the air fan was turned off.

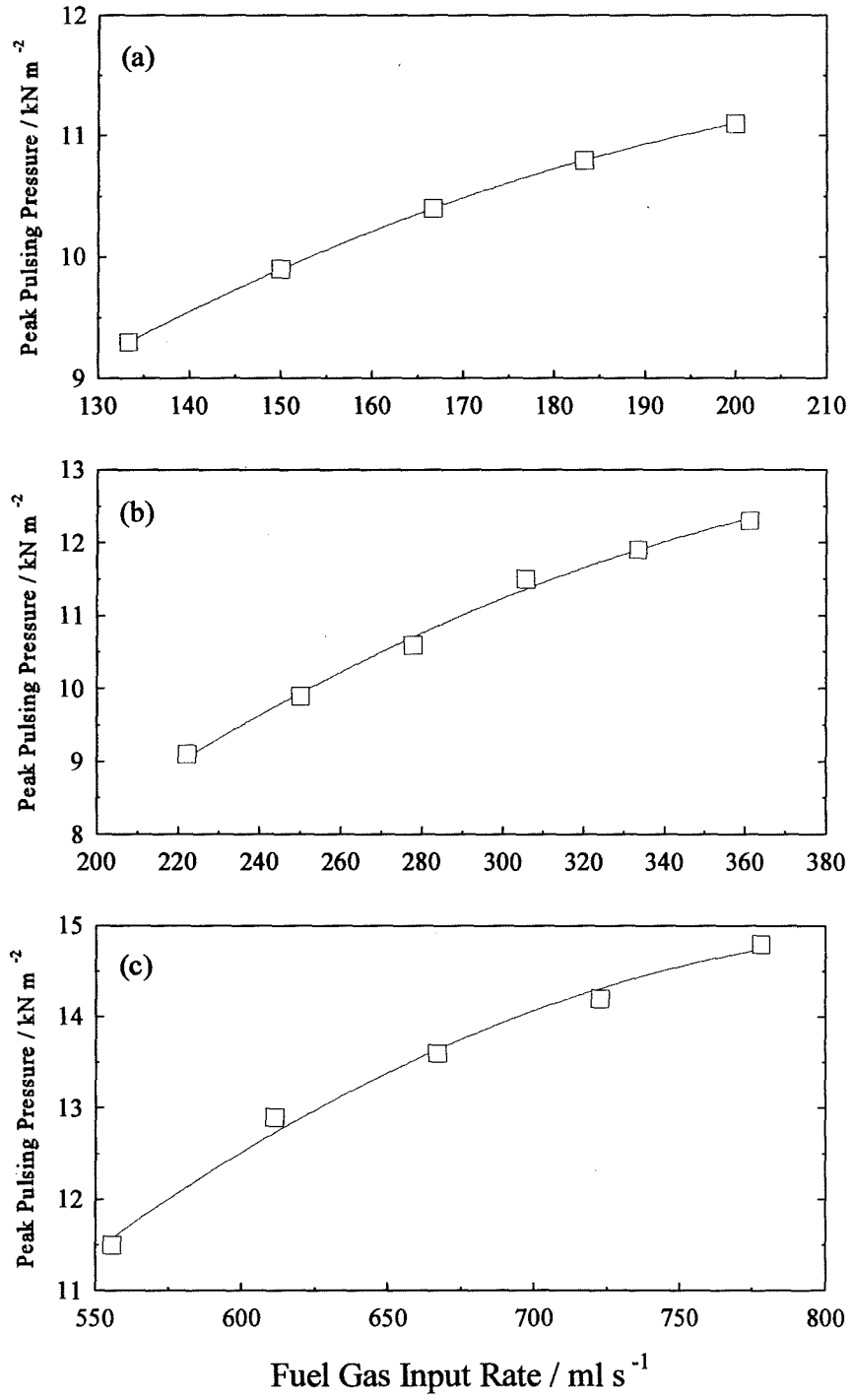

Fig. 5.1 Variation of peak pulsing pressure with gas input rate for a) the 7.5 kW combustor with combustion chamber volume of 110 ml, b) the 15 kW combustor with combustion chamber volume of 370 ml and c) the 30 kW combustor with combustion chamber volume of 1270 ml. Tailpipe length and flapper valve thickness were 2000 mm and 0.15 mm respectively.

At a fixed gas input rate of 360 ml s^{-1}, combustion chamber volume of 370 ml and tailpipe length of 1500 mm, the peak pulsing pressure increased from 12 kN m^{-2} when the fan was switched off to 14 kN m^{-2} when the fan was left on after ignition. Two possible explanations are proposed:

i) increased heat release per cycle. From the results shown in Fig. 4.3, for a fixed gas input rate the frequency of operation decreased when the air fan was turned on. This in turn increased the heat release per cycle for a fixed gas input rate, which in turn may have caused the observed pressure rise.

ii) increased inlet pressure from the fan. When the fan was on, the mixture pressure was higher than when the fan was turned off. For a given fixed gas input rate the volume flow rate of the inlet air increased by an average of 500 ml s^{-1}.

These possibilities are considered in detail below.

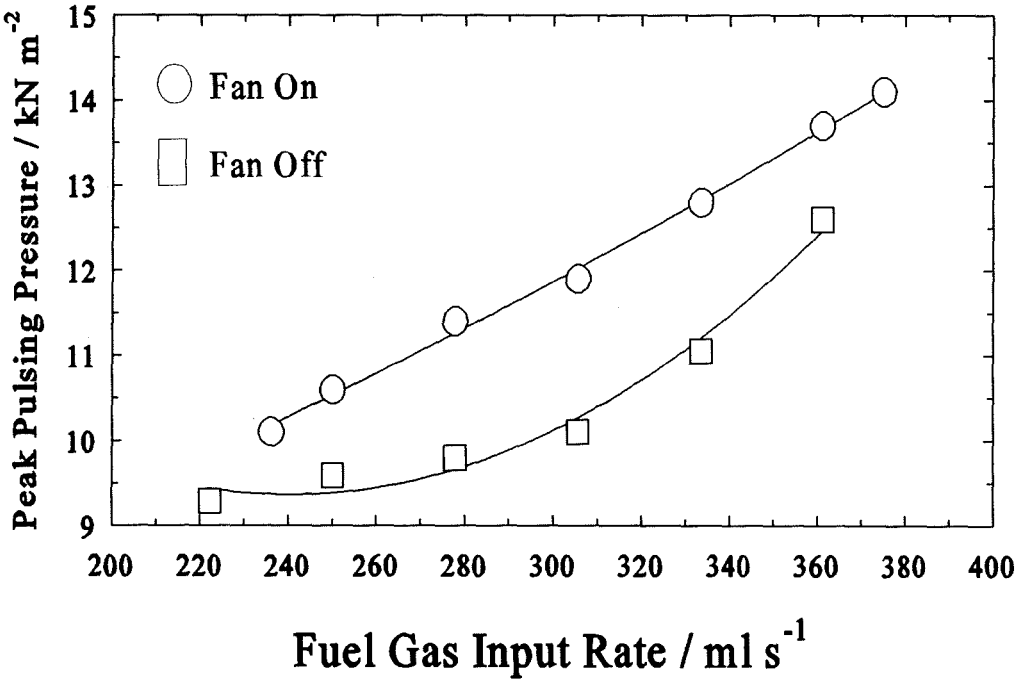

Fig. 5.2 Effect of increasing air flow rate, by leaving the air fan on after ignition, upon the peak pulsing pressure of the nominally 15 kW pulsed combustor at various fuel gas flow rates. The combustion chamber volume and tailpipe length were kept constant at 370 ml and 1500 mm respectively.

5.2.3 Effect of the Dilution of Mixture Charge with Nitrogen

To obtain a better insight into the fundamental processes involved in the operation of a pulsed combustion system, the effect of adding nitrogen to the inlet air and hence diluting the mixture charge of air and gas was studied. For this study the nominally 15 kW pulsed combustor was used with fixed combustion chamber volume (CCV) of 370 ml, tailpipe length of 1500 mm and flapper valve thickness of 0.13 mm. During these experiments the natural gas volume input rate was kept constant at 277 ml s^{-1}. As the N_2 was added, the total air plus nitrogen remained constant at around 3100 ml s^{-1} (Fig. 5.3a) resulting in constant adiabatic flame temperature (calculated) at about 1875 °C as shown in Fig. 5.3b.

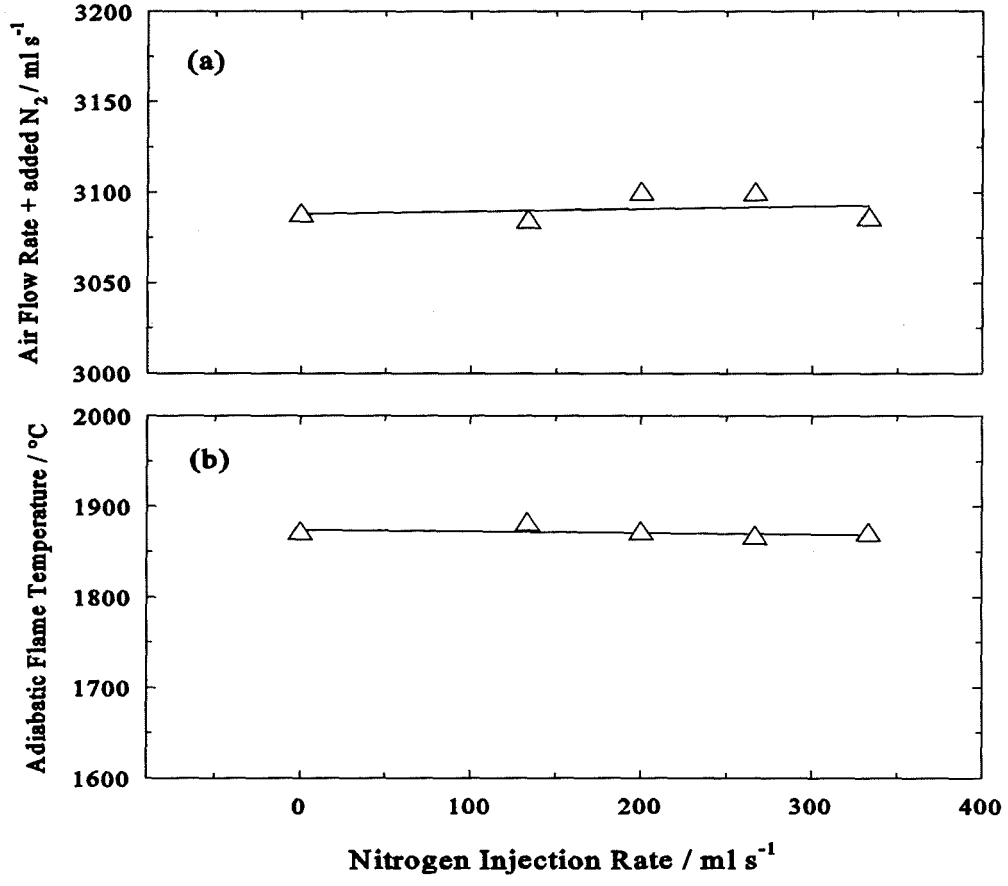

***Fig. 5.3** Variation of a) total air + nitrogen and b) calculated adiabatic flame temperature with N_2 injection rates. For the 15 kW combustor, tailpipe length of 1500 mm, combustion chamber volume of 370 ml and flapper valve thickness of 0.13 mm was used.*

Under the above conditions, with a fixed geometry of the combustor, the operating frequency and the peak pulsing pressure at the outlet of the exhaust tube were measured, as the volume flow rate of N_2 diluent was increased. The results of these measurements are shown in Fig. 5.4.

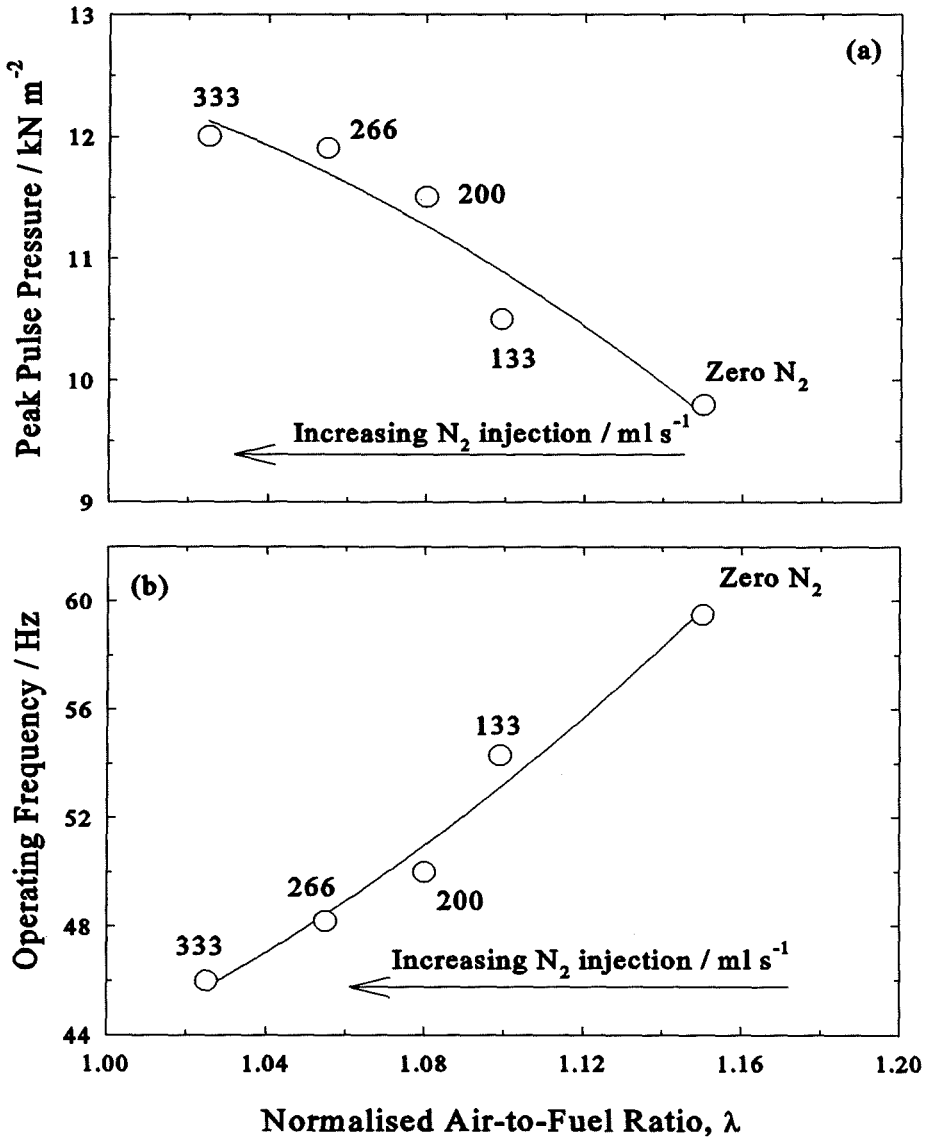

Fig. 5.4 Variation of a) peak pulsing pressure and b) operating frequency with rate of N_2 injection as a function of normalised A/F(λ), at constant fuel gas rate of 277 ml s^{-1}. Figures adjacent to points indicate nitrogen injection rates in ml s^{-1}. Configuration as in Fig. 5.3.

Oxygen measurements in the exhaust gases provided a measure of the excess air ratio, λ (see Appendix IV). As the N_2 was progressively injected, λ decreased because the N_2 replaced part of the air going into the system and the peak pulse pressure increased while operating frequency decreased (Fig.5.4). The results showed that as the N_2 flow rate increased from 0 to 333 ml s^{-1} the operating frequency decreased from 60 to 46 Hz (Fig. 5.4b) and the peak pulsing pressure increased from 10 to 12 kN m^{-2} (Fig. 5.4a) at the given fixed configuration.

5.3 Discussion of Results for Fixed Configurations

In this section the results presented so far are discussed in more detail. These results were obtained at a fixed configuration of the developed pulsed combustors, i.e. constant combustion chamber volume, tailpipe length and flapper valve thickness.

5.3.1 Effect of Fuel Gas Rate

It was shown earlier that the operating pressure amplitude of the pulsed combustors increased as the fuel gas input rate increased (Fig. 5.1). Further analysis of these data as shown in Fig. 5.5 indicated that the trend of results obtained is in consistent with the following equation, showing the pressure rise in the combustion chamber due to combustion heating alone [Dhar *et al.*, 1982]:

$$P_h = \frac{RU}{VC_v} \tag{5.1}$$

where, P_h is the pressure rise inside the combustion chamber, R is the specific gas constant, U is the internal energy, V is the combustion chamber volume and C_v is the specific heat at constant volume. Equation (5.1) is obtained from approximation of the pressure, volume and temperature behaviour of the gases inside combustion chamber by

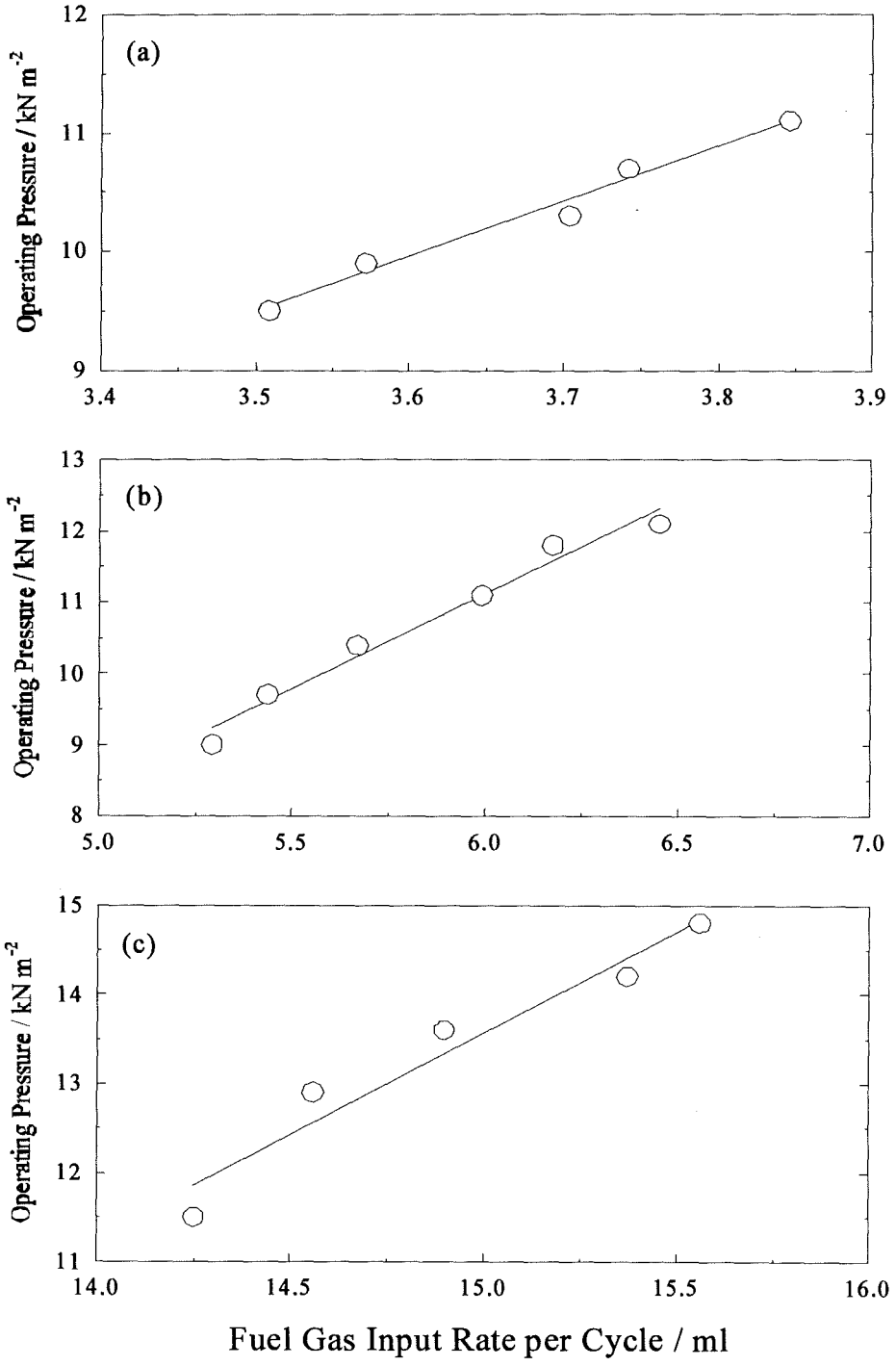

Fig. 5.5 ***Variation of fuel gas per cycle upon peak pulsing pressure for the a) 7.5 kW combustor with CCV of 110 ml, b) the 15 kW combustor with CCV of 370 ml and c) the 30 kW combustor with CCV of 1270 ml. Tailpipe length of 2000 mm with flapper valve thickness of 0.15 mm were used.***

the ideal gas equation of state.

The analysis in Fig. 5.5 is obtained from data given in Fig. 5.1 and 4.1. It can be seen from the figure that for a fixed configuration of a pulsed combustor, the peak pulsing pressure increased as the fuel gas per cycle and hence the heat release per cycle increased. Clearly, from the trend of results shown in Fig. 5.5, it can be deduced that the principal contributing factor to the rise of pressure inside the combustion chamber with constant volume is the heat release per cycle. The increase of heat release inside the combustion chamber as a result of increased fuel gas flow rate, increased the internal energy and subsequently raised the pressure inside the chamber.

Other workers [e.g. Keller *et al.*, 1989] have shown that factors such as phase difference between heat release and pressure oscillations has an influence on pressure amplitude inside the combustion chamber as discussed in Chapter 1 section 1.8. However, phase angle data was not obtained in this study.

An interesting and clearly important finding emerging from the data presented is that the maximum pressure amplitudes occurred at the higher gas input rates where the A/F was near to stoichiometric indicating that optimum operation of the developed combustors in terms of pressure swing could be obtained with low excess air. It is reported an increase in amplitude of oscillations may result in improved mixing, heat transfer and combustion [Dec and Keller, 1989 ; Zinn, 1992].

5.3.2 Effect of Running with the Air Fan On

Experimental data were shown in Fig. 5.2 and 4.3. The peak pulse pressure was higher with the fan on but frequency was lower for a fixed fuel gas input rate. The variation of the peak pulsing pressure with the fuel gas injected per cycle is shown in Fig. 5.6. The analysis brings all the data into a single line. For a given fuel gas rate, the frequency was lower with the fan on than with it turned off (see Fig. 4.3), so the fuel gas per cycle was increased; this resulted in the higher pulse pressure in the former instance. Conformance of the trend of results with equation (5.1) indicates that the higher peak pulsing pressure with the fan on, was not influenced significantly by the pressure rise at

the inlet due to the fan.

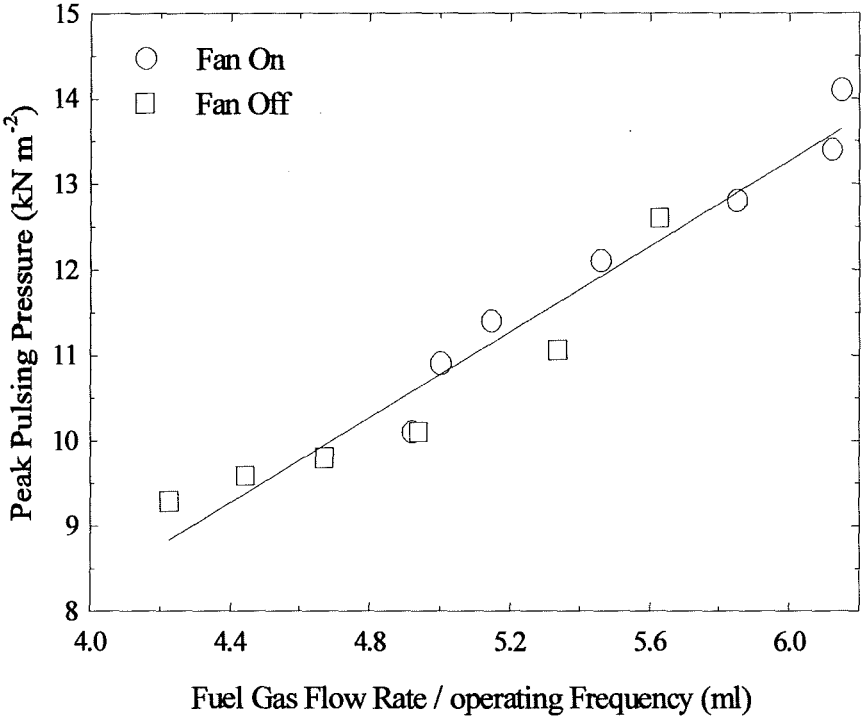

Fig. 5.6 Variation of peak pulsing pressure with fuel gas injection per cycle at two operating conditions of air fan on and off for the 15 kW combustor after ignition. Configuration as in Fig. 5.2.

5.3.3 Effect of Nitrogen Injection

Experimental data are shown in Fig. 5.4. Increasing N_2 injection, at a fixed fuel gas rate, resulted in increasing peak pulsing pressure but lower frequency of operation. The pulsing pressure amplitude plotted against fuel injected per cycle is shown in Fig. 5.7. This representation brings all the data for various fuel gas rates (Fig. 5.7a) and nitrogen injection rates (Fig. 5.7b) into a single straight line confirming that the heat release per cycle was the principal factor controlling the magnitude of the pressure pulses in this type of combustor.

These findings, for operation with N_2 injection, correlate closely with those of Keller *et al.* [1989] where in their results injection caused the system to change towards

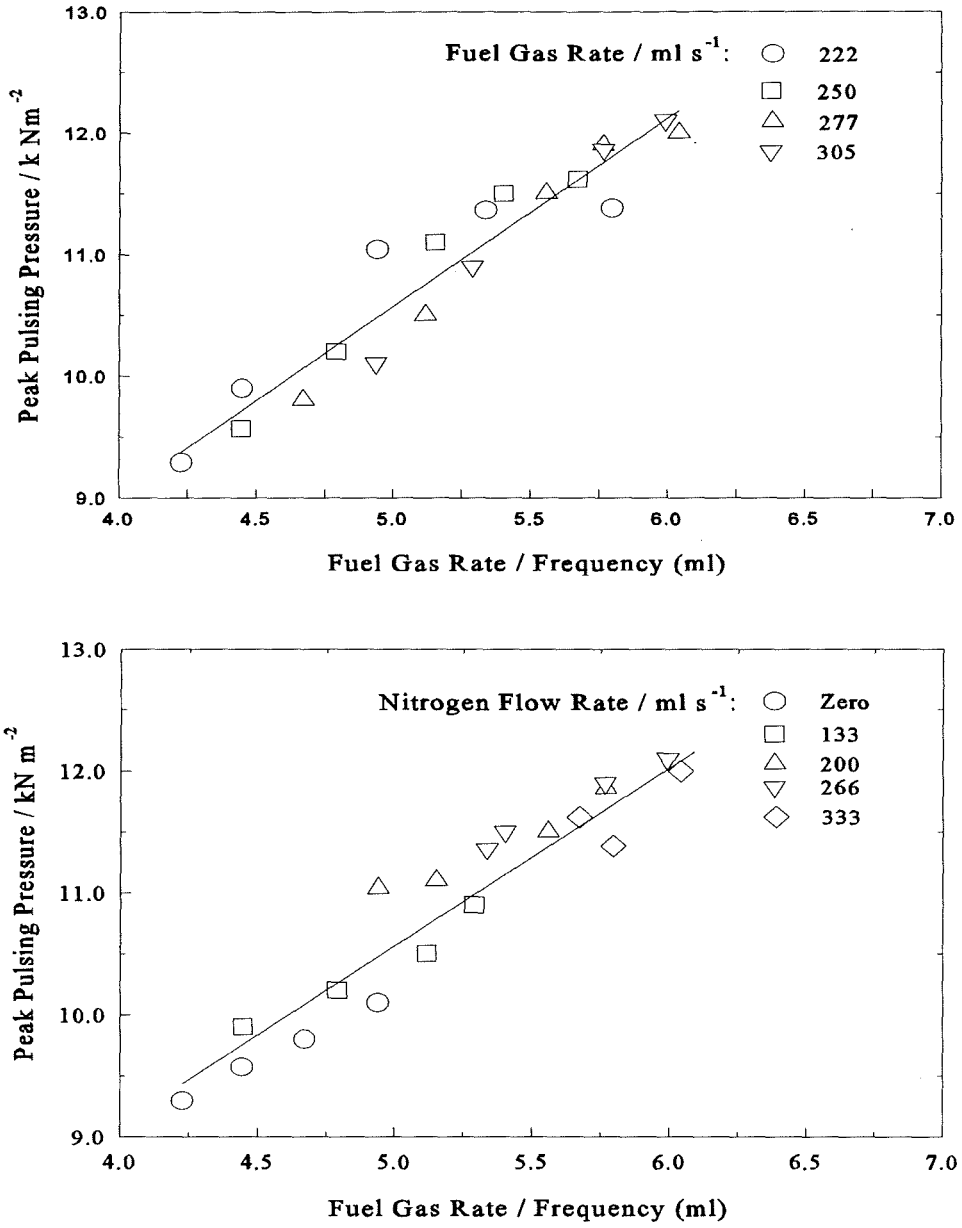

Fig. 5.7 Peak pulsing pressure vs fuel gas volume per cycle a) for various fuel gas rates and b) various N_2 injection rates. Combustor used was the 15 kW unit with tailpipe length of 1500 mm, combustion chamber volume of 370 mm and flapper valve thickness of 0.13 mm.

the stoichiometric condition with pressure increasing from 6 to 10 kPa while frequency decreased from 68 to 52 Hz approximately. Keller *et al.*[1989] interpreted their data with reference to the Rayleigh criterion proposing that the pulse pressure was maximised when the heat release was precisely in phase with the resonant pressure oscillation; the phase angle varied with N_2 injection because progressive N_2 dilution resulted in increasing total delay time via $\tau_{kinetic}$ (equation 1.6). Based on their interpretation it seems that the addition of N_2 diluent delayed the energy release despite the fact that the gas input rate was constant. Such delay of energy release could result from slower chemical reactions which in turn increased the total ignition delay time according equation (1.6) [Keller *et al.*, 1989].

As the rate of N_2 injection was increased oxygen was replaced by nitrogen in the reactant gases. It was seen in Chapter 4 from equation (4.1) that the rate of reaction is a function of oxygen available. Therefore, as the N_2 diluent was added the reaction rate decreased due to decrease of O_2 and this caused an increase of kinetic time, $\tau_{kinetic}$, through a decrease in the probability of a collision occurring between species (i.e. O_2 and fuel gas). Since the total ignition delay time, τ_{total}, is an increasing function of the characteristic times [Keller *et al.*, 1989] an increase of kinetic time increased the total ignition delay time. It seems that prolonging τ_{total} via addition of N_2 caused an improvement in the coupling of the energy release and the resonant pressure wave and hence resulted in the observed trend of data.

The above was based upon the Keller *et al.* [1989] interpretation and their assumption of the characteristic times (see Chapter 1). There seems little doubt that N_2 injection resulted in ignition delay and consequent reduction in pulsing frequency. As mentioned earlier, this was as a result of decreased oxygen concentration which modified the rate of the chemical reactions. It follows from this that as the fuel gas rate was held constant, the mass of fuel gas entering the combustion chamber per cycle increased in inverse proportion to the frequency of operation. Thus, as the N_2 injection rate was increased the fuel gas charge per cycle increased and the heat released per cycle increased resulting in an increased peak pulse pressure.

5.4 Results for Varying Combustor Configurations

In the following sections, the results obtained for various configurations of the developed pulsed combustors are discussed. These included results due to changes of the combustion chamber volume, tailpipe length and flapper valve thickness.

5.4.1 Effect of Combustion Chamber Volume

Results showing the peak pulsing pressure as a function of combustion chamber volume (CCV) for the three developed combustors are presented in Fig. 5.8. This shows that at a fixed fuel gas input rate, tailpipe length and flapper valve thickness, the peak operating pressure of each pulsed combustor decreased as the CCV increased. For a given fixed gas input rate the peak pulsing pressure decreased from 12.5 to 11 kN m^{-2} for the 7.5 kW combustor (Fig. 5.8a), 13.2 to 10 kN m^{-2} for the 15 kW combustor (Fig. 5.8b) and 14.7 to 13 kN m^{-2} for the 30 kW combustor (Fig. 5.8c) when the CCV increased from 85 to 110 ml, 300 to 385 ml and 1160 to 1270 ml for the 7.5, 15 and 30 kW combustors respectively. This was expected according to equation (5.1) indicating a reciprocal relation of pressure with volume of the combustion chamber with the assumption that the combustion gas behaved as an ideal (perfect) gas.

Further analysis of data for a fixed input of fuel gas per cycle and hence heat input per cycle for each combustor is shown in Fig. 5.9 and 5.10. Data in Fig. 5.10 are obtained from Fig. 5.9 for a fixed input fuel gas per cycle for each of the three combustors. Earlier it was shown that heat release per cycle is the principal determining factor controlling peak pulsing pressure in this type of combustor. In Fig. 5.10 the effect of CCV on pressure change at constant heat release per cycle is shown; the peak pulsing pressure vs V^{-1} shows a straight line with positive slope as predicted by equation (5.1).

With reference to the Rayleigh criterion and the characteristic times, when fuel gas input rate and air flow rate were constant, the characteristic time for chemical reactions to occur ($\tau_{kinetic}$) and the characteristic time required to mix the reactants with hot products (τ_{mixing}) were expected to be constant and since the systems were premixed the

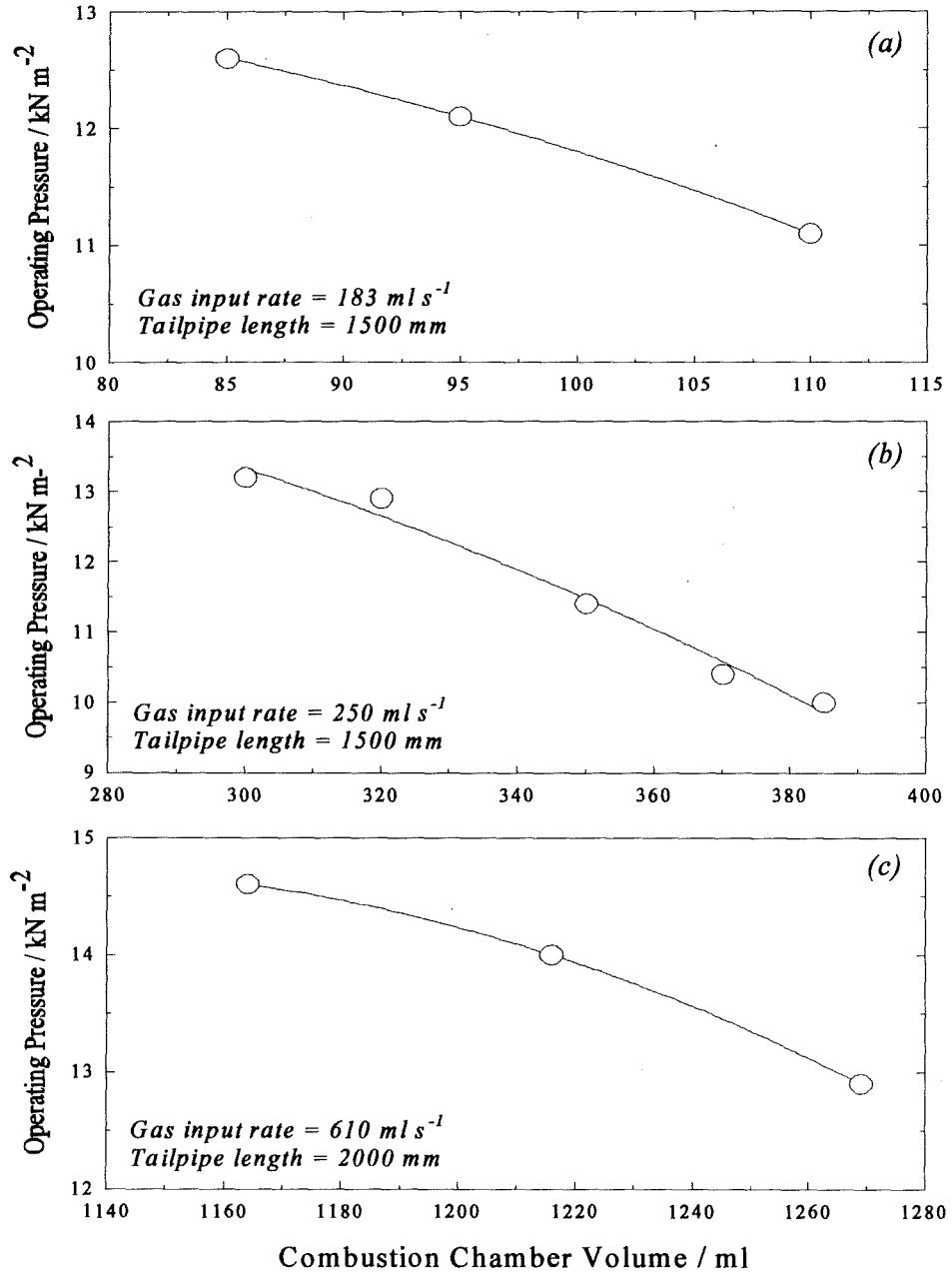

***Fig. 5.8** Variation of peak pulsing pressure with combustion chamber volume at a given fixed fuel gas input rate and tailpipe length for a) the 7.5 kW combustor, b) the 15 kW combustor and c) the 30 kW combustors. Flapper valve thickness of 0.15 mm was used.*

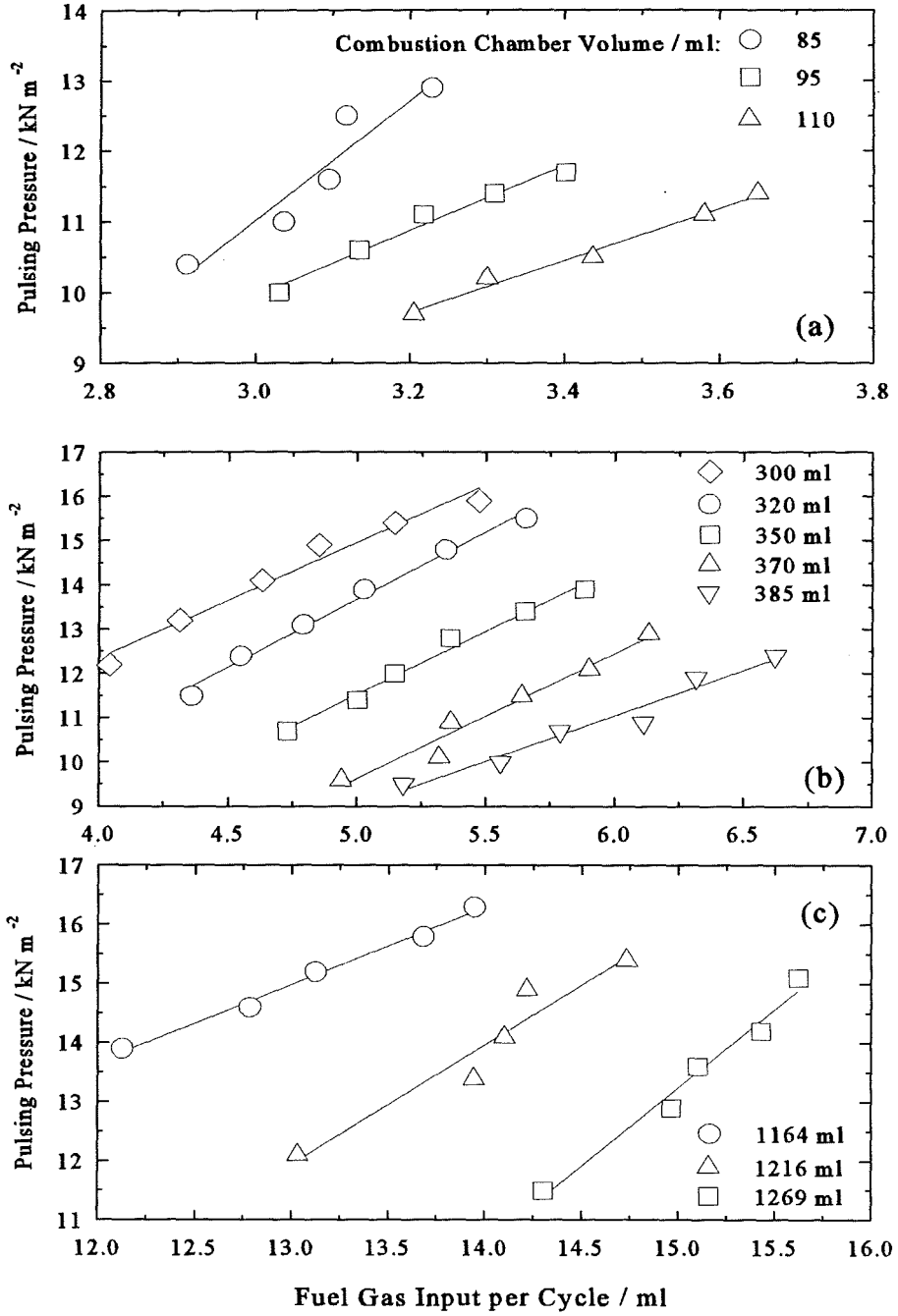

Fig. 5.9 Variation of peak pulsing pressure with fuel gas input per cycle for the combustors a) 7.5 kW with tailpipe length of 1500 mm, b) 15 kW with tailpipe length of 1500 mm and c) 30 kW with tailpipe length of 2000 mm. Combustion chamber volumes are shown.

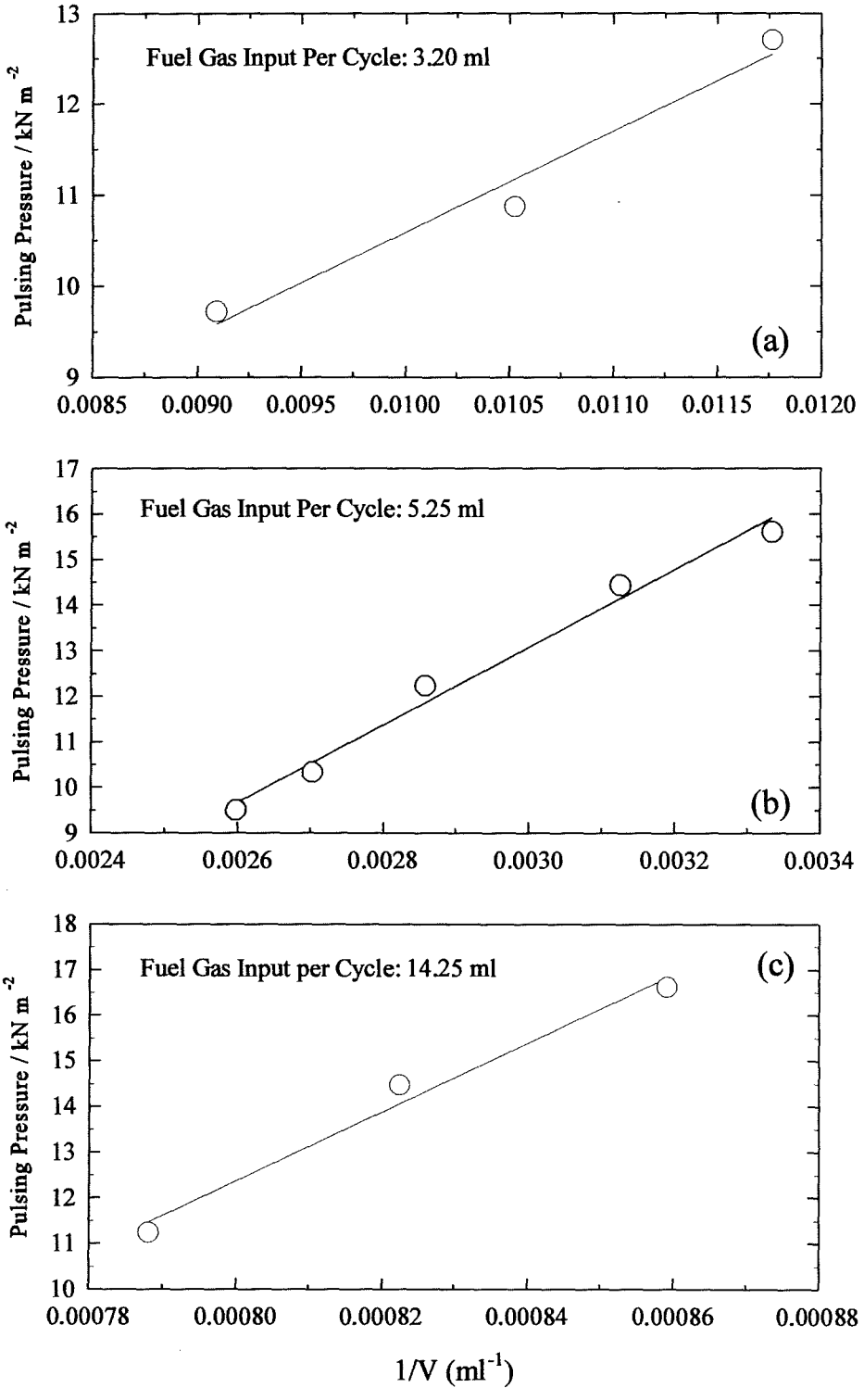

Fig. 5.10 ***Peak pulsing pressure vs 1/V, where V is the combustion chamber volume for the three developed combustors: a) the 7.5 kW, b) the 15 kW and c) the 30 kW. Configurations as in Fig. 5.8.***

$\tau_{species}$ also should have been constant. Thus, the total ignition delay time should have remained constant. However, the frequency of oscillation decreased as the CCV increased (see Fig. 4.8) resulting in an increase of the period of pressure oscillation and hence some change in phase relationship between the heat release and pressure oscillations (i.e. delaying pressure maximum). The change in coupling between heat release and pressure oscillations may also have modified the magnitude of pressure amplitude as described in Chapter 1 [Keller *et al.*, 1989]. In this study no data was available to confirm the theory. Clearly there is a need for more study on this area.

5.4.2 Effect of Tailpipe Length

The peak pulsing pressures of the 7.5 and 15 kW pulsed burners were measured with variation of the tailpipe length. The experimental results are shown in Fig. 5.11 and 4.11 (for the frequency measurements). During these measurements the fuel gas volume input rate, combustion chamber volume and flapper valve thickness were kept constant as the tailpipe length was varied. The results show that the peak pulsing pressure of the two combustors decreased as the tailpipe length was increased (Fig. 5.11).

A similar analysis was applied to data in Fig. 5.11 and 4.11 as was used for the other parametric studies above; i.e. the peak pulse pressure at the tailpipe outlet was plotted vs the fuel gas volume per cycle as shown in Fig. 5.12. This case indicates a different result to those noted previously in that the pressure at the outlet decreased as the fuel gas per cycle increased. The observed change in the trend of peak pulsing pressure with an increase of tailpipe length may be attributed to three factors:

i) Frictional effects between the exiting gas and the inner walls of the tailpipe. As the tailpipe length was increased the friction on the tailpipe wall increased and more damping and acoustic losses occurred, resulting in the observed decrease of peak pulsing pressure with an increase of tailpipe length.

ii) Modified coupling of heat release and pressure oscillations as described in section 5.4.1. Although the time of heat release remained constant when the rate of input fuel gas was kept constant an increase in the tailpipe length increased the period of

oscillations as seen in Fig. 4.11, thereby delaying the pressure maximum. This in turn modified the phase difference and the coupling between heat release and pressure oscillations resulting in a lower pressure amplitude [Keller *et al.*, 1989]. This suggests that there is a limit for the length of tailpipe that each pulsed unit can incorporate to satisfy the Rayleigh criterion and operate successfully.

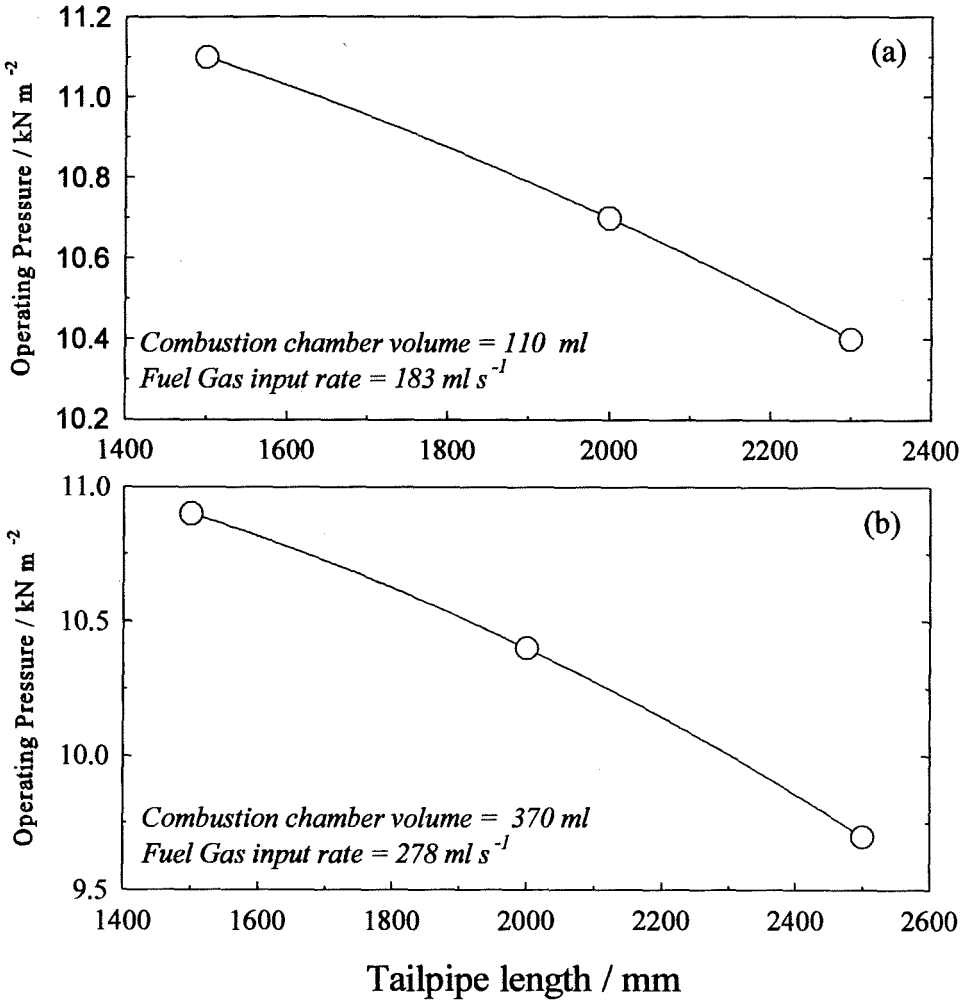

Fig. 5.11 ***Effect of change of the tailpipe length upon the peak pulsing pressure for a) the 7.5 kW combustor and b) the 15 kW combustor at given fixed combustion chamber volumes and fuel gas input rates.***

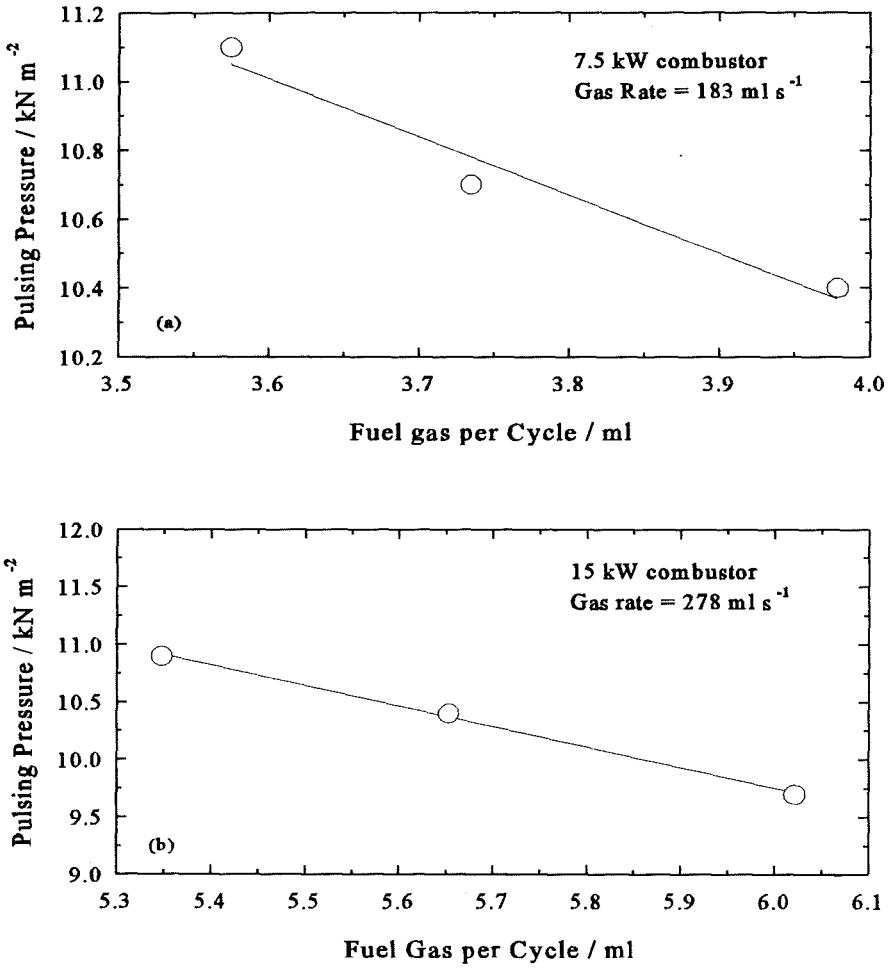

Fig. 5.12 ***Variation of peak pulsing pressure vs fuel gas per cycle for a) the 7.5 kW combustor and b) the 15 kW combustor. The data as in Fig. 5.11 showing various tailpipe lengths for each combustor.***

However, in some cases, for example that reported by Francis *et al.* [1963], the pulsed unit may adjust itself by jumping to a new mode (i.e. higher acoustic harmonic) resulting in successful operation by causing the maximum pressure and heat release again to be in phase (i.e. Rayleigh criterion).

3) Additional expansion of combustion gases as the tailpipe length was increased due to the increase of the internal volume of the tailpipe. However, since some of the

combustion gases remain inside the tailpipe after each cycle, the influence of this factor on the observed peak pulsing pressure changes with the change of the tailpipe length is thought to be minimal compared to the above two other factors.

5.4.3 Effect of Flapper Valve Thickness

Together with the frequency measurements (Fig. 4.12) the peak pulsing pressure at the outlet of the exhaust was measured when using PTFE-coated fibre glass flapper valves with thicknesses ranging from 0.13 mm to 0.36 mm. The results are shown in Fig. 5.13. Clearly the flapper valve thickness exerted a considerable influence on both the frequency of operation as shown in Fig. 4.12 and the peak pulsing pressure shown in Fig. 5.13.

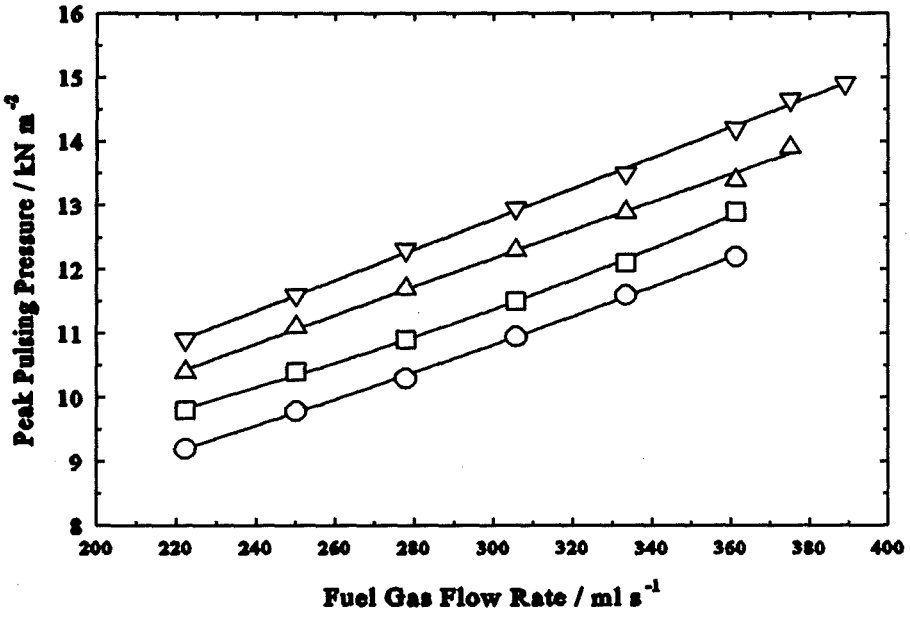

Fig. 5.13 ***Effect of flapper valve thickness on peak pulsing pressure of the 15 kW combustor. Combustion chamber volume 370 ml and tailpipe length 1500 mm. Symbols as in Fig. 4.12.***

An analysis of the peak pulsing pressure vs fuel gas volume per cycle is shown in Fig. 5.14. All the data fall on a single line confirming that the heat release per cycle was the primary factor controlling the peak pulsing pressure in this type of combustor.

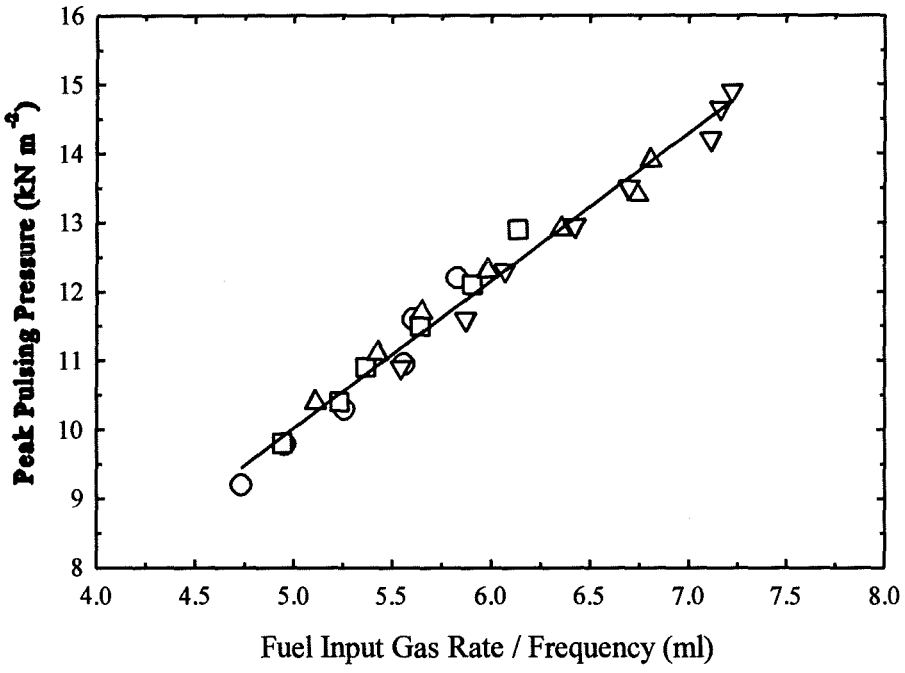

Fig 5.14 ***Variation of peak pulsing pressure as a function fuel gas volume per cycle for various flapper valve thickness. Symbols as in Fig. 4.12.***

Further analysis was carried out by plotting all the measured peak pulsing pressure data at fixed configuration of the 15 kW combustor (i.e. fixed tailpipe length and combustion chamber volume) against fuel gas volume per cycle as shown in Fig. 5.15. This has been done for the fan on/fan off conditions over a range of firing rates (data in Fig. 5.6), nitrogen injection at various rates (Fig. 5.7b) and a range of flapper valve thickness (Fig. 5.14). As can be seen all the data, can be represented by a single straight line through the origin. This provides further confirmation that peak pulse pressure was primarily controlled by heat release per cycle in the present design of pulsed combustors according equation (5.1).

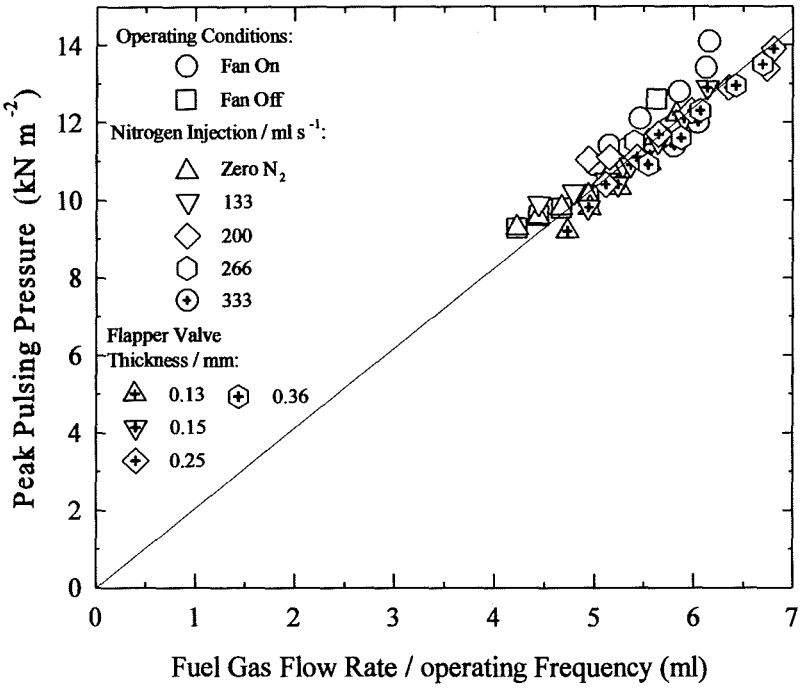

Fig. 5.15 ***Variation of peak pulsing pressure with fuel gas rate divided by operating frequency for given various operating conditions. Line shown is the best straight line through the points and origin.***

5.5 Summary and Conclusions

Peak pulsing pressure measurements for the three developed 7.5, 15 and 30 kW combustors were made at the end of the tailpipe under various operating conditions. Parameters included fuel gas input rate, combustion chamber volume, tailpipe length and flapper valve thickness. In addition, the effect of operating the 15 kW combustor with the air fan on and the addition of nitrogen to the inlet air was studied.

The results obtained indicated that for a fixed configuration of the pulsed units, the peak pulsing pressure increased when;

a) the fuel gas input rate increased,

b) the pulsed combustor was run with the air fan kept switched on,

c) the nitrogen injection rate was increased.

When the obtained data were plotted as a function of fuel gas volume per cycle it was found that the data fell on a single line for each operating condition. From these analyses it can be concluded that for a fixed configuration of the pulsed units, the peak pulsing pressure was principally controlled by the increase in heat release per cycle within the combustion chamber. However, phase angle data would provide additional information on effects that modify the peak pulse pressure of this type combustor. A number of studies, including Keller *et al.* [1989] Jones and Leng [1994] have shown that there is a significant influence of phase angle on operating pressure of the pulsed combustors.

For a fixed fuel gas input rate results showed that the peak pulsing pressure was affected by the configuration of the units. The peak pulsing pressure increased as the CCV and tailpipe length decreased. The pattern of variation of peak pulsing pressure with CCV was expected and was in the conformance with theory. With increasing tailpipe length, frictional interaction between the exiting gases and the internal surface of the tailpipe resulted in a decrease in the measured peak pulsing pressure at the exit. Modified coupling between heat release and pressure oscillations may also have been a factor responsible for lower peak pulsing pressure as the tailpipe was increased.

The pulsing pressure increased with increasing thickness of the flapper valve. The results obtained indicated that this is primarily because of increased amount of heat release per cycle associated with a thicker flapper valve due to modification of the frequency.

Chapter Six

GASEOUS EMISSIONS

6.1 Introduction

It is well known that pulsed combustion systems generally operate with low emissions of nitrogen oxides. During the last 20 years, there have been a number of published works investigating the factors that affect the NO_x emissions and the mechanism that controls the formation of NO_x from pulsed combustion systems [Corliss *et al.*, 1984 ; Keller and Hongo, 1990; Keller *et al.*, 1994a ; Lindholm, 1995 ; Jones and Leng, 1996; AU-Yeung *et al.*, 1998]. Some of the findings of these authors are described in Chapter1.

Regulations on NO_x emission becoming increasingly stringent and other low NO_x combustion technologies are gaining ground. Therefore, there is yet a need for a more systematic study of NO_x and CO emissions from pulsed combustion systems. In addition data are generally lacking on the variations of levels of combustion products from a premixed gas-fired pulsed combustor, that result from differences in the size and configuration of pulsed combustor or from operating a given combustor at various input gas rates or with change of fuel gas composition.

In this chapter an extensive body of data on combustion gases for the three developed pulsed combustors is presented. The data include the relation of NO_x and CO emissions with input firing rate, excess air ratio, combustor configuration (i.e. combustion chamber volume and tailpipe length), water bath temperature and input fuel gas composition. Moreover, in an attempt to reduce the NO_x emission from the pulsed combustors, the effects of diluting the inlet mixture charge of air and gas with nitrogen or argon were studied.

The information obtained from the analysis of these data is a step towards the optimization of the performance and configuration of pulsed combustors of this type. Furthermore, it provides a better understanding of the parameters influencing the

formation of NO_x and CO in this type of pulsed combustor and can be used as a guide to employing suitable methods to reduce emission of these pollutant gases from such combustors.

6.2 General

As shown in Chapter 2 the combustors were designed to allow considerable variation in their configurational parameters; these included tailpipe dimensions (length and diameter), combustion chamber volume (choice of combustor size and aspect ratio of the combustion chamber) and flapper valve thickness. Other variables were fuel gas flow rate, air flow rate and the temperature of water in the water bath.

A PTFE-coated glass fibre flapper valve of 0.15 mm thickness was used throughout the work unless specifically noted otherwise. The water bath temperature was maintained constant at 65 ±1°C, which was above the dew point of flue gas at the stoichiometric condition [Appendix VI]. During a typical test, the pulsed combustor was operated at a particular air-to-fuel ratio until all readings stabilised.

At the tailpipe exit, analysis was carried out for CO, CO_2, NO_x ($NO + NO_2$) and O_2. In this study N_2O values were not taken into account. Apparatus employed for the experimental measurements was described in Chapter 3.

Dilution effects for NO_x and CO were eliminated by correcting to zero oxygen content [see Appendix V]. The excess air and hence air flow rate was calculated based on oxygen (for fuel-lean mixture) and CO (for fuel-rich mixture) measurements [Appendix IV]. The stoichiometric air-to-fuel ratio was calculated for mains natural gas using the fuel gas analysis supplied by North London Gas Board and was updated weekly using the current value in a particular test. A typical value for the stoichiometric air-to-fuel ratio was 9.66.

6.2.1 Correlation between CO_2 and O_2

For a given fuel gas composition, the oxygen and carbon dioxide levels in the exhaust

are simply related, providing that the CO level is low (e.g. < 0.1 %). This is readily shown for the special case where the fuel gas is 100 % methane and complete combustion takes place in air as follows:

$$CH_4+2\lambda(O_2+3.76N_2)\rightarrow CO_2+7.52\lambda N_2+2H_2O+2(\lambda-1)O_2 \qquad (6.1)$$

λ is the actual A/F divided by the stoichiometric A/F. Writing CO_2 concentration (%) as s and the O_2 concentration (%) as p, where both are on a dry basis it is readily shown that

$$p=\frac{200(\lambda-1)}{9.52\lambda-1} \qquad (6.2)$$

and

$$s=\frac{100}{9.52\lambda-1} \qquad (6.3)$$

Eliminating λ between equations (6.2) and (6.3) leads to

$$s=\frac{100}{8.52}-\frac{4.76}{8.52}p \qquad (6.4)$$

or

$$s=11.74-0.56p \qquad (6.5)$$

Equation (6.5) indicates that a plot of s vs p (i.e. CO_2 vs O_2) should be a straight line with intercept of 11.74 (at p = 0) and a slope of -0.56. Equation (6.5) for the natural gas with composition given in Appendix II becomes:

$$s=11.88-0.57p \qquad (6.6)$$

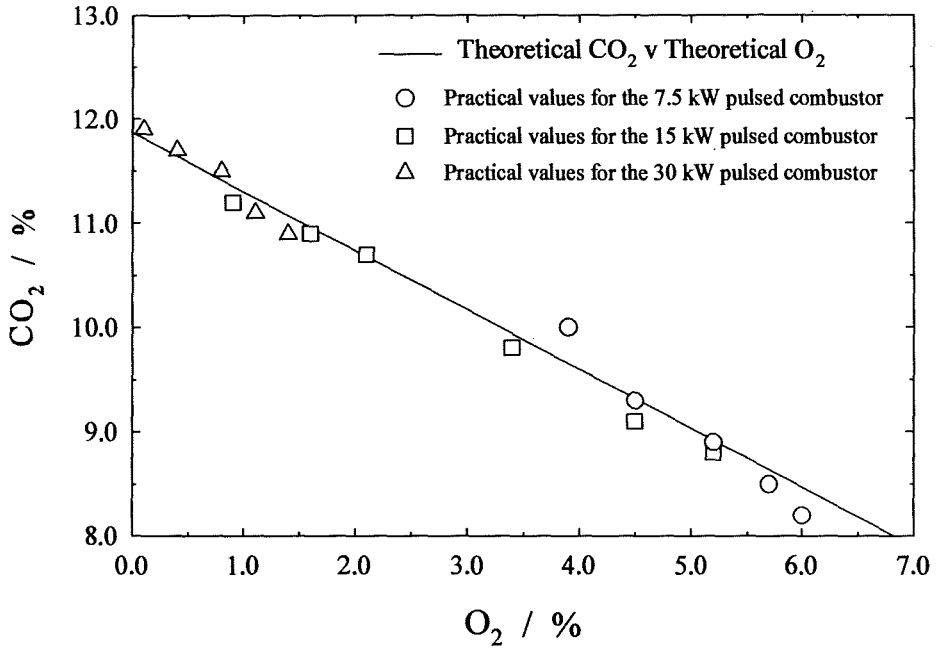

Fig. 6.1 Comparison of theoretical and practical values of O_2 and CO_2 for the three pulsed combustors.

This analysis provides a useful check on the analytical system. In Fig. 6.1 experimental values are shown and compared with the theoretical line according to equation (6.6) which takes account of the actual composition of the fuel gas. Agreement between theory and experiment is considered satisfactory providing confidence in the sampling procedure and gas analysis for CO_2 and O_2.

6.3 Results

The results obtained from a systematic investigation on NO_x and CO emissions using the three developed nominally 7.5, 15 and 30 kW pulsed combustors are presented below. The data represented here show the influence of the changeable parameters upon emission of these pollutant gases which then are discussed in more depth in later sections.

6.3.1 Influence of Fuel Gas Input Rate

Burning mains natural gas only, the effect of varying fuel gas input rate upon emission of NO_x and CO was studied. The study also enables the optimum fuel gas input rate to be identified for the present design of pulsed combustors in terms of these pollutant gases. Figures 6.2, 6.3 and 6.4 show the typical pattern of combustion products in relation to increasing gas input rates for the three developed combustors. The measurements were made using combustion chamber volumes of 110, 370 and 1270 ml for the nominally 7.5, 15 and 30 kW combustors respectively. The tailpipe length in each case was 2000 mm with outside diameter of 12, 15 and 22 mm for the 7.5, 15 and 30 kW combustors respectively.

From these figures (Fig. 6.2-6.4) some general observations may be made as follows:

- The oxygen level and hence air-to-fuel ratio (A/F) tended to decrease as the size of the combustor increased from nominally 7.5 to 15 and to 30 kW.
- The oxygen concentration and hence excess air decreased as the fuel gas rate increased. The decrease in oxygen level and hence excess air arises from the fact that the appliances were self-aspirating combined with the throttling effect of the air intake. The variation of calculated excess air and airflow rate with input fuel gas rate are shown in Fig 6.5.
- The CO_2 concentration and heat input increased almost linearly with increasing fuel gas input rate. The increase in CO_2 was a reflection that the oxygen concentration decreased approximately linearly with increasing fuel gas rate. Linearity of one (CO_2 or O_2) must result in linearity of the other because CO_2 and O_2 are themselves linearly related (equation 6.6). The CO_2 emission levels generally ranged from 7.5 to 11% for the three combustors.
- NO_x concentrations for the three developed combustors increased with increasing fuel gas rate ranging from 10 ppm at the highest percentage excess air to 70 ppm at highest fuel gas input rate and corresponding lowest percentage excess air.

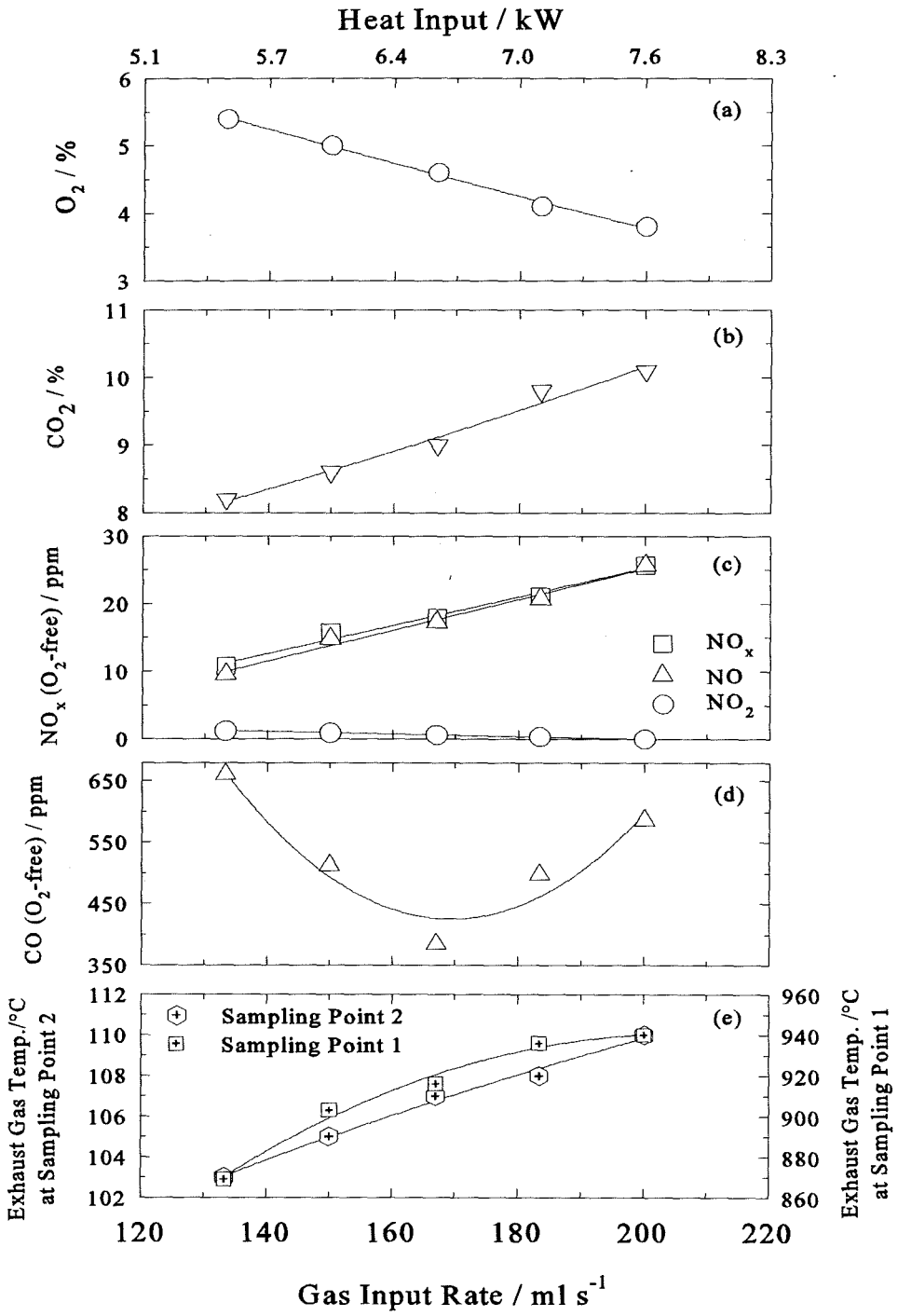

Fig. 6.2 Variation of a) O_2, b) CO_2, c) NO_x, d) CO concentrations and e) exhaust gas temperature at two sampling points with fuel gas input rate for the nominally 7.5 kW combustor at fixed combustion chamber volume of 110 ml and tailpipe length of 2000 mm.

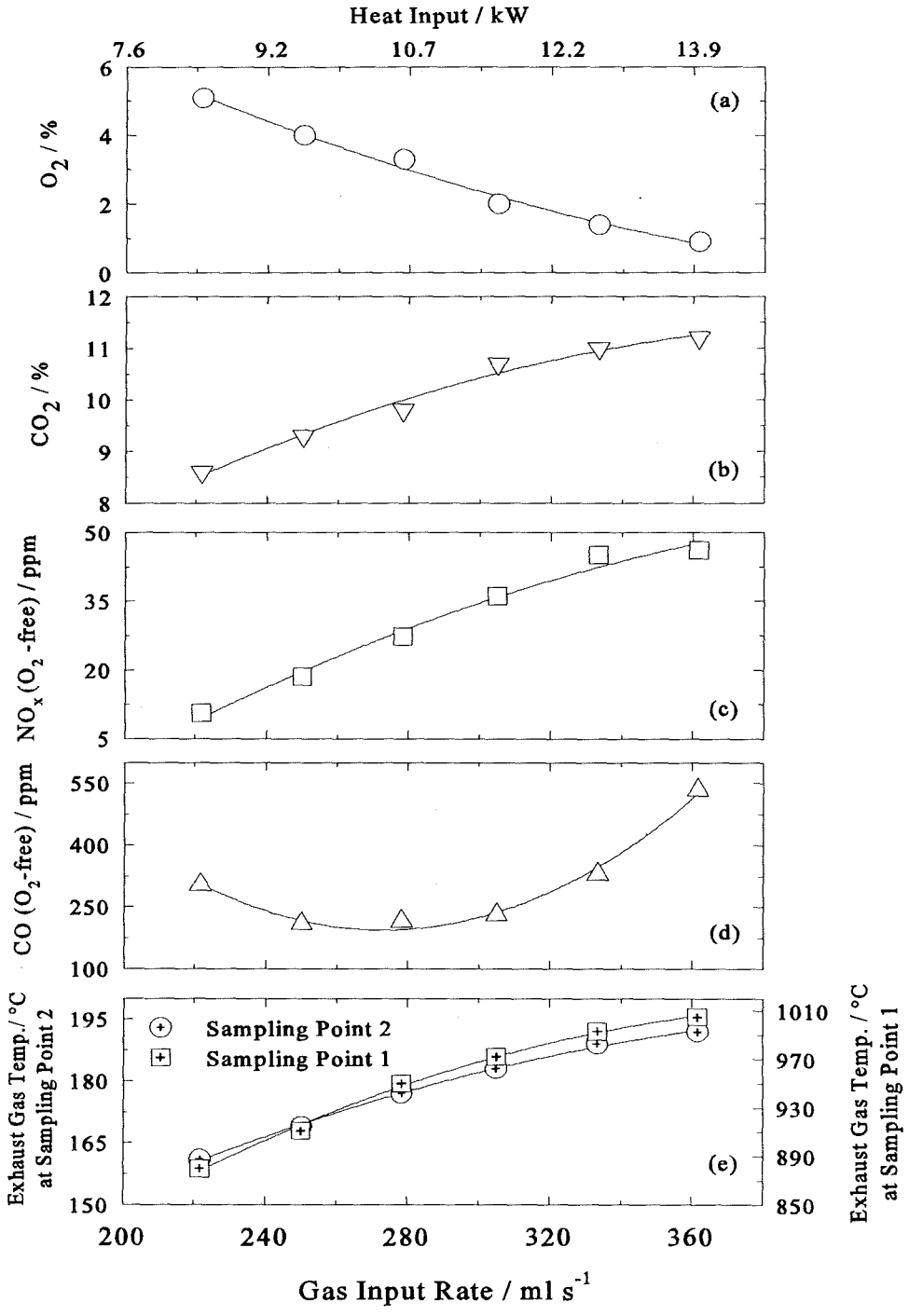

***Fig. 6.3** Variation of a) O_2, b) CO_2, c) NO_x, d) CO concentrations and e) exhaust gas temperature at two specified sampling points with fuel gas input rate for the nominally 15 kW combustor at fixed combustion chamber volume of 370 ml and tailpipe length of 2000 mm.*

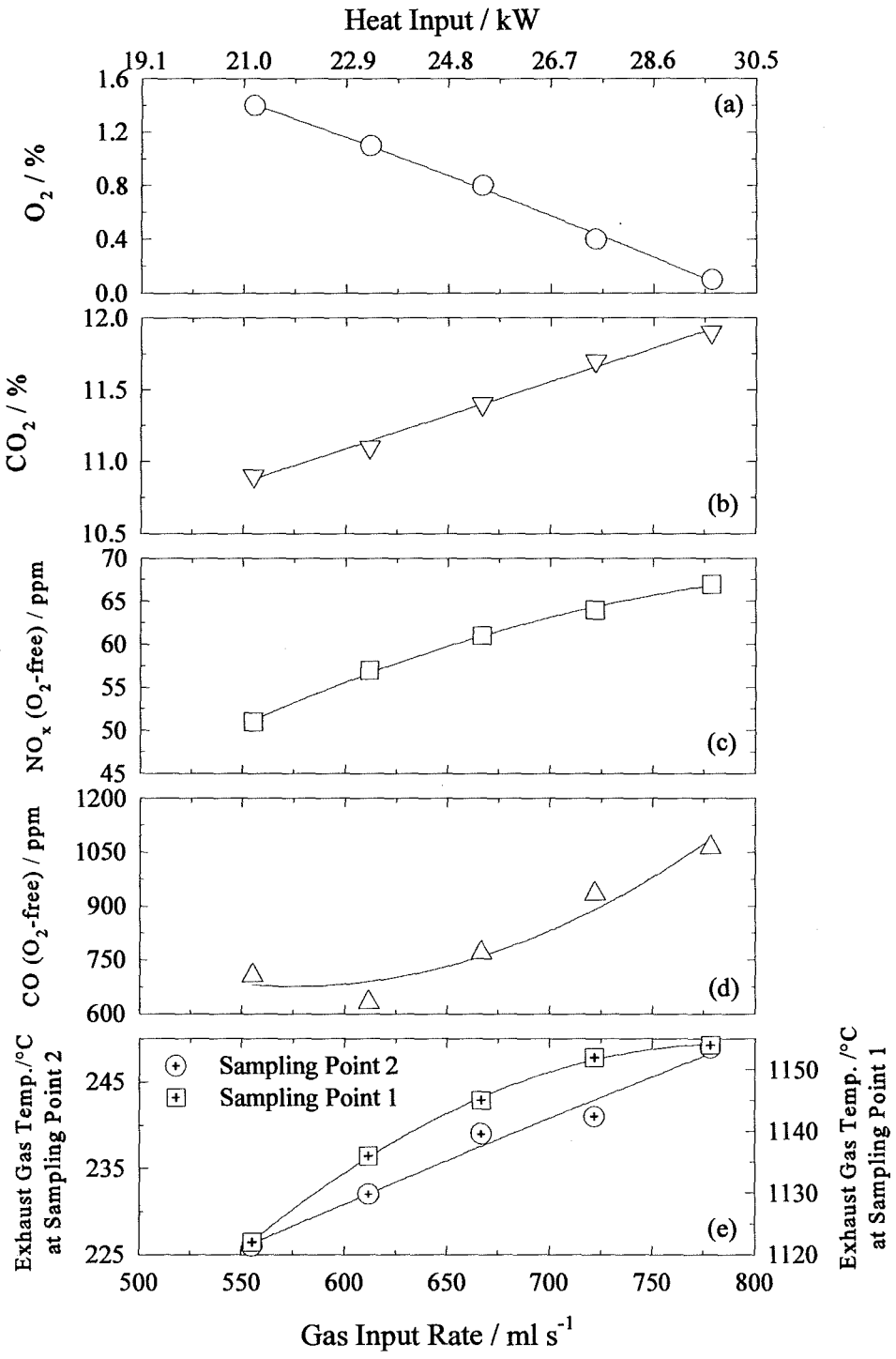

***Fig. 6.4** Variation of a) O_2, b) CO_2, c) NO_x, d) CO concentrations and e) exhaust gas temperature at sampling points 1 and 2 for the nominally 30 kW combustor using fixed combustion chamber volume 1270 ml and tailpipe length of 2000 mm.*

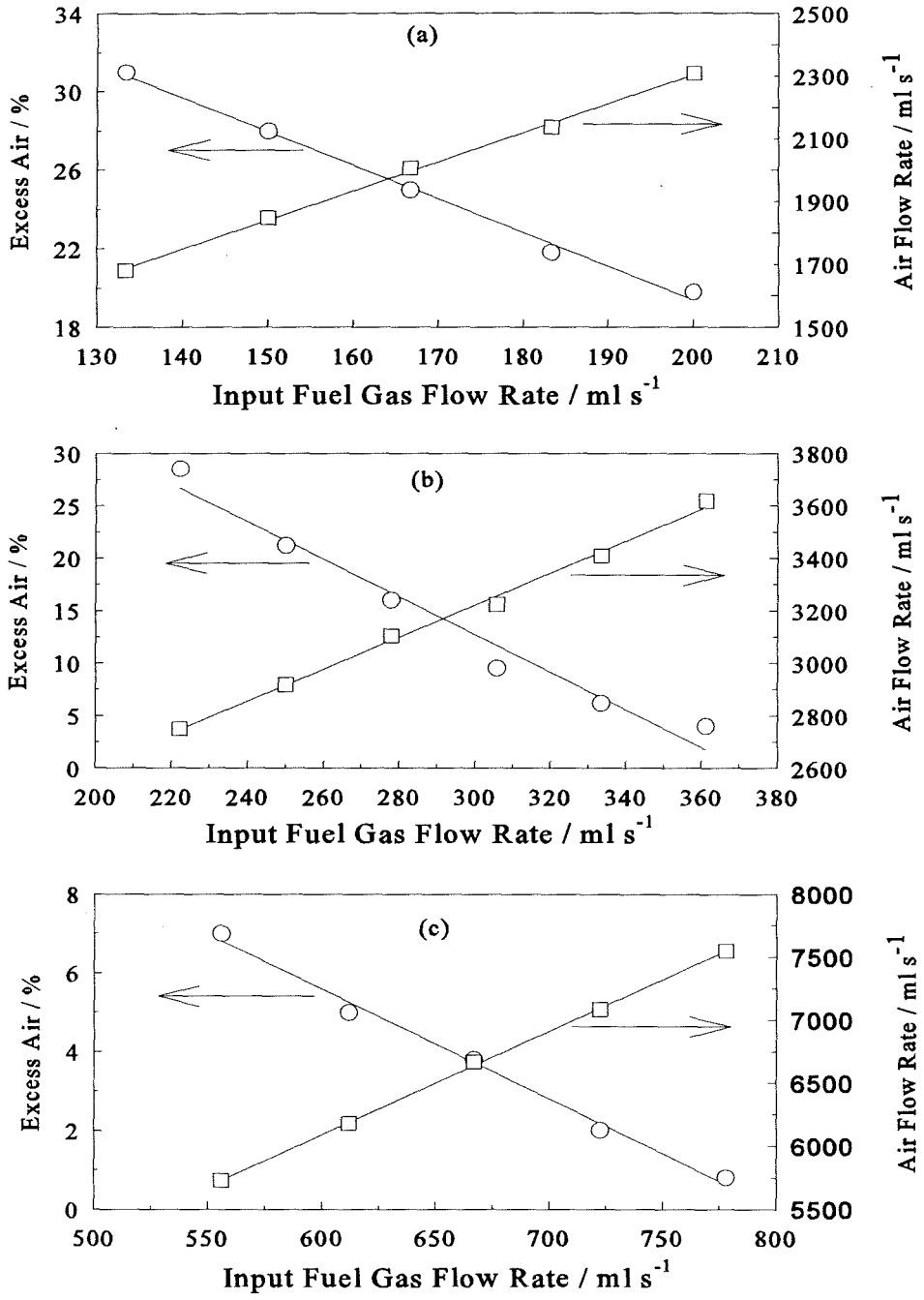

***Fig. 6.5** Variation of excess air and air flow rate as a function of fuel gas flow rate for a) the 7.5 kW combustor, b) 15 kW combustor and c) the 30 kW combustor with combustion chamber volumes of 110, 370 and 1270 ml respectively and fixed tailpipe length of 2000 mm.*

- During the measurements of NO_x it was conspicuous that nearly all of the NO_x was emitted as NO. Only when the excess air was above 30 %, was NO_2 formed (up to 15% of total NO_x) as shown in Fig. 6.2c. Studies of NO_x formation and oxidation of NO to NO_2 have shown [Hargreaves *et al.*, 1981; Bowman, 1992] that at high flame temperatures (i.e. >1500 K) the oxidants such as HO_2 are not stable for reaction with NO to cultivate NO_2 (see Chapter 1 for the mechanism of formation of NO_2). In the present work the calculated adiabatic flame temperature was generally above 1850 K, although the actual flame temperature inside the combustion chamber is expected to be lower.
- The CO/CO_2 ratio was generally below 0.01 and within the British Standards [B.S 5258, 1986] requirements. Carbon monoxide concentration showed a U-shaped curve when plotted against fuel gas flow rate; values were typically in the range of 200-1100 ppm when combustion air was in excess (Fig. 6.2d, 6.3d and 6.4d).
- Exhaust gas temperatures measured at each end of the tailpipe increased with the nominal combustor size, 7.5 - 30 kW. They also increased with increase of fuel gas flow rate (Fig.6.2e to 6.4e); this was as a result of the decreasing A/F with increasing fuel gas rate (Fig. 6.5) which resulted in increased flame temperature.

The above findings are in line with most reported studies including: Windmill [1984], Belles *et al.* [1988], Suthenthiran [1988], Keller *et al.* [1994a] and Jones and Leng [1996].

6.3.2 Effect of Air Flow Rate on NO_x and CO emissions

The present design of pulsed combustors does not allow direct measurement of air flow rate to the combustors. This is because of substantial pressure fluctuations in the air delivery system consequent to the pulsed process of the combustors which would lead to unstable readings of the air flow rate. Moreover, employing a flowmeter within the air delivery system was found to restrict the air intake through the air delivery system to the mixer head and so prevented the system from pulsing. Thus air flow rate was calculated from the oxygen concentration in the exhaust and the fuel gas flow rate and

composition. Air flow rate could however be modified (increased) by running the combustor with the air fan remaining switched on after the ignition sequence. The amount of combustion air was varied by modifying the speed of fan.

Fig. 6.6 shows the variation of NO_x and CO with air flow rate when operating with a fixed input gas rate of 222 ml s^{-1}. It can be seen that as the air flow rate increased from 2650 to 3050 ml s^{-1} the NO_x concentrations (Fig. 6.6a) decreased from 18 to 7 ppm and exhaust gas temperature decreased from 940 to 870 °C (Fig. 6.6b). The reduction of combustion gases temperature was due to the rise of excess air following from the increase of air flow rate (Fig. 6.6b). At the same time for the given range of air flow rate the measured CO values showed a substantial increase of around 500 ppm, rising from 120 to 650 ppm corresponding to the minimum and maximum observed air flow rates respectively.

Figure 6.7 compares the variation of composition of combustion products and their temperatures when the 15 kW combustor was run with the air fan switched "on" and "off". Running the combustor with the air fan on resulted in lower NO_x values and as expected higher oxygen levels (Fig. 6.7) and A/F as shown in Fig. 6.8a. On the other hand, the CO values, presented as CO/CO_2 (Fig. 6.7), were higher than those values measured when the air fan was switched off. Also shown in Fig. 6.8b is the air flow rate vs input fuel gas rate at the two operating conditions. It can be seen that for a given fixed fuel gas input rate the air flow rate was higher with the air fan on, compared to when operating the unit with the air fan switched off as expected.

6.3.3 Influence of Combustion Chamber Volume

A series of tests was conducted to measure the concentrations of combustion products at various combustion chamber volumes (CCV) for each pulsed unit. The combustion chamber volumes ranged from 85 to 110 ml, 300 to 385 ml and 1170 to 1270 ml for the three nominally 7.5, 15 and 30 kW pulsed units respectively. Figures 6.9 to 6.11 display the variation of measured and calculated quantities with fuel gas flow rate at the specified CCV. The results show that at any given fixed heat input for each given

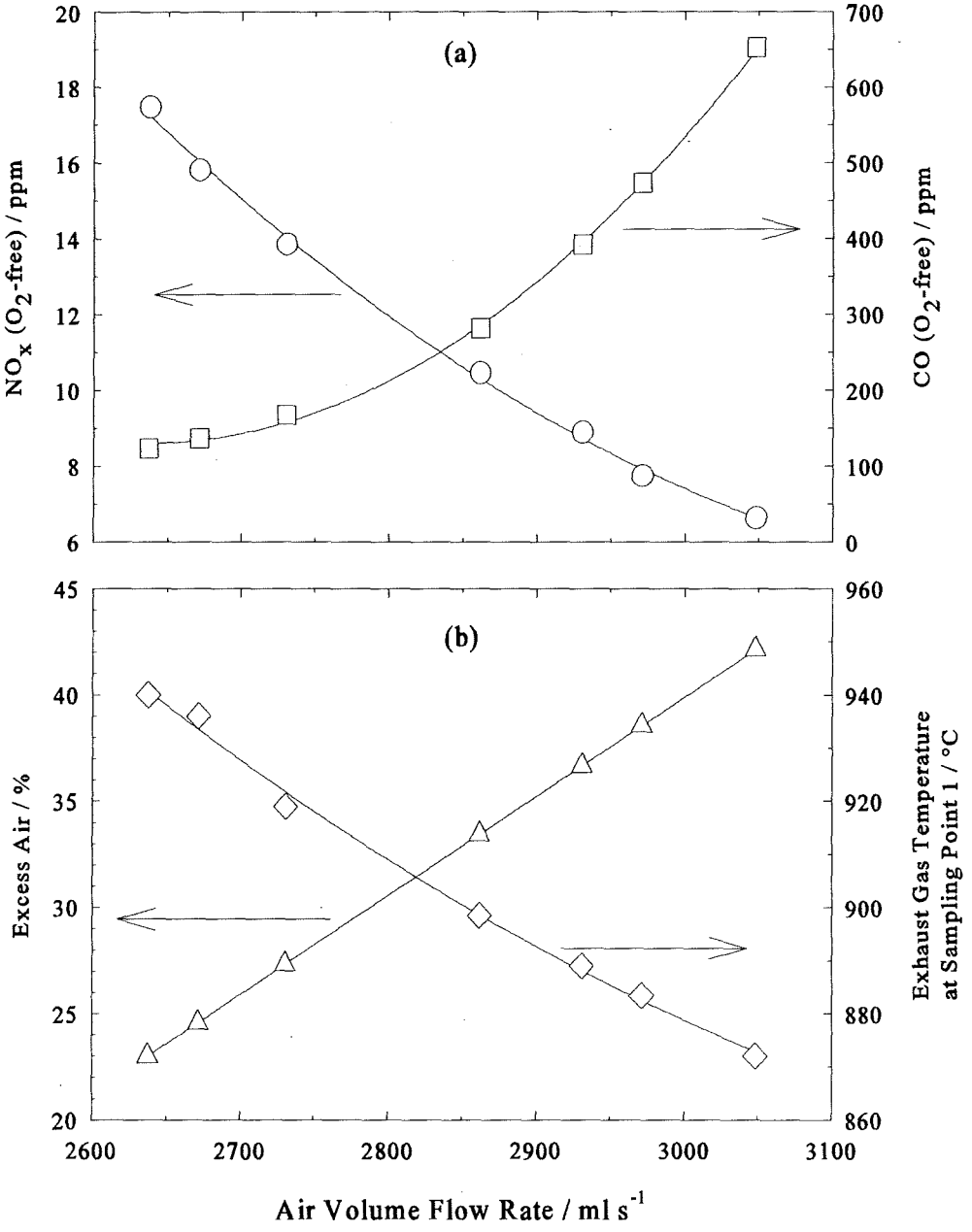

***Fig. 6.6** Effect of increasing air volume flow rate upon a) NO_x and CO emissions and b) amount of excess air and exhaust gas temperature within the combustion chamber, for the nominally 15 kW combustor at constant fuel gas input rate of 222 ml s^{-1}. The unit was operated using a combustion chamber volume of 350 ml and tailpipe length of 1500 mm. Flapper valve thickness was 0.13 mm.*

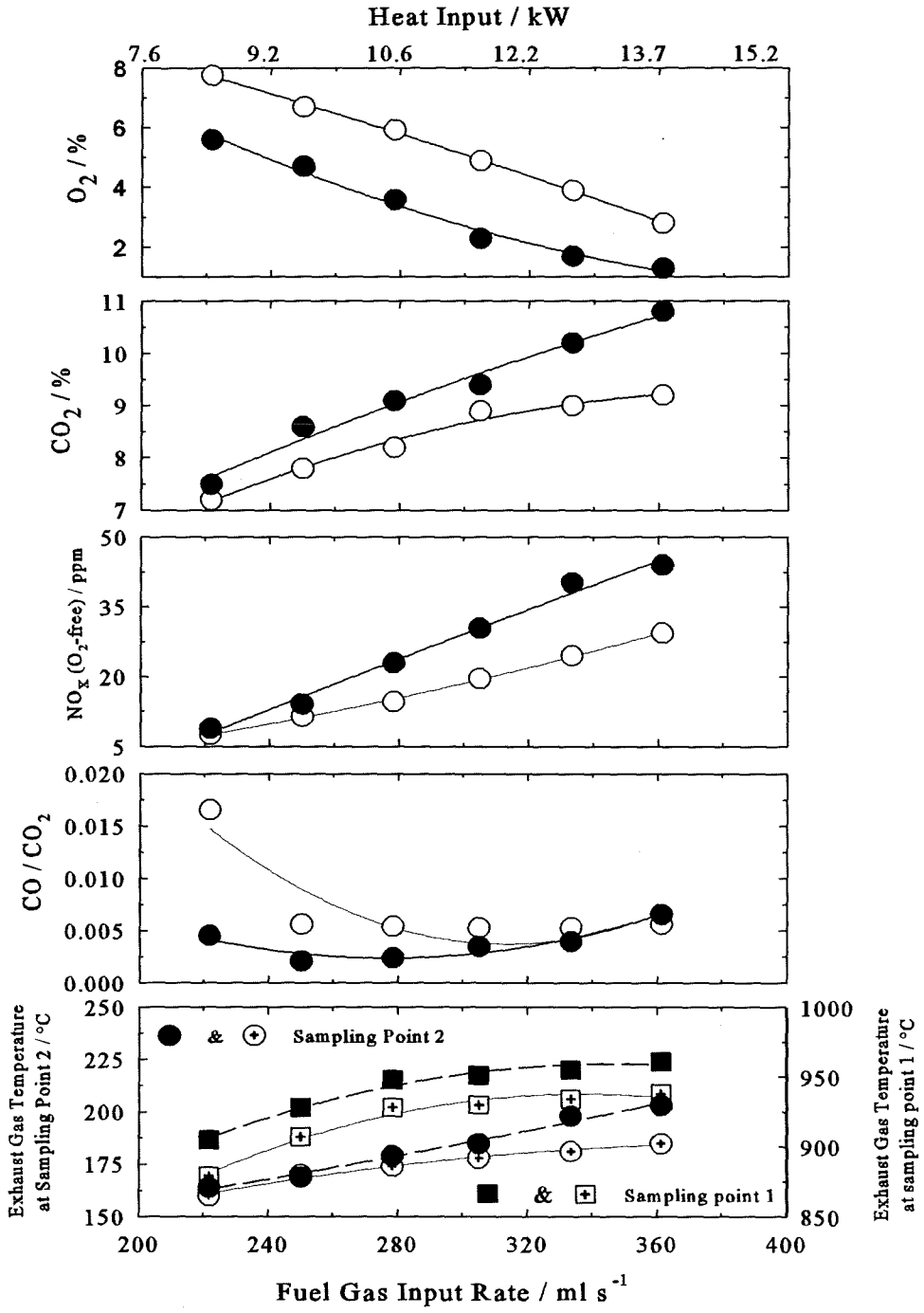

Fig. 6.7 Comparison of the combustion products and exhaust gas temperature when the nominally 15 kW combustor was run with the air fan switched "on" (white symbols) and "off" (black symbols). The configuration as in Fig. 6.6.

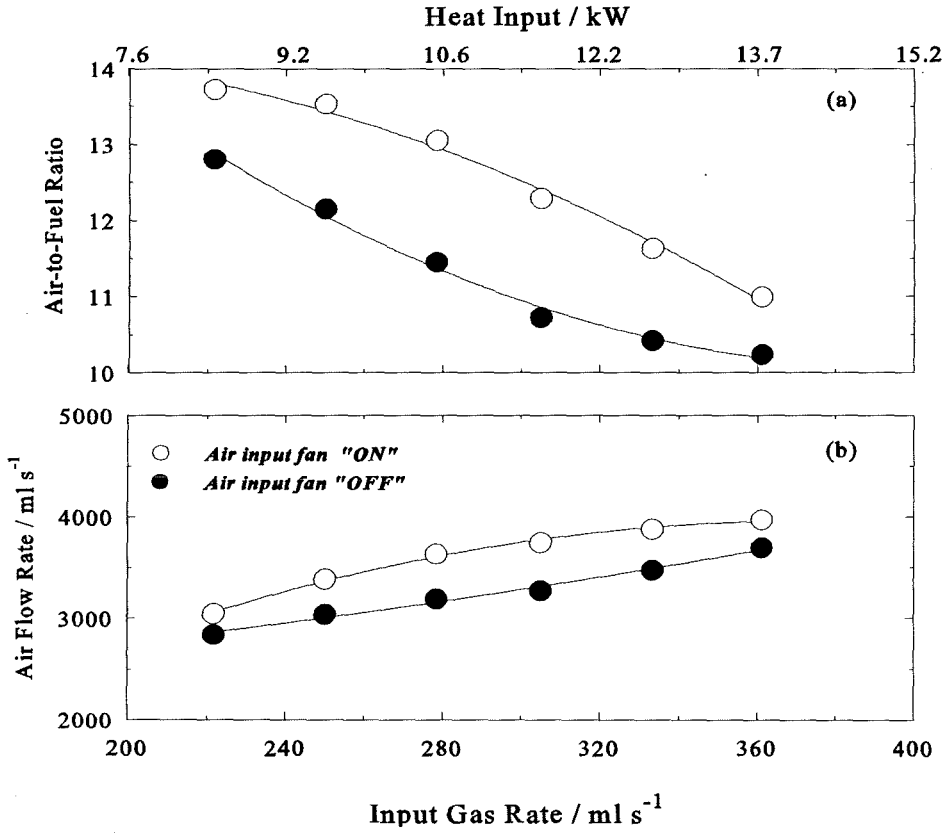

Fig.6.8 ***Variation of a) air-to-fuel ratio and b) air flow rate with mains natural gas flow rate using the 15 kW combustor with the fan on compared with when running the system with the fan switched off. The combustion chamber volume was 350 ml and tailpipe length 1500 mm. Flapper valve thickness chosen to be 0.13 mm.***

combustor the oxygen level (Fig. 6.9a - 6.11a), percentage excess air and air flow rate (Fig. 6.9g - 6.11g) decreased as the combustion chamber volume increased. For example, in the case of the nominally 15 kW combustor at a fixed gas input rate of 280 ml s^{-1}, the O_2 levels (Fig 6.10a) and excess air (Fig. 6.10g) fell from 5.0 and 30 % to 3.0 and 15 % respectively as the CCV was increased from 300 to 385 ml. Results also indicate that as the CCV was increased the NO_x concentration increased and CO emission decreased.

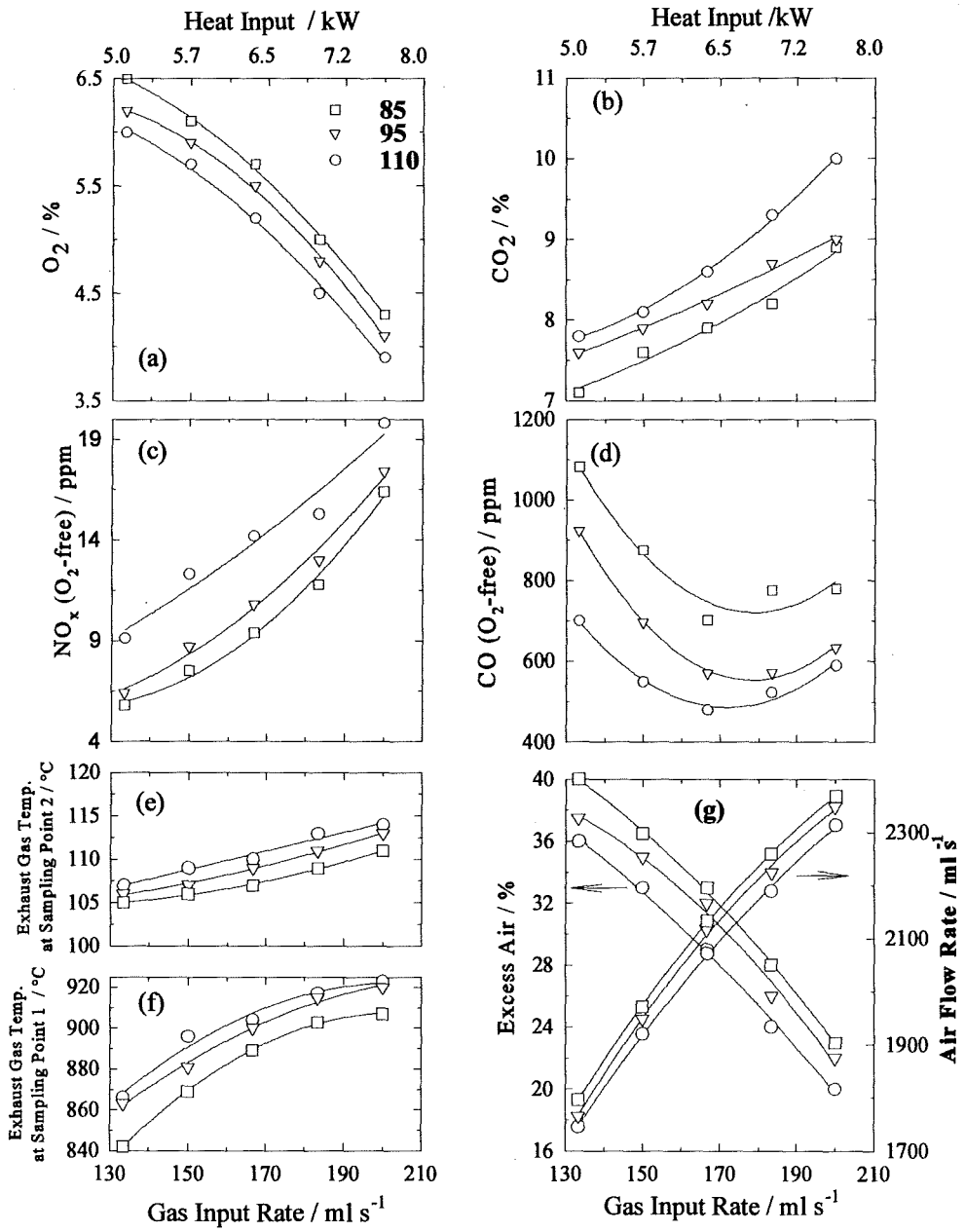

Fig. 6.9 ***Variation of a, b, c and d) combustion products, temperature of exhaust gas at e) sampling point 2, f) sampling point 1, g) excess air and air flow rate with input gas flow rate for the nominally 7.5 kW combustor at the specified combustion chamber volumes/ ml. The***

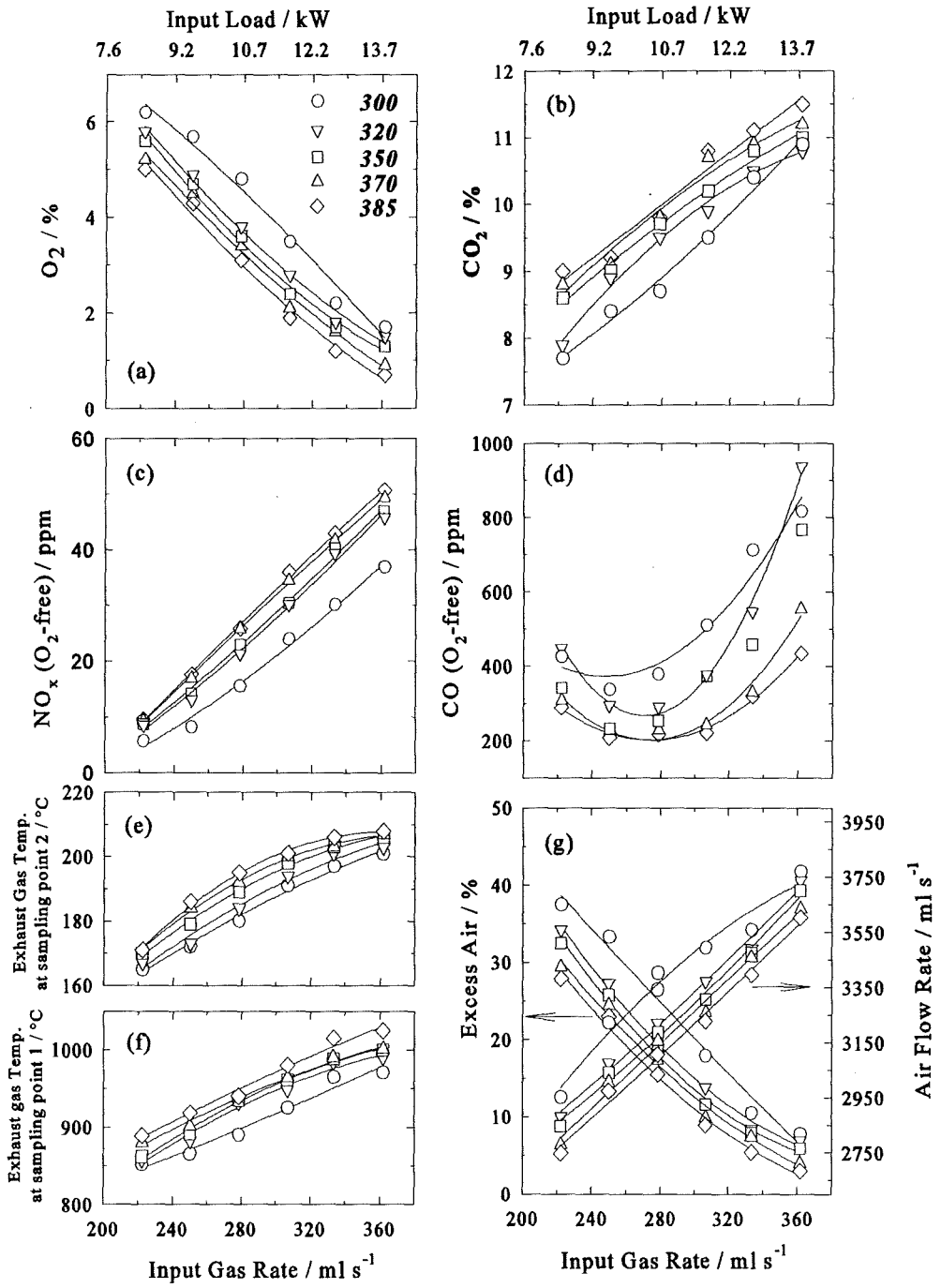

Fig. 6.10 ***Variation of a, b, c and d) combustion products, temperature of flue gas at e) sampling point 2, f) sampling point 1, g) excess air and air flow rate with gas input rate for the nominally 15 kW combustor at the specified combustion chamber volumes / ml. The tailpipe length was 1500 mm.***

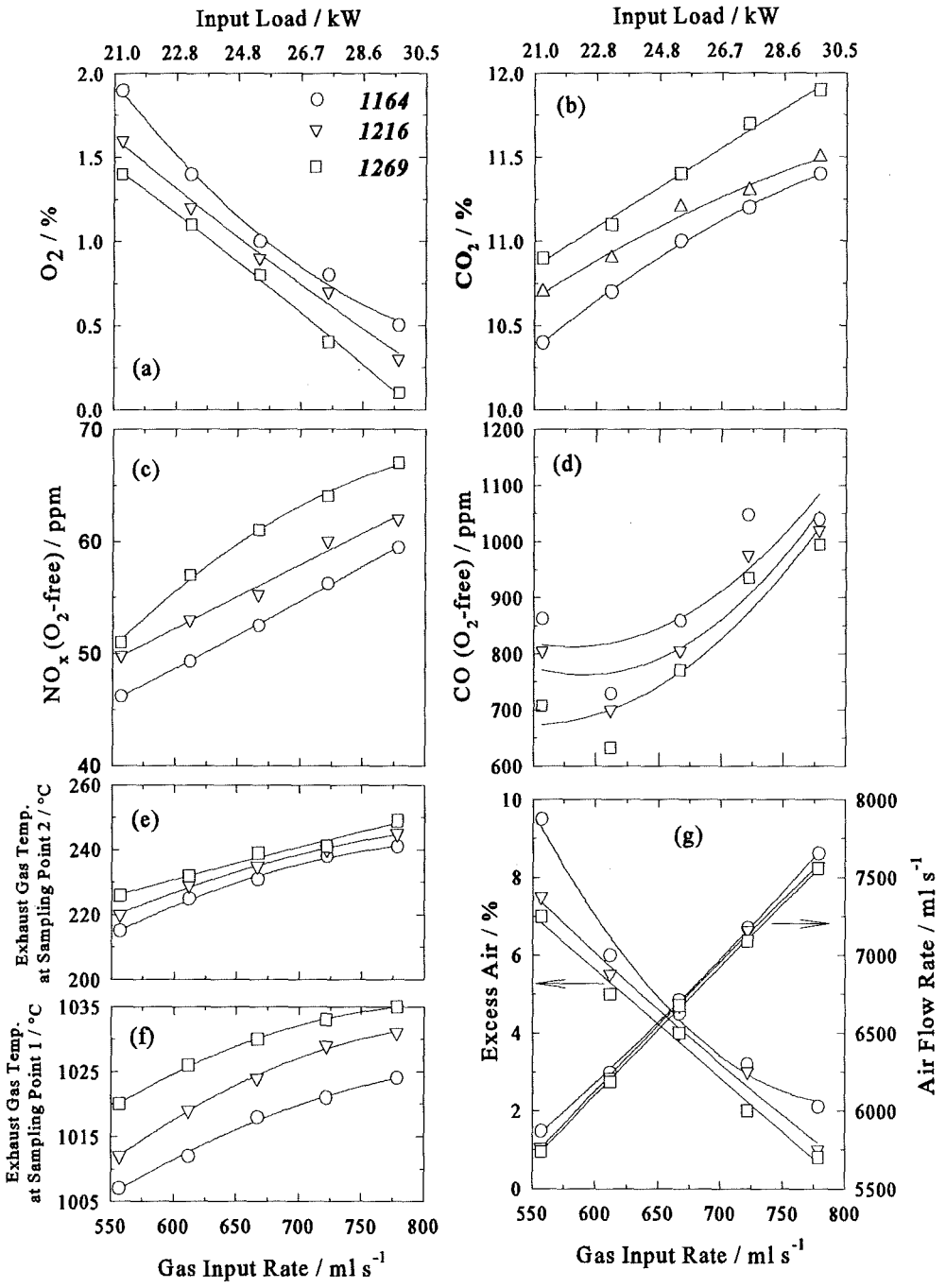

Fig. 6.11 ***Variation of a, b, c and d) combustion products, temperature of exhaust gases at e) sampling point 2, f) sampling point 1, g) excess air and air flow rate with gas input rate for the nominally 30 kW combustor at the specified combustion chamber volumes / ml. The tailpipe length was 1500 mm.***

6.3.4 Influence of Tailpipe Length

The effect of varying the tailpipe length on gaseous emissions was studied in a series of investigations. For the 7.5 and 15 kW burners the tailpipe length was varied from 1500 to 2300 mm and 1500 to 2500 mm respectively. The outside diameter of tailpipes used for the nominally 7.5 kW and 15 kW combustors were 12 and 15 mm respectively. Results for the nominally 7.5 and 15 kW combustors each with fixed combustion chamber volume, but three different tailpipe length are shown in Fig. 6.12 and 6.13 respectively. In the smaller combustor, at a given fuel flow rate, the NO_x concentration increased as the tailpipe length increased (Fig. 6.12c and 6.13c). At the same time the excess air reduced and combustion gas temperature increased (Fig. 6.12f and 6.13f). In the larger 15 kW combustor, at the given fuel input rate, NO_x was little influenced by tailpipe length (Fig. 6.13c). It is notable that the changes in oxygen level (Fig. 6.13a) and excess air also were not substantial (Fig. 6.13g).

Results for CO emission vs fuel gas flow rate (Fig. 6.12d and 6.13d) displayed a U-shape characteristics regardless of tailpipe length. However, there was no monotonic variation in CO with tailpipe length for the 7.5 kW combustor and little influence of tailpipe length for the 15 kW combustor. But the trend of results obtained indicates that CO increased as the tailpipe length decreased.

6.4 Discussion

In the following sections detailed analyses of the obtained results on NO_x and CO emissions are presented. Further, the effect of dilution of the mixture charge of air and gas with N_2 or Ar together with the effect of water bath temperature upon emission of NO_x and CO are presented, analysed and discussed.

6.4.1 Emissions of Nitrogen Oxides

NO_x formation can be attributed to three distinct chemical processes: these are thermal

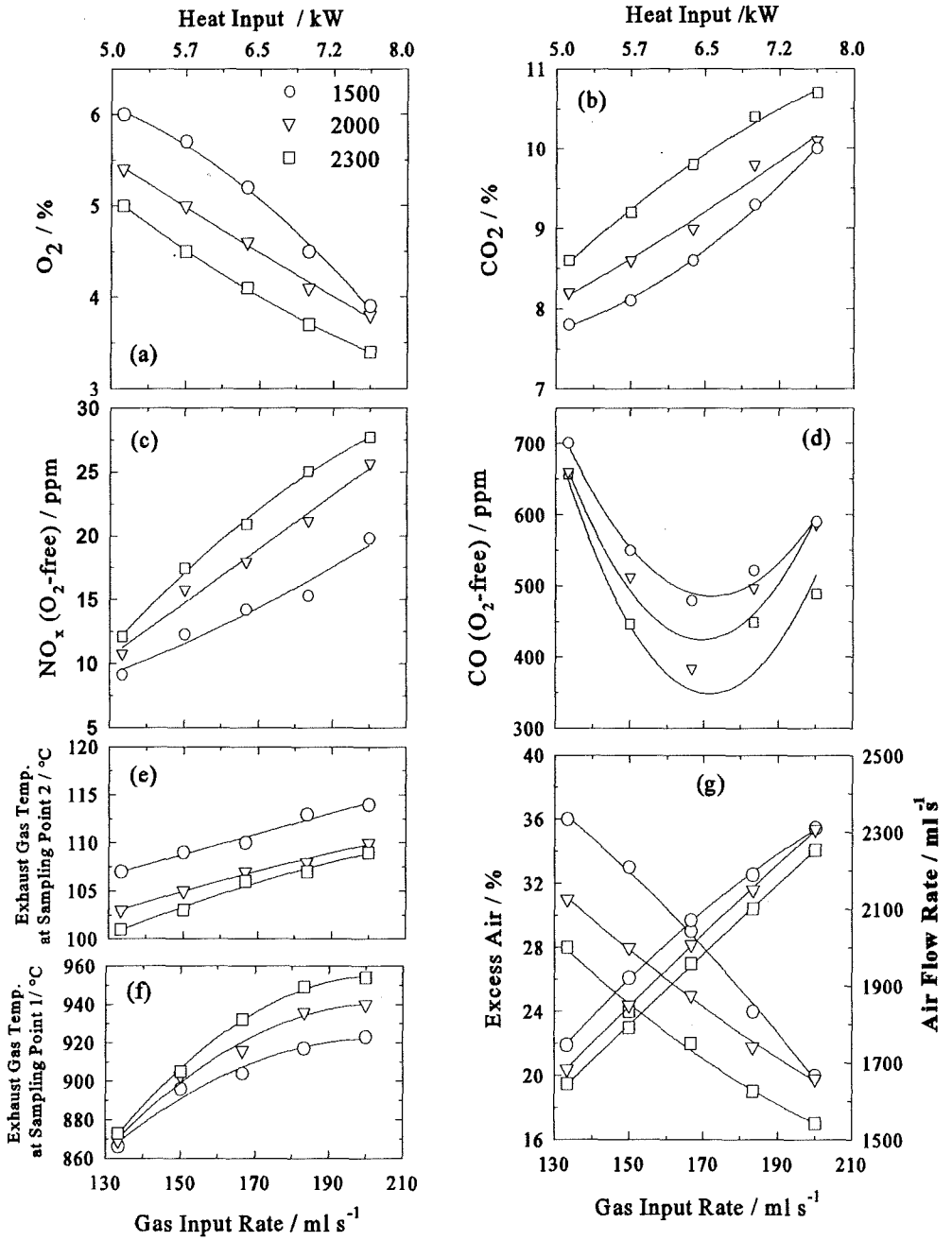

Fig. 6.12 ***Variation of a, b, c, and d) combustion products, temperature of exhaust gas at e) sampling point 2, f) sampling point 1 and g) excess air and air flow rate with input gas rate for the nominally 7.5 kW combustor at the specified tailpipe lengths / mm. Combustion chamber volume was kept constant at 110 ml.***

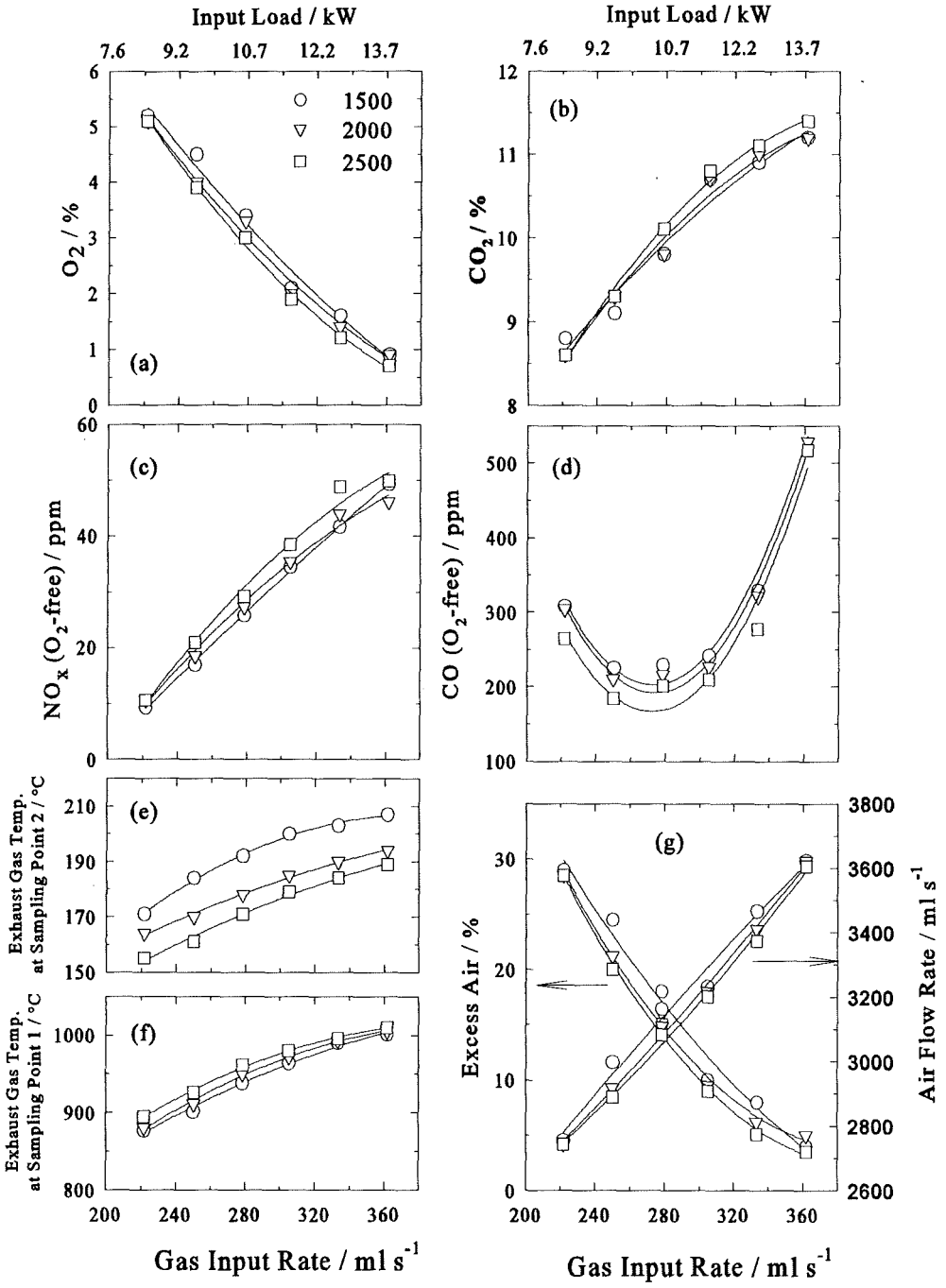

Fig. 6.13 ***Variation of a, b, c and d) combustion products, temperature of exhaust gas at e) sampling point 2, f) sampling point 1, g) excess air and air flow rate with gas input rate for the nominally 15 kW combustor at the specified tailpipe lengths / mm. The combustion chamber volume was kept constant at 370 ml.***

NO_x (the Zeldovich mechanism), prompt NO_x (the Fenimore mechanism) and fuel NO_x. A complete description of these processes were given in Chapter 1. Since the developed combustors were generally operated lean premixed and the burnt fuel was natural gas, the last two mechanisms are not significant in the present work and the NO_x formed as considered to arise via the thermal route. However, under very lean (low flame temperature) conditions the NO_x production can be attributed to mechanisms that form NO at a rate faster than Zeldovich mechanism such as non-equilibrium O and OH concentrations and the three body recombination involving N_2O [Bowman, 1992 ; Keller *et al.* 1994a].

Providing there is a substantial amount of oxygen (i.e. a fuel-lean flame), the rates of consumption of nitrogen atoms is equivalent to its rate of formation. Hence, making a steady-state assumption for the nitrogen atom and assuming the oxygen atom concentration is in equilibrium, the maximum NO formation rate due to the Zeldovich mechanism can be expressed by [Bowman, 1992]:

$$\frac{d[NO]}{dt} = [O_2]_{eq}^{1/2}[N_2]_{eq} 1.45\times10^{17} T^{-1/2} \exp\left(\frac{-69460}{T}\right) \qquad (6.7)$$

in mol ml^{-1} s^{-1} where T is temperature in Kelvin and [ ] denotes species concentrations in mol ml^{-1}. The above equation indicates that the NO_x concentration is an exponential function of temperature in the post flame gases and linear in time as a result of the Zeldovich mechanism. The formation rate of NO_x is very temperature-sensitive as is clear from the exponential term in equation (6.7) and shown in a number of studies [Keller and Hongo, 1990 ; Bowman, 1992; Jones and Leng, 1996; William *et al.*, 1997].

It is well known that in a premixed conventional combustion process NO_x emissions decrease as the air-to-fuel ratio (A/F) is increased. The reason for this is that raising the A/F dilutes the charge with air so reducing the flame temperature. This is also valid for the present design of pulsed combustor as shown in Fig. 6.14. The figure shows a plot of average measured exhaust gas temperature at sampling point 1 against excess air ratio, λ, at various operating conditions. Clearly, these measured temperatures do not

represent the peak temperature of combustion gases inside the combustor; however, the trend of results indicates that the combustion temperature was controlled primarily by the excess air ratio in these premixed pulsed combustors. The temperature within the combustion chamber was also lowered by two other effects:

- the rapid mixing of the fresh combustion gases with cooler residual of gases from the previous cycle,
- quenching of the combustion reactions on the relatively cool walls of the combustion chamber.

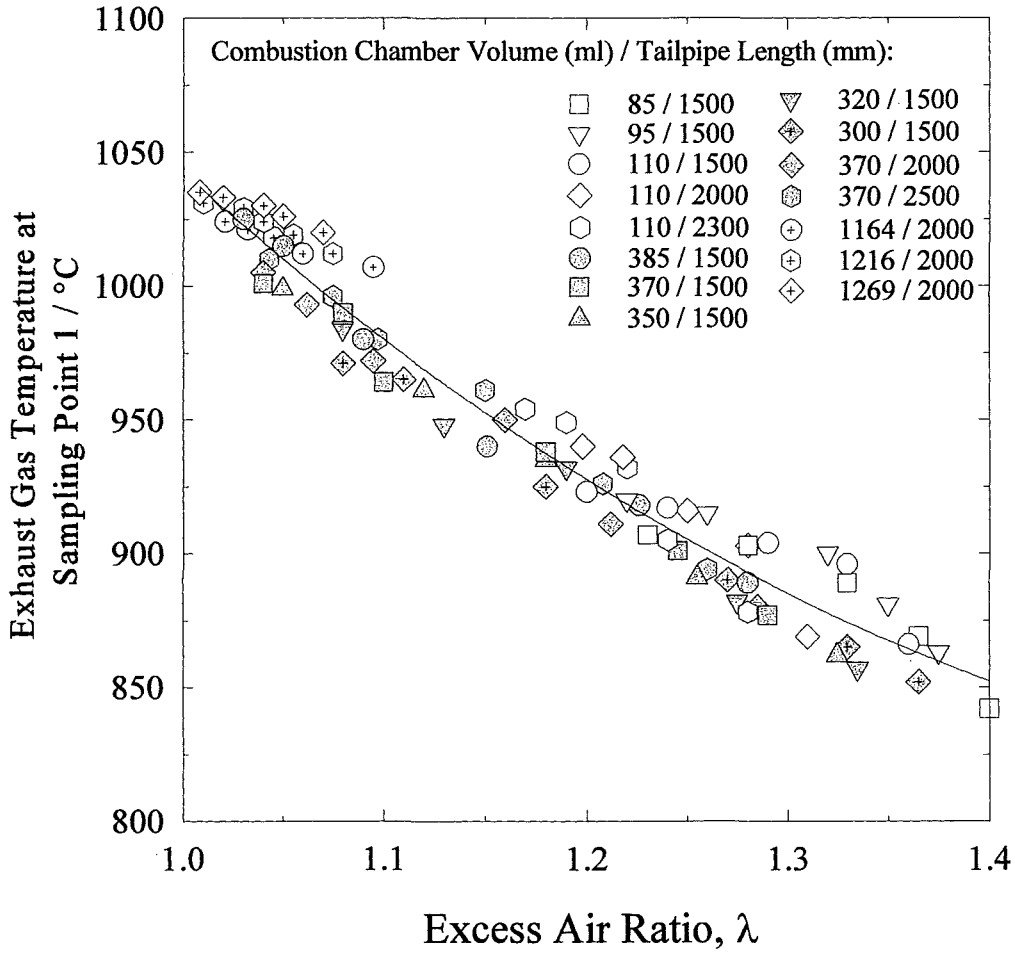

Fig.6.14 ***Variation of average measured exhaust gas temperature within the combustion chamber as a function of excess air ratio for the three pulsed combustors at the given configurations of the pulsed units.***

Since the combustors were operated in a premixed mode it is therefore sensible to plot NO_x emissions as a function of excess air ratio, λ. The NO_x data shown in Fig. 6.9 to 6.13 are presented in this way in Fig. 6.15. The scatter about the best second order line through the points is ±5 ppm and may be accounted for by localised variations in mixture strength and hence temperature within the combustion chamber. This will be discussed later when CO data was analysed in detail. The important point to note here is that for the range of combustion chamber volumes and tailpipe lengths employed for the three developed combustors, all the points follow a single curve (Fig. 6.15).

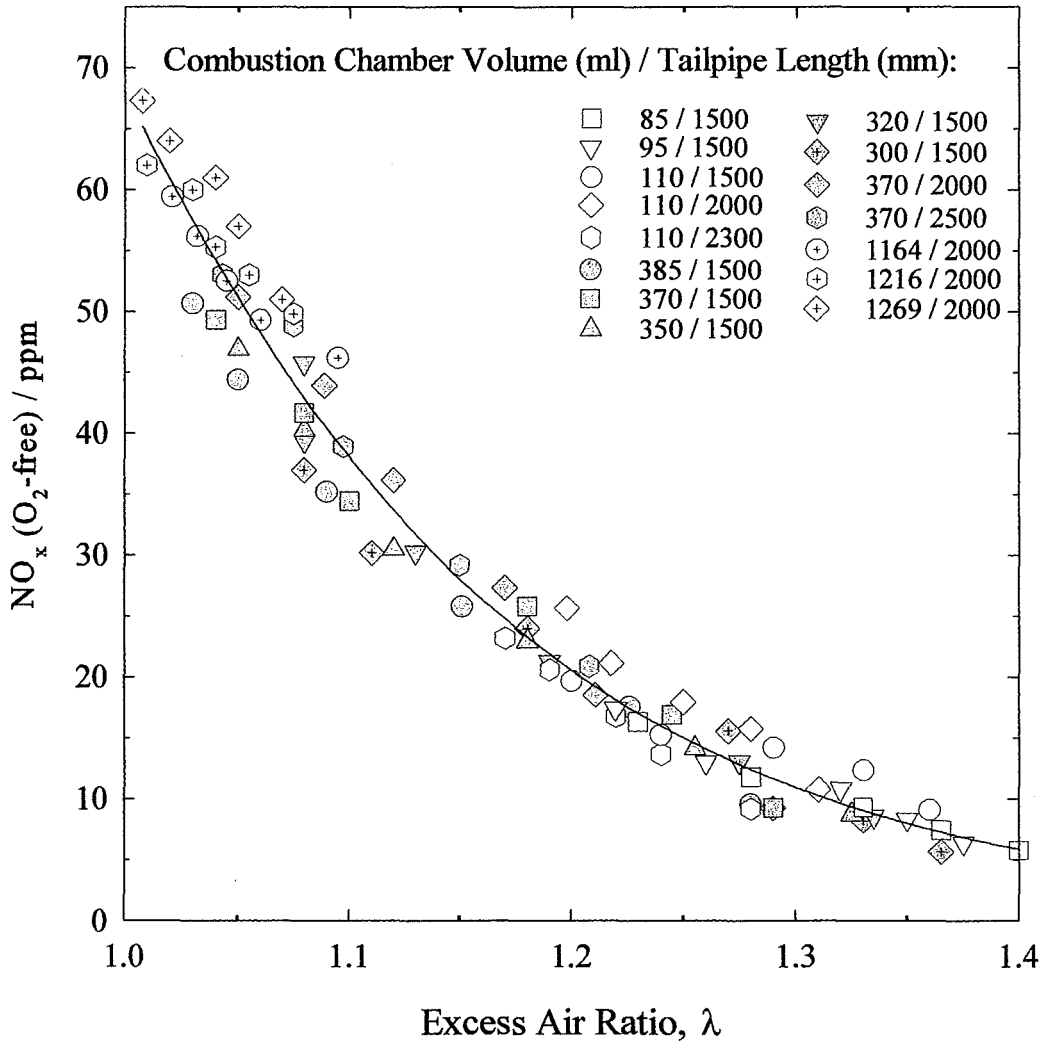

Fig.6.15 ***NO_x as a function of excess air ratio, λ, for the three developed pulsed combustors at the given configurations of the units.***

From Fig. 6.15 it is clear that the smallest combustor (i.e. 7.5 kW) operated at higher A/F, with λ values ranging from 1.4 to 1.2 whereas the nominally 15 and 30 kW pulsed combustors operated within λ values of 1.35 to 1.05 and 1.10 to 1.00 respectively. It is also apparent from Fig. 6.15 that the NO_x values were generally lower for the 7.5 kW pulsed combustor increasing from 4 to 30 ppm at the above given range of λ. The higher λ associated with the 7.5 kW pulsed combustor induced a lower peak temperature within the combustion chamber resulting in a decrease in NO_x emission levels. Combining the data in Fig. 6.14 and 6.15 allows the average measured NO_x to be plotted vs measured exhaust gas temperature at sampling point 1 (Fig. 6.16). As expected all the data fall on a single curve demonstrating that the measured average NO_x values were principally a function of temperature within the combustion chamber. It

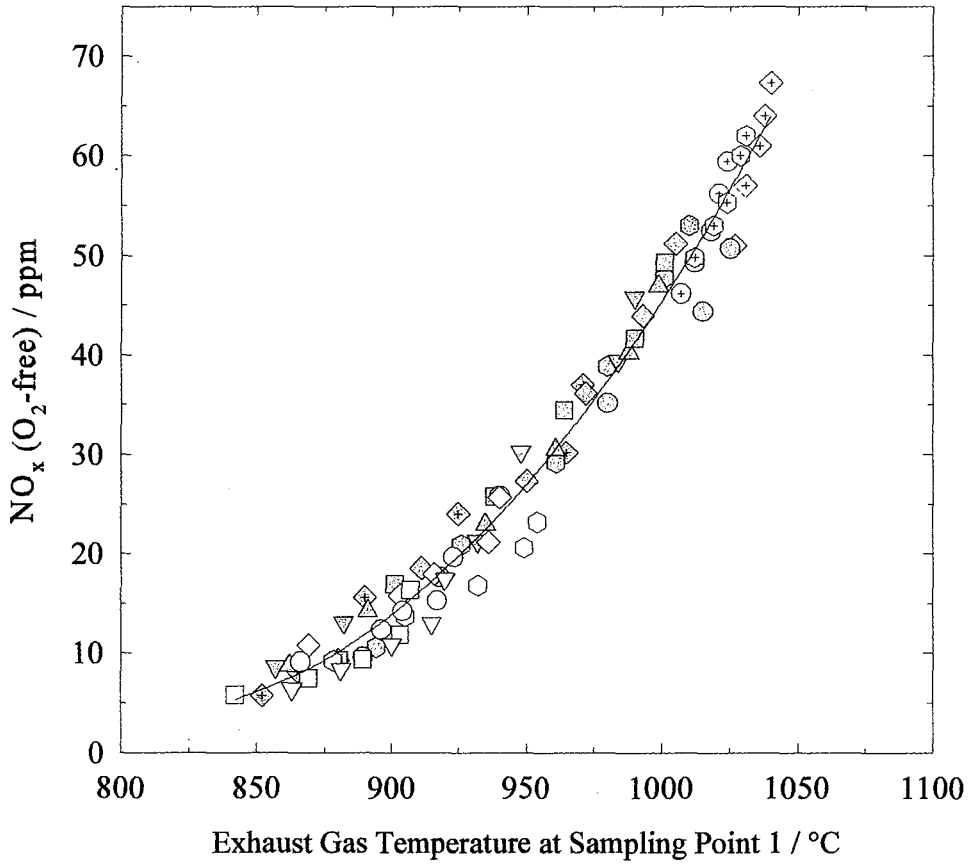

Fig. 6.16 ***NO_x vs measured average exhaust gas temperature within the combustion chamber for the three combustors. The configurations were as in Fig. 6.15.***

should be noted that here the trend of averaged measured NO_x at the end of tailpipe only is being discussed.

Clearly, these measured temperatures do not represent the flame temperature inside the combustion chamber. Thus, the adiabatic flame temperature was calculated and used as a guide for determination of the mechanisms involved for the formation of NO_x in the present design of pulsed combustors. Other workers [Jones and Leng, 1996] also proposed the use of the calculated adiabatic flame temperature as the relevant temperature for analysis of NO_x emission data. The adiabatic flame temperature (calculated for the mains fuel gas used in this work [Appendix VII]) is shown as a function of λ in Fig. 6.17. For the range of A/F used in this work the calculated adiabatic flame temperature varied from 1620 to 2050 °C, a range of 430 °C. The use of the adiabatic flame temperature is probably sensible because a) it shows a similar trend to the plot of measured average temperature of flue gases vs λ, increasing with decrease of excess air ratio and b) the maximum temperature of the flame during combustion is that relevant to NO_x formation. The reason for latter is that the activation energy in equation (6.7) is high indicating that the rate of formation of NO increases rapidly with increasing temperature. Thus, as soon as the combustion gases begin to be cooled significantly below the initial flame temperature, the rate of formation of NO becomes small compared with the initial rate. Therefore, the majority of the NO_x formed may be considered to be formed at the maximum temperature.

A plot of measured NO_x values versus calculated adiabatic flame temperature is shown in Fig. 6.18 and as expected the data fall on a single curve, indicating that in these combustors the NO_x formation is primarily dependent upon flame temperature. According to equation (6.7) a plot of natural logarithm of NO_x concentration vs 1/T should reveal a straight line with slope related to the activation energy E_a. Such a plot is shown in Fig. 6.19. The data do follow a straight line indicating an exponential dependence of NO_x emissions upon temperature according to an Arrhenius-type relationship. From the slope an activation energy of approximately 200 kJ mol^{-1} was calculated. This value is somewhat lower than the figure of 319 kJ mol^{-1} [Etzkorn *et al.*, 1992], expected for the Zeldovich mechanisms for the NO formation, although values

of around 19 kJ mol^{-1} have also been reported for a non-premixed pulsed combustor [Jones and Leng, 1996].

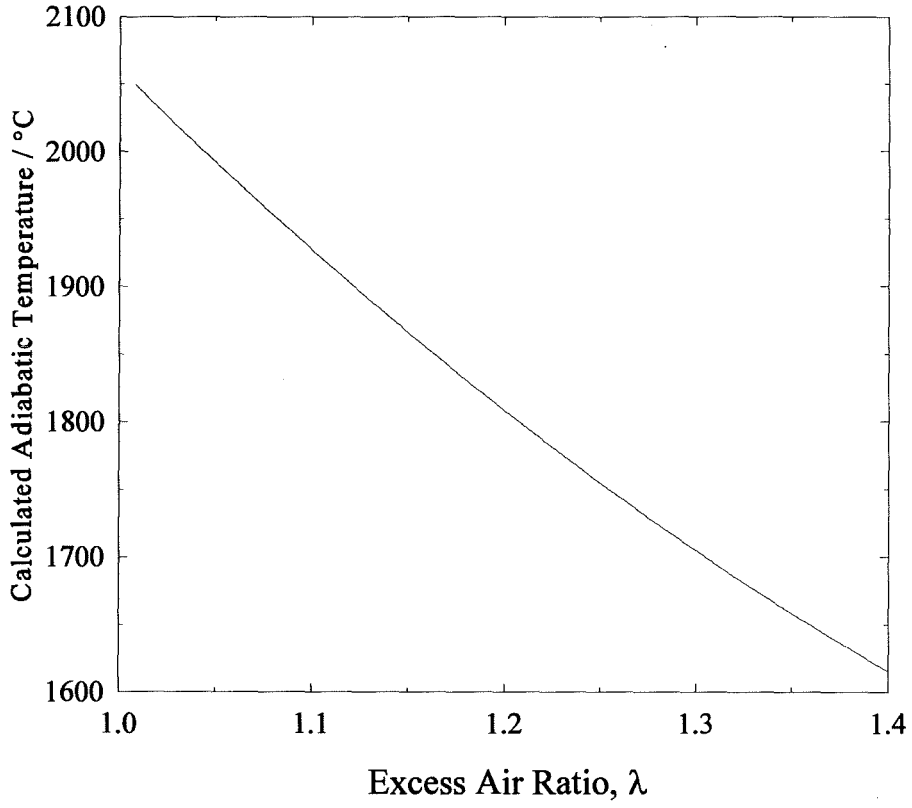

Fig.6.17 ***Calculated adiabatic flame temperature vs excess air ratio for the range of A/F in which the three combustors were operated.***

It should be noted that the adiabatic flame temperature was calculated assuming that the gas and air were well mixed prior to combustion. Any imperfect mixing of fuel and air prior to the combustion may effect the reactions for formation of NO through the effect upon the activation energy. In addition, in the above methodology any effect of mixing of the reactants with combustion gases from the previous cycle and any local fluctuations in temperature or mixing strength have been ignored. Indeed, in the present investigation the relatively higher measured levels of NO_x (i.e. average of 20 ppm @ 20 % excess air) compared to the other reported values (e.g. 12 ppm @ 20 % excess air) [Keller *et al.*, 1994a] may have their origin in such effects. However, the observed

pattern of obtained results in Fig 6.16 to 6.19 show that the formation of NO was controlled principally by the temperature at which combustion occurred. Also they indicate the dominant contribution of the Zeldovich mechanism on NO production in the present design of pulsed combustor.

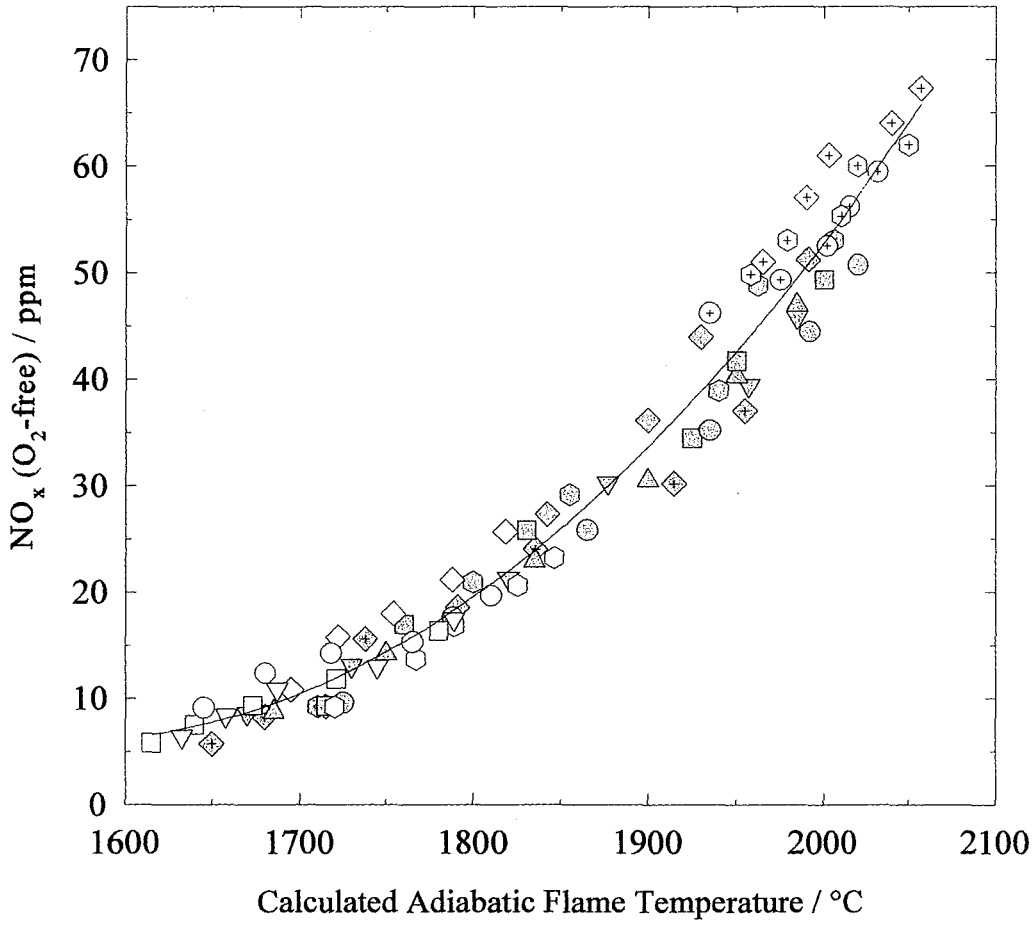

Fig. 6.18 ***Measured NO_x values corrected to zero oxygen vs calculated adiabatic flame temperature for the three nominally 7.5, 15 and 30 kW combustors. Combustors configurations as specified in Fig. 6.15.***

It is also notable that almost all NO_x values measured were in the form of NO. This was due to the high flame temperature inside the combustion chamber. As shown in Fig.

6.18, the minimum adiabatic flame temperature was above 1850 K. It was explained earlier in this chapter and also in Chapter 1 that at sufficiently high temperature (i.e. T > 1500 K) there were insufficient oxidant radicals present for oxidization of NO to NO_2.

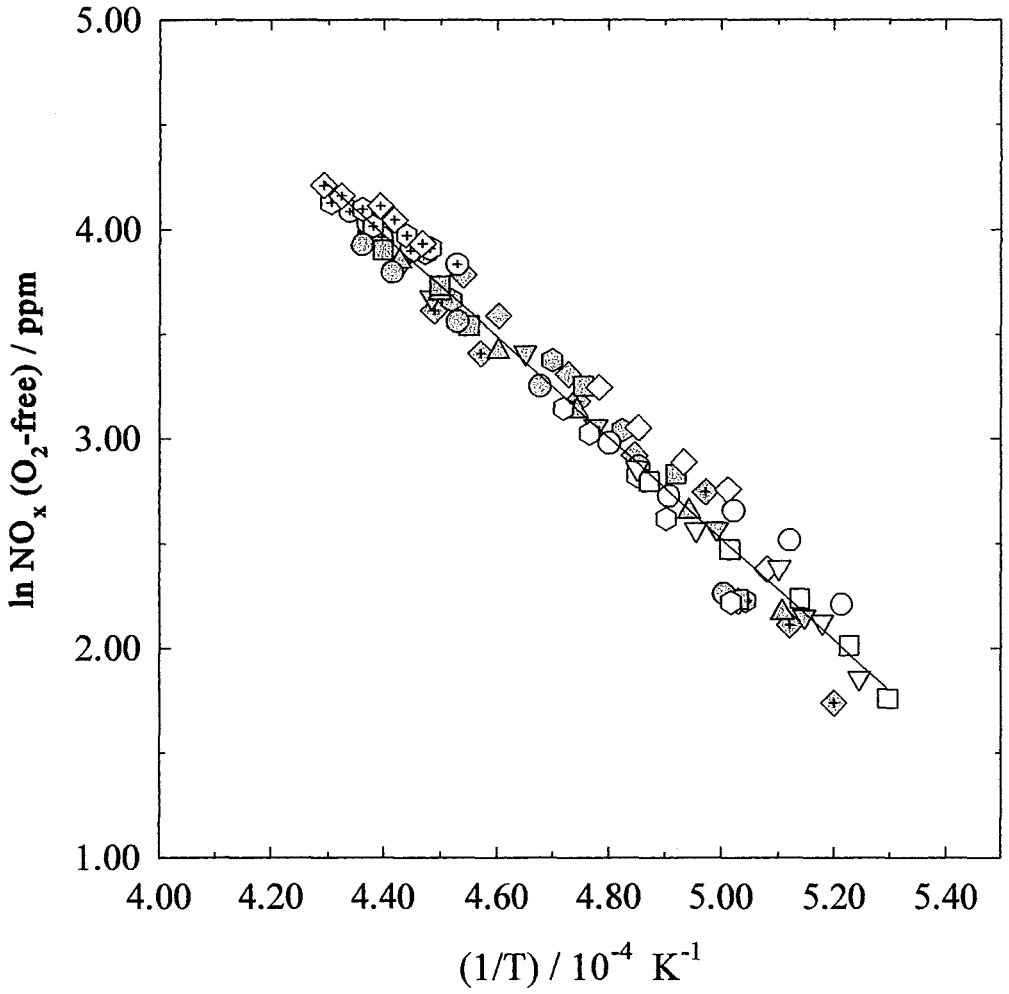

Fig. 6.19 ***Data from Fig. 6.18 plotted as logarithm of NO_x concentration vs reciprocal of calculated adiabatic flame temperature. The best straight line through the points from a linear regression analysis is shown.***

6.4.1.1 Influence of Added Air, Nitrogen and Argon

So far it has been shown that measured average NO_x emissions at the end of the tailpipe from the present type of pulsed combustors were principally dependent upon flame

temperature. It was also deduced that in the present type of combustors the contribution of NO_x formation via the Zeldovich mechanism was great particularly due to the fact that the combustors operated in fuel-lean conditions with high combustion temperatures.

It has been suggested that one of the reasons for the low NO_x levels associated with pulsed combustion systems is internal exhaust gas recirculation (EGR) [Murphy and Putnam, 1985]. Of course, as described in Chapter 1, exhaust gas recirculation is a well-known method of reducing NO_x in combustion systems, the dilution effect resulting in lowered combustion temperature. Exhaust gases are relatively complex mixtures of gases. The addition of simple gases lends itself more readily to detailed analysis which can then subsequently be extended to complex mixtures. In this study the gases chosen for dilution were air, nitrogen and argon. Air and nitrogen have similar molecular heats (equivalent to specific heat but on molar and hence volume basis) and nitrogen (present also in air) is an active species in the Zeldovich mechanism. Argon has a substantially lower molecular heat, is non-reactive and is not involved in the Zeldovich mechanism.

Addition of Air

Results on the influence of air flow rate on average measured NO_x at the end of tailpipe were presented earlier in Fig. 6.6 and 6.7. It was shown that the NO_x decreased as the air flow rate increased. From data generated, the NO_x emission was plotted vs excess air ratio, λ, as shown in Fig. 6.20. Also shown on the figure is the best line through the points in Fig. 6.15. It can be seen that all the data in Fig. 6.6 and Fig. 6.7 fall on the same line as in Fig. 6.15. Dilution of mixture charge by added air reduced the temperature within the combustion chamber resulting in the observed reduced NO_x values. This is somewhat the same as the principle of EGR where cool exhaust gases are introduced into the combustion chamber with reactants reducing the flame temperature by a dilution effect. This again clearly indicated the importance of flame temperature upon formation of NO_x in this type of pulsed combustor.

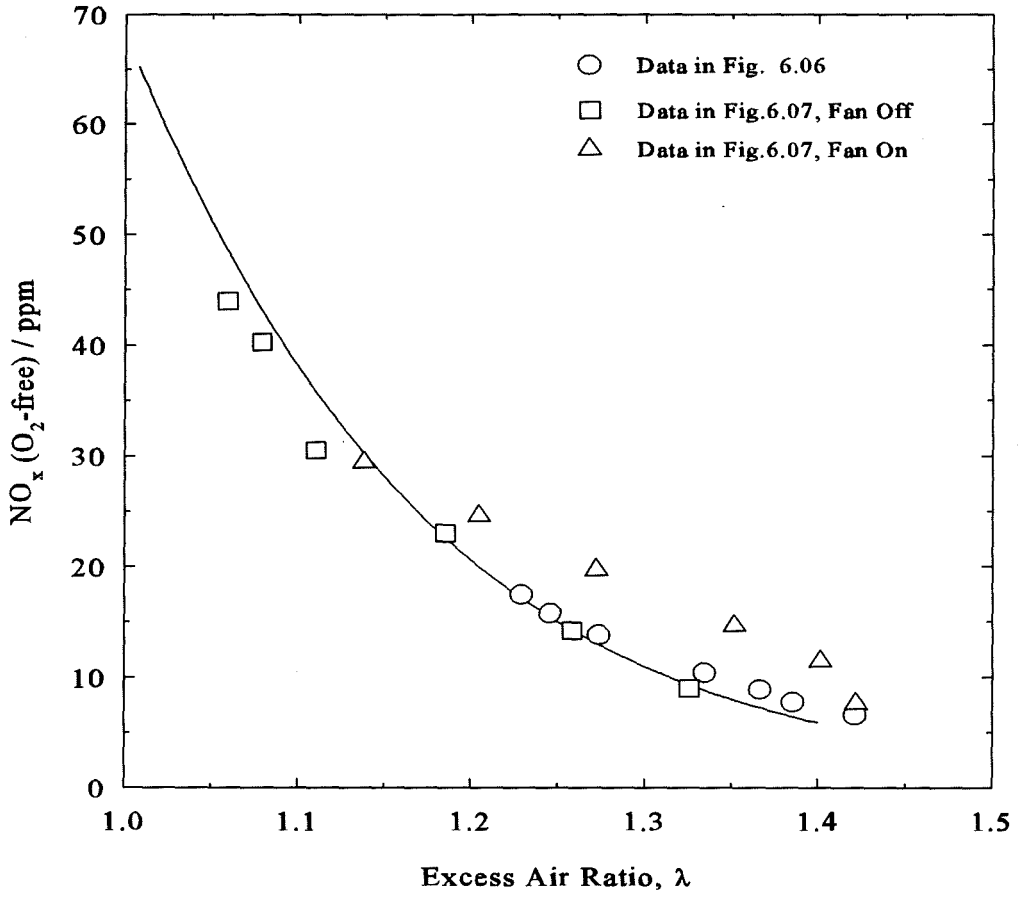

Fig. 6.20 ***Variation of NO_x with λ using data in Fig. 6.6 and 6.7. Line is the best curve though the results in Fig. 6.15.***

Addition of Nitrogen

Nitrogen from a bottle was injected into the inlet air stream of the nominally 15 kW pulsed combustor via the air decoupler prior to mixing with fuel gas. The configuration employed was: combustion chamber volume 370 ml; tailpipe length 1500 mm; flapper valve thickness 0.13 mm. The data obtained from this study are shown in Fig. 6.21. Clearly, at a given A/F the NO_x values decreased with increasing nitrogen addition. Two competing effects were anticipated. Adding N_2 diluted the system leading to lower temperature at a given value λ; on the other hand adding N_2 increased the nitrogen concentration which would be expected to increase the NO_x according to equation (6.7).

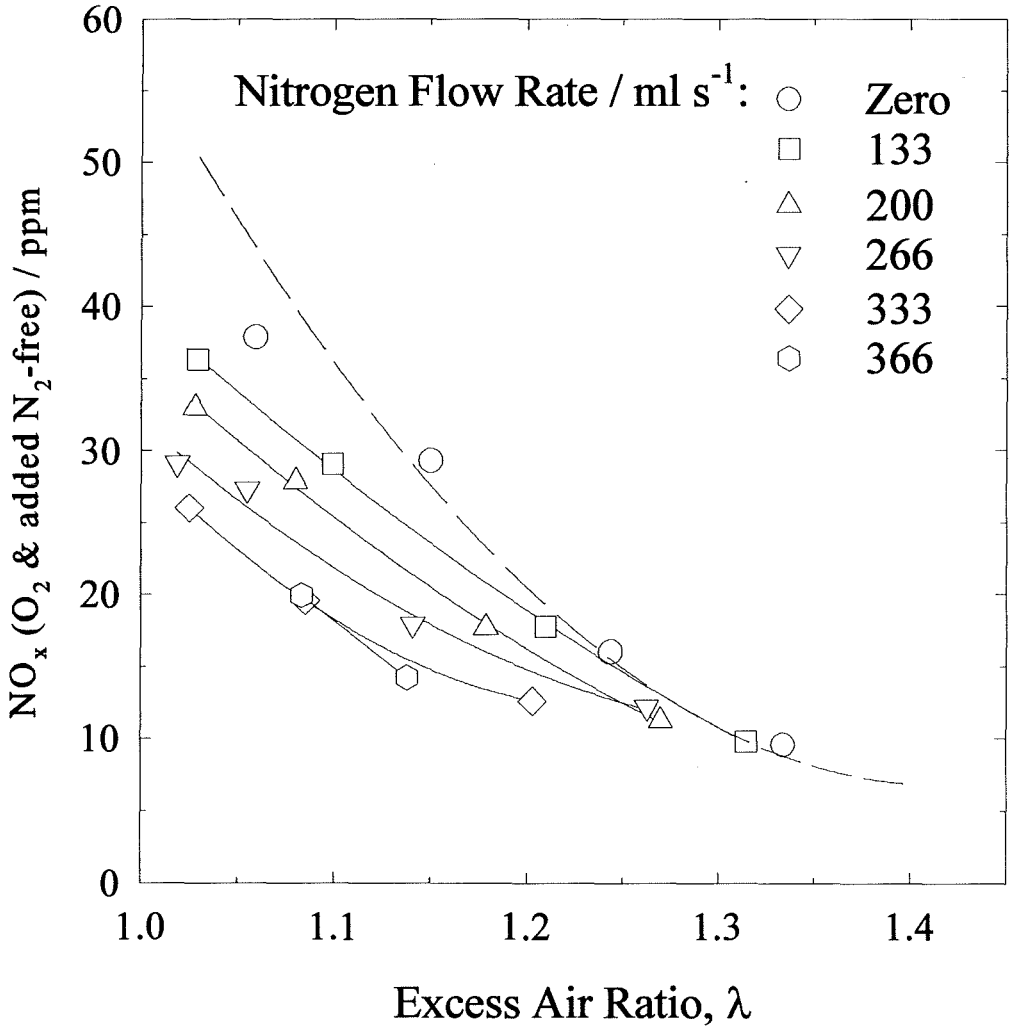

Fig. 6.21 ***Variation of NO_x values corrected for dilution to zero excess air and to zero injected N_2 as function of excess air ratio for various flow rates of N_2 diluent. The broken line represents the best line through the NO_x vs λ data for the nominally 15 kW combustor at various configuration of the units. The line through the points refer to given nitrogen flow rates. The configuration used here: combustion chamber volume 370 ml, tailpipe length 1500 mm and flapper valve thickness 0.13 mm.***

However, because air contains some 78 % N_2, the further addition of N_2 resulted in only a small increase in N_2 concentration. The reduction in NO_x with N_2 addition indicates that the effect due to temperature reduction outweighed that due to N_2 concentration increase.

The data in Fig. 6.21 are shown again in Fig. 6.22 but with lines drawn through points of constant fuel gas flow rate. These show that NO_x increased and decreased with increasing N_2 injection at low and high fuel gas input rates respectively. The explanation of this is as follows. At low fuel gas flow rates, with increasing N_2 diluent, the temperature rise due to the decreasing A/F outweighed the temperature decrease due to dilution of the nitrogen. At high fuel gas rates, with increasing N_2 addition, the temperature rise due to the decreasing A/F was outweighed by the temperature decrease due to the dilution of the mixture. This is confirmed by the analysis represented in Fig. 6.23 and 6.24.

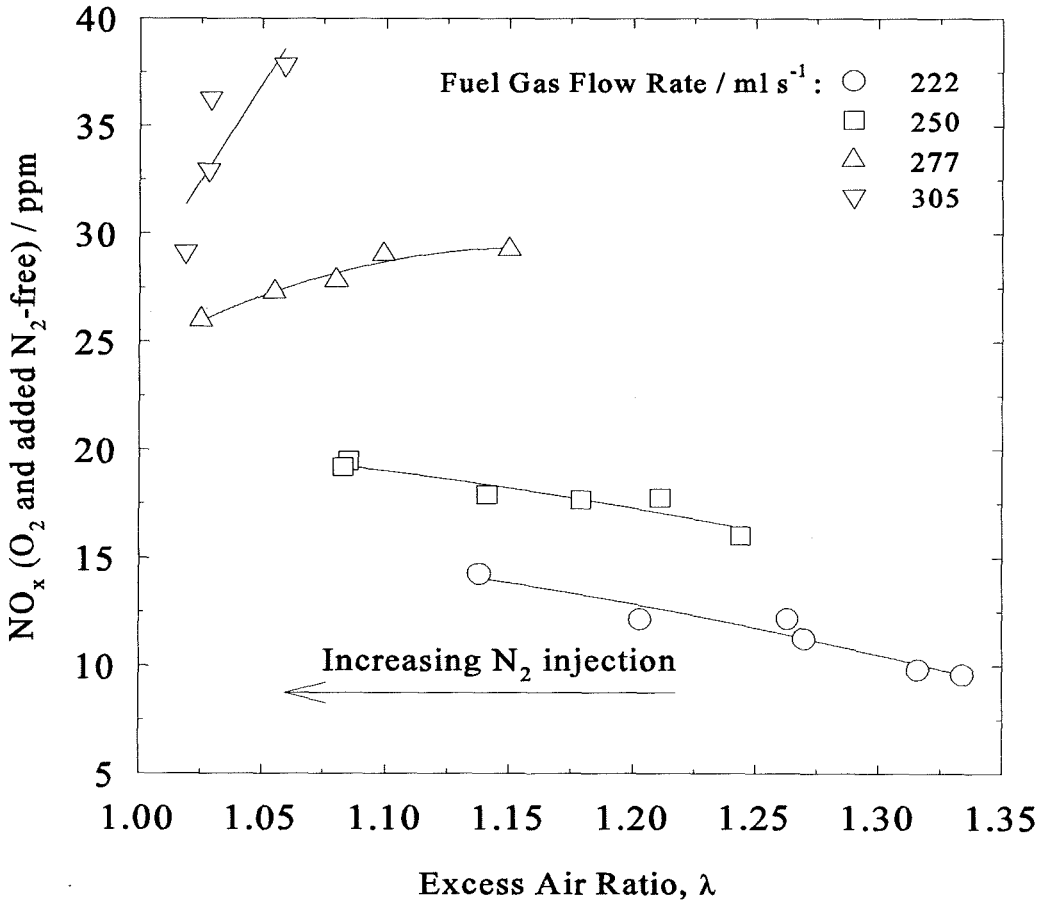

Fig. 6.22 ***The drawn indicate the effect of N_2 injection at constant fuel gas flow rates. Configuration as in Fig. 6.21.***

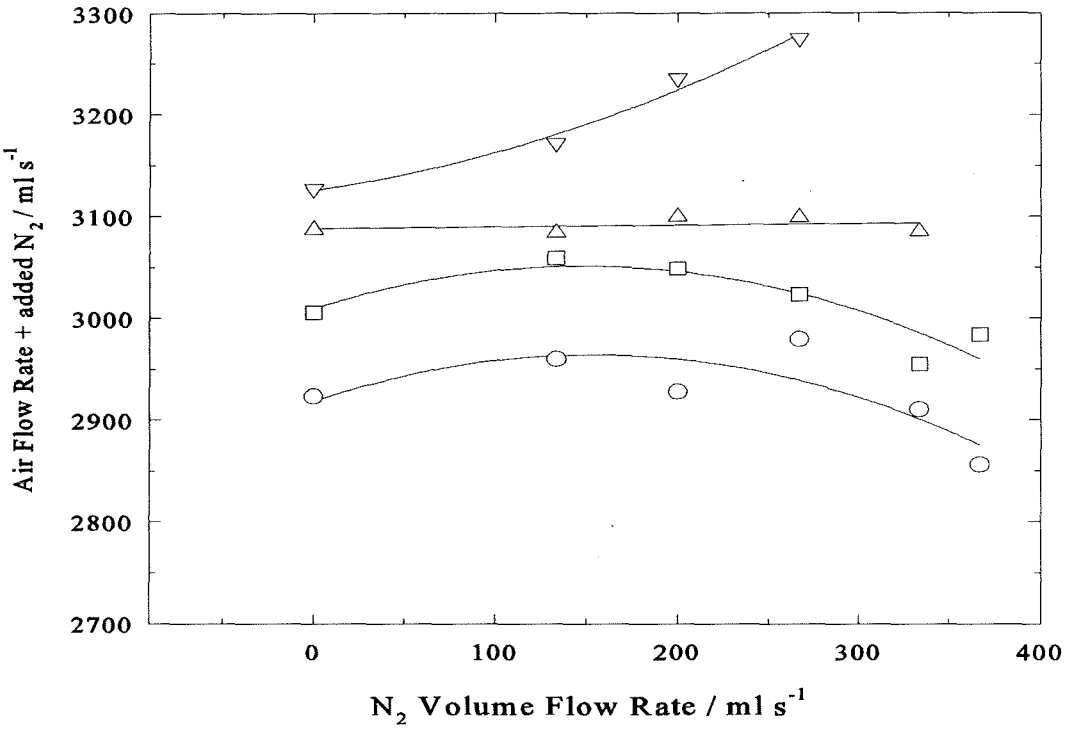

Fig.6.23 ***The total air+nitrogen flow rate into the combustor vs nitrogen injection rate at various fuel gas rates. Data and symbols corresponds to Fig. 6.22.***

Considering first Fig.6.23, for the lower fuel gas rates in the range of 222-277 ml s^{-1}, as N_2 was injected the added air plus nitrogen flow rate varied very little, that is the nitrogen injected was replaced by air on a volume for volume basis. At the highest fuel gas flow rate of 305 ml s^{-1} as N_2 was injected there was a reduction in the air but it amounted to only about one half of the N_2 flow rate, so that the total air plus nitrogen increased with increasing N_2 addition. These data then enable the adiabatic flame temperature to be calculated as shown in Fig. 6.24. Thus as mentioned earlier, since the molecular heats of air and nitrogen are very similar (i.e. 29.2 and 29.4 kJ $kmol^{-1}$ K^{-1}), replacing air by N_2 volume for volume resulted in little change in thermal capacity of the mixture. Hence, the finding that for the fuel gas flow rate of 277 ml s^{-1} the adiabatic

flame temperature was sensibly independent of nitrogen rate. In general terms the slopes of the lines in Fig. 6.23 and 6.24 explain the slopes found in Fig. 6.22. This confirms the explanation from equation (6.7) that NO_x is mainly thermally generated in this system and increases with increasing combustion temperature. In fact, the NO_x data shown in Fig. 6.21 fall on a single curve when plotted as a function of adiabatic flame temperature as shown in Fig. 6.25. Indeed, this reinforces the point made earlier, that changes in nitrogen concentration in equation (6.7) resulted in insignificant changes in NO_x compared with the effect due to flame temperature.

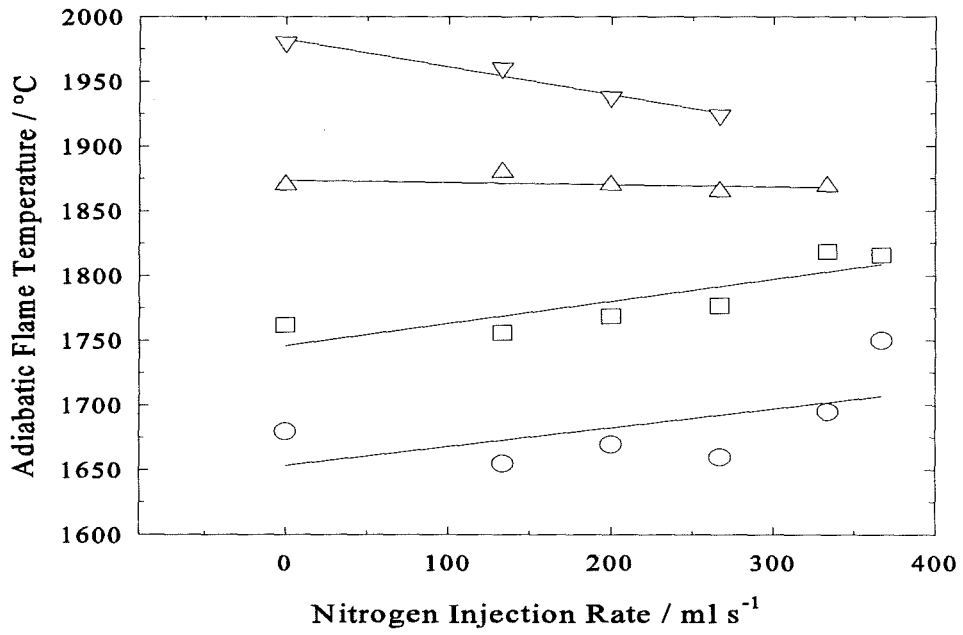

Fig. 6.24 ***Calculated adiabatic flame temperatures vs N_2 injection rate at various fuel gas rates. Data and symbols correspond to Fig. 6.22 and 6.23.***

Addition of Argon

In the same way that nitrogen was employed as a diluent above, argon from the bottle was injected into the air stream and thereby it diluted the mixture charge of air and gas prior to combustion. The complementary diagrams to Fig. 6.21-6.24 (for N_2) but for

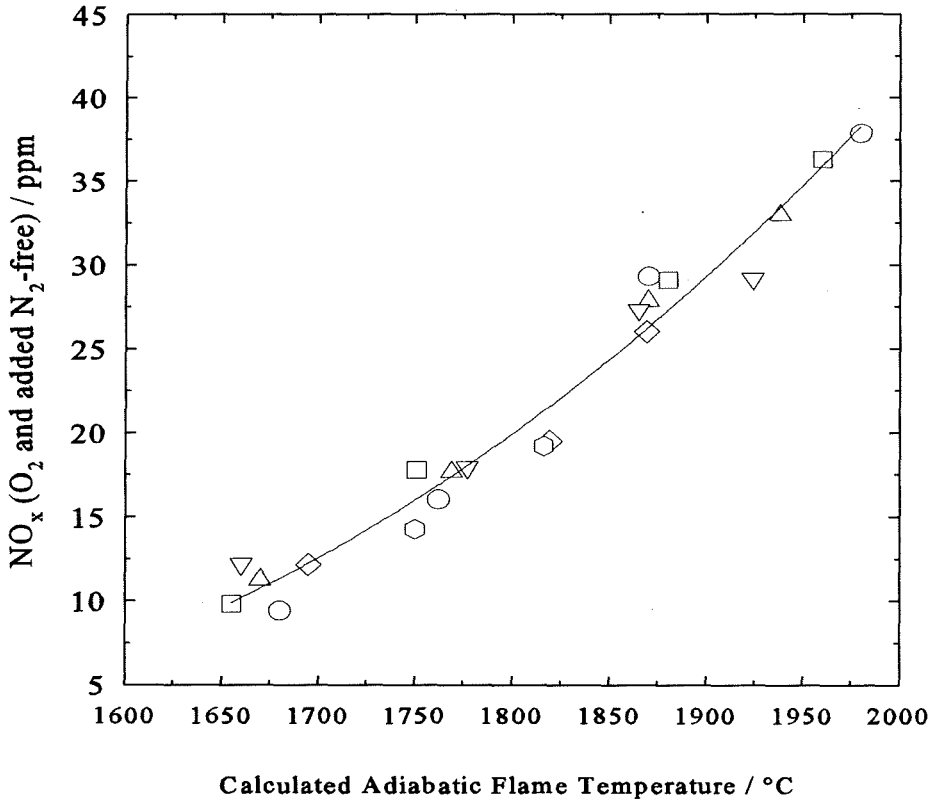

Fig. 6.25 ***Variation of NO_x with calculated adiabatic flame temperature for various N_2 injection rates. Symbols as in Fig. 6.21. Line shown is the best second order curve through the points.***

argon injection are shown in Fig. 6.26-6.29. It can be seen that the general features of the two sets of figures are very similar. Clearly for a given λ value NO_x reduced as the argon flow rate increased (Fig. 6.26).

The plot of NO_x vs calculated adiabatic flame temperature is shown in Fig. 6.30 and compared with the data for N_2 injection (from Fig. 6.25) in the Fig. 6.31. The correlation between the data for N_2 and Ar is close; it should be remembered that the cooling effect for dilution with argon is less than that of dilution with nitrogen as a result of the differing specific heats. Yet clearly temperature is the main factor controlling the NO_x emission. Nitrogen concentration was a small factor in comparison.

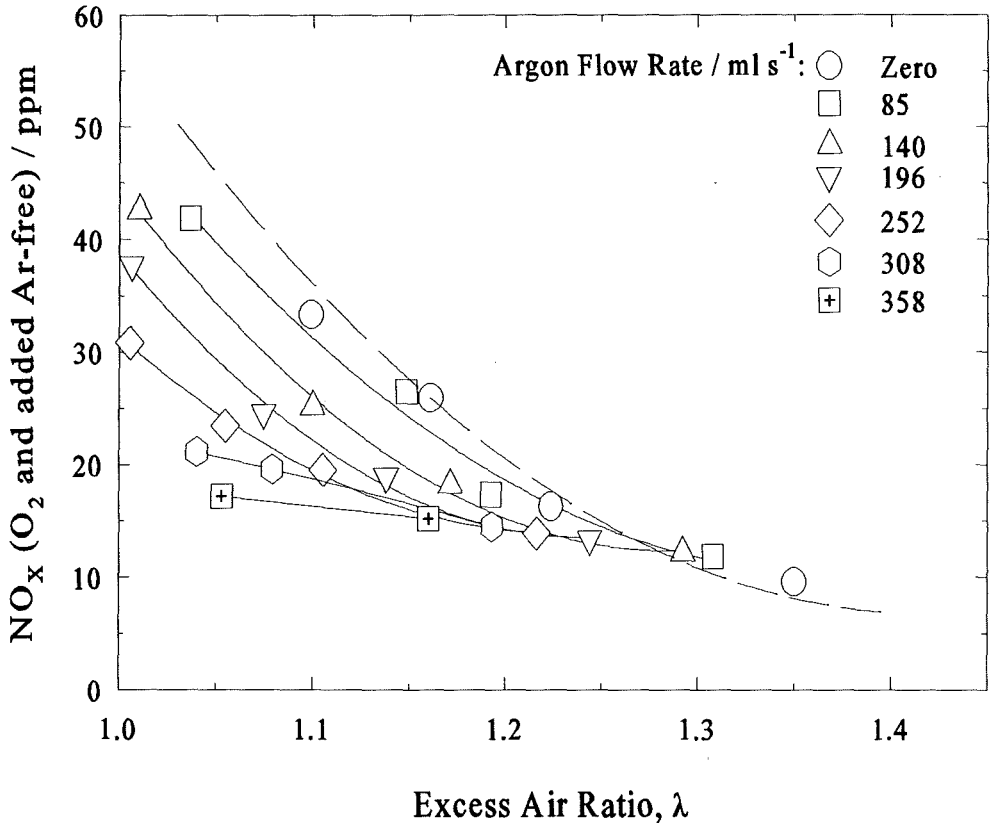

Fig. 6.26 ***Variation of NO_x corrected to zero oxygen and added argon with λ at various rates of Ar injection. The broken line represents the NO_x vs λ at various operating condition of the 15 kW combustor with zero argon injection. Configuration used here: combustion chamber volume of 370 ml, tailpipe length of 1500 mm and flapper valve thickness 0.13 mm.***

The addition of more air by running the fan, of nitrogen or of argon diluted the fuel gas/air charge lowering the flame temperature. The results show that all the data essentially follow a single curve when NO_x emission is plotted against calculated adiabatic flame temperature. So this work involving injection of these gases is further confirmation of the earlier findings that in the present design of pulsed combustors, the average measured NO_x emissions at the end of tailpipe are principally dependent upon the flame temperature.

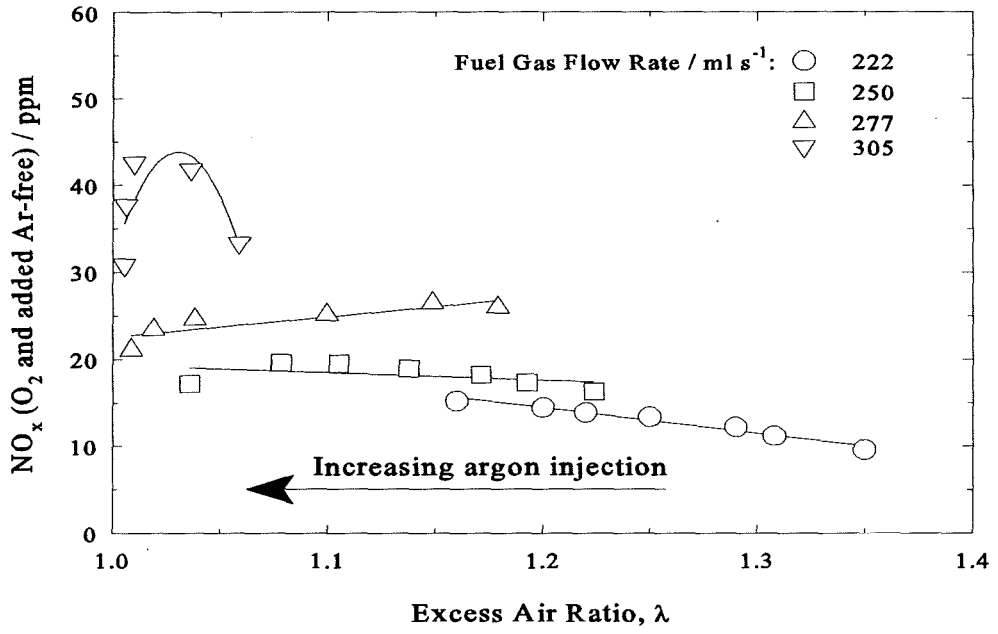

Fig. 6.27 ***NO_x vs argon excess air ratio, λ at various gas input rates. Data and configuration as in Fig. 6.26.***

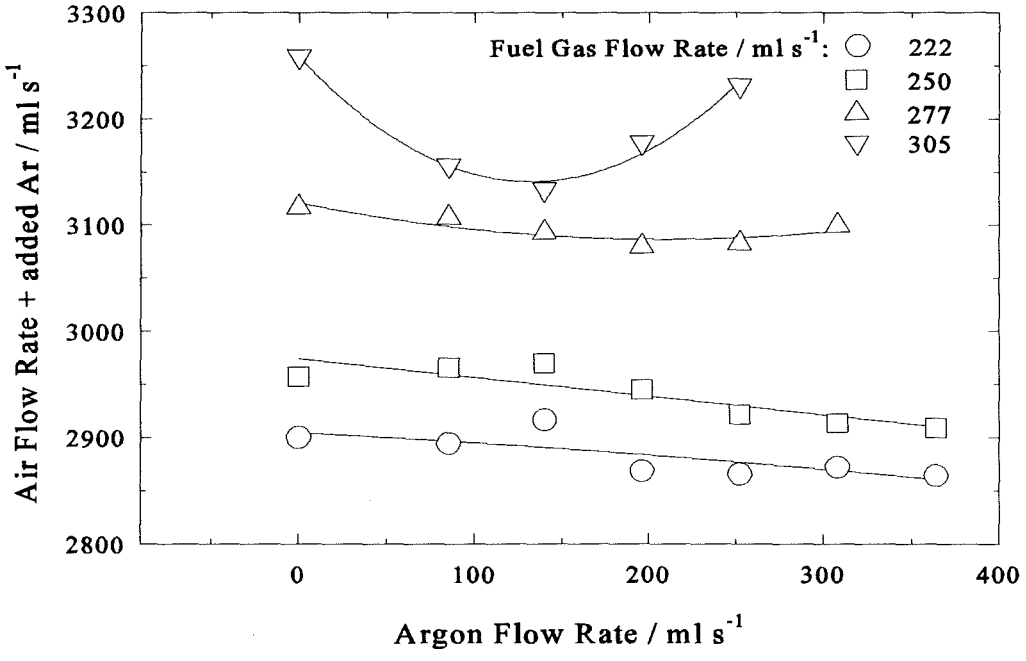

Fig. 6.28 ***The total air + argon flow rate as a function of argon injection rate at various fuel gas input rates. Configuration as in Fig. 6.26.***

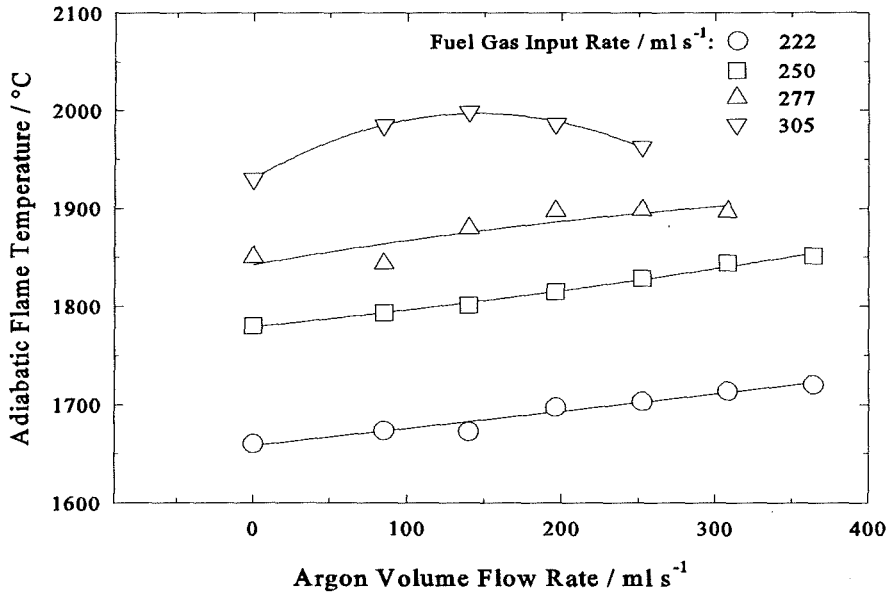

Fig. 6.29 ***Calculated adiabatic flame temperature vs argon injection rate at various fuel gas flow rates. Data as in Fig. 6.27.***

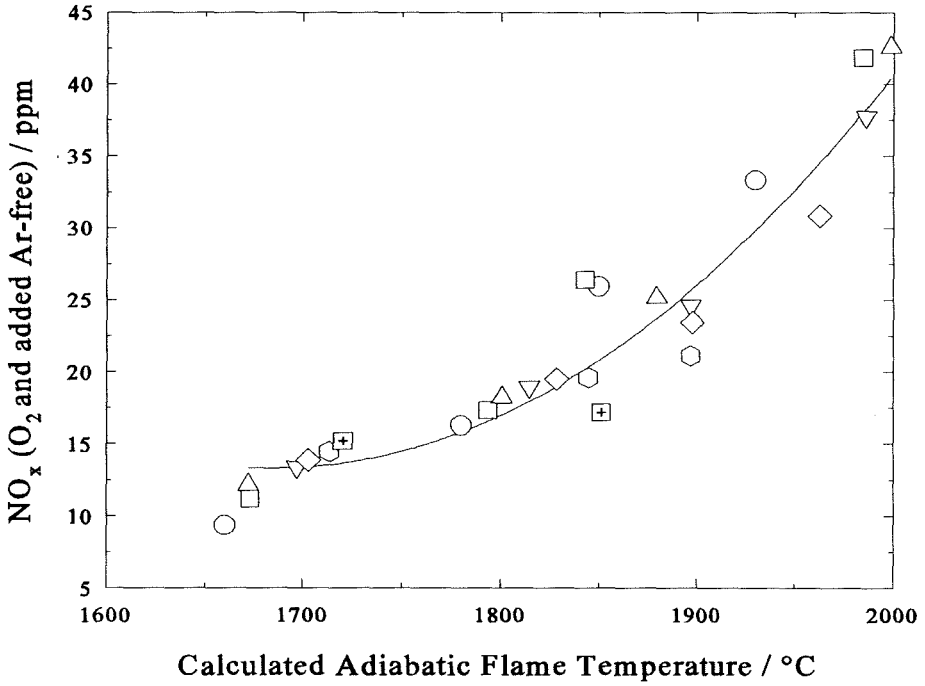

Fig. 6.30 ***Variation of NO_x (corrected to zero oxygen and added argon) as a function of calculated adiabatic flame temperature at various rates of argon from zero to 350 ml s^{-1}. Configuration and symbols as in Fig. 6.26.***

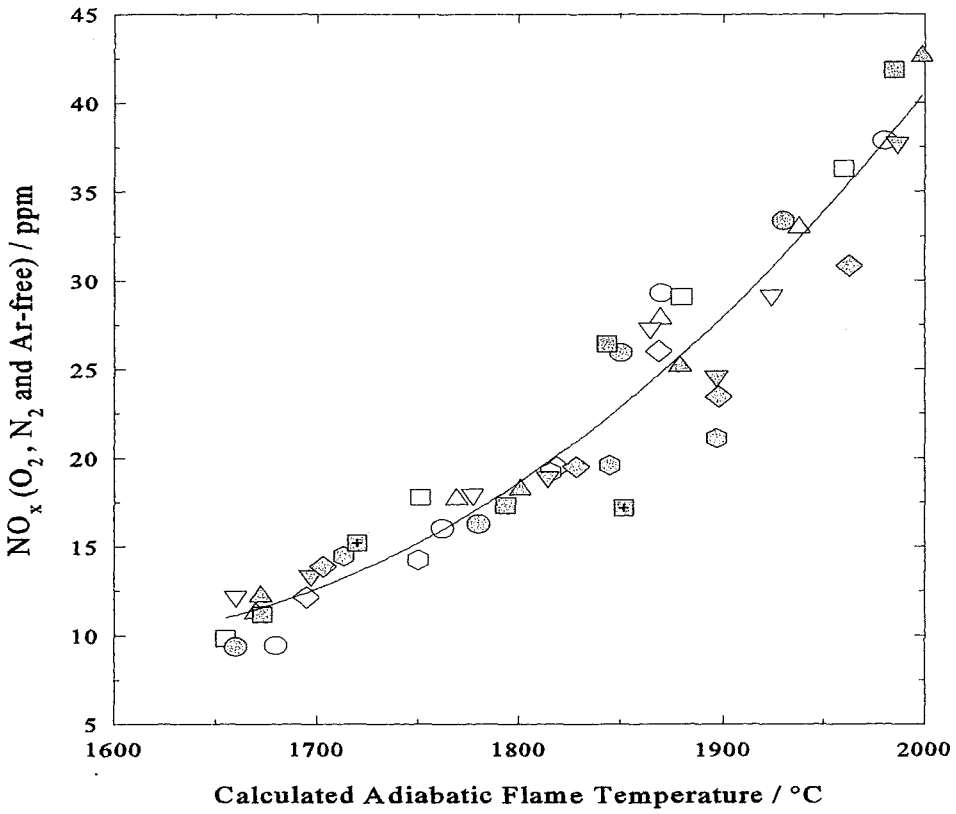

Fig. 6.31 ***Comparison of NO_x vs calculated adiabatic flame temperature for argon injection (gray symbols) and nitrogen injection (white symbols). Symbols as in Fig 6.21 and 6.26.***

6.4.2 Emission of Carbon Monoxide

It was shown earlier that the excess air ratio decreased towards a λ value of unity as the fuel rate was increased. This in turn increased the flame temperature as was shown earlier. Thus, a variation in CO emission would be expected with changes in λ, according to equation (1.26). This is investigated below for the data in Fig. 6.9 to 6.13 where the CO was measured at various operating conditions.

Plots of average measured CO concentration against λ for the three combustors, with a fixed tailpipe length for each and with combustion chamber volume (CCV) as a parameter are shown in Fig. 6.32 to 6.34. Generally the results display U-shaped

characteristics with CO values which are high at both high and low values of λ. A high value of CO associated with lower excess air ratio, λ, can be ascribed to the incomplete mixing of air and gas in the mixer head prior to combustion. As described in section 1.8.5, imperfect mixing of air and gas prior to combustion generates fuel-rich pockets and consequently results in production of CO. This can also considered to be one main reason that the CO values were generally higher for the 30 kW combustor despite the high combustion temperature and existence of sufficient oxygen which should result in low CO concentrations. On the other hand, the rise of CO values in the high λ region can be attributed to dilution with excess air, thus resulting in lower temperatures and high CO concentrations according to equation (1.26).

It can be seen from these figures (Fig. 6.32-6.34) that there is a significant dispersion among the values of CO, particularly in the low λ region (i.e λ<1.15) for various combustion chamber volumes with fixed tailpipe length. In general terms for a given combustor and λ value, there was a trend towards lower CO values with increasing CCV. However, when CO was plotted against λ at a fixed CCV but various tailpipe lengths (Fig. 6.35 and 6.36), it was observed that CO levels were little influenced by tailpipe length for a given λ value. Possible influences of CCV upon CO emissions are the followings:

a) increased amplitude of pulsing pressure as the CCV decreased. It was shown in Chapter 5 that as the CCV decreased the peak pulsing pressure increased. It is reported [Zinn, 1992 ; Lindholm, 1995] that higher pressure amplitude leads to enhanced heat transfer and hence lower temperatures within the combustor and consequently higher CO values.

b) increased thermal quenching as the CCV was decreased. It was shown in Chapter 4 that as the CCV was decreased the operating frequency increased. This in turn influences the fluid dynamic mixing environment and increases the thermal quenching mechanism. Hence higher CO values might be associated with smaller CCV.

c) localised variation of mixture strength. With smaller CCV there would be less space for mixing of new reactants with hot gases (inside combustion chamber) from

the previous cycle compared with a larger CCV, which in turn would result in localised variation of mixture strength and hence temperature. Moreover, cycle time increased as the CCV was increased (see Fig. 4.8) resulting in more time available for burn-out of the CO. In addition, a larger combustion chamber would allow better mixing of hot gases inside combustor with new reactants as well as improved mixing of air and fuel gas within the mixer head. This in turn results in lower CO emissions.

d) with increasing CCV the flame can travel a longer distance and provide more complete combustion and hence result in lower CO emissions. It should be noted that CCV increase was achieved by increasing the length of the combustion chamber while the diameter was remained constant.

Factors a) and b) would be expected to lead to a significant change in NO_x production with changing CCV but this was not found, suggesting that these factors were not appropriate to explain the CO results shown in Fig. 6.32-6.34. Factors c) and d) seem more likely to be the primary reasons for the observed CO emissions. Also, as CCV was reduced the influence on CO values was more pronounced in the lower λ region (where imperfect mixing was considered an important factor for high CO emissions) thus factor c) is considered to be the most probable explanation of the CO results (Fig.6.32-6.34). Clearly this is an area which would benefit from research with more advanced combustion diagnostics.

It was noted earlier that for a fixed CCV and λ value the CO values did not change significantly with change of tailpipe length (Fig. 6.35 and 6.36). This may be because the combustion occurred almost totally within the combustion chamber. Measurements of CO_2 at the inlet and the exit of tailpipe showed similar values (within experimental uncertainty) as shown in table 6.1. Therefore, it is expected that there would be little influence of factors c) and d) described in above on CO values by variation of tailpipe length as was found experimentally. It should also be noted that for the given range of combustion chamber volumes and tailpipe lengths for each combustor, variation in frequency was more sensitive to change of CCV compared with change of tailpipe length (see figures 4.8 and 4.11).

More details on CO formation in the present design of the pulsed combustors is discussed in later sections.

Gas Input Rate / ml s^{-1}	CO_2 / % Sampling Point 1	CO_2 / % Sampling Point 2
133	8.2	8.3
150	8.6	8.6
167	9.0	9.1
183	9.8	9.8

Table 6.1 Measured CO_2 values at two sampling points for the 7.5 kW combustor.

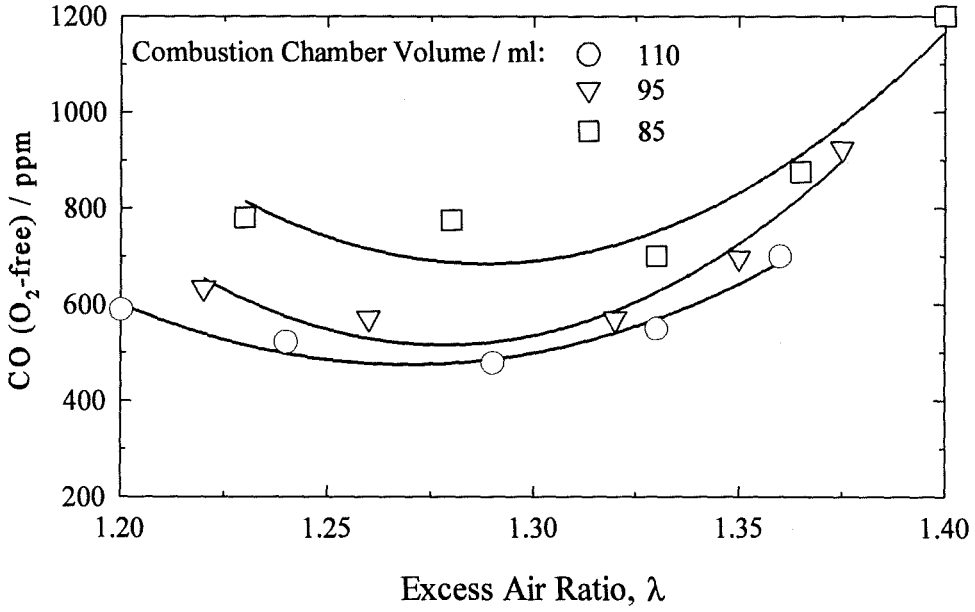

Fig. 6.32 CO values vs λ for the nominally 7.5 kW combustor at fixed tailpipe length of 1500 mm and the specified combustion chamber volumes.

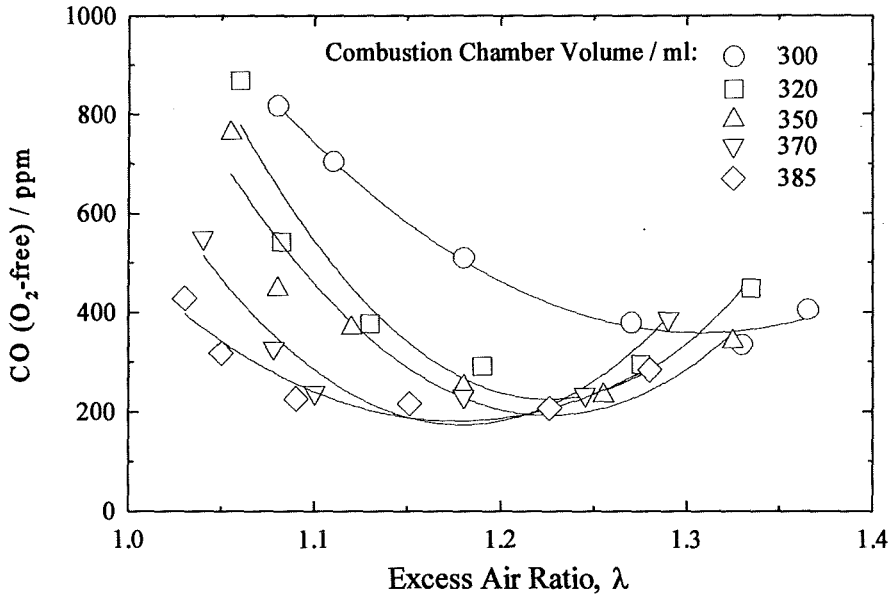

Fig. 6.33 ***CO as a function of excess air ratio for the nominally 15 kW combustor, using fixed tailpipe length of 1500 mm and the specified combustion chamber volumes.***

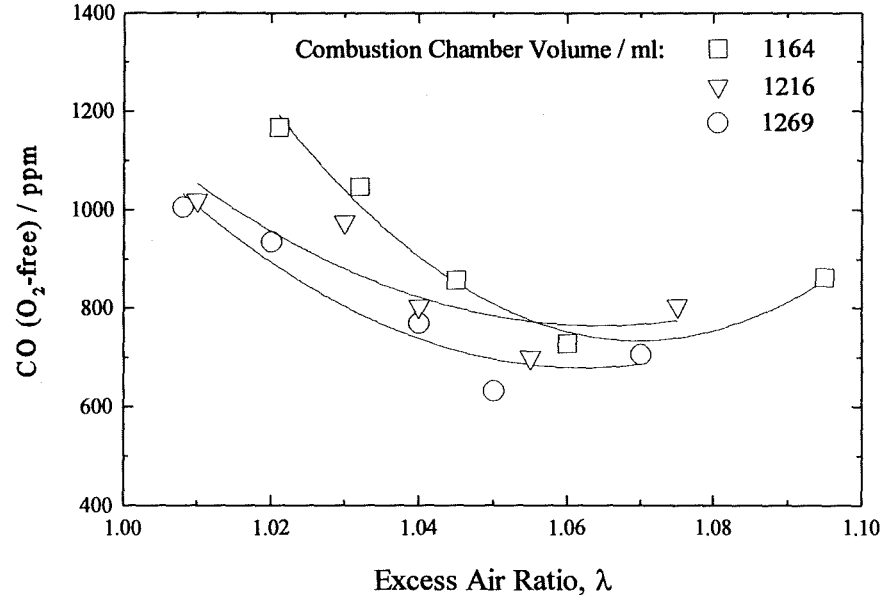

Fig,6.34 ***Variation of CO with λ for the nominally 30 kW combustor, using fixed tailpipe length of 2000 mm and the specified combustion chamber volumes.***

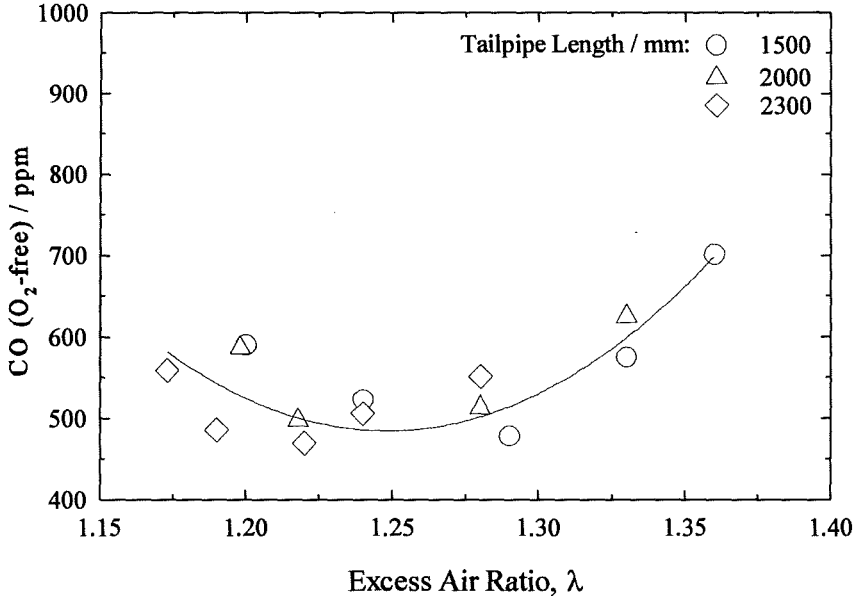

Fig. 6.35 ***CO concentrations vs excess air ratio for the nominally 7.5 kW combustors, using fixed combustion chamber volume of 110 ml and the specified tailpipe lengths.***

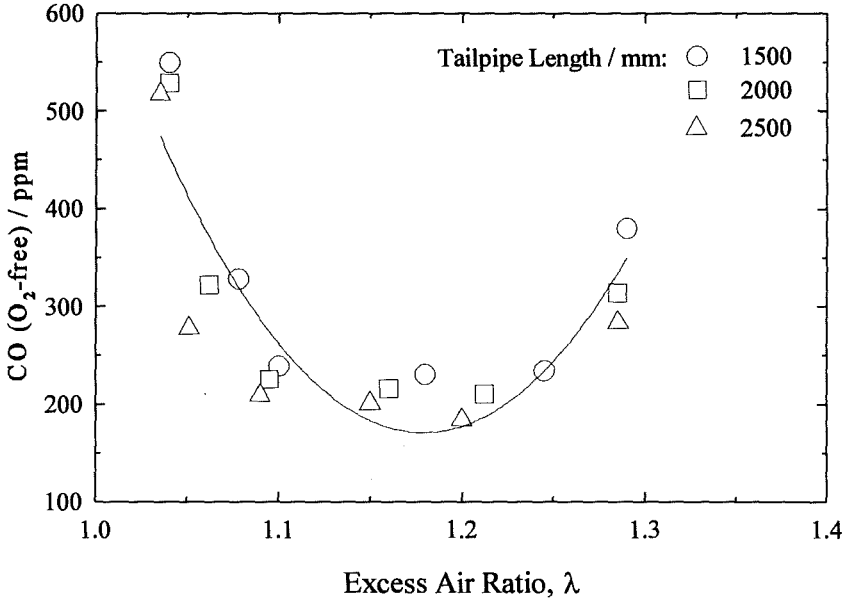

Fig. 6.36 ***CO vs λ for the nominally 15 kW combustor when combustor operated at combustion chamber volume of 370 ml and the specified tailpipe lengths.***

6.4.2.1 Influence of Added Nitrogen and Argon

It was shown in section 6.4.1.1 that dilution of the mixture charge of air and gas with additional gases reduced the NO_x emission as a result of lowered flame temperature. Here, the effect of nitrogen and argon upon CO levels is studied.

Carbon monoxide emissions are shown vs excess air ratio for a fixed configuration of the combustor in Fig. 6.37. The general U-shaped pattern of the CO values vs λ is similar for all the measurements including zero injected N_2 and at different added volume rates of nitrogen. Nitrogen injection resulted in a narrowing of the width of the U-shaped curve, the effect being progressive with increasing N_2 injection. There was little influence of N_2 injection on the low λ side but a major influence in the high λ region, with minimum values of CO (for each N_2 injection rate) moving towards lower λ values. In the region for λ values from 1.20 to 1.35 CO levels increased progressively with increasing N_2 dilution at any given normalised A/F. This may be due to decreased flame temperature resulting from dilution.

Further, it is proposed that the sharply increasing CO levels with decreasing λ in the range of λ from 1.15 to 1.00 were an indication of imperfect mixing. As a λ value of unity was approached, macro pockets of fuel-air charge of sub-stoichiometric composition would have become increasingly prevalent. Additional results favouring this explanation are presented in following section 6.4.2.2.

Results of CO vs λ for various argon injection rates are shown in Fig. 6.38. The results were similar to those for nitrogen injection. As the argon flow rate increased the CO level increased. The argon replaced oxygen, pushing mixture strength towards stoichiometric and at the same time reducing the flame temperature. This effect is quite clear at higher λ values, where the CO increased from 300 ppm to 500 ppm with increase of argon flow rate from zero to 350 ml s^{-1}.

In both conditions of nitrogen or argon addition, reduction in CO was less than expected at the higher values of λ with increasing injection rate of diluent (see Fig. 6.37 and 6.38). This is because although the nitrogen or argon injection reduced the flame temperature and consequently raised the CO levels, moving towards lower λ values as a result of increased injection rate of diluent increased the flame temperature which

according to equation (1.26) reduced the CO.

At lower values of λ the trends were less clear-cut with Ar than with N_2 (Fig. 6.37 and 6.38), i.e. points were more scattered for argon than for nitrogen injection. However, the CO values were generally high in this region which was attributed to poor mixing of the fuel gas and air.

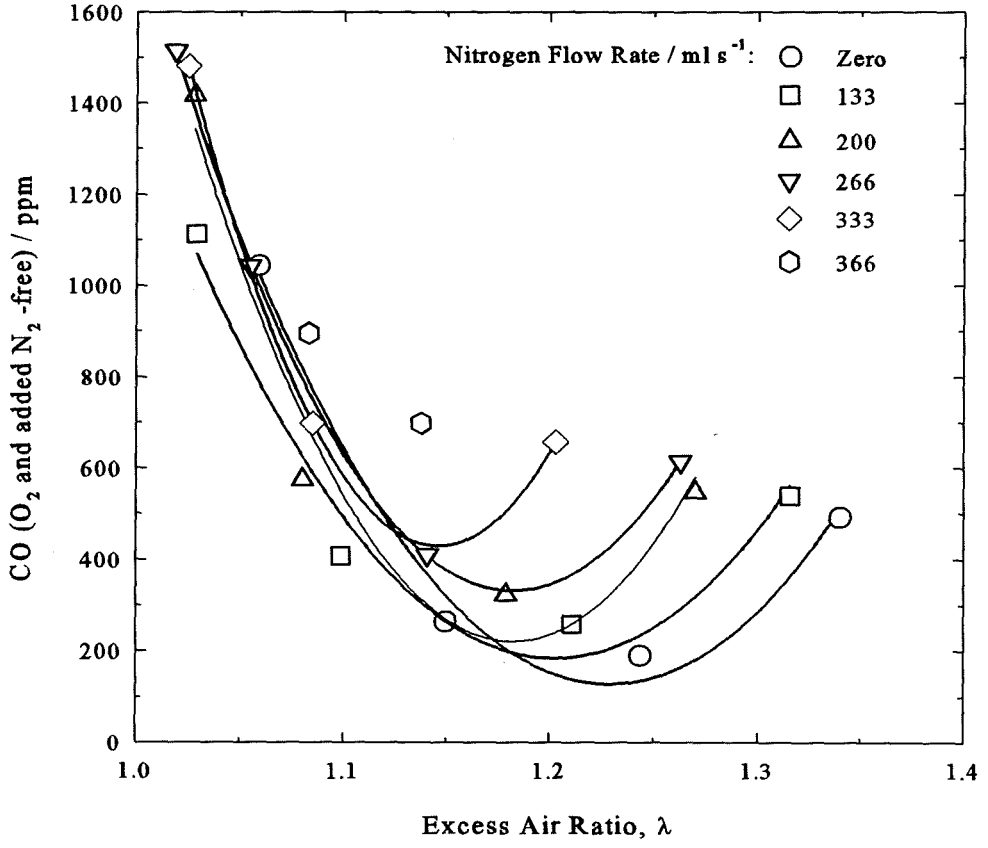

Fig. 6.37 ***Carbon monoxide emissions corrected for dilution to zero excess air and to zero injected N_2 vs λ for various rates of nitrogen injection as shown.***

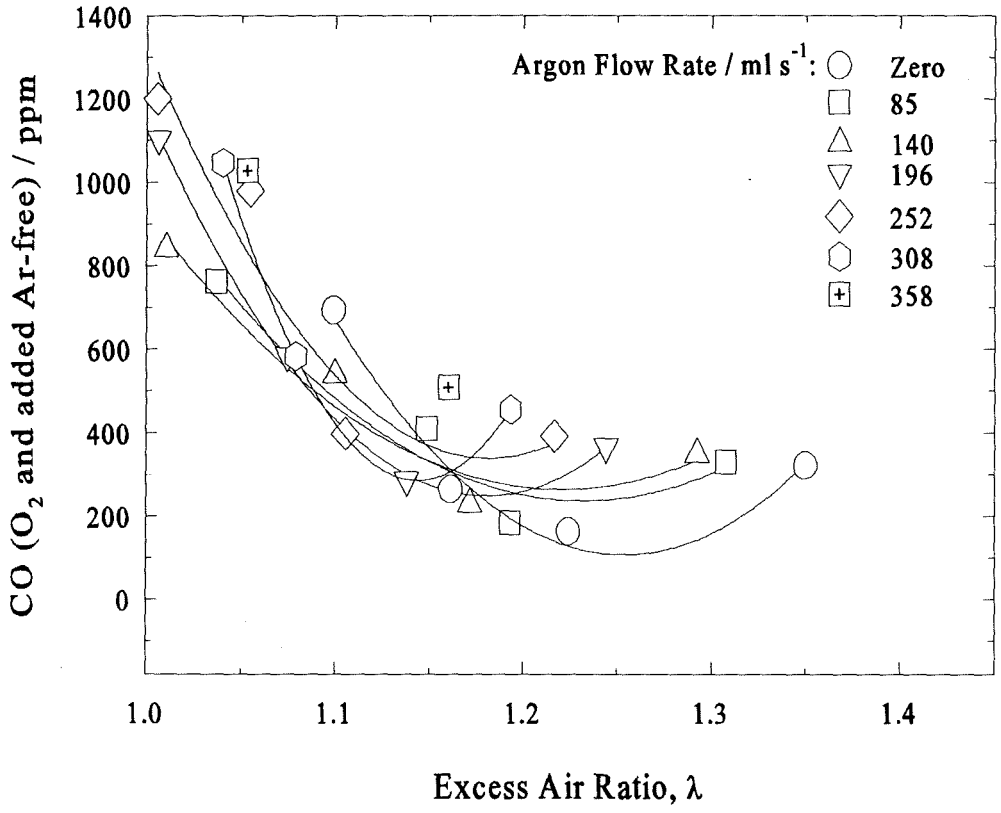

Fig. 6.38 ***Variation of CO emissions corrected for dilution to zero excess air and to zero injected argon with excess air ratio for the various rates of argon injection.***

6.4.2.2 Effect of water bath temperature

It has been postulated by a number of workers including Kitchen [1982] and Blomquist *et al.* [1982] that the CO emissions from a pulsed combustors can be attributed to the followings:

a) quenching effect on the walls of the combustion chamber,

b) imperfect mixing of air and gas prior to combustion.

Kitchen [1982] described the quenching of the combustion products in the combustion chamber of the Lucas Rotex boiler which resulted in high CO levels in the exhaust gas. On the other hand the Blomquist *et al.* [1982] data on heat transfer did not support

quenching. Kitchen suggested that insufficient residence time of combustion gases in the combustion chamber may have caused the high CO emission levels in his experimental burner.

None of these workers has shown clear validity of their statements. Therefore, a series of experiments was conducted measuring the concerned combustion products at various water bath temperatures (WBT). The purpose of this experiment was to modify heat losses from the combustion gases to the walls of the combustion chamber by varying the WBT. For these experiments the nominally 15 kW combustor was used burning mains natural gas. Figure 6.39 shows the variation of CO with λ at various water bath temperatures. A clear trend is evident with water bath temperature, CO levels decreasing as WBT was raised. As the WBT was raised so the temperature of the walls of the combustion chamber increased. The results therefore indicate that quenching of the flame at the walls was an important contributor to the generation of CO; the degree of quenching increased as WBT decreased. But it can be seen that at values of λ approaching 1.05, WBT became relatively unimportant; thus the high CO levels at low λ would not appear to be due to quenching. So the proposition that the effect was due to imperfect mixing described in previous section seems to be reasonable. The result implies that in the low λ region where the A/F is near to the stoichiometric and the temperature of the combustion gases is higher, the degree of mixing air and gas is the more important factor if CO levels are to be kept low. Further analysis of the data is shown in Fig. 6.40 where the CO is plotted against WBT for the chosen values of λ determined from the best lines through the points. It can be seen that the lines become less steep with decreasing λ illustrating a decreasing dependence upon WBT at low λ values. The effect can be clearly seen in Fig. 6.41. These figures confirm that the effect of WBT on CO emission was substantial for $\lambda > 1.15$ but became insignificant as λ approached 1.00. The CO generated at λ values above 1.20 had two main sources: part was formed in the main bulk of the combustion gas via reaction (1.26); a further part was formed close to the walls of the combustion chamber where the gas layer was cooler than the bulk due to conduction and radiation and thus CO was formed due to quenching of the flame. A possible third component in this λ region was imperfect mixing though

the results provide no evidence for this proposition at this stage.

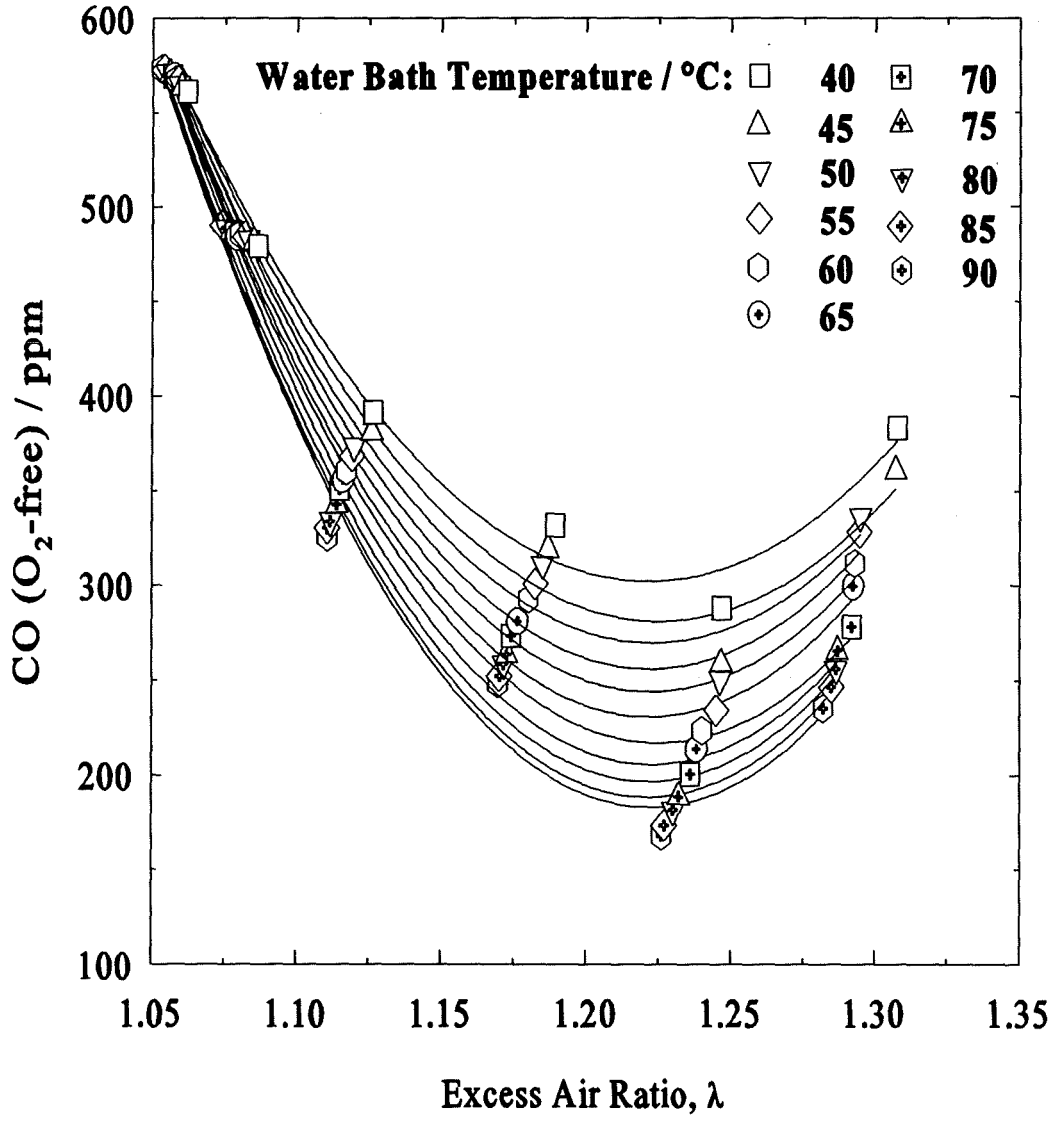

Fig. 6.39 ***CO emissions vs λ with water bath temperature (WBT) as a parameter. Lines represent the best second order line through the points for a given WBT. Combustion chamber volume 370 ml, tailpipe length, 1500 mm and flapper valve thickness 0.15 mm.***

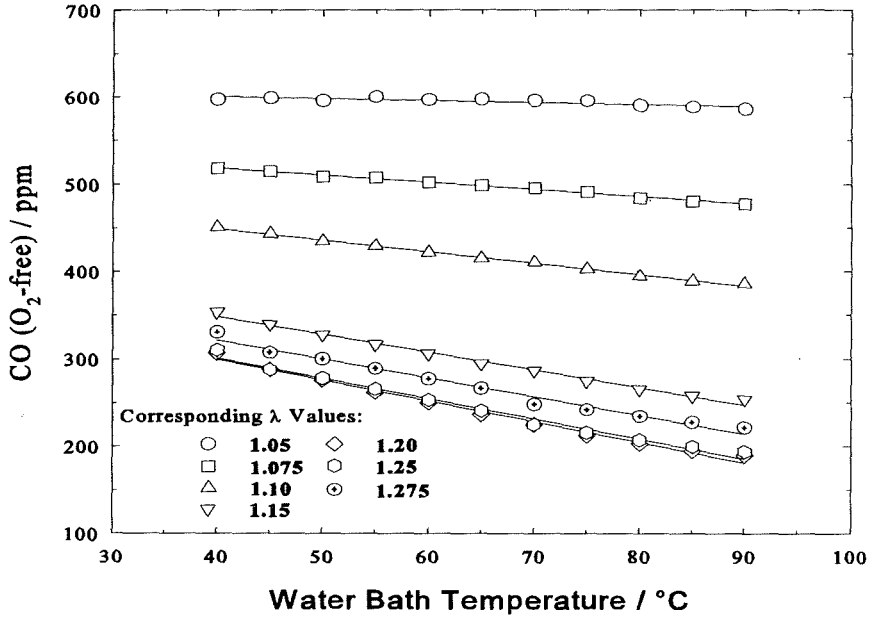

Fig. 6.40 ***CO emissions vs water bath temperature for given values of λ. The data shown for λ = 1.05 were obtained by extrapolating beyond the range of the primary data. Data are from Fig. 6.39.***

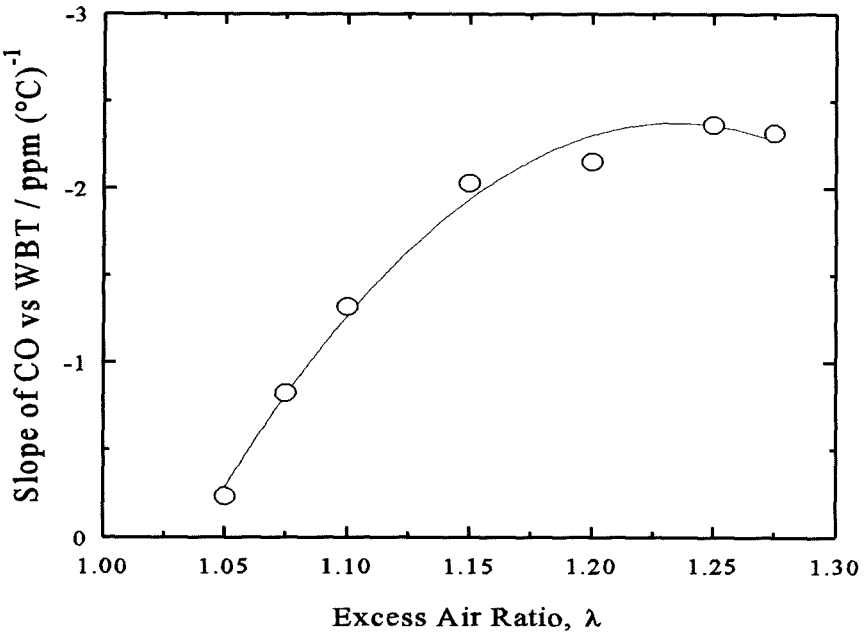

Fig. 6.41 ***Slopes of lines in Fig. 6.40 vs excess air ratio, λ.***

The discussion so far has ignored any effect that WBT may have had on flame temperature in the bulk of the burnt gas. This is because it was considered that incoming gases had insufficient time, upon entering the system, to receive significant heat from the water bath to cause a rise in their temperature prior to ignition. Results for NO_x emission presented in Fig. 6.42 confirm that this is a reasonable assumption; the effect of raising WBT was probably effectively to increase the time at maximum temperature due to reduced radiation losses.

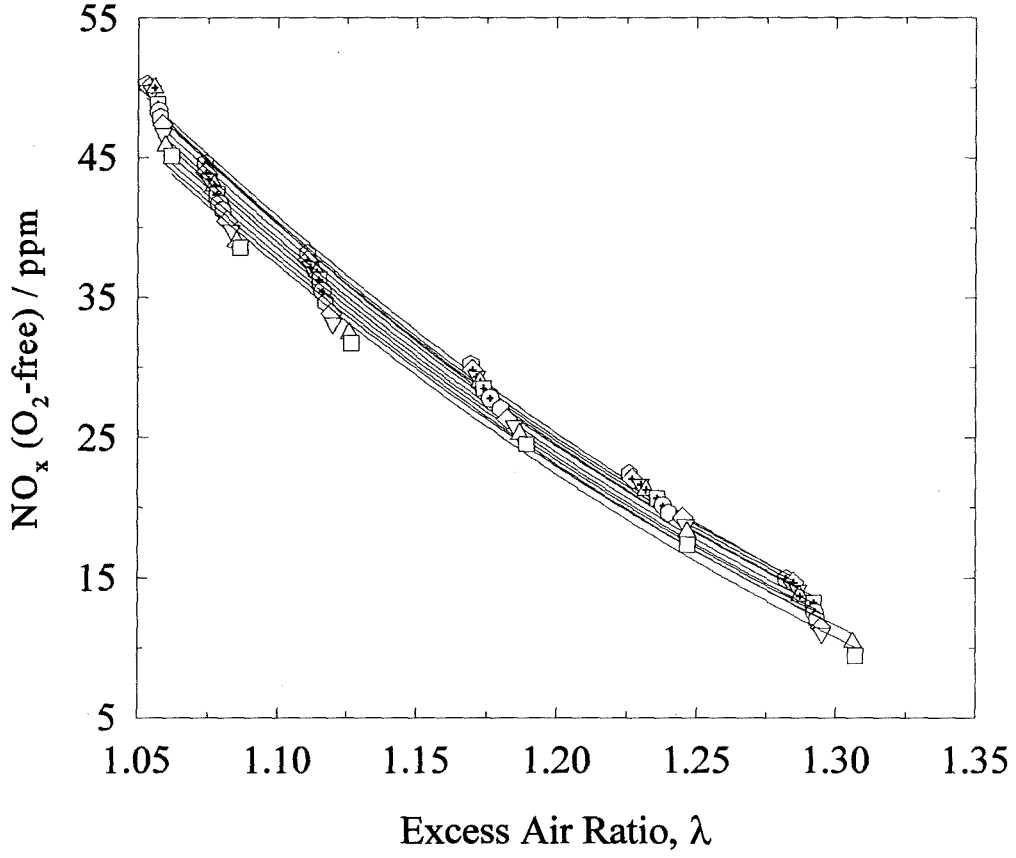

Fig. 6.42 ***NO_x emissions vs λ with water bath temperature (WBT) as a parameter. Lines represent the best second order line through the points for a given WBT. Symbols and configuration as in Fig. 6.39.***

6.4.2.3 Sub-Stoichiometric Operation

Sub-stoichiometric combustion of hydrocarbon fuels is generally undesirable because of the generation of large amounts of toxic CO and decrease in thermal efficiency of the combustor. It was found that of the three combustors only the largest, the nominally 30 kW unit, would run in a sub-stoichiometric condition; this was when the volume of combustion chamber was increased to a value above 1300 ml. A few measurements were made around the stoichiometric point and are presented in Fig. 6.43. Sub-stoichiometric operation was shown by the oxygen decreasing to zero and the CO rising sharply. The further effect was the decrease in exhaust gas temperature (Fig. 6.43d). The above trend is typical of incomplete combustion where the fuel burns with less than the overall stoichiometric air requirement.

Combustion of a fuel with less than the stoichiometric air requirement is a complex situation which involves chemical equilibria and reaction kinetics. However, a simplified mechanism is conventionally assumed which enables a straightforward estimation of the products of combustion to be carried out. This mechanism consists of the following sequence of events [Hanby, 1993]:

a) the available oxygen firstly burns all the hydrogen in the fuel to water vapour,
b) all the carbon in the fuel is then burned to carbon monoxide,
c) the remaining oxygen is consumed by burning carbon monoxide to carbon dioxide.

The above listed procedure is only pertinent if there is sufficient oxygen to attain stages (a) and (b). Fig. 6.44 shows the relations of the above where the measured CO and CO_2 from the nominally 30 kW pulsed combustor are plotted as a function of the excess air ratio, λ. As the air supply fell below the stoichiometric requirement (i.e. $\lambda < 1.00$) the percentage of carbon monoxide (CO) in the flue gas increased rapidly. CO was close to its minimum value with $\lambda=1.00$ while CO_2 exhibited its maximum value at this point.

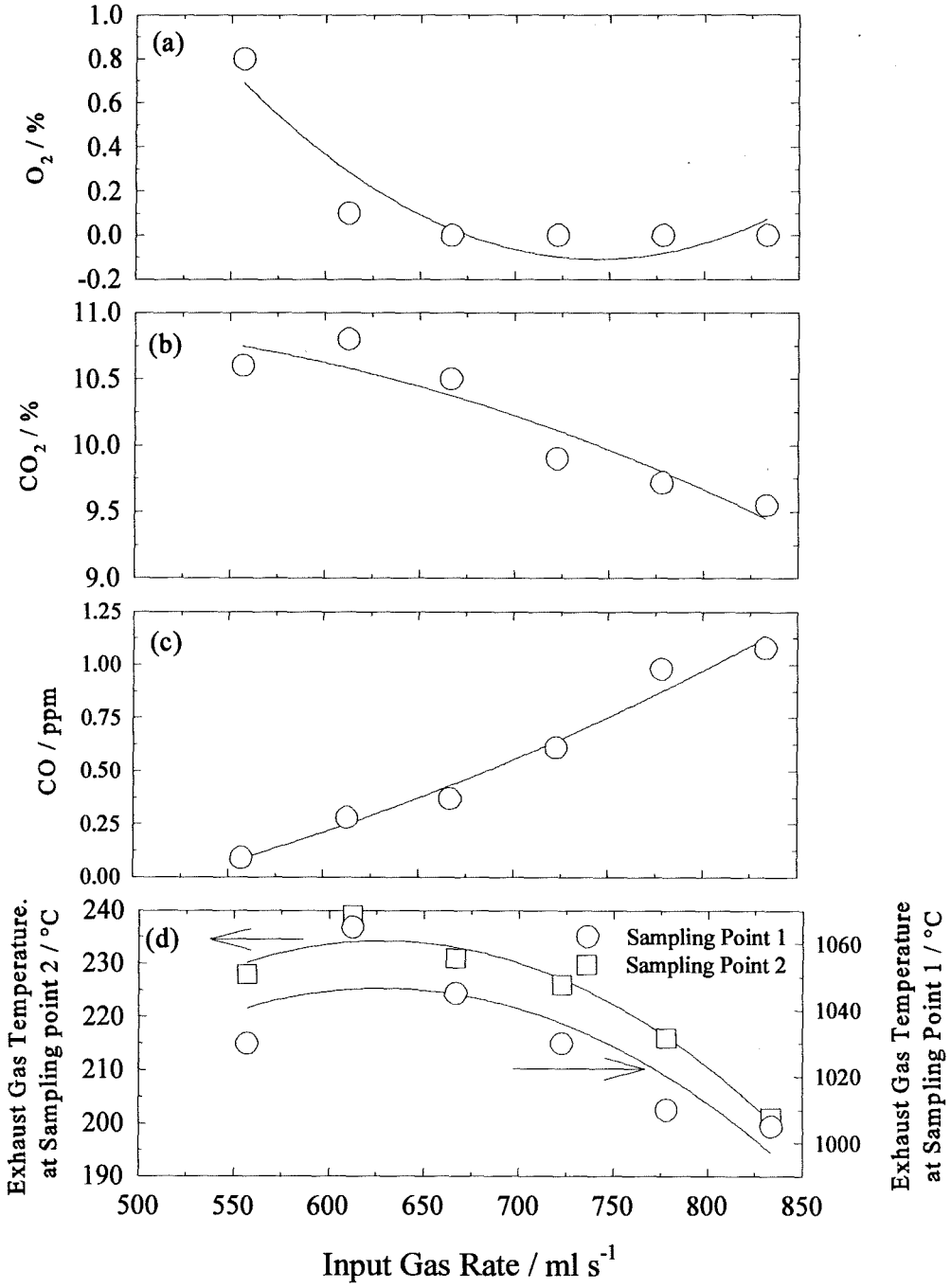

Fig. 6.43 ***Effect of sub-stoichiometric combustion upon the a) O_2, b)CO_2, c)CO and d) exhaust gas temperature at two sampling points. The 30 kW combustor was operated with combustion chamber volume of 1370 ml, tailpipe length of 2000 mm and flapper valve thickness of 0.15 mm.***

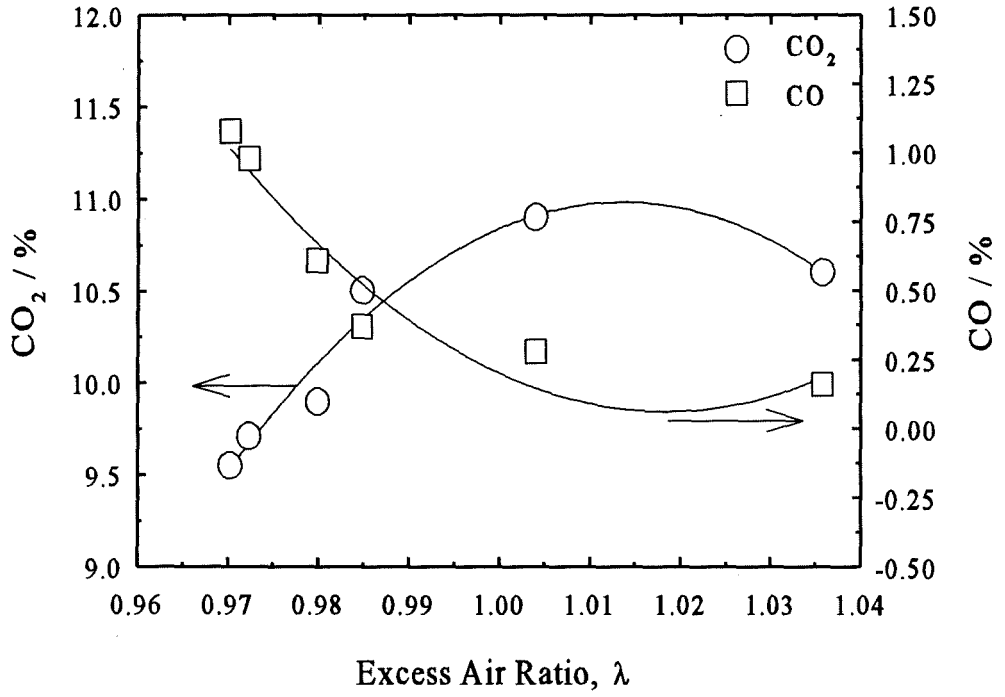

Fig. 6.44 ***Variation of CO_2 and CO with excess air ratio for the nominally 30 kW pulsed combustor. Configuration as in Fig. 6.43.***

6.5 Effect of Input Fuel Gas Composition

One of the characteristics of combustors which should be considered is the interchangeability of one gaseous fuel with another. Moreover, it is a requirement of the British Standards Institute that the appliance performance should be checked against a number of gases representing limiting compositions of gases such as incomplete combustion, light back and flame lift, which might be distributed to customers under emergency conditions [Jones, 1989]. Earlier in Chapter 1 it was mentioned that there are two important factors that determine the suitability of a fuel for a particular burner;

a) the ratio of the calorific value of a fuel to the square root of its density relative to air (i.e. Wobbe number of the gaseous fuel) [see Appendix II],

b) the rate at which a flat flame front is propagated through a static medium (i.e. burning velocity).

It has been pointed out that a pulsed combustor which burns satisfactorily one type of fuel gas such as mains natural gas with a high content of methane may fail to operate successfully or deteriorate markedly with other fuel gases. For instance, Jones and Leng [1994] have shown that addition of hydrogen and/or propane affects the operation of a pulsed combustor. Their non-premixed pulsed system failed to operate satisfactory with gas mixtures containing more than 20% hydrogen by volume generating high contents of carbon monoxide and failing to satisfy the Rayleigh criterion. Similarly, Kunsagi [1971] reported the operating failure of a pulsed combustor which was successfully operated in the UK with town gas containing 48 % H_2 when burning natural gas with 96 % methane. Other workers also reported such deterioration of performance of their pulsed combustors burning fuels containing a higher percentage of higher hydrocarbons [Keller and Westbrook, 1986].

This section represents data on the fuel flexibility and performance of the present developed pulsed combustors in terms of pollutant emissions which were investigated by burning various fuel gas compositions: namely test gases NGB, NGC and NGD supplied by the British Gas Research Centre. The detailed compositions of these test gases are given in Appendix II. Discussion of the concept of flame stability was presented previously in Chapter 1. Because of the limited supply of the test gases, only the nominally 15 kW combustor was employed for this study. Measurements of the composition of combustion products and flue gas temperature were carried out using a fixed configuration of the combustor. Details of the experimental arrangement for these tests were given in Chapters 2 and 3.

6.5.1 Analysis of Combustion Products

At a fixed combustion chamber volume of 360 ml, tailpipe length of 2500 mm and flapper valve thickness of 0.15 mm a series of tests was conducted and measurements of the composition of combustion gases at the tailpipe exit were carried out. Figure 6.45

shows the variation of combustion products with heat input when burning test gases NGB, NGC and NGD. From the results obtained it is clear that the trend of the variation of concentrations of combustion products with heat input is similar to those obtained from burning mains natural gas (see Fig. 6.3); the average measured NO_x concentrations at end of the tailpipe increased with increasing heat input. However, from the experimental data (Fig. 6.45) it is apparent that the test gas NGC with heat release of 0.031 kW for one ml s^{-1} of gas, produced slightly lower NO_x (average of 15 ppm) compared to NGB (average of 25 ppm) and NGD (22 ppm) which have heat inputs of 0.047 and 0.036 kW for every ml s^{-1} input gas respectively. The measurement of combustion gas temperature at the sampling point 1 (Fig. 6.46b) was consistent with the trend of the above average measured NO_x data. The calculated adiabatic flame temperatures (Fig.6.47) revealed lower values for NGC than the other two test gases for a given heat input.

It is known that the theoretical air requirement for combustion of hydrogen is lower than for hydrocarbons particularly propane which has a significantly higher theoretical air requirement [Jones, 1989]. Therefore, it is expected that more air remains from each cycle when burning the NGC gas with 36 % by volume hydrogen content compared to burning the NGB gas with a trace of H_2 and over 17 % by volume propane. This is illustrated in Fig. 6.48. Moreover, for a given fuel gas flow rate, the rate of heat release decreases as the hydrogen level increases. Therefore, the observed lower flame temperature associated with NGC and higher flame temperature associated with NGB gas in Fig. 6.47 may have contributed by the above. Knowing that the NO_x concentration is very sensitive to combustion temperature, Fig. 6.46b and 6.47 clearly enable the observed behaviour of the NO_x emissions (i.e. Fig. 6.45c) in relation to burning these test gases at various fuel input rate to be explained. As before (i.e. when burning mains natural gas) it was found that the NO_x concentrations were in the form of NO.

Similar to the combustion of mains natural gas, burning the test gases NGB and NGD showed a U-shaped characteristic for CO emission as shown in Fig. 6.45d. CO values were high at lower heat input when the excess air was high and the flame

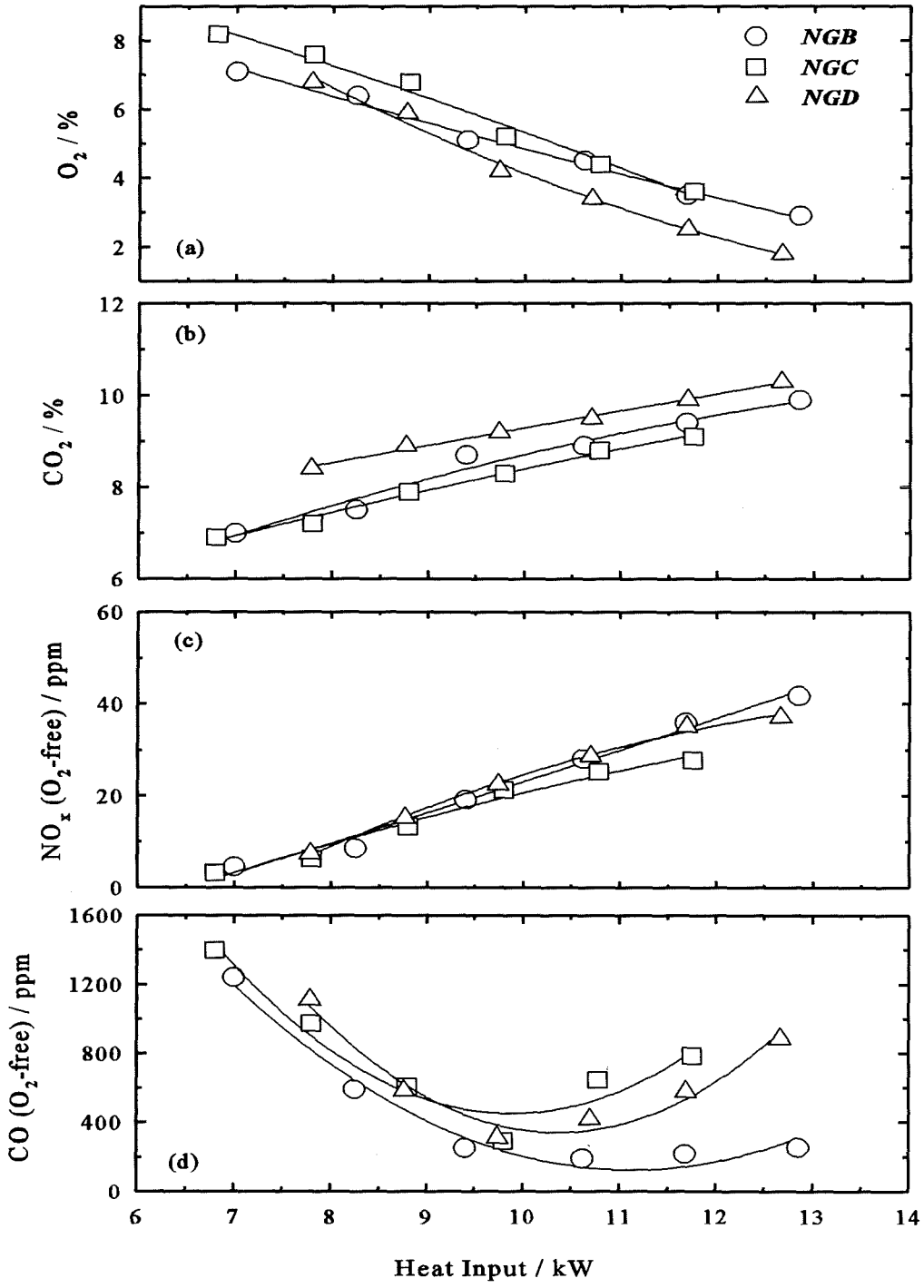

Fig. 6.45 ***Variation of concentrations of combustion products a) O_2, b) CO_2, c) NO_x and d) CO concentrations with heat input burning test gases NGB, NGC and NGD. Configuration: combustion chamber volume 360 ml, tailpipe length 2500 mm and flapper valve thickness 0.15 mm.***

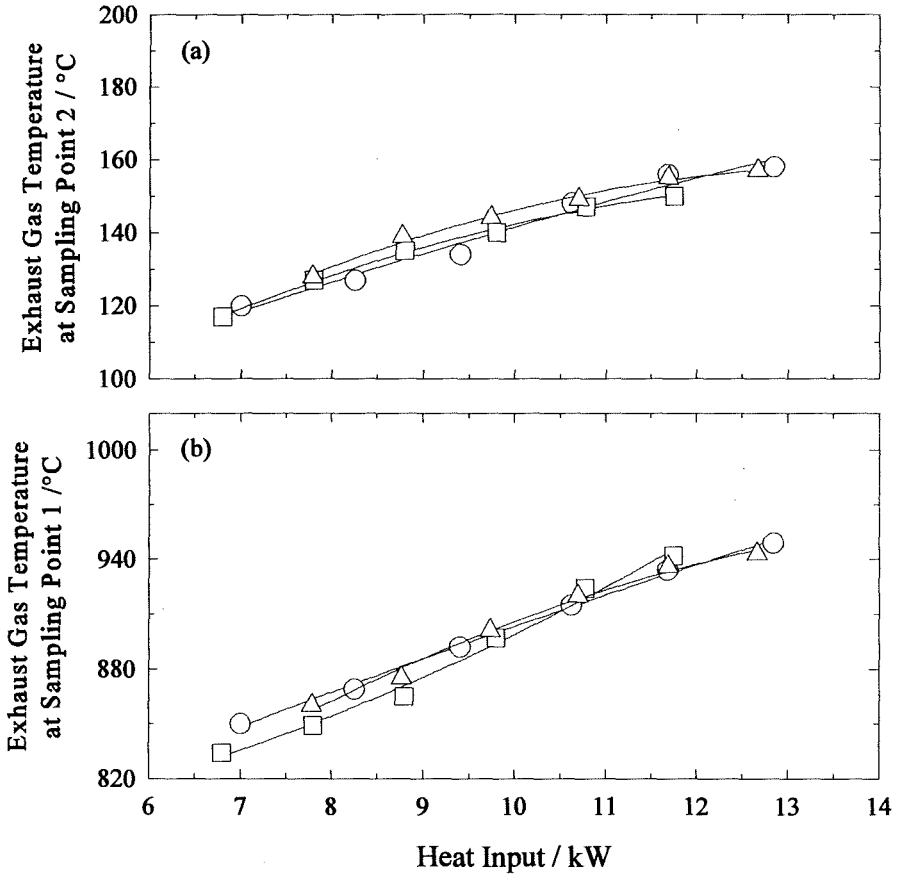

Fig. 6.46 ***Variation of flue gas temperatures at two a) sampling point 2 and b) sampling point 1, burning the test gases NGB, NGC and NGD at fixed configuration as in Fig. 6.45.***

temperature low. Then the CO values reduced progressively as the heat input was increased. Further increase of heat input resulted an increase of the carbon monoxide values again (Fig.6.45d) presenting a U-shaped characteristic. It can be seen from Fig. 6.45 that in contrast to the NO_x concentrations the CO values were generally higher when burning NGC gas, particularly in the higher heat input region (average CO of 600 ppm) compared to NGB and NGD gas with average CO emission levels of 400 ppm and 300 ppm respectively. This also can be attributed to the flame temperature. As seen in Fig. 6.47 the NGC had the lowest flame temperature compared to the other two test

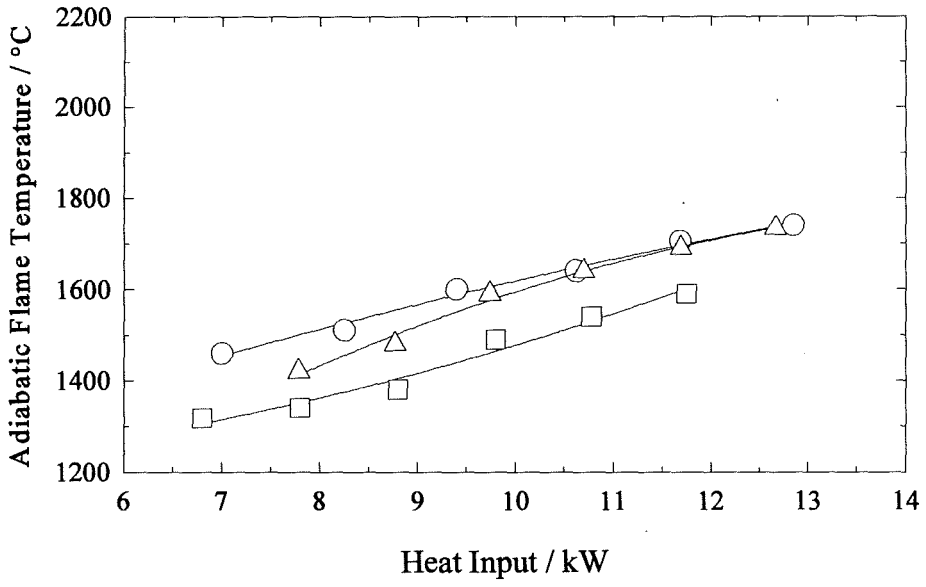

Fig. 6.47 ***Variation of calculated adiabatic flame temperature as a function of heat input rate for the three test gases NGB, NGC and NGD. The configuration and symbols as in Fig. 6.45.***

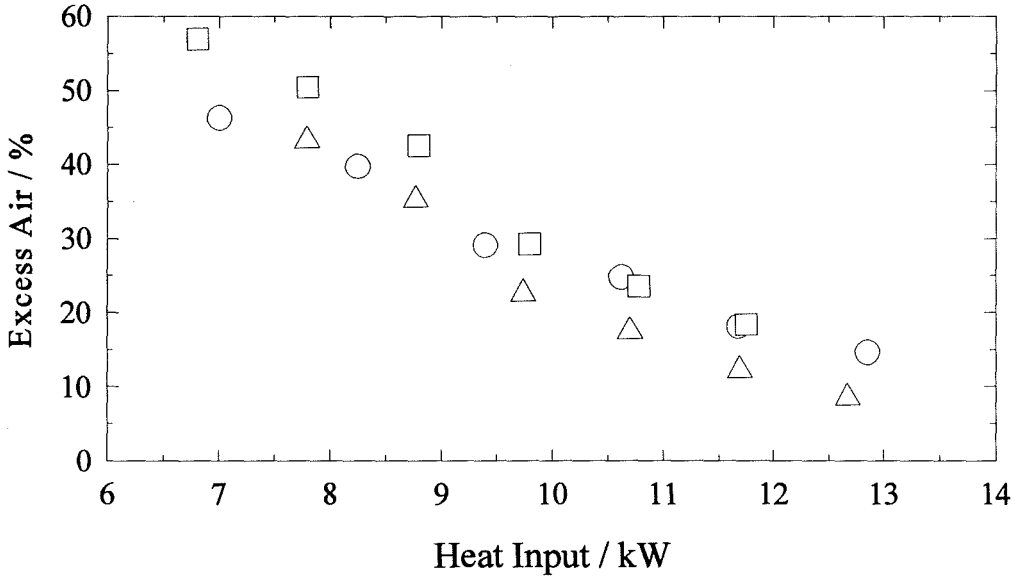

Fig. 6.48 ***Variation of excess air with heat input for combustion of the test gases NGB, NGC and NGD. Configuration used as in Fig. 6.45.***

gases for a given heat input which in turn resulted in the observed increase of CO according to equation (1.26). One other possible reason for the high levels of CO associated with burning NGC gas may be due to light back nature of NGC gas in which flame propagates back through the burner and lack of air at the upstream of the combustion chamber results in unsatisfactory combustion and associated high concentrations of CO. High CO levels were also observed by workers such as Jones and Leng [1996] and Windmill [1984] when burning hydrocarbon fuel with added H_2 or fuel with high contents of hydrogen. Jones and Leng [1996] concluded that such a rise of CO was due to incomplete combustion which in turn lowered the flame temperature and resulted in high levels of CO. Incomplete combustion was implicated in the successive damping effect arising from a change in the phase relationship between heat release and pressure oscillations so failing to satisfy the Rayleigh criterion. Windmill [1984] also reported relatively high levels of CO emission associated with burning NGC gas compared to NGB and NGD gas. Indeed, the trend of results obtained for CO emissions in this study is in line with his results, although, he did not indicate the reasons for his observations.

6.6 Overall Efficiency

In the earlier sections it was shown that in the present type of pulsed combustors under study the combustion temperature was controlled mainly by A/F and NO_x concentrations were significantly influenced by temperature. Clearly, any change in temperature would be expected to affect the overall efficiency of the combustors. Thus, the variation of the overall efficiency of the developed combustors with excess air ratio, λ, was investigated.

The direct measurement of the developed combustor's efficiency is a complex task since carefully controlled operating conditions and environment together with appropriate instrumentation are required. Therefore, in this study the overall efficiency of the three developed pulsed combustors was calculated.

The driving forces for heat transfer in the combustors are the temperature and flow of the combustion gases. Figure 6.49 shows measured temperatures as a function of

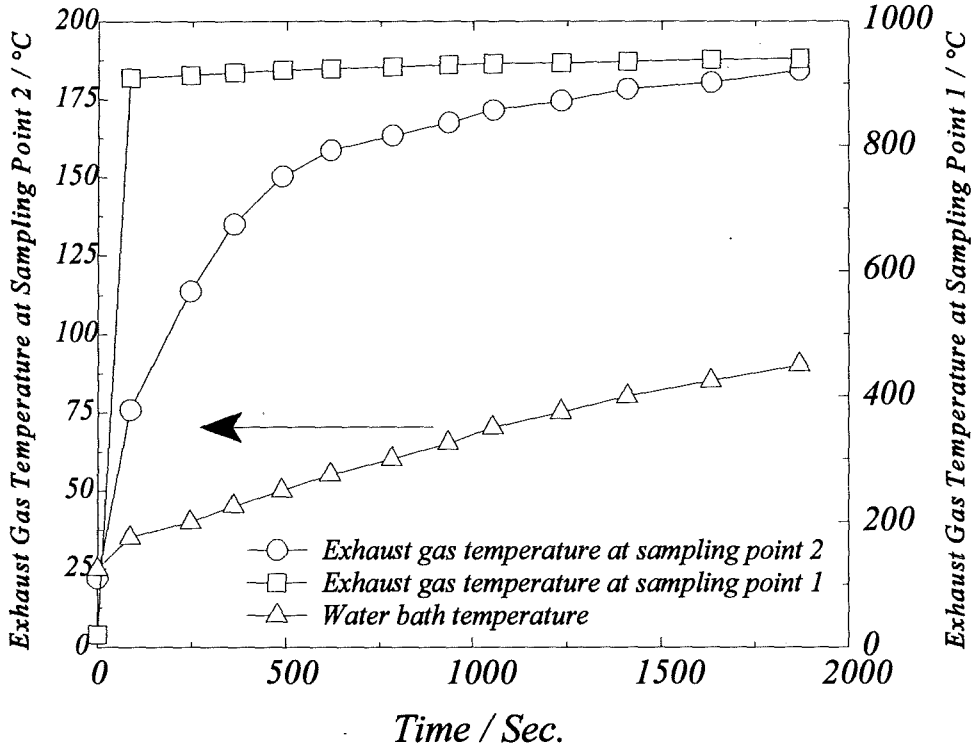

Fig. 6.49 ***Variation of exhaust gas temperature as a function of time for the nominally 15 kW combustor burning natural gas at the rate of 250 ml s^{-1}. Configuration: combustion chamber volume 370 ml and tailpipe length 1500 mm.***

time. The temperature inside the combustion chamber increased rapidly after ignition and then levelled off, while the temperature at the end of tailpipe together with the temperature of the water in the tank continuously increased with time. The temperature difference between two sampling points 1 and 2 is a clear indication of the high convective heat transfer rates in the present design of pulsed combustor.

In this study a simple approach was used to calculate the overall efficiency of the pulsed combustors. The calculation was based upon readings which enable the enthalpy losses in the flue gas (per unit mass of fuel) to be related to the calorific value of the fuel. In this calculation it is assumed that there was negligible case loss in the system giving the general energy balance of the system as [Hanby, 1993]:

$$CV = (H_P - H_R) + Q_u \tag{6.8}$$

where CV is the calorific value of the fuel, Q_u is the useful heat and the term in the bracket represents the difference between the enthalpy of fuel and air at room temperature and that of the combustion products.

Given that the efficiency of the system is defined by Q_u / CV, then using equation (6.8), the overall efficiency, η, can be written as [Hanby 1993]:

$$\eta = 1 - [\frac{(H_P - H_R)}{CV}] \tag{6.9}$$

This equation assumes complete combustion with negligible CO in the products. Since measurements of combustion products were carried out above the flue gas dew point (typically above 60°C) it is appropriate to carry out the calculations based upon net calorific value of the mains natural gas, excluding the latent heat of condensation of the water vapour. However, if the combustion gases were cooled below the dew point, enabling the recovery of latent heat present in the water vapour in the flue gas then the use of gross calorific value of the fuel would be more appropriate.

Fig. 6.50 shows the variation of overall efficiency of the three pulsed combustors as a function of excess air ratio , λ. The results obtained indicate that the changes, in the given ranges, of A/F had insignificant effect upon overall efficiency of the pulsed combustors, remaining at above 90 % in all cases.

6.7 Summary and Conclusions

Measurements of flue gases temperature and gaseous emissions from the three developed pulsed combustors at various operating conditions were made. The results show that the combustion temperature was principally fixed by the excess air ratio, λ, in these premixed combustors.

It was shown that the NO_x varied with gas input rate, increasing when fuel gas input rate was increased. In addition, for a given fuel gas input rate the NO_x values increased as the CCV and tailpipe length were increased. Further analysis of data indicated that combustion temperature was the principal factor controlling the concentration of NO_x

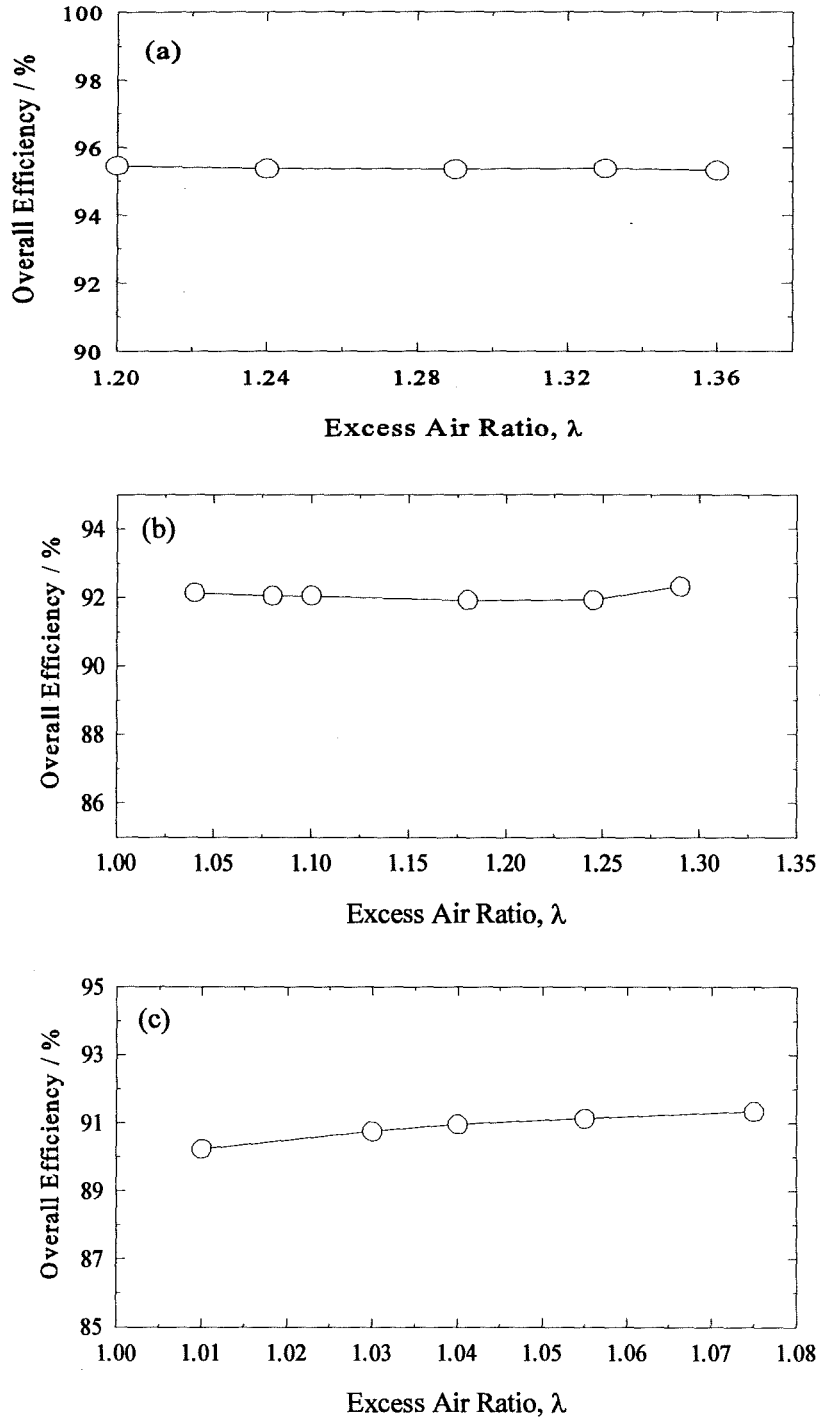

Fig. 6.50 ***Variation of overall efficiency (based on net calorific value) with excess air ratio, λ for a) the 7.5 kW, b) the 15 kW and c) the 30 kW combustors. The employed configuration was as in Fig. 6.2 to 6.4 respectively.***

for these premixed combustors and any influence of CCV and tailpipe length on NO_x was as a result of their effect on combustion temperature. It was demonstrated that NO_x values, as a function of calculated adiabatic flame temperature for all the operating conditions, followed a single curve. Further analysis of the data showed that NO_x emissions in these premixed combustors with high combustion temperatures was an exponential function of flame temperature indicating the formation of NO_x was mainly via the Zeldovich mechanism. Almost all the NO_x emitted was in the form of NO. This is believed to be the result of high flame temperatures which were generally above 1850K.

The significance of flame temperature upon measured average NO_x emissions at the end of the tailpipe was further confirmed by dilution of the mixture charge of air and gas with nitrogen or argon. For a given A/F, NO_x concentration was reduced as the rate of diluent gas was increased.

Experimental data showed that for a given configuration CO values were high in both the lower λ and higher λ regions resulting in a U-shaped characteristic. Increased CO levels at higher λ values were thought to be due to reduced flame temperatures, while it was proposed that the rising CO levels as λ approached 1.0 resulted from imperfect mixing of fuel and air prior to combustion. It was found that the quenching effect on the walls of the combustion chamber was an important contributor to CO emissions. This was demonstrated by measuring the CO concentration at various water bath temperature for the range of λ values. It was found that for $\lambda>1.15$ the CO values were substantially influenced by WBT whereas for $\lambda< 1.10$ the WBT had no influence at all.

The results obtained from all the tests indicated three main sources for CO emissions. The first was that found at low λ values which is thought to indicate imperfect mixing of the fuel gas and air before combustion. The second was that formed in the bulk of the combustion gases via reaction (1.26) which was pushed to the left at low flame temperatures and the third was quenching of the combustion reactions on the relatively cool walls of combustion chamber.

Finally, the pulsed units operated successfully with test gases NGB (incomplete

combustion sooting gas), NGC (light back gas) and NGD (flame lift gas). The variations of NO_x and CO vs input heat for these test gases showed similar trends to those for mains natural gas. NO_x increased as the fuel gas input rate increased and CO showed a U-shape curve. However, the NGC gas showed the lowest NO_x concentrations which was compatible with its having the lowest calculated adiabatic flame temperature.

In general, the results obtained regarding NO_x measurements indicated that the apparent influence of scale of the unit, tailpipe length and combustion chamber volume were simply due to the effect of these parameters on the temperature within the combustor which was principally controlled by the A/F. These results indicated that the influence of frequency of pulsing was insignificant upon quantities of the average NO_x emissions measured at the end of tailpipe in the present design of pulsed combustors.

Chapter Seven

Noise Characteristics of the Developed Pulsed Combustors

7.1 Introduction

Excessive operating noise is probably the most serious problem in applying pulsed combustion technology, and one of the design constraints, particularly for residential and light commercial equipment which must be reasonably quiet to be acceptable. It is generally agreed that the most annoying noises are characterised by magnitude of above 80 dB, by frequencies above 1500 Hz and by rapid fluctuations in both sound intensity and frequency. There have been a number of reports on sound characteristics of pulsed burners and various methods of noise reduction including work carried out by American Gas Association Laboratories [Belles *et al.*, 1982] and the Toshiba Corporation, Japan [Saito *et al.*, 1986] where the noise level was reduced down to 45 dB from a 17 kW combustor. But for any design and application of a pulsed combustor it is necessary to know how much noise will be emitted from the combustor, how it may be attenuated and at what penalty. In this chapter an investigation on noise emission levels from the present design of pulsed combustors was conducted, mapping out variations with input load and combustor configuration. In addition, suitable noise reduction methods were employed to reduce the noise from the present combustors to an acceptable level.

7.2 Identifying Sources of Noise

Before any noise control technique it is important to identify the main elements contributing to the noise problem. These can be listed as follows [Warring, 1974]:

i) the source, which generates the noise,

ii) the path which transmits the noise from the source to receiver,

iii) the receiver who hears the noise,

though, the last has not considered in this study.

It was shown earlier in Chapter 1 (Fig. 1.1) that periodic controlled explosions are an inherent operational characteristic of the pulsed combustors. These explosions showing similarity to a two cycle engine (e.g. motorcycles) probably are the main source of the unwanted sound waves which are annoying noise to human ears. Furthermore, it is well known fact that the premixed gas burners (such as the design used in this study) have a tendency to excite unacceptable acoustic resonances when incorporated within sealed combustion systems.

Technically, by proper noise control, the acoustic energy emitted from the combustion chamber can be reduced and modified so as to produced a sound spectrum acceptable to the normal human ear. But here, before applying any noise controlling methods, a series of tests was conducted to identify the noise sources and the paths which contribute to the noise levels emitted from the present design of pulsed combustors. Using the sound level meter described in Chapter 3, the initial measurements of noise from the developed pulsed combustors was carried out. The details of instrumentation and experimental techniques employed for theses tests were given in Chapter 3. Before starting up the combustors the background noise was measured. First the background noise emitted from the ventilation systems and other equipment such as analysers was measured, indicating a noise level of around 56 dBA. Then the background noise level was measured when the booster pump was started, recording a noise level of around 70 dBA with the pump used for 15 and 30 kW combustors and 64 dBA from the smaller gas booster pump which was employed for the 7.5 kW combustor. These noise values also included all background noise mentioned above. Once the total amount of background noise was established, then noise measurements at constant configuration and input fuel gas rate from each pulsed combustor were carried out. These measurements revealed that at three points the noise level generated from each combustor was highest:

i) at the air inlet,

ii) above the combustion chamber and

iii) at the outlet to atmosphere of the exhaust gases.

The measured values at these three points are given in tables 7.1 to 7.3 (the third column from left). The given values have been corrected by subtracting the background noise from the total measured noise (see Appendix VIII).

Clearly the contribution of noise generated from the flue gas outlet to the overall noise of the combustors was greater than those emitted from either the combustion chamber or air inlet system. The results indicate that the noise emitted from the exhaust outlet was some 17 dBA higher than the noise generated at the combustion chamber and 7 dBA higher than noise emitted at the air inlet.

But the highest noise level was expected from the combustion chamber rather than the other points. This is because:

a) it contained flapper valve,

b) the pressure fluctuations were greater.

It has been reported that valveless combustors have lower noise levels (around 3-8 dBA) than those with flapper valve(s) [Ohiwa and Yamaguchi, 1989]. This may be because it is the only moving part in this type of combustor. In addition, combustion takes place inside the combustion chamber where the temperature of gases and maximum pulsing pressure are at their highest. It is well established that there is a close relation between pressure fluctuation and noise emission level; that is higher pressure oscillations result in higher noise levels [Saito *et al.* 1986]. Therefore, in view of the above, the noise emitted from the combustion chamber should be higher than at the other two points. But as seen from the results this was not the case. This was because each pulsed combustor had the combustion chamber fully immersed in a water bath; water acted as an attenuating medium reducing the external noise level. This was in addition to reduction of noise as a result of thick fabrication of the combustion chamber.

Location	Silencing Component	Noise Level before Silencing Component /dB(A)	Noise Level after Silencing component /dB(A)
At The Air Inlet to the Mixer Head	Pipe Elbow	78.4	77.2
	Expansion Chamber and Elbow	78.4	71.8
Above Combustion Chamber	None	70.0	70.0
At the Exhaust Outlet	Exhaust Silencer Chamber	86.0	67.0
Overall Noise Level at 1 metre from Middle of the Pulsed Unit	With all the above Silencers	79.5	64.1

Table 7.1 ***Overall noise levels emitted from the nominally 7.5 kW combustor measured before and after silencing. Tailpipe length used was 2000 mm with outside diameter of 12 mm. The combustion chamber volume was 110 ml, burning fuel gas rate of 167 ml s^{-1}.***

Location	Silencing Component	Noise Level before Silencing Component /dB(A)	Noise Level after Silencing Component /dB(A)
Above Air Inlet	Pipe Elbow	82.0	80.0
	Expansion Chamber and Elbow	82.0	76.0
Above Combustion Chamber	None	74.7	74.7
Above Exhaust Outlet	Exhaust Silencer Chamber	91.0	78.4
Overall Noise Level at 1 metre from Middle of the Pulsed Unit	With all the above Silencers	81.0	72.0

Table 7.2 ***Overall noise levels emitted from the nominally 15 kW pulsed unit before and after silencing. The used tailpipe had length of 2000 mm and diameter of 15 mm. The used combustion chamber volume was 370 ml and gas input rate was at 333 ml s^{-1} .***

Location	Silencing component	Noise Level before Silencing Component /dB(A)	Noise Level after Silencing Component /dB(A)
Above Air Inlet	Pipe Elbow	88.0	85.8
	Expansion Chamber and Elbow	88.0	78.4
Above the Combustion Chamber	None	78.4	78.4
Above Exhaust Outlet	Exhaust Silencer Chamber	94.9	81.7
Overall Noise Level At 1 metre from the Middle of the Pulsed Burner	With all the above Silencers	89.0	76.0

Table 7.3 ***Overall noise levels from the nominally 30 kW pulsed combustor measured before and after silencing. The length of Tailpipe employed was 2000 mm with outside diameter of 22 mm. Combustion chamber volume employed was 1270 ml with input gas rate of 722 ml s^{-1}.***

7.3 Noise Control

Noise control methods usually fall into three categories [Warring, 1974]:

I) use of protective measures at the receiver,

ii) reduction of noise at the source,

iii) use of a suppressor in the noise transmission path.

In this study only the use of a suppressor in the noise transmission path was considered. It is apparent that if more than one noise suppressor is used the attenuation provided by each method cannot be added arithmetically. Instead, all suppressors must be treated as a single integrated unit, a procedure that requires very tedious calculations [Alebon *et al.*, 1963]. Here complex calculations were avoided by using proper noise measuring equipment in conjunction with preliminary noise control design. This technique has been found to be easier and more economic because it has been shown that simple modifications to preliminary design result in fairly acceptable sound levels from a pulsed combustor [Vishwanath, 1984].

7.3.1 Directional Change

It is reported that bends in air ducts act as low pass filters by reflecting high frequency sound waves [Alebon *et al.*, 1963]. Since, at low frequencies there is no wave reflection, no attenuation is possible [Harris, 1957]. In the present design of nominally 7.5, 15 and 30 kW pulsed systems 15, 22, and 28 mm x 90° standard pipe elbows were located respectively at the air inlet to the mixer head to control high frequency sound emissions. Direct noise measurements at this point showed that the use of elbow reduced the overall sound levels by an average of 2 dB A in each case. The measured values are presented in tables 7.1 to 7.3.

7.3.2 Acoustic Filters

Acoustic filters or mufflers are normally used when sound transmission through a gas

or air transport line is excessive. In simple terms, sound suppression in mufflers is obtained by correctly designed discontinuities such as expansion and constriction that reflect sound energy back to the source. But it is important that the mufflers are designed such that the pressure fluctuations present at the exhaust exit are attenuated without significant effect upon the pulsations present in the combustion chamber or tailpipe [Vishwanath, 1985]. This is because, pulsing pressure in this type of combustor is related to combustion intensity, the successful operation of the pulsed unit and noise level. Therefore, any noise reduction technique which results in reduction of the pressure amplitude would consequently have an adverse effect on these parameters.

Figure 7.1 shows the variation of measured overall noise with heat input per unit combustion chamber volume for the three 7.5 (Fig. 7.1a), 15 (7.1b) and 30 kW (7.1c) combustors. These graphs clearly indicate the dependence of noise of pulsed combustors on the firing rate; noise level increased as the heat input was increased. It can also be deduced that combustion intensity was related to excess air ratio in these self-aspirating combustors. Hence, there should be a trade-off point concerning the combustion intensity and noise reduction.

Tests have shown that the acoustical filters which consist of an acoustic system designed to generate a pressure wave at the tailpipe exit which is out of phase with combustion wave have effective influence on silencing the systems [Hargrave *et al.*, 1986]. But such a system also eliminates the acoustical oscillations through the acoustical system of the tailpipe, thereby halting the operation of the combustor [Hargrave *et al.*, 1986]. However, the use of suitable expansion chambers (with respect to what is described above) have been shown to be effective in silencing the combustion devices. These expansion chambers or decouplers are essentially employed to decouple the pressure pulsations in the combustion chamber and tailpipe from the inlet and exit ducts. In this investigation this has been incorporated using a simple expansion chamber at the air inlet. The nominally 7.5, 15 and 30 kW pulsed combustors were fitted with cylindrical air inlet expansion chambers having volumes of 550, 1300 and 1800 ml respectively which not only reduced the noise level (up to 5 dBA) but also resulted in more stable operation of the pulsed combustors. Later, significant reduction of noise

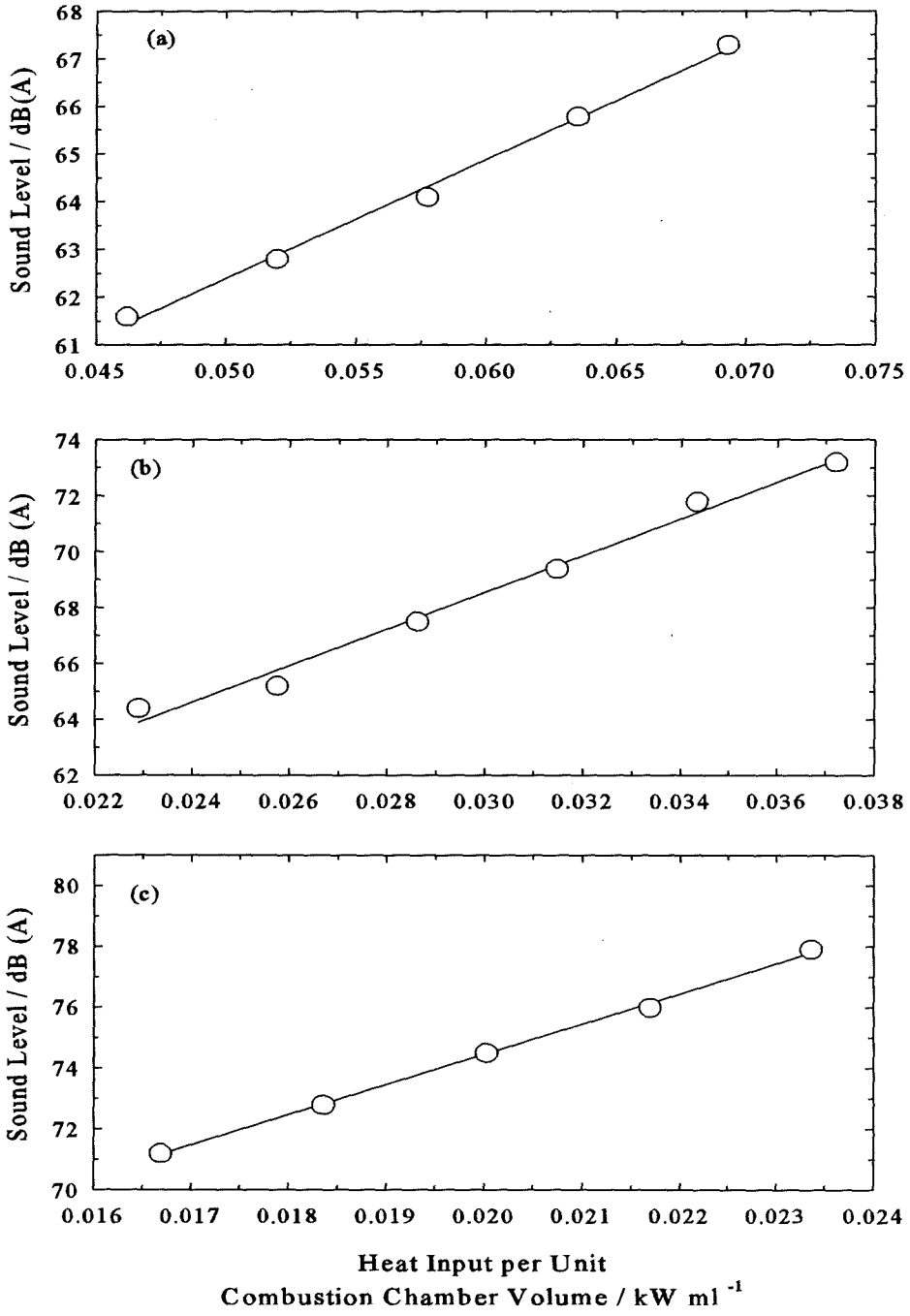

***Fig. 7.1** Variation of sound level with heat release per unit combustion chamber volume for a) the nominally 7.5 kW combustor with combustion chamber volume (CCV) of 110 ml, b) the 15 kW combustor using CCV of 370 ml and c) the 30 kW combustor using CCV of 1270 ml. The tailpipe length employed for the three combustors was 2000 mm. Flapper valve thickness used was 0.15 mm for each combustor.*

level was achieved by employing a well-baffled multi-hole motor car-type silencer at the exit of tailpipe. The exhaust decoupler had a volume of 6000 ml which as is shown below resulted in reduction of high frequency noise generated by the high velocity gases. Noise measurements showed that the use of these expansion chambers together with the directional change technique can reduce the overall noise levels of the pulsed units by up to 15 dBA.

Figures 7.2 and 7.3 show the typical frequency spectra of the pulsed combustors when the combustor was run without (Fig.7.2) and with exhaust silencer (Fig.7.3). The sound pressure levels are the root mean square (RMS) values of the pressure wave amplitude, enabling a steady reading to be registered for the rapidly fluctuating pressure. The figures show a number of discrete peaks in the low frequency range and the rest is of a broad-band type. The peaks are the family of harmonics with fundamental frequency of around 50 Hz which was in fact the basic operating frequency of the combustor.

Comparing the two figures it is clear that the use of a silencer was mainly effective at higher frequencies. This was as expected since it is known that there is no wave reflection at lower frequencies and hence no noise attenuation. Interestingly, when using the silencer the peak at the fundamental frequency was greater. This may have been due to the larger diameter of the vent pipe incorporated with the silencer which was three times greater than the diameter of the tailpipe used.

7.4 Effect of Combustion Chamber Volume

A series of tests was conducted measuring sound levels of the three developed combustors at various combustion chamber volumes (CCV) using fixed tailpipe dimensions. The results obtained are illustrated in Fig. 7.4. It can be seen that the sound emission levels increased as the combustion chamber volume decreased.

From Fig 7.1 it was noted that an increase of combustion intensity increased the operating noise level. It is apparent that decrease in combustion chamber volume increased the combustion intensity for a given fixed heat input and hence, the observed

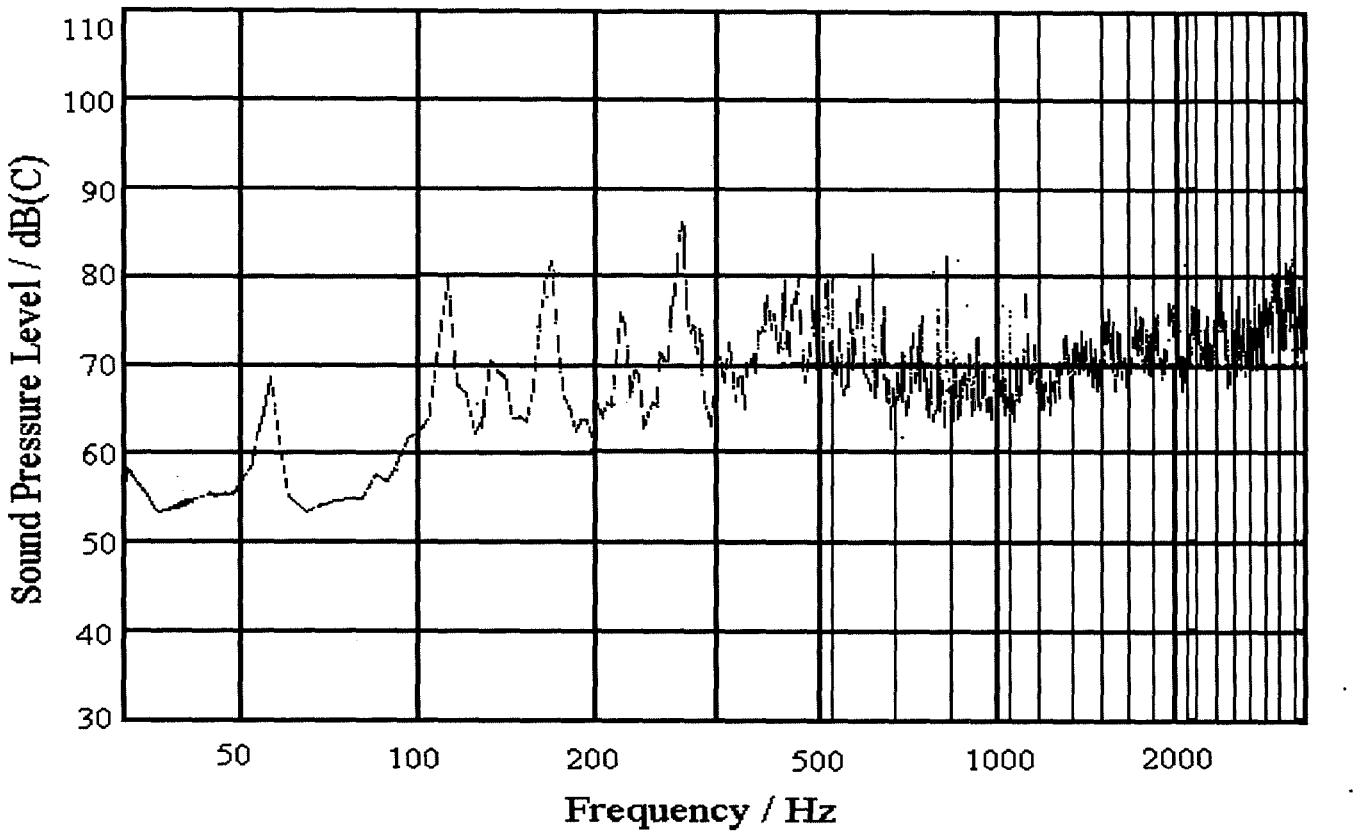

Fig. 7.2 ***A typical frequency spectrum for the developed pulsed combustors. The spectrum refers to the nominally 15 kW combustor without use of exhaust silencer. The tailpipe of 1500 mm and combustion chamber volume of 360 ml was used. The input firing rate was 250 ml s^{-1}.***

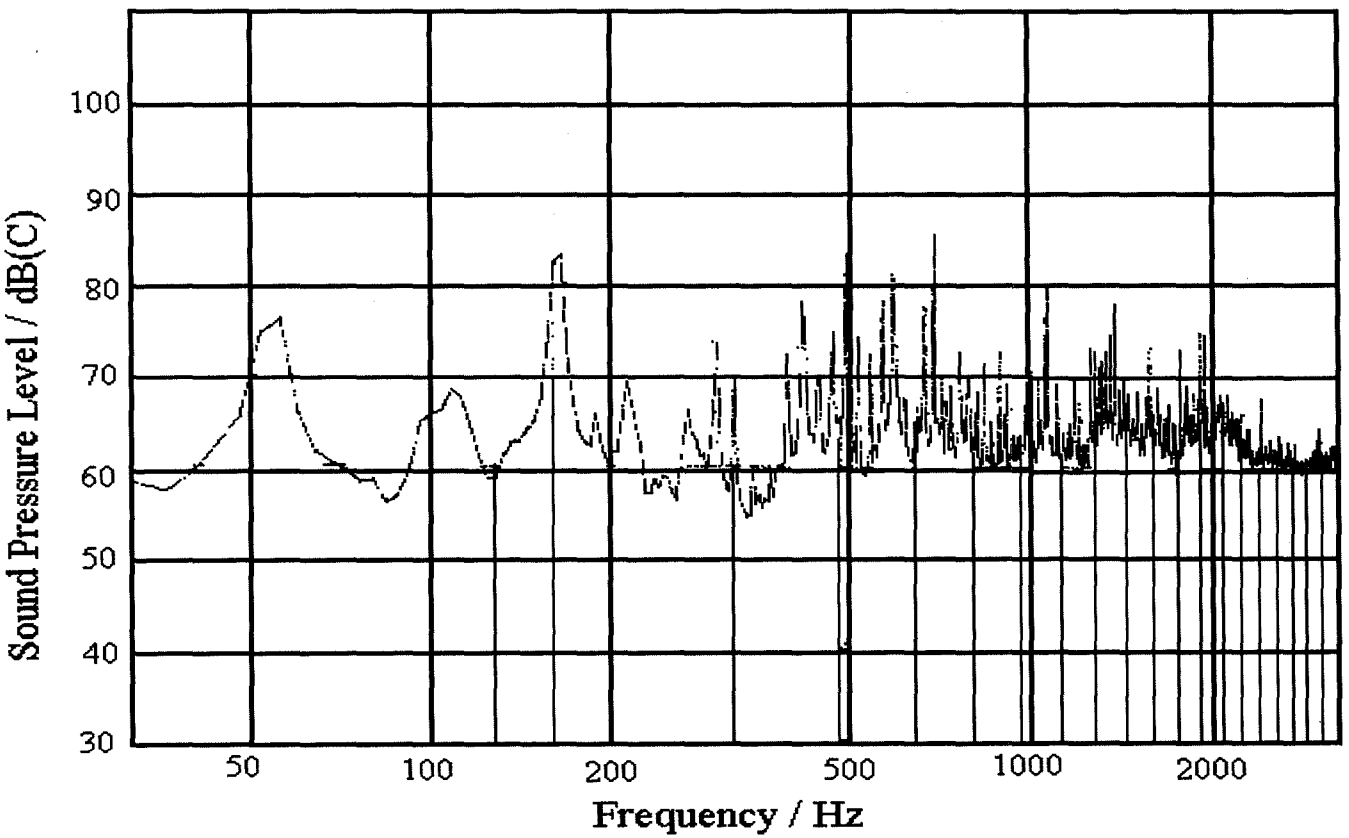

Fig. 7.3 ***A typical frequency spectrum for the developed pulsed combustors. The spectrum refers to the silenced nominally 15 kW combustor using exhaust silencer at the exhaust exit. The tailpipe of 1500 mm and combustion chamber volume of 360 ml was used with an input fuel gas rate of 250 ml s^{-1}.***

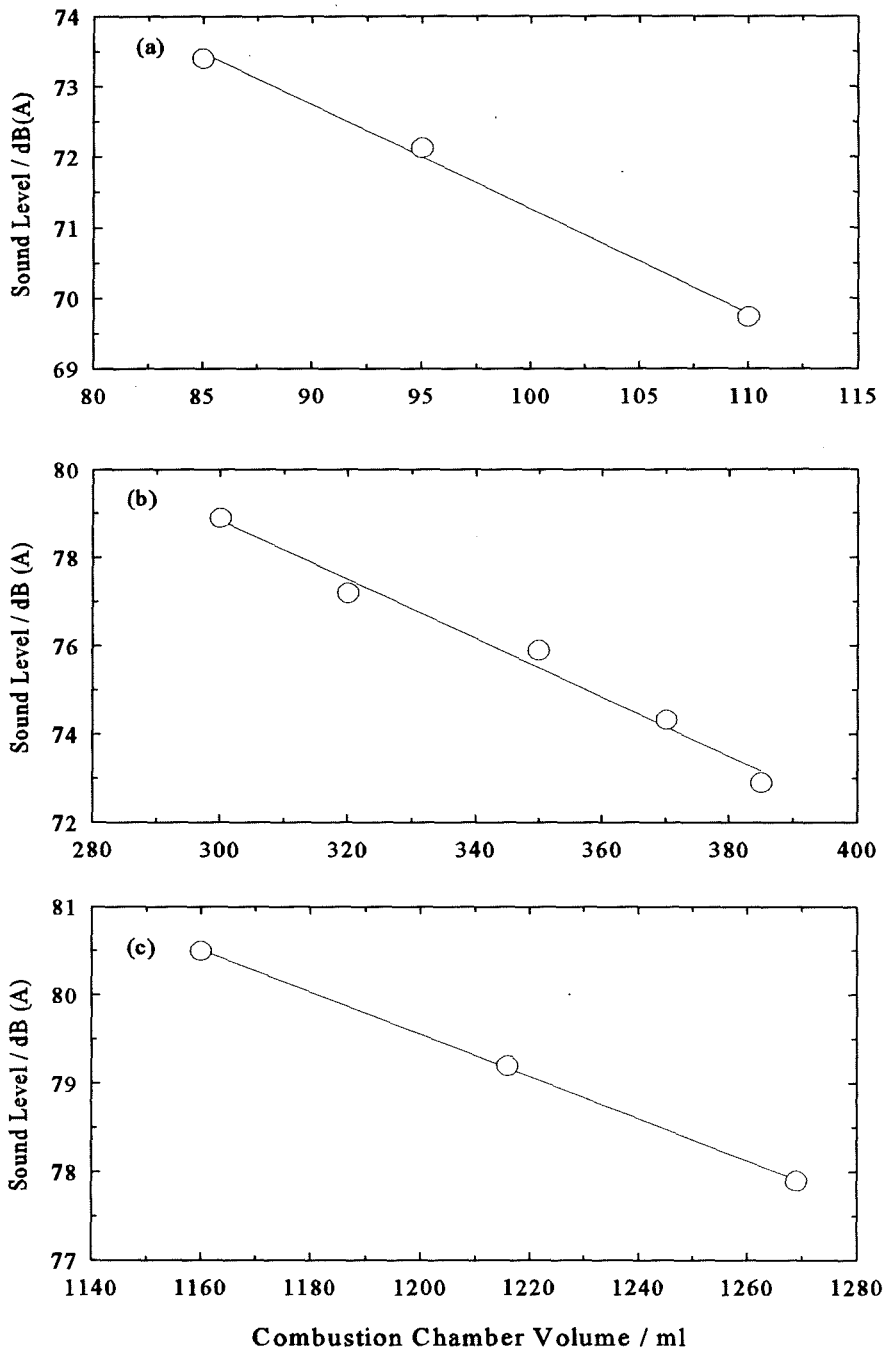

***Fig. 7.4** Variation of noise level with combustion chamber volume for a) the 7.5 kW combustor with tailpipe length of 1500 mm and diameter of 12 mm, b) the 15 kW combustor with tailpipe length of 1500 mm and diameter of 15 mm and c) the 30 kW combustor with tailpipe of 2000 mm and diameter of 22 mm. The combustors were operated at firing rates of 200, 361 and 778 ml s^{-1} respectively.*

increase of noise with smaller combustion chamber volume. Increase in combustion intensity resulted in an increase in magnitude of pressure oscillations and hence high noise level.

7.5 Influence of Tailpipe Length

The study on influence of configuration upon noise emission levels was taken a step further by direct measurements of overall noise from the nominally 7.5 and 15 kW combustors using various tailpipe lengths at constant CCV. The tailpipe used in the present design of pulsed combustors was a simple copper tube acting as a resonator. Thus, it was expected to induce transmission loss providing its effective length was equal to one quarter of a wavelength. The results of the noise measurements from the combustors as a function of tailpipe length is shown in Fig.7.5 where the tailpipe length was varied from 1500 to 2500 mm. The obtained results indicated that lengthening the tailpipe reduced the overall noise level of the combustor. This was as expected because increasing tailpipe length raised the fluid resistance resulting in greater friction loss. Thus, the pressure of pulsing decreased which may have lowered the noise level. This is also expected to be the case when the tailpipe diameter is smaller. The 30 kW combustor had the largest tailpipe diameter (i.e. 22 mm) compared to the other two combustors. Despite having a larger combustion chamber volume it displayed a higher noise level compared with the other two developed combustors.

7.6 Summary and Conclusions

Noise measurement from the three developed pulsed combustors were carried out. The results showed that the noise level increased as the firing rate at constant configuration increased.

At fixed gas input rate noise levels were increased as the combustion chamber volume and the tailpipe length were decreased. The decrease in noise level with

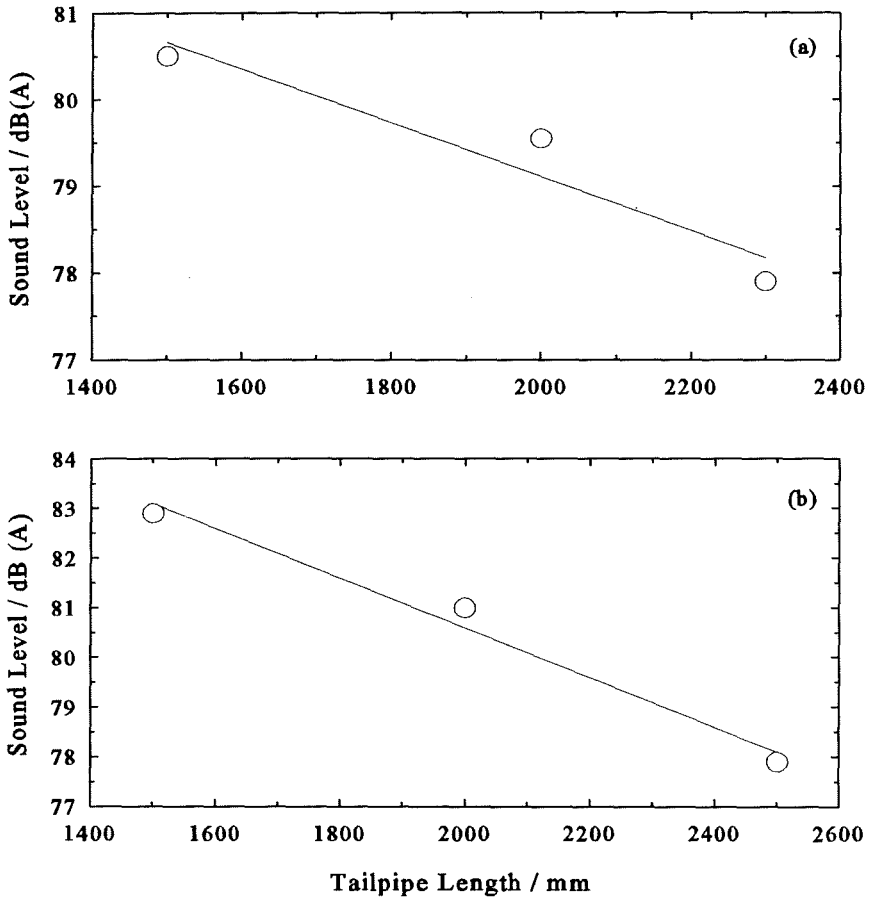

Fig. 7.5 Influence of tailpipe length on noise emission level from a) the 7.5 kW combustor with gas input rate of 167 ml s^{-1} and b) the 15 kW combustor using gas input rate of 333 ml s^{-1}. The combustion chamber volumes of the combustors were 110 ml and 370 ml respectively and the noise measurements refer to unsilenced values.

increased CCV was associated with decreased combustion intensity and magnitude of pressure fluctuations. The reduction of noise resulting from lengthening the tailpipe was due to the fact that the tailpipe acted as a resonator, in addition to increased friction losses and fluid resistance.

The application of noise control methods, including use of expansion chambers at the air inlet and the exhaust gases exit, resulted in reduction of the noise levels from the three combustors to a tolerable level of a minimum of around 65 dBA.

Chapter Eight

Conclusions and Future Work

8.1 Introduction

The contributions of this study can be categorized into three parts:

i) design and development,

ii) operational characteristics and stability,

iii) emissions of pollutant gases.

Measurements on the developed pulsed combustors took account of as many parameters as possible to obtain a clear picture of the factors influencing the operation of the developed pulsed combustors. The information obtained from this systematic study of performance of the designed pulsed combustors is a step forward towards better engineering and use of pulsed combustors as heating devices and provides valuable feedback for theoretical models.

8.2 Design and Development of the Pulsed combustors

Two pulsed combustors of nominally 15 and 30 kW input with cylindrical components were designed and developed. The combustors were of Helmholtz-type, operating in a premixed mode. The flow of the mixture of air and gas was controlled mechanically with the aid of a flapper valve. The basic elements of the pulsed combustors were considered to be the mixer head, combustion chamber and tailpipe and since the operating functions were interrelated, the other components and their dimensions developed in relation to these basic elements. Consequently, the design evolved by trial and error and from empirical correlations. The design of the developed combustors was based upon the existing 7.5 kW combustor which was also developed previously at Middlesex University. Tests showed that complete combustion occurred within the combustion chamber. Thus, it was considered to be the main component for scaling the

combustors. By a trial and error procedure it was found that the required input rates could be achieved by scaling up or down each combustion chamber dimensions linearly by a factor of 1.5, while maintaining the geometry identical. Initial tests showed that the developed combustors could operate successfully at various configurations and fuel gas input rates yielding overall thermal efficiency in excess of 90 % after silencing. However, there were limits of operation in terms of configuration and heat input. The maximum obtainable turn-down ratio was 1.8:1 when burning mains natural gas.

The three developed premixed pulsed combustors generally operated lean although, at certain operating conditions the 30 kW combustor ran with a fuel-rich mixture. Tests showed that each combustor operated with higher excess air compared to the next larger combustor. The 7.5 kW operated with a minimum of 20% excess air whereas the 15 and 30 kW could operate near to the stoichiometric condition.

8.3 Operating Characteristics and Stability

The stability of the developed combustors was systematically studied in terms of their operating frequency and pulsing pressure. The results confirmed that the developed pulsed systems behaved as Helmholtz resonators and that the frequency was a fundamental parameter in these acoustical devices. Measurements showed that the frequency with which the process occurred was controlled by the configuration of the combustor and the temperature within the combustion chamber. The operating frequency of the three combustors increased as the combustion chamber volume, tailpipe length and flapper valve thickness were reduced.

From the obtained frequency data, including those measured during the combustion of natural gas with added nitrogen, it was concluded that stable operation of the pulsed combustor dependent upon the existence of a delay time between admission of the mixture of air and gas into the combustion chamber and the occurrence of combustion. Peak pulsing pressure and operating frequency of the pulsed units were influenced by N_2 injection. The decrease in frequency resulting from N_2 injection was attributed to ignition delay as a consequence of slower combustion kinetics due to the reduction in

concentration of oxygen. The increase of peak pulsing pressure with N_2 injection was explained as resulting from increased heat release per cycle. The effect of heat release per cycle upon peak pulsing pressure became clearer when tests showed that all measured peak pulsing pressure data including that for addition of air, various nitrogen injection rates and a range of flapper valve thickness fall on a single line through the origin when plotted against fuel gas rate divided by operating frequency. Thus, in general it was concluded that the magnitude of peak pulsing pressure was a strong function of heat release per cycle.

8.4 Combustion Products

Tests evaluating the influence of excess air ratio, λ (i.e. the actual A/F divided by the stoichiometric A/F), on the combustion of mains natural gas indicated that temperature in the combustion chamber varied with mixture strength. Measured temperature of the exhaust gases at the exit of the combustion chamber (i.e. sampling point 1), increased as air-to-fuel (A/F) decreased. Analysis of temperature data indicated that any influence of configuration upon temperature was primarily from consequent change of A/F in the present design of pulsed combustors.

Operation of the three combustors on mains natural gas at various fuel gas flow rates, combustion chamber volumes and tailpipe length resulted in NO_x emissions which all fell on a single curve when plotted vs excess air ratio, λ. The scale and configuration of the developed combustors, i.e. 7.5, 15 or 15 kW, had no influence upon NO_x emission except in so far as it modified temperature within combustion chamber.

Injection of nitrogen or argon into the system resulted in reduced NO_x emissions at a given A/F; the effect was progressive with increasing rate of injection of either diluent.

A plot of NO_x emission vs calculated adiabatic flame temperature showed that all the points obtained for all the operating conditions employed followed a single curve. This representation eliminated variations due to rate of nitrogen or argon injection or configuration of the combustors showing that maximum flame temperature was the dominant factor controlling NO_x formation in these pulsed combustion systems. Further

analysis of data showed that the average measured NO_x at the end of tailpipe was an exponential function of temperature. Moreover, combustors generally operated lean premixed with high combustion temperatures. Therefore, it is concluded that the NO_x production in this type of combustors was principally controlled by a thermally activated process (Zeldovich mechanism).

Almost all the NO_x values recorded in this study were in the form of NO which was attributed to the high flame temperature (i.e. typically above 1850 K) associated with the combustors. Only under certain operating conditions of the nominally 7.5 kW combustor was a concentration of NO_2 observed. At low fuel gas flow rate together with the smallest combustion chamber volume, the 7.5 kW combustor had the highest excess air which lead to the lowest flame temperature resulting in formation of NO_2.

Carbon monoxide (CO) emissions showed the typical U-shaped curve, with high values near to the stoichiometric condition and at high levels of excess air. This was found to be as a result of three factors; a) low flame temperature observed at high values of excess air b) imperfect mixing of air and gas the effect of which was most pronounced at near to the stoichiometric condition and c) quenching of flame at the walls of the combustion chamber. The last influence became quite clear when the combustion products were measured at various water bath temperatures (WBT). Water bath temperature influenced gaseous emissions, particularly CO, substantially when operated at high λ values (>1.15). The dependence of CO emission on WBT decreased as λ decreased, tending to show little dependence for $\lambda < 1.1$. This behaviour at higher values of λ indicated that quenching on the walls of the combustor was an important factor in the generation of CO. From the results obtained it was concluded that the emission of CO at low λ values resulted principally from incomplete mixing of the air and fuel gas.

Measurements of CO vs λ, when combustion chamber volume (CCV) was maintained constant while tailpipe length was varied, followed a separate single line for each nominal combustor; with CO values being highest for the smallest appliance. However, when the tailpipe was kept fixed and the CCV varied then CO vs λ followed a separate line for each CCV, with CO values generally increasing as the CCV was

decreased. This thought to be due to localised variation of mixture strength and hence temperature with change in CCV for a given A/F. Measurements of CO_2 at two sampling points indicated that the combustion did not continue in the tailpipe. Thus as mentioned in above, there was a little influence of tailpipe length upon CO emission for a fixed CCV and λ value.

8.4.1 Fuel Gas Composition

In order to evaluate the effect of changes in fuel gas composition the developed 15 kW pulsed performance was investigated burning gases which represent limiting composition of gas which could be distributed to customers. In this study the test gases NGB, NGC and NGD were used which had similar composition and flame stability to the standard test gases, G21, G222 and G23 of the second family group H of test gases respectively. In this way the susceptibility of the developed combustors to incomplete combustion, light back and flame lift was tested. The developed 15 kW combustor operated successfully burning all the above test gases using the same configuration as for burning mains natural gas. The trend of measured combustion products at the outlet of the tailpipe was similar for all the test gases used. Analysis of these measurements indicated the influence of flame temperature upon emissions of NO_x and CO.

8.5 Noise

The overall noise generated from the developed pulsed combustors was subjectively rated as objectionable. However, by utilization of noise control techniques the noise level was reduced to the tolerable level of a minimum of 65 dBA. Tests showed that the main noise sources were the air inlet and exhaust outlet. Thus, by employment of expansion chambers at these two points, noise level was reduced by up to 20 dBA for each combustor. Frequency analysis of the noise spectrum showed that the use of an expansion chamber reduced only the high frequency noise with no effect on low

frequency noise.

Analysis of noise measurement at various configurations and heat input confirmed the direct relation of emitted noise level with pressure fluctuations of each combustor.

8.6 Recommendation for Future Work

In this study due to limitations in diagnostics, conventional experimental measuring techniques were employed. These conventional methods, without a doubt, provide valuable qualitative and quantitative information. But in order to develop theoretical modelling and create greater understanding of the processes involved and how they should be controlled, other advanced experimental techniques such as Laser Doppler Velocimetry (LDV), Coherent Anti-Stokes Raman Scattering (CARS), various type of high speed shadowgraphy of the combustion cycle, chemiluminescence and Schlieren images of the flows are required. Such advanced experimental methods provide quantified information on time and space resolved velocities and temperature and the phase relationship between different periodic properties which then leads to better determination of the processes occurring in the combustion chamber. Having said that the studies undertaken as such have shown that these methods also have their limitation. For instance, laser techniques such as Schlieren photography are useful in symmetrical flows, for following the high temperature interface between unburnt reactants and the burned combustion products in the flame, but provide little direct information on the combustion chemistry and hence the possible coupling between chemistry and fluid motion. Furthermore, the spatial resolution of Schlieren visualization is limited in highly turbulent flows.

Further insight might be obtained by determining the phase angle between the heat release and pressure oscillations. Such measurements have been reported by using an optical system comprising an appropriate narrow bandpass optical filter and photomultiplier permitting to monitor the emissions of CH, C_2 and OH radicals. The intensities of such emissions are indicative of the rate of heat release during combustion process [Jones and Leng, 1994]. From measurements of pulsing pressure and rate of

heat release, it is possible to determine the phase angle between the two oscillations.

In this study CO was generally observed at higher levels than the reported values elsewhere. Although this study pinpointed the parameters that attributed to such high CO levels and generally these measured values of CO were below the British standards requirements for clean combustion, further investigation is required to reduce the CO levels to ultra-clean combustion levels. One of the options to be considered is the improvement of mixing of the air and fuel gas prior to combustion. This could be achieved by variation in configuration of the mixer head allowing better mixing of air and gas before entering the combustion chamber. Imperfect mixing of fuel gas and air can also be a contributing factor to the emission of NO_x.

Because of a limited supply of test gases, systematic stability tests including operating frequency and pulsing pressure could not be carried out. This study indicated that such measurements and data analysis provided great insight on the operating condition of the pulsed combustors. Thus, it is recommended that systematic measurements of frequency and pulsing pressure burning test gases G21, G222 and G23 be carried out. This study clearly demonstrated the effect of configuration of pulsed combustors upon emission of combustion products operating frequency and peak pulsing pressure. However, parameters such as the effect of gas orifice size, vent pipe length and longer tailpipes were omitted. These parameters may influence the pumping capacity and operational stability of the pulsed combustors and required further investigations.

References

Adams C.W., (1982) "Performance Results of the Lennox Pulse Combustion Furnace Field Trials", *Proceedings of the International Symposium on Pulse Combustion Applications*, Atlanta, Georgia, USA, pp. 18-1 to 18-12, March 2-3, 1982.

Ahrens F.W., (1979) "Prediction of Heat Transfer in Pulse Combustion Burners", *Proceedings of the International Symposium on Pulse combustion Technology for Heating Applications*, ANL/EES-TM-87, Argonne, Illinois, pp. 46-66, November 1979.

Alebon J., Lee K., and Geller L.B., (1963) "A Pulsating Combustion System for Space Heating", *Proceedings of the Boyar Conference*, Montreal University, Canada, pp. 61-75, May 1963.

Allen J., (1990) "Low NO_x Burner Systems", *Energy World Publication*, pp. 13-15, November 1990.

Anderson J.S. and Anderson M.B., (1993) "Noise: its Measurements, Analysis, Rating and Control", *Avebury Technical, Ashgate Publishing Ltd*, Aldershot, Hants, England, UK, pp. 70-78, 1993.

Arai N., 1994, "Emissions of Nitric Oxide from Stationary Combustion Sources" *Journal of the Institute of Energy*, Vol. 67, pp. 61-69, June, 1994.

AU-Yeung H.W., Garner C.P., Hanby V.I., (1998) "An Experimental Study of the Effects of Combustion Frequency and Pressure Amplitude on the NO Emissions from Pulse Combustors", *Journal of The Institute of Energy,* Vol. 71, pp. 204-208, December 1988.

AU-Yeung H.W., Garner C.P., Hanby V.I., (1999) "Modelling the Effects of Combustion Frequency and Pressure Amplitude on NO Formation in a Gas-Fired Pulse Combustor", *Journal of The Institute of Energy,* Vol. 72, pp. 70-76, September 1999.

Babkin Yu. L., (1965) "Pulsating Combustion as Furnaces for Steam Boilers", *Thermal Engineering*, Vol. 12, pp. 23-27, 1965.

Bagwell F.A., Rosenthal K.E., Breen B.P., Bayard de volo N. and Bell A.W., (1970) "Oxides of Nitrogen Emission Reduction", *Proceedings of the 32 American Power Conference*, Institute of Technology, Illinios, Chicago, USA, pp. 227-236, April 1970.

Barr P.K., Dwyer H.A. and Bramlette T.T., (1987) "A One Dimensional Model of a Pulsed Combustor", *Sandia Report No. SAN D86-8864,* Sandia National Laboratories, Livermore, USA, 1987.

Barr P.K. and Keller J.O., (1991) "Pulse Combustion Importance of Flame Extinction by Fluid Dynamics Strain", *Proceedings of the International Symposium on Pulsating Combustion*, Monterey, CA, USA, Paper D-5, August 1991.

Baulch D.L., Drysdall D.D., Horne D.G. and Lloyd A.C., (1973) "Evaluated Kinetic Data for High Temperature Reactions", *Butterworth & Co. (Publishers)*, London, UK, Vol. 2, pp. 23, 1973.

Belles F.E., Vishwanath P.S. and Ives J.E., (1982) "Sound Characteristics of a Family of Pulse Burners at Various Heat Release Rate", *Proceedings of the International Symposium on Pulsed Combustion Applications*, Atlanta, Georgia, USA, pp. 21-1 to 21-7, March 2-3, 1982.

Belles F.E, (1986) "Pulse Combustion Design Research", *Report on Contract No. GRI-5086-260-1271*, Gas Research Institute, Chicago, IL, USA, pp. 1-7, December 1986.

Belles F.E., (1988) "Correlation of Boiling Water Heat Transfer Data for a Family of Pulse Combustors", *Proceedings of 12 Annual Symposium on Fossil Fuels Combustion*, The American Society of Mechanical Engineers (ASME), pp. 43-48, April 1988.

Bhaduri C.B., Baxi C.B., Gill B.S. and Mukhopadhyay N., (1968) "A Theoretical Study of Pulsating Combustion", *Indian Journal of Technology*, Vol. 6, pp. 245-248, 1968.

Blomquist C.A., Clinch J.M. and Chiu H.H., (1982) "Operational and Heat Transfer Results from an Experimental Pulse Combustion Burner", *Proceedings of the International Symposium on Pulse Combustion Applications*, Atlanta, Georgia, USA, pp. 1-1 to 1-20, March 2-3, 1982.

Bollin B., Doos, B.R., Jager J. and Worrick R.A., (1986) "The Green House Effect: Climate Change and Ecosystems", *Published by John Wiley and Sons*, pp. 529, 1986.

Bowman C.T., (1992) "Control of Combustion Generated Nitrogen Oxides Emissions: Technology Driven by Regulation", *Proceedings of the Twenty Fourth Symposium (International) on Combustion*, Combustion Institute, Pittsburgh, PA, USA, pp. 859-878, July 1992.

Briffa F.E.J. and Staddon P.W., (1982) "An Application of Fluid-Logic Technique to Pulsed Combustion", *Proceedings of the International Symposium on Pulse Combustion Applications*, Atlanta, Georgia, USA, pp. 12-1 to 12-18, March 2-3, 1982.

British Standards Institute, (1986) "Specification for Safety of Domestic Gas Applications", *BS 5258*, BSI, London, pp. 1-6, 1986.

British Standards Institute, (1992) "Thermocouple Materials and Their Characteristics", *BS 1041, Part 4,* BSI, London, pp. 6-8, 1992.

British Standards Institute, (1993) "Recent Gas Analysis Instruments", *BS 3048*, BSI, London, pp. 63-66, August 1993.

British Standards Institute, (1993) "Clarification of Test Gases", *BS EN 437*, BSI, London, pp. 3-7, 1993.

Carvalho J.A., Wang M.R., Miller N., Daniel B.R. and Zinn B.T., (1984) "Controlling Mechanism and Performance of Cool Burning Rijke Type Pulsating Combustors", *Twentieth Symposium (International) on Combustion*, The Combustion Institute, Pittsburgh, PA, USA, pp. 2011-2017, 1984.

Cheng X.C., Daniel BR., Jagoda J.I. and Zinn B.T., (1988) "Dependence of Pulse Combustor Frequency upon Combustion Process" *Journal of American Society of Mechanical Engineers (ASME)*, Vol. 25, pp. 39-42, 1988.

Chiu H.H., Clinch J.M., Blomquist C.A. and Croke E.J., (1981)"Pulse Combustion Noise: Problems and Solutions", *Proceedings of 1981 International Gas Research Conference*, Los Angeles, USA, pp. 1530-1539.

Clark P.H. and Craigen J.G., (1976) "Mathematical Model of a Pulsating Combustor", *Proceedings of the Sixth Thermodynamics and Fluid Mechanics Convention*, Durham, UK, pp. 221-228, 1976.

Coe W.W., (1980) "Combustion: Efficiency vs NO_x", *Selections from API, NPRA and GPA Meetings, Hydrocarbon processing*, Houston, USA, pp. 130-134, May 1980.

Cowgill U.M., (1989) " Acid Precipitation: A Review "; *Environmental Problems and Solutions (Veziroglu T. N, Ed.),* Hemisphere Publishing Corporation, London, pp. 111-117, 1989.

Corliss J.M., Putnam A.A., Murphy M.J. and Locklin D.W., (1984) "NO Emission from Several Pulse Combustors", *Presented at the 105th ASME Winter Annual Meeting*, New Orleans, USA, Paper No. 84-JPGC-APC-2, pp. 1-4, December 1984.

Corliss J.M., Creamer K.S. and George P.E., (1987) "Frequency and Time Domaine Effect on the Operation of Valved Pulsed Combustors" *Presented at Battelle-Columbus Laboratories Annual Meeting*, Fuels and Combustion Technologies Section, Columbus,

OH, USA, Paper No. NT-87-14-4, pp. 1632-1645, 1987.

Dandy D.S. and Barr K.P., (1991) "Model-Based Control Strategies for Pulse Combustion", *Proceedings of the International Symposium on Pulsating Combustion*, Monterey, CA, USA, Paper C-1, August 5-8, 1991.

Dec J.E. and Keller J.O., (1989) "Pulsed Combustor Tailpipe Heat Transfer Dependence on Frequency Amplitude and Mean Flow Rate", *Combustion and Flame,* Vol. 77, pp. 359-374, 1989.

Dhar B., Huang H.C.G., Lee J.H., Soedel W. and Schoenhals R.J., (1982) "Dynamic and Thermal Characteristics of a Pulsed Combustion Gas-Fired Water Heater", *Proceedings of the International Symposium on Pulse Combustion Applications*, Atlanta, Georgia, USA, pp. 4-1 to 4-27, March 2-3, 1982.

Edmonds J.A., Wuebbles D.L. and Scott M., (1989) " Energy and Radiative Precursor Emissions"; *Environmental Problems and Solutions (Veziroglu T. N, Ed.),* Hemisphere Publishing Corporation, London, pp. 353-354, 1989.

Etzkorn T., Muris S., Wolfrum J., Dembny C., Bockhorn H., Nelson P.F., Attia-Shahin A. and Warnatz J., (1992) "Destruction and Formation of NO in Low Pressure Stoichiometric CH_4/O_2 Flames", *Twenty Fourth Symposium (International) on Combustion*, The Combustion Institute, Pittsburgh, PA, USA, pp. 925-932, 1992.

Fenimore C.P., (1971) "Formation of Nitric Oxide" *Thirteenth Symposium (International) on Combustion*, The Combustion Institute, Pitsburgh, PA, USA, pp. 373, 1971.

Fenimore C.P., (1972), "Formation of Nitric Oxide from Fuel Nitrogen in Ethylone Flame" *Combustion and Flame*, Vol. 19, pp. 289-296, 1972.

Francis W.E., Hoggarth M.L. and Reay D., (1963) "A Study of Gas-Fired Pulsating Combustors for Industrial Applications", *I.G.E. Journal*, Vol. 3, pp. 301-320, 1963.

Fureby C. and Lundgren E., (1993) " One-Dimensional Models for Pulsating Combustion", *Journal of Combustion Science and Technology*, Vol. 94, pp. 337-351, 1993.

Gill B.S. and Bhaduri D., (1978) "Prediction of Pressure and Frequency in Helmholtz Pulsating Combustion Systems", *Indian Journal of Technology*, Vol. 16, pp. 171-176, May 1978.

Griffiths J.C. and Weber E.J., (1969) "The Design of Pulsed Combustion Burners", *Research Bulletin 107,* American Gas Association Laboratories, USA, pp. 21-40, May 1969.

Griffiths J.C., Connelly S.M. and DeRemer R.B., (1982) "Effect of Fuel Gas Composition on Appliance Performance" *Topical Report No. GRI-82/0037*, Gas Research Institute, Chicago, IL, USA, pp. 1-10, 1982.

Hanby V.I. and Brown D.J., (1968) "A 50 Ib/h Pulsating Combustor for Pulverized Coal", *Journal of the Institute of Fuel (now Energy)*, Vol. 41, pp. 423-426, November 1968.

Hanby V.I., (1969) "Convective Heat Transfer in a Gas-Fired Pulsating Combustor", *ASME, Journal of Eng. for Power*, Vol. 91, pp. 48-52, 1969.

Hanby V.I., (1971) "Basic Considerations on the Operation of a Simple Pulse Combustor", *Journal of the Institute of Fuel (now Energy)*, Vol. 44, pp. 595-598, November 1971.

Hanby V.I., (1979) "An Appraisal of Gas-Fired Pulse Combustors for Space Heating",

The Heating and Ventilating Engineer, pp. 6-8, February 1979.

Hanby V.I., (1993) "Combustion and Pollution Control in Heating Systems", *Published by Springer-Verlag Ltd.*, London, pp. 61-75 and 103-113, 1993.

Hanson R.K. and Salimian S., (1984) "Survey of Rate Constants in H/N/O Systems", *Combustion Chemistry*, (W.C. Gardiner Ed.), pp. 361, 1984.

Hargrave G.K., Kilham J.K., and William A., (1986) "Operating Characteristics and Convective Heat Transfer of a Natural Gas-Fired Pulsating Combustor", *Journal of the Institute of Energy*, pp. 63-69, June 1986.

Hargreaves K.J.A. and Smith D.B., (1976) "The Construction and Performance of a Low Pressure Chemiluminescent NO_x Analyser", *Project L164*, British Gas plc, UK, pp. 6-10, August 1976.

Hargreaves K.J.A., Harvey R., Roper F.G. and Smith D.B., (1981) "Formation of NO_2 by Laminar Flames", *Eighteenth Symposium (International) on Combustion*, The Combustion Institute, Pittsburgh, PA, USA, pp. 133-144, 1981.

Hargreaves K.J.A. and Patterson M.C., (1986) "Advance Combustion Systems for High Efficiency Domestic Appliances", *Proceedings of 1986 International Gas Research Conference*, Toronto, Canada, pp. 80-90.

Harris C.M., (1957) "Noise Control Hand Book", *Published by McGraw-Hill Book Co.*, Toronto, Canada, pp. 14-18, 1957.

Harris R.J., Nasralla M. and Williams A., (1976) "The Formation of Oxides of Nitrogen in High Temperature CH_4-O_2-N_2 Flames", *Journal of Combustion Science and Technology*, Vol. 14, pp. 85-94, 1976.

Harrison R.M., (1992) "Understanding our Environment: An Introduction to Environmental Chemistry and Pollution" *Published by The Royal Society of Chemistry*, Cambridge, UK, pp. 12-16, 1992.

Hayhurst A.N. and Vince I.M., (1983) " The Origin and Nature of Prompt Nitric Oxide in Flame", *Combustion and Flame*, Vol. 50, pp. 50-61, 1983.

Hollowell G.T., (1987) "Development of a Commercial Pulsed Combustion Water Heater", *Annual Report No. NT-14-1,* Gas Research Institute, Chicago, IL, USA, pp.1-50, November 1987.

Iverach D., Basden K.S. and Kirov N.Y., (1973) "Formation of Nitric Oxide in Fuel-lean and Fuel-Rich Flames", *Fourteenth Symposium (International) on Combustion*, The Combustion Institute, Pittsburgh, PA, USA, pp. 767, 1973.

Jasper G., Glennon E. and Ketteridge R.C., (1990) "Gas Service Technology", *Benn Technical Book, Published by Ernest Benn Ltd*, Croydon, UK, pp. 26-37, 1990.

Johnson S.A. and Rawdon A.H., (1977) "NO_x Control by Furnace Burner Design", *Power Technology Trends*, USA, Vol. 9, pp. 335-348, 1977.

Johnson G.M., Smith M.Y. and Mulcahy M.F.R., (1979) "Presence of NO//2 in premixed Flames", *Seventeenth Symposium (International) on Combustion*, Combustion Institute, Pittsburgh, PA, USA, pp. 647-660, 1979.

Jones H.R.N., (1989) "The Application of Combustion Principles to Domestic Gas Burner Design", *Published by E.& F.N. Spon Ltd. in Association with British Gas plc*, London, UK. pp. 7-15 and 106-118, 1989.

Jones H.R.N. and Leng J., (1994) "The Effect of Hydrogen and Propane Addition on the Operation of a Natural Gas-Fired Pulsed Combustor", *Combustion and Flame*, Vol.

99, pp. 404-412, 1994.

Jones H.R.N. and Leng J., (1996) " The Influence of Fuel Composition on Emissions of CO, NO and NO_2 from a Gas-Fired Pulsed Combustor", *Combustion and Flame*, Vol. 104, pp 419-430, 1996.

Kantrowits A., (1948) "Heat Engines Based on Wave Processes", *Annual Meeting Report,* The American Society of Mechanical Engineers (ASME), Anaheim, California, USA, pp. 25-29, June 1948.

Keller J.O, (1985) "The Dynamics of Injection, Mixing and Combustion in a Valved Pulse Combustor", *Fall Meeting of the Western State Section of the Combustion Institute,* Davice, California, USA, Paper WSS/C185-38, October 21-22, 1985.

Keller J.O. and Westbrook C.K., (1986) "Response of a Pulse Combustor to Changes in Fuel Composition", *Twenty-first Symposium (International) on Combustion*, The Combustion Institute, Pittsburgh, PA, USA, pp. 547, 1986.

Keller J.O., Bramlette T.T., Dec J.E. and Westbrook C.K., (1989) "The Importance of Characteristic Times", *Combustion and Flame*, Vol 75, pp. 33-44, 1989.

Keller J.O. and Hongo I., (1990) "Pulsed Combustion: the Mechanisms of NO_x Production", *Combustion and Flame,* Vol. 80, pp. 219-237, 1990.

Keller J.O., Bramlette T.T., Westbrook C.K. and Dec J.E., (1990) " Pulse Combustion: The Quantification of Characteristic Times" *Combustion and Flame*, Vol. 79, pp. 151-161, 1990.

Keller J.O., Bramlette T.T., Barr, P.K. and Alvarez J., (1994a) "NO_x and CO Emission from a Pulse Combustor Operating in a Lean Premixed Mode", *Combustion and Flame,* Vol. 99, pp. 460-466, 1994a.

Keller J.O., Barr P.K. and Gemmen R.S., (1994b) "Premixed Combustion in a Periodic Flow Field, Part I: Experimental Investigation", Combustion and Flame, Vol. 99, pp. 29-42, 1994b.

Kelly J., Woodworth R. and Grant C., (1991) "Reducing Gas-Fired Pulse Combustor NO_x Emissions", *Proceedings of the International Symposium on Pulsating Combustion*, Monterey, CA, USA, Paper B-7, August 5-8, 1991.

Kentfield J.A.C., (1971) "The Flow Rectifier, A Fluidic Alternative to the Pulsed combustor Non-Return Valve", *Proceedings of First International Symposium on pulsating combustion*, (DJ Brown Ed.) Sheffield, England, pp. 18-1 to 18-27, 1971.

Kentfield J.A.C., (1986) "The Noise-Producing Characteristics of Highly Loaded Valveless Pulse Combustors", *Winter annual meeting, Report No.86-WA/NCA-34*, The American Society of Mechanical Engineers (ASTHMA), Anaheim, California, USA, pp. 1-9, Dec. 7-12, 1986.

Kishimoto K., (1991) "A Numerical Approach to Valveless Pulse Combustion" *Proceedings of the International Symposium on Pulsating Combustion*, Paper C-5, Monterey, CA, USA, August 5-8, 1991.

Kitchen J.D., (1962) "Pulsed Combustion Promises Chapter Furnace Installations", *Product Design and Engineering*, Vol. 67, pp. 50, 1962.

Kitchen J.A., (1982) "Pulsating Combustion Chambers for Heating Equipments", *Proceedings of the International Symposium on Pulse Combustion Applications*, Atlanta, Georgia, USA, pp. 20-1 to 20-9, March 2-3, 1982.

Kunsagi L., (1971) " Silent Valveless Pulsating Combustor for Industrial Applications", *Proceedings of First International Symposium on Pulsating Combustion*, (DJ Brown Ed.) Sheffield, UK, pp. 17-1 to 17-10, September 1971.

Lawton E.A., Irwin L. and Lawer A., (1982) "Development of a Gas-fired Pulse Combustion Commercial Water Heater", *Proceedings of the International Symposium on Pulse Combustion Applications*, Atlanta, Georgia, USA, pp. 19-1 to 19-29, March 2-3, 1982.

Leckner B. and Gustavsson L., (1991) "Reduction of N_2O by Gas Injection in CFB Boiler", *Journal of the Institute of Energy*, Vol. 44, pp 176-182, 1991.

Lindholm A., (1995) "Combustion Characteristics in Pulsed Combustors Using NO_x Recirculation Methods", *Proceedings of 1995 International Gas Research Conf*erence, Canns, France, pp. 331-340.

Lindholm A., Lundgren E. and Moller S.I., (1996) "Pulse Combustors of Helmholtz Type-Simulation and Measurements of the Combustion Processes in the Combustion Chamber", *Proceedings of First European Conference on Small Burner Technology and Heating Equipments*, Zurich, pp. 405-413, September 25-26, 1996.

Lockwood R.M., (1964) "Pulsed Reactor Low Cost Lift-Propulsion Engine", *American Institute of Aeronautics and Astronautics (AIAA),* Paper No. 64, pp. 172, 1964.

Lockwood R.M., (1982), "Guidelines for Design of Pulse Combustion Devices, Particularly Valveless Pulse Combustors", *Proceedings of the International Symposium on Pulse Combustion Applications*, Atlanta, Georgia, USA, pp. 14-1 to 14-24, March 2-3, 1982.

Lyngfelt A., Amand L.E., Karlsson M. and Leckner B., (1995) "Reduction of N_2O Emissions from Fluidised Bed Combustion by Reversed Air Staging", *Proceedings of Combustion and Emissions Control II*, Institute of Energy, London, UK, pp. 89-93, December 4-5, 1995.

Manganiello E.J., (1948) "Pulse Jet", *Journal of Coast Artillery*, Vol. 91, pp. 9-13, Jan-

Feb 1948.

Michel Y. and Belles F.E., (1991) "Experimental Study of NO_x Production of a Family of Water-Backed Pulse Combustors", *Fossil Fuel Combustion Symposium*, Petroleum Division, ASME, New York, USA, PD-Vol. 33, pp 87-91, 1991.

Miller J.A. and Bowman C.T., (1989) "Mechanism and Modelling of Nitrogen Chemistry in Combustion", *Progress in Energy and Combustion Science,* Vol. 15, pp. 287-338, 1989.

Morel T., (1993) "Comprehensive Model of a Pulse Combustor", *Journal of Combustion Science and Technology*, Vol. 94, pp. 379-409, 1993.

Moseley P.E. and Porter W.J., (1969) "Helmholtz Oscillation in Pulsating Combustion Chamber", *The Journal of the Acoustical Society of America*, Vol. 46, Number 1, Part 2, pp. 262-266, 1969.

Muller J.L., (1971) "Theoretical and Practical Aspects of the Application of Resonant Combustion Chambers in a Gas Turbine", *Journal of Mechanical Eng. Sci.*, Vol. 13, pp. 137-150, 1971.

Murphy M.J. and Putnam A.A., (1985) "Burner Technology Bulletin: Control of NO_x Emissions from Residential Gas Appliances, a Reference Guide for Gas Burner Designers", *Contract No. 5082-24-0772A.G.A.*, Gas Research Institute, Chicago, IL, USA, pp. 4-21, April 1985.

Ohiwa N. and Yamaguchi S., (1989) "A Valveless Pulse Combustor with Wide Operation Range and Low Noise Level", *Journal of Energy Resources Technology*, Vol. 111, pp 187-193, September 1989.

Ponizy B. and Wojcickis B., (1984) "On Modelling of Pulse Combustors", *Twentieth*

Symposium (International) on Combustion, The Combustion Institute, Pittsburgh, PA, USA, pp. 2019-2024, 1984.

Porges G., (1977) "Applied Acoustics", *Edward Arnolds Publishers Ltd*, London, UK, pp.1-8, 1977.

Pugh R.R., (1985) "A Reappraisal of Pulsed Combustion for Liquid Heatings", *British Gas Research and Development*, Project M/6201, London, UK, Part 2, pp. 1-9, August 1985.

Putnam A.A., (1971a) "Combustion Driven Oscillations in Industry", *American Elsevier Publishing Company, Inc.* New York, USA, pp. 1-5, 1971a.

Putnam A.A., (1971b) "General Survey of Pulse Combustion",*Proceedings of First International Symposium on Pulsating Combustion*, (DJ Brown Ed.) Sheffield, UK, pp. 1-1, 1-40, September 1971b.

Putnam A.A., (1979) "A Review of Pulse Combustor Technology", *Proceedings of the Symposium on Pulse Combustion Technology for Heating Applications*, Argon National Laboratory, ANL/EES-TM-87, pp. 1-12, November 1979.

Putnam A.A., Belles F.E. and Kentfield J.A.C., (1986) "Pulse Combustion", *Progress in Energy and Combustion Science*, Vol. 12, pp. 43-79, 1986.

Randall R.H., (1951) "An Introduction to Acoustics", *Published by Addison-Wesley,* Cambridge, Mass., USA, pp. 110, 1951.

Rayleigh (Lord), (1945) "The Theory of Sound", *Dover, New York,* Vol. 2, *Section 322g*, pp. 226, 1945.

Reader G.T., (1978) "Aspects of Pulsating Combustion", *Proceedings of 13th*

Intersociety Energy Conservation Engineering Conference., Vol. 1, pp. 548-555, 1978.

Reay D., (1963) "A study of Gas-Fired Pulsating Combustors", *Journal of Institute of gas Engrs.* Vol. 4, pp. 305-323, 1963.

Rogers G.F.C. and Mayhew Y.R., (1988) "Thermodynamics and Transport Properties of Fluids", *Published by Basil Blackwell Ltd, Fourth Edition,* Oxford, UK, 1988.

Ross C.C., (1954) "Combustion Instability in Liquid Propellant Rocket Motors"; A Survey, Selected Combustion Problems, *Butterworths & Co. (Publishers)*, pp. 25-29, 1954.

Saito T., Tanaka S., Saito K. and Hisaoka S., (1986) "Noise Reduction of Pulse Combustion Water Heaters", *Proceedings of 1986 International Gas Research Conference*, Toronto, Canada, pp. 447-485.

Saito T., Saito K. and Mitoni A., (1989) "Study on NO_x Formation Mechanism in Gas-Fired Pulse Combustors", *Proceedings of 1989 International Gas Research Conference*, Tokyo, Japan, pp. 386-377.

Severyanin V.S., (1969) "The Combustion of Solid Fuel in a Pulsating Flow", *Thermal Engineering,* Vol. 16, pp. 9-13, 1969.

Severyanin V.S. and Dereschuk E.M., (1977), "Future Prospects for the Use of Pulsating Combustion", *Energetika*, Vol. 5, pp. 138-141, (translated by Mrs. Dennis J. Brown, University of Sheffield), 1977.

Severyanin V.S., (1982) "Application of Pulsating Combustion in Industrial Installations", *Proceedings of the International Symposium on Pulsed Combustion Applications*, Atlanta, Georgia, USA, pp. 7-1 to 7-23, March 2-3, 1982.

Skinner B.A., (1989) "New Concept in Air Conditioning", *Gas Engineering and Management*, Vol. 29, pp. 26-32, 1989.

Sommers H., (1952) "Experiences with Pulsating Tube Firing in an Experimental Installation", *Pulsating Combustion-The collected works of F.H. Reynst*, (M.W. Thring Ed.), Progamon Press, NewYork, pp. 262-274, 1952.

Sran B.S. and Kentfield J.A.C., (1982) "Twin Valveless Pulse Combustors Coupled to Operate Antiphase", *Proceedings of the International Symposium on Pulse Combustion Applications*, Atlanta, Georgia, USA, pp. 3-10 to 3-12, March 2-3, 1982.

Suthenthiran A., (1988) "Initial Measurements of Pressure at the Exhaust Outlet", *Report 2 to British Gas Research Centre*, Middlesex University, London, pp. 17, July 1988.

Suthenthiran A., (1989) "Combustor Operation with a Range of Test Gases ", *Report 4 to British Gas Research Centre*, Middlesex University, London, pp. 3-5, March 1989.

Suthenthiran A., (1990) "Construction of Mark 2 Pulsed Combustor", *Report 7 to British Gas Research Centre*, Middlesex University, London, pp. 1-10, January 1990.

Tang Y.M., Waldherr G., Jagoda J.I. and Zinn B.T., (1995) "Heat Release Timing in a Non-Premixed Helmholtz Type Pulse Combustor", *Combustion and Flame*, Vol. 100, pp. 251-261, 1995.

Thrasher W.H. and Strassemeyer E.H., (1987) "A Second Generation Pulse Combustion Space Heater", *Report No. NT-87-14-3,* Gas Research Institute, Chicago, IL, USA, pp. 1619-1631, 1987.

Thring M.W., (1968) "Theoretical Study of Pulsating Combustion", *Twelves Symposium (International) on Combustion*, The Combustion Institute, Pittsburgh, PA, USA, pp.

163, 1968.

Turner D.W. and Siegmand C.W., (1972) "Staged Combustion and Flue Gas Recirculation", *Proceedings of 1st American flame days,* American flame research committee, Chicago, USA, pp. 156-164, September 1972.

Vishwanath P.S., (1984) "Decoupler Design Guidelines for Improving Sound Levels and Stability of Pulsed Burner", *Proceedings of 1984 International Gas Research Conference*, Washington D.C., USA, pp. 912-921, 1984.

Vishwanath P.S., (1985) "Advancement of Development Technology for Pulsed Combustion Applications", *Final Report GRI-85/0280*, Gas Research Institute, Chicago, IL, USA, pp. 3-23, 1985.

Vishwanath P.S. and Thrasher W.H., (1986) "Stand-alone Pulse Combustion Water Heater System", *Proceedings of 1986 International Gas Research Conference*, Toronto, Canada, pp. 122-130, 1986.

Warring R.H., (1974) "Hand Book of Noise and Vibration Control" *2nd Edition, Trade and Technical press Ltd.* Surrey, UK, pp. 7-76 and 171-183, 1974.

Whitlock D., Favors S. and Reuter G., (1982) "Field Tests on Pulse Combustion Boilers for Residential Space Heating and Domestic Water Heating", *Proceedings of the International Symposium on Pulse Combustion applications*, Atlanta, Georgia, USA, pp. 17-1 to 17-12, March 2-3, 1982.

Williams A., Jones J.M. and Rowlands L., (1997) "A Review of NO_x Formation and Reduction Mechanisms in Combustion Systems with Particular Reference to Coal", *Proceedings of Combustion and Emission Control III*, Institute of Energy, Bath, UK, pp. 2-4, 1997.

Williams A., (1990) "Combustion of Liquid Fuel Sprays" *Butterworths & Co. (Publishers)* Ltd., London, UK, pp. 85, 1990.

Willis J.W., Lee A.R., Karagozian A.R. and Smith O.L., (1991) "Acoustic Mode Alteration in a Dual combustor Arising from Halon Addition", *Proceedings of the International Symposium on Pulsating combustion*, Monterey, CA, Paper B-1,August 5-8, 1991.

Windmill S.A., (1984) "An Investigation of the Factor Affecting the Performance of an Experimental Pulsed Combustion Unit", *Internal Progress Report,* British Gas plc, pp. 1-19, 1984.

Wood A., (1949) "A Text Book of Sound", *Published by G. Bell and Sons Ltd.*, London, UK, pp. 214-216, 1949.

Zimmer J.A., (1991) "Analytical Model for Pulse Combustion" *Proceedings of the International Symposium on Pulsating Combustion*, Monterey, USA, Paper C-7, August 5-8, 1991.

Zinn B.T., (1986) "Pulse Combustion: Characteristics- Applications and Research Needs", *21st Intersociety Conference in Energy Conservation Engineering*, American Chemistry Society, CA, USA, pp 7-11, August 25-29, 1986.

Zinn B.T., (1992) " Pulse Combustion: Recent Applications and Research Issues", *Twenty Fourth Symposium (International) on combustion*, The Combustion Institute, Pittsburgh, PA, USA, pp. 1297-1305, 1992.

Appendix I

Calculation of the Combustion Chamber Volume

AI.1 Volume of main cylinder, V_C (ml):

$$V_C = \pi r^2 L \qquad \text{(AI.1)}$$

where, r is the radius of the combustion chamber and L is the length of combustion chamber.

AI.2 Volume of conical cylinder end, V_E (ml):

Volume of a cone is = $(1/3\ \pi r^2)$ (height)

then,

$$V_E = \left[\frac{1}{3}(\pi r^2)\ \frac{r}{\tan 30°}\right] - \left[\frac{1}{3}(\pi r_c^2)\ \frac{r_c}{\tan 30°}\right] \qquad \text{(AI.2)}$$

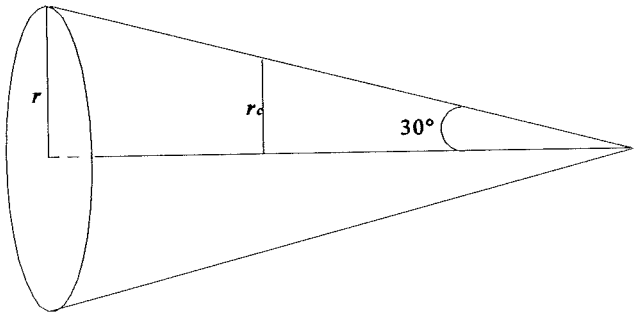

where r_c is the radius of the conical cylinder end.

AI.3 Volume of valve holder, V_H (ml):

$$V_H = \pi r_H^2 L_H \quad \text{(AI.3)}$$

where r_H is the radius of valve holder and L_H is the length of valve holder.

Let "X" be the distance from the rim of the valve holder to the top surface of the front flame trap lock ring. Then, the remaining volume inside the valve holder incorporated into the combustion chamber, V_F (ml):

$$V_F = 2[\pi (r_{LR}^2) L_{LR}] + [(\pi r_H^2) L_{RH}] + [(\pi r_H^2) X] \quad \text{(AI.4)}$$

where r_{LR} is the radius of lock rings, L_{LR} is the length of lock rings and L_{RH} is the remaining length inside the valve holder between components.

Let "Y" be the distance from the rim of the cylinder V_C to the valve holder. Therefore, the effective volume of the combustion chamber, V_{CC} (ml):

$$V_{CC} = V_C + V_E + V_F - V_H - [(\pi r^2) Y] \quad \text{(AI.5)}$$

Appendix II

Composition and Properties of the Test Gases

AII.1 Test Gases

Four types of fuel gas were used in this study. The three of these fuel gases were the test gases supplied by British Gas plc, namely: NGB, NGC and NGD. The fourth fuel gas employed was the mains natural gas designated as NGA. In this appendix the composition and some of the properties of these test gases are given.

AII.1.1 Test Gas NGA

This is the mains natural gas used for most of the experiments conducted in this study. Typically its composition (by volume) according to the North London Gas Board was as follows:

CH_4 = 92.54 %, C_2H_6 = 3.25 %, C_3H_8 = 0.68 %, n-C_4H_{10} = 0.15 %, i-C_4H_{10} = 0.11 %, n-C_5H_{12} = 0.04 %, i-C_5H_{12} = 0.05 %, N_2 = 2.91 % and CO_2 = 0.27 % .

The relative density of the NGA gas to dry air was about 0.58 with Gross Calorific Value (CV_g) of 38.06 MJ m^{-3}. Hence the Wobbe number can be obtained as follows:

$$Wobbe\ Number = \frac{38.06}{\sqrt{0.58}} = 49.97 \qquad MJ\ m^{-3}$$

AII.1.2 Test Gas NGB

This was one of the three test gases provided by British Gas plc to investigate the fuel flexibility and performance of the developed pulsed combustor. The composition and flame stability of the NGB gas is similar to the standard test gas G21 which belongs to

gases of the second family group "H" and categorised as incomplete combustion limit gas. The detailed composition and property of G21 was given in Chapter 1.

The composition of the NGB gas (by volume) according to British Gas plc was as follows:

CH_4 = 73.78 %, C_2H_6 = 2.57 %, C_3H_8 = 17.31 %, n-C_4H_{10} = 0.14 %, i-C_4H_{10} = 0.22 %, He = 0.03 %, N_2 = 5.48 % and CO_2 = 0.47 %.

The CV_g for the NGB gas was 46.83 MJ m^{-3} with relative density (dry gas relative to dry air) of 0.773. Therefore;

$$Wobbe\ Number = \frac{46.83}{\sqrt{0.773}} = 53.26 \qquad MJ\ m^{-3}$$

AII.1.3 Test Gas NGC

The second test gas under study was NGC with a high contents of hydrogen. NGC is a light back limit gas similar to the known standard test gas G222 with 23 % H_2 content [B.S. EN 437]. The NGC gas contained the following gases (by volume):

CH_4 = 55.84 %, C_2H_6 = 2.23 %, C_3H_8 = 3.63 %, n-C_4H_{10} = 0.18 %, i-C_4H_{10} = 0.16 %, N_2 = 1.94 %, H_2 = 35.83 %, CO_2 = 0.19 %.

Relative density of dry NGC gas to dry air was 0.443, with CV_g of 30.87 MJ m^{-3}. Therefore;

$$Wobbe\ Number = \frac{30.87}{\sqrt{0.443}} = 46.38 \qquad MJ\ m^{-3}$$

AII.1.4 Test Gas NGD

The last test gas used in this study was NGD with lift flame stability similar to G23 test

gas [B.S. EN 437]. The composition of NGD gas (by volume) was as follows:

CH_4 = 87.20 %, C_2H_6 = 2.54 %, C_3H_8 = 0.49 %, n-C_4H_{10} = 0.27 %, i-C_4H_{10} = 0.19 %, N_2 = 9.27 %, and He = 0.04 %.

The CV_g of the NGD test gas was 35.80 MJ m^{-3} with relative density of 0.619 to dry air and Wobbe number was calculated as follows:

$$Wobbe\ Number = \frac{35.80}{\sqrt{0.619}} = 45.50 \qquad MJ\ m^{-3}$$

AII.2 Calculation of Input Load For the Gases NGA, NGB, NGC, and NGD

In the following sections the input load for the gases used for this study are calculated.

AII.2.1 Input Load at Volume Flow Rate of One ml s^{-1} for the NGA Gas:

Gross Calorific Value (CV_g) of NGA gas	= 38.06 MJ m^{-3}
one cubic meter is 1000 litre, hence;	
CV_g for one litre NGA gas	= 38.06 kJ l^{-1}
Therefore, heat input at one ml s^{-1}	= 0.0381 kJ s^{-1}
or	
	= 0.0381 kW.

AII.2.2 Input Load at Volume Flow Rate of One ml s^{-1} for the NGB Gas:

CV_g for the test gas NGB	= 46.83 MJ m^{-3}
	= 46.83 kJ l^{-1}

heat input at one ml s^{-1} = 0.0468 kJ s^{-1}

or = 0.0468 kW.

AII.2.3 Input Load at Volume Flow Rate of One ml s^{-1} for the NGC Gas:

CV_g for the test gas NGC = 30.87 MJ m^{-3}

= 30.87 kJ l^{-1}

heat input at one ml s^{-1} = 0.0309 kJ s^{-1}

or = 0.0309 kW.

AII.2.4 Input Load at Volume Flow Rate of One ml s^{-1} for the NGD Gas:

CV_g for the test gas NGD = 35.80 MJ m^{-3}

= 35.80 kJ l^{-1}

heat input at one ml s^{-1} = 0.0358 kJ s^{-1}

or = 0.0358 kW.

Appendix III

Correction of the Rotameter Readings

When the fluid flows through the tube of a rotameter, the float rises and takes up a position such that the pressure loss through the annular space between the float and the tube wall balances the immersed weight of the float. At this stage the float will be in equilibrium. Then,

Weight of float	=	$V_f \rho_f g$	(AIII.1)
Pressure force	=	$(P_1 - P_2)A_f$	(AIII.2)
Upthrust	=	$V_f \rho g$	(AIII.3)

where: V_f is the volume of float,

ρ_f is the density of float,

A_f is the cross sectional area of float,

ρ is the density of fluid,

g is acceleration due to gravity,

P_1, P_2 are the pressures acting on the float (i.e. P_1 from bottom and P_2 from top of the float).

At the equilibrium condition;

$$V_f \rho_f g = (P_1 - P_2) A_f + V_f \rho g \qquad \text{(AIII.4)}$$

therefore;

$$P_1 - P_2 = \frac{V_f(\rho_f - \rho)g}{A_f} \qquad \text{(AIII.5)}$$

According to Bernoulli's equation:

$$P_1 = P_2 + \rho\frac{v^2}{2} \quad \text{(AIII.6)}$$

hence;

$$v^2 = \frac{2(P_1 - P_2)}{\rho} \quad \text{(AIII.7)}$$

Substituting equation (AIII.5) into equation (AIII.7):

$$v^2 = \frac{2v_f(\rho_f - \rho)g}{A_f\rho} \quad \text{(AIII.8)}$$

Volume flow rate, V_{fr}, can be written as:

$$V_{fr} = C_d\, Av \quad \text{(AIII.9)}$$

where C_d is the coefficient of discharge.

Thus by substituting equation (AIII.8) into equation (AIII.9) gives;

$$V_{fr} = C_d.A\sqrt{\frac{2V_f(\rho_f - \rho)g}{A_f\rho}} \quad \text{(AIII.10)}$$

since ρ is very small compared to ρ_f it can be neglected and hence the volume flow rate become:

$$V_{fr} \propto \frac{1}{\sqrt{\rho}} \quad \text{(AIII.11)}$$

or

$$V_{fr} \propto \frac{1}{\sqrt{\sigma}} \qquad \text{(AIII.12)}$$

where σ is the relative density of fluid.

If the test gas G_2 is passed through the flow meter designed for the gas G_1 then the relationship below can be written:

$$V_{G_1} \propto \frac{1}{\sqrt{\sigma_{G_1}}} \qquad \text{(AIII.13)}$$

$$V_{G_2} \propto \frac{1}{\sqrt{\sigma_{G_2}}} \qquad \text{(AIII.14)}$$

$$V_{G_2} = V_{G_1}\sqrt{\frac{\sigma_{G_1}}{\sigma_{G_2}}} \qquad \text{(AIII.15)}$$

where V_{G2} is the actual value of the volume flow rate of the G_2 gas, V_{G1} is the scale reading of G_2 volume flow rate, σ_{G1} is the relative density of gas G_1 and σ_{G2} is the relative density of gas G_2.

Appendix IV

Combustion Calculations

AIV.1 Calculation of Excess Air Ratio (λ) Burning the Mains Natural Gas (NGA) Based on O_2 Measurements

The equation for combustion of one mole of NGA gas at given percentage excess air, "x" can be written as:

$$NGA+2.03(O_2+3.76N_2)(1+\frac{x}{100})\rightarrow 1.03CO_2+7.633(1+\frac{x}{100})N_2+2.0H_2O+2.03\frac{x}{100}O_2 \quad \text{(AIV.1)}$$

then, volume percentage O_2 in dry products can be given as follows:

$$\%\ O_2 = \frac{2.03x}{1.03+7.633(1+\frac{x}{100})+\frac{2.03x}{100}} \quad \text{(AIV.2)}$$

By re-arranging the above equation, the percentage excess air can then be obtained as follows:

$$\%\ x = \frac{8.663\ \%O_2}{2.03-9.663\frac{\%O_2}{100}} \quad \text{(AIV.3)}$$

The excess air ratio λ* is defined as:

$$\lambda = \frac{actual\ A{:}F\ ratio}{stoichiometric\ A{:}F\ ratio} \quad \text{(AIV.4)}$$

*λ is also referred as normalised air-to-fuel ratio.

which is equal to *(1+x)*. Hence, by knowing the value of x, the λ can be evaluated.

Moreover, the input air volume flow rate can be calculated as follow:

$$Air\ Volume\ Flow\ Rate\ =\ q\,9.66\ (1+\frac{x}{100}) \qquad \text{(AIV.5)}$$

where q is the volume flow rate of input fuel gas and 9.66 is the typical stoichiometric air-to-fuel ratio value for NGA gas.

AIV.2 Calculation of λ for a Fuel-Rich Mixture

In this study when burning a rich mixture of air and gas, the excess air ratio was calculated based upon CO readings. The combustion reaction of 1 mole of the mains natural gas when $\lambda<1$ can be written as:

$$NGA+m(O_2+3.76N_2)\rightarrow yCO_2+3.76mN_2+zCO+2H_2O \qquad \text{(AIV.6)}$$

let S be the volume fraction of CO, then it can be written on a dry basis as:

$$S=\frac{z}{y+z+3.76m} \qquad \text{(AIV.7)}$$

From equation (AIV.6), and composition of NGA gas as given in (Appendix II), balancing the carbon:

$$1.03\ =\ y\ +\ z \qquad \text{(AIV.8)}$$

then,

$$z = 1.03 - y \tag{AIV.9}$$

and when balancing oxygen:

$$2.03m = 2y + z + 2 \tag{AIV.10}$$

substituting the equation (AIV.9) into equation (AIV.10) follows:

$$y = 2.03m - 3.03 \tag{AIV.11}$$

and thus, z can be evaluated by eliminating y from equation (AIV.10) using equation (AIV.11):

$$z = 4.06 - 2.03m \tag{AIV.12}$$

Now by substituting the values of "*y*" and "*z*" into equation (AIV.7) *S* can be obtained as follows:

$$S = \frac{4.06-2.03m}{2.03m-3.03+4.06-2.03m+3.76m} \tag{AIV.13}$$

By rearranging the above equation (AIV.13) "m" can be evaluated as follows:

$$m(3.76S+2.03) = 4.06 - 1.03S \tag{AIV.14}$$

$$m = \frac{4.06 - 1.03S}{3.76S + 2.03} \quad \text{(AIV.15)}$$

Then m can be evaluated by use of the measured CO so that;

$$\lambda = \frac{m}{2.03} \quad \text{(AIV.16)}$$

AIV.3 Calculation of λ, for the Test Gases NGB, NGC and NGD

A similar procedure to that used for the NGA gas is employed here to obtain excess air and λ values for the test gases NGB, NGC and NGD with stoichiometric A/F values of 11.83, 7.54 and 9.10 respectively. The combustion reaction for one mole of NGB test gas can be written as follows:

$$NGB + 2.486(O_2 + 3.76N_2)(1 + \frac{x}{100}) \rightarrow 1.336CO_2 + 9.347N_2(1 + \frac{x}{100}) + \frac{2.486x}{100}O_2 + 2.30H_2O \quad \text{(AIV.17)}$$

The percentage excess air, x can be calculated as follows (dry basis):

$$\%x_{NGB} = \frac{10.683\ \%O_2}{2.486 - 11.833\frac{\%O_2}{100}} \quad \text{(AIV.18)}$$

The combustion reaction for burning 1 mole of NGC gas can be written as:

$$NGC + 1.583(O_2 + 3.76N_2)(1 + \frac{x}{100}) \rightarrow 0.730CO_2 + 5.95N_2(1 + \frac{x}{100}) + 1.706H_2O + \frac{1.583x}{100}O_2 \quad \text{(AIV.19)}$$

The percentage excess air can therefore be evaluated on a dry basis as follows:

$$\%x_{NGC} = \frac{6.68\ \%O_2}{1.583 - 7.533\frac{\%O_2}{100}} \qquad \text{(AIV.20)}$$

Finally, when burning NGD gas the combustion reaction can be written as follow:

$$NGD + 1.90(O_2 + 3.76N_2)(1 + \frac{x}{100}) \rightarrow 0.96CO_2 + 7.2N_2(1 + \frac{x}{100}) + 1.88H_2O + \frac{1.90x}{100}O_2 \qquad \text{(AIV.21)}$$

Excess air then can be evaluated as follow:

$$\%x_{NGD} = \frac{8.16\ \%O_2}{1.90 - 9.10\frac{\%O_2}{100}} \qquad \text{(AIV.22)}$$

AIV.4 Calculation of λ, with N_2 Injection

Combustion equation for burning NGA with N_2 addition can be written as follow:

$$NGA + yN_2 + 2.03(O_2 + 3.76N_2)(1 + \frac{x}{100}) \rightarrow 1.03CO_2 + 7.633(1 + \frac{x}{100})N_2 + yN_2 + 2.0H_2O + \frac{2.03x}{100}O_2 \qquad \text{(AIV.23)}$$

where

$$y = \frac{volume\ rate\ of\ flow\ of\ N_2}{volume\ rate\ of\ flow\ of\ NGA} \qquad \text{(AIV.24)}$$

The value of y can be obtained from direct measurements of N_2 and NGA flow rates. Since the measurements of combustion products has been carried out on a dry basis the

term for H_2O can be eliminated. From oxygen measurements and y values the "x" can be calculated as follows:

$$\%x = \frac{(8.663 + y)\%O_2}{2.03 - 9.663\frac{\%O_2}{100}} \quad \text{(AIV.25)}$$

Hence, the $\lambda = 1 + x$.

AIV.5 Calculation of λ, with Ar Injection

The chemical reaction for burning NGA gas with added Ar is:

$$NGA + y'Ar + 2.03(O_2 + 3.76N_2)(1 + \frac{x}{100}) \rightarrow 1.03CO_2 + 7.633(1 + \frac{x}{100})N_2 + y'Ar + 2.0H_2O + \frac{2.03x}{100}O_2 \quad \text{(AIV.26)}$$

where the y' value is defined as:

$$y' = \frac{volume\ flow\ rate\ of\ Ar}{volume\ rate\ of\ flow\ of\ NGA} \quad \text{(AIV.27)}$$

Then, the percentage of excess air can be obtained by:

$$\%x = \frac{(8.663 + y')\%O_2}{2.03 - 9.663\frac{\%O_2}{100}} \quad \text{(AIV.28)}$$

As before $\lambda = 1 + x$.

Appendix V

Correction of measured NO_x and CO Values

AV.1 Correction of NO_x and CO Readings to Zero O_2

It was shown earlier in section AIV.1 that excess air ratio, λ, for NGA gas is equal to:

$$\lambda = 1 + x = \frac{2.03 - O_2}{2.03 + 9.66 O_2} \qquad \text{(AV.1)}$$

where O_2 is the measured volume fraction of oxygen. According to equation (AIV.1) with excess air the number of moles of exhaust products for burning 1 mole of NGA is 8.66 + 9.66 x (on a dry basis). With zero excess air this is 8.66 moles. So in order to correct the measured emission data (e.g. NO_x) to zero excess air these values must be multiplied by the factor given below:

$$Multiplying\ Factor = \frac{(8.66 + 9.66x)}{8.66} \qquad \text{(AV.2)}$$

Substituting x by equation AIV.3 the above equation becomes:

$$Mutiplying\ Factor = \frac{0.21}{0.21 - O_2} \qquad \text{(AV.3)}$$

A similar method to the above can be used for other test gases.

AV.2 Correction of NO_x and CO Data for Excess Air and Injected N_2

The combustion equation with the N_2 addition was given in Section AIV.23. Addition of nitrogen dilutes all the combustion products down by a factor:

$$\frac{1.03+2.03\frac{x}{100}+7.63(1+\frac{x}{100})}{1.03+2.03\frac{x}{100}+7.63(1+\frac{x}{100})+y} = \frac{8.66+9.66\frac{x}{100}}{8.66+9.66\frac{x}{100}+y} \qquad \text{(AV.4)}$$

where y is defined as in equation AIV.24. With excess air and injected N_2 the number of moles of exhaust products is $8.66 + 9.66x + y$, but with zero excess air and zero nitrogen this is 8.66 moles. Therefore, to correct the emission data to zero excess air and zero nitrogen the concentration of measured emissions must be multiplied by the factor below:

$$Multiplying\ Factor = \frac{8.66+9.66x+y}{8.66} \qquad \text{(AV.5)}$$

Substituting for x as given in equation AIV.25 the multiplying factor becomes:

$$Multiplying\ Factor = \frac{0.21}{0.21-O_2}\left[\frac{8.66+y}{8.66}\right] \qquad \text{(AV.6)}$$

Now by multiplying the above factor with measured concentrations of pollutant gases such as NO_x and CO, their values for zero O_2 and N_2 can be determined.

AV.3 Correction of NO_x and CO Values for Excess Air and Added Ar

A similar procedure as for nitrogen injection (shown in section AV.2) was carried out to correct the NO_x and CO readings to zero excess air and added argon volume rate.

Appendix VI

Calculation of Flue Gas Dew Point

The dew point of flue gases from the combustion of the mains natural gas (NGA) at stoichiometric condition can be calculated using the combustion equation for burning 1 mole of NGA gas:

$$NGA + 2.03(O_2 + 3.76N_2) \rightarrow 1.03CO_2 + 7.633N_2 + 2H_2O \qquad \text{(AVI.1)}$$

From the above equation it can be seen that 1 kg of NGA gas requires 16.17 kg air (taken to be dry). The saturated moisture content "g_s"can be calculated using the equation below [Hanby, 1993]:

$$g_s = \frac{0.624 P_s}{P_{atm} - 1.004 P_s} \qquad \text{(AVI.2)}$$

where P_s is the saturated pressure at the given temperature and P_{atm} is the atmospheric pressure. At a typical laboratory temperature of 15 °C, P_s = 0.01704 bar [Rogers and Mayhew, 1988]. Substituting this value into equation (AVI.2), gives a saturation moisture content of 0.01067 kg water per kg dry air at the standard atmospheric pressure. However, the typical value for the relative humidity of the ambient air was 60 %. Therefore, for the above given temperature and relative humidity, the moisture content of air would be 0.00640 kg kg^{-1} dry air. At a moisture content of 0.00640 kg kg^{-1} dry air, the required quantity of air to burn 1 kg NGA contains 0.103489 kg water vapour.

Hence, the combustion of 1 kg NGA produces:

	2.63	kg	CO_2
	12.4	kg	N_2
and	2.20	kg	H_2O

To find the volume fraction of water vapour in these products we need to obtain the mole fraction of water vapour. The number of moles of each of the constituents is:

	CO_2	(2.63÷44)	0.060
	N_2	(12.4÷28)	0.443
and	H_2O	(2.20÷18)	0.122
			Total = 0.625

The mole fraction of water vapour is thus:

$$0.122 \div 0.625 = 0.1952 \qquad \text{(AVI.3)}$$

The partial pressure of water vapour in the flue gas is thus:

$$0.1952 \times 1.01325 = 0.198 \qquad \text{(AVI.4)}$$

in bar. From the steam tables [Rogers and Mayhew, 1988] and by interpolating the tabulated values, the corresponding saturation temperature is 60.0 ±1 °C. Therefore, the dew point of the combustion gases at stoichiometric condition is 60.0 ±1 °C.

It should be noted that the above atmospheric pressure used here is the standard value; in practice, its value was updated by direct readings from a barometer daily. Similarly, the temperature and relative humidity of the laboratory was monitored daily.

Appendix VII

Calculation of Adiabatic Flame Temperature

The temperature of the flame especially as it enters the heat exchanger has a significant effect upon the performance of any device. In this calculation an energy balance was used to estimate the temperature of the flame inside the combustors. It was assumed that combustion took place under adiabatic conditions i.e. no heat transfer between the gas and surroundings. The implication of this was that there is no useful heat and case loss. With this assumption the energy balance can be written as [Hanby 1993]:

$$CV_n + H_R = H_p \qquad \text{(AVII.1)}$$

where CV_n is the net calorific value of the fuel, hence H_p contains only sensible heat terms. The value of CV_n for the mains natural gas typically was 48.7 MJ kg^{-1} and the enthalpy of the reactants (H_R) at a reference temperature of 25°C was calculated as follows:

$$H_R = (T_i - 25) \sum (mC_p)_R \qquad \text{(AVII.2)}$$

where T_i is the initial temperature and the value of H_R is the sensible heat in the reactants. The summation$\sum$ was carried out for each of the species present in the reactants by mass (kg). Using appropriate tables [Rogers and Mayhew, 1988] the specific heats (C_p) of the fuel, oxygen and nitrogen at constant pressure were obtained at a mean temperature calculated as follows:

$$\frac{T_i + 25}{2} \qquad \text{(AVII.3)}$$

According to equation AVII.1 the enthalpy of the products H_p is the sum of calorific value of the fuel gas and the enthalpy of reaction which can be defined as [Hanby, 1993]:

$$H_p = (T_f - 25) \sum (mC_p)_P \qquad \text{(AVII.4)}$$

where T_f is the flame temperature. The above relationship can not be solved directly for T_f due to the considerable difference between T_f and the reference temperature. Hence, the value of T_f was required to evaluate the specific heats of the combustion products. A value for T_f was estimated and was used to obtain the specific heats (i.e. C_p), of the combustion products at the average temperature between the flame and the reference temperature. Using the obtained values for C_p and the mass of combustion products equation (AVII.4) was solved for T_f. Finally, the new value of T_f was compared with the original estimated value and if there was a substantial differences (i.e. > 5 °C) the new value was used to re-evaluate the specific heats (iterative method) and the process of calculation was continued as before.

This method is one of many ways of calculating the adiabatic flame temperature. It is a straightforward well-known technique of successive substitution which is generally used in engineering calculations [Hanby 1993]. However, no dissociation effect was considered which reduce the flame temperature. This is because dissociation is an endothermic process, absorbing energy from enthalpy of the gas mixture. When a detailed prediction of composition of the combustion products is required it is necessary to carry out equilibrium composition calculations.

Appendix VIII

Correction for Background Noise

The measured noise levels from pulsed combustors were corrected to zero background noise as follows. Let "C" to be the corrected value, which can be obtained using the equation below [Anderson and Anderson, 1993]:

$$C = -10 \log(1 - 10^{\frac{-[SPL_t - SPL_{bg}]}{10}}) \qquad \text{(AVIII.1)}$$

Where SPL_t is the total measured noise and SPL_{bg} is the measured background noise. Hence the actual emitted sound pressure level from the combustor can be written as:

$$SPL = SPL_t - C \qquad \text{(AVIII.2)}$$

in dB. The equation (AVIII.1) is derived from the fact that the decibel scale is a logarithmic scale applied in acoustics to the ratio of sound intensities or ratio of sound pressure. The sound pressure level (SPL) is an important quantity characterising sound and can be measured easily. Sound pressure level can be defined as [Anderson and Anderson, 1993]:

$$SPL = 20 \log \frac{P_{rms}}{P_{ref}} \qquad \text{(AVIII.3)}$$

in dB. The value of reference pressure (P_{ref}) is approximately the value of the root mean square sound pressure (P_{rms}) corresponding to very faint sound that can be heard in the mid-frequency range. The reference sound pressure value is 20μPa. The multiplying factor in the equation (AVIII.3) was introduced to avoid a scale which was too compressed.

Appendix IX

Flue Gas Analysis Methods

A.IX.1 Gas Analysis by Infra-red Absorption

Most gases have absorption spectra with characteristic absorption bands in the infra-red. Not all gases can be differentiated however, the notable exceptions being nitrogen, oxygen, argon, chlorine, helium and hydrogen. Sensitive detecting elements are available for measuring by comparison the amount of radiation absorbed, and can be calibrated to give the concentration of the particular gas sought. The infra-red analyser can be applied with accuracy and reliability for flue gases such as carbon monoxide and carbon dioxide.

A.IX.1.1 Principle of Method

Shown in Fig. AIX1, is the recording infra-red absorption gas analyser [BS 3048, 1993]. Two radiators in the form of nickel-chromium wire spirals are heated electrically to give two sources of infra-red radiation of equal intensity. The produced infra-red beams are interrupted periodically by a rotating shutter. The beams pass through filter chambers (if fitted) and one passes through a comparison chamber filled with dry air while the other passes through an analysis chamber into which the filtered and dried sample gas is passed. Both beams then pass to a sensitive detector element which measures by difference the amount of radiation absorbed by the specimen in the analysis chamber. One form of detector unit consists of two small measuring chambers separated by a flexible metal membrane which is part of an electrical condenser. The radiation in the analysis chamber is proportional to the amount of absorbing gas in the sample. The periodic warming of the gas in the measuring chamber beyond the analysis chamber is less than that in the comparison measuring chamber. This difference in heating causes the pressures in the two measuring chamber to be different, and since the radiation is being chopped by mechanical shutter, a periodic movement of the condenser membrane occurs. The electrical capacity changes are measured and amplified sufficiently to

operate an indicator or recorder. The sensitivity of the measuring unit is a function of the pressure of the filled gas.

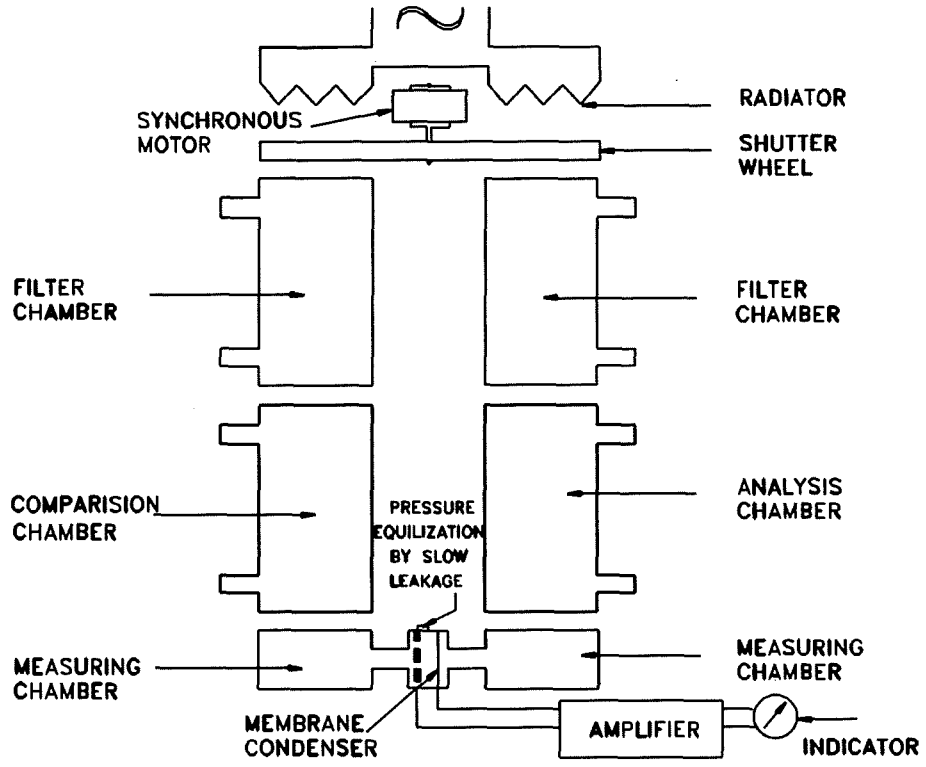

Fig. AIX1 ***A schematic representation of the infra-red absorption gas analyser [After BS 3048, 1993].***

A.IX.2 Oxygen Measurements by Magnetic Means

Compared to other gases, oxygen has a high magnetic susceptibility. Oxygen is a paramagnetic gas which seeks the strongest part of a magnetic field, unlike some other gases which seek the weakest part of a magnetic field (i.e. diamagnetic). The oxygen content can be determined from its magnetic susceptibility by direct deflection method, method utilizing the loss of paramagnetism caused by heating and/or indirect method depending on the change in the viscosity of oxygen in a magnetic field [BS 3048, 1993]. A detailed descriptions of these methods are reported in British standards 3048, 1993.

A.IX.3 Chemiluminescent Method of NO_x Measurements

There are number of methods for determination of oxides of nitrogen which are generally tedious and not readily adaptable to on-line monitoring of emissions. These methods include: the Greiss-Saltzman method, optical and electrical method and finally chemiluminescent analysis. Of the three methods the latter is the most satisfactory method for measuring concentrations of nitrogen oxides. This is because the two former methods have presented awkward problems such as: calibration problems for the Greiss-Saltzman method which requires the quantative conversion of NO to NO_2 or difficulties of obtaining rapid response in a continuous monitoring instrument associated with the optical and electrical methods owing to utilization of long-path infrared spectroscopy which uses large volume cells [Murphy and Putnam, 1985].

The method of chemiluminescent analysis is simple in principle and highly specific to nitric oxide. However, the phenomenon has been used to measure the concentrations of a number of atmospheric pollutants including sulfides, ethylene, PAN and ozone. The method is very sensitive and it arises in high exothermic reactions when there is sufficient energy for reaction products to be formed in excited states [Hargreaves and Smith 1976]. Then the excited products either undergo collisional deactivation or decay to their ground state by radiation. In principle the method is dependent upon the reaction between the oxide and ozone. Here in this study the principle of operation of the chemiluminescent analyser (Rotork analyser model 443) used is as follows. After the sample gas enters the chemiluminescent NO_x analyser it is mixed with ozone (O_3) within the reaction chamber in front of a photomultiplier tube. The ozone is generated internally within the instrument and after the reaction any residual of O_3 is catalytically destroyed. The photomultiplier tube monitors the production of photons. Nitric oxide reacts with ozone to produce nitrogen dioxide some molecules of which are in the ground state and some in an excited state. The reactions are as follows:

$$NO + O_3 \rightarrow NO_2 + O_2 \qquad \text{(AIX.1)}$$

$$NO + O_3 \rightarrow NO_2^* + O_2 \qquad \text{(AIX.2)}$$

$$NO_2^* \rightarrow NO_2 + hv \qquad \text{(AIX.3)}$$

$$NO_2^* + M \rightarrow NO_2 \qquad \text{(AIX.4)}$$

where *hv* is the energy of a photon. The first equation refers to production of nitrogen dioxide, the second equation refers to production of electronically excited nitrogen dioxide, the third equation corresponds to chemiluminescence and finally the last equation refers to collisional deactivation. A molecule of electronically excited nitrogen dioxide decays to the ground state either by loss of a photon or by energy transfer to another species (i.e. M) by collision. "M" can either be the walls of the chamber, or other molecules of gas in the sample flow. With sufficient presence of ozone before and after reaction, the intensity of emitted light is linear with nitric oxide concentration. This can be monitored by using the photomultiplier tube.

NO_2 is not one of the reactants in the chemiluminescent reaction. Using a catalytic converter the NO_2 can be converted to NO prior to entering the chamber, allowing determination of NO_x. NO_2 is obtained by difference after measuring total NO_x and NO. The instrument used in this study can be operated as a NO_x or NO analyser by switching the converter in or out of stream.

List of Publications

i. Barham, K.J.A. Hargreaves, H. Ipakchi and W.C. Maskell, *in Proceedings of the Fifth International Conference on Technologies and Combustion for a Clean Environment,* Lisbon, Portugal, Volume 1, pp. 481-488, July 12-15, 1999.

ii. Barham, K.J.A. Hargreaves, H. Ipakchi and W.C. Maskell, *in Proceedings of Mediterranean Combustion Symposium (International),* Antalya, Turkey, pp. 255-264, June 20-25, 1999.

iii. P. Barham, K.J.A. Hargreaves, H. Ipakchi and W.C. Maskell, *in Proceedings of Fourth International Conference on Technologies and combustion for a Clean Environment*, Lisbon, Portugal, Volume 1, section 29.3, pp. 17-23, July 1997.

iv. Barham, K.J.A. Hargreaves, H. Ipakchi and W.C. Maskell, *Combustion and Emission Control III*, Institute of Energy, Bath, UK, pp. 481-488, 1997.